

**Identification and Characterisation of Novel
Mechanisms that Regulate TRAIL-Receptor Signalling
Complexes**

Thesis submitted for the degree of
Doctor of Philosophy
at the University of Leicester

by

Adam Peall BSc (Hons)

MRC Toxicology Unit

University of Leicester

September 2016

Identification and Characterisation of Novel Mechanisms that Regulate TRAIL-Receptor Signalling Complexes

Adam Peall, MRC Toxicology Unit, University of Leicester, Leicester, UK, LE1 9HN

Activation of death receptors by their cognate ligands can induce apoptosis through the formation of death receptor signalling complexes. TRAIL has been demonstrated to selectively induce apoptosis in transformed cells, but not normal cells, by binding to its death receptors, TRAIL-R1 and TRAIL-R2 and inducing DISC formation. However, the use of TRAIL as a cancer therapeutic has been hampered by widespread intrinsic and acquired resistance to TRAIL in tumours. Gaining a better understanding of the mechanisms which regulate TRAIL signalling in both tumour and normal cells, will enable new strategies to overcome tumour resistance to TRAIL-induced apoptosis. Therefore, the aim of this thesis was to identify and characterise novel mechanisms which regulate TRAIL signalling using protein complex isolation, mass spectrometry and functional assays.

By isolating the TRAIL DISC and unstimulated TRAIL-R1/R2 using wild-type TRAIL and TRAIL-R1 or -R2 specific TRAIL mutants, novel protein interactors were identified. Oxysterol binding protein related protein 8 (ORP8) was shown to specifically interact with unstimulated TRAIL-R1/R2 and regulate the cell surface expression of TRAIL-R2. An SCF complex, composed of S-phase kinase associated protein 1 (Skp1), cullin-1 (CUL1) and F-box only protein 11 (FBXO11), was shown to interact with unstimulated TRAIL-R1/R2. The role of this complex was hypothesised to regulate ubiquitination and proteasomal degradation of TRAIL-R1/R2. The serine/threonine phosphatase, PP2A was demonstrated to interact with both the TRAIL DISC and unstimulated TRAIL-R1/R2. PP2A is likely to regulate TRAIL signalling by de-phosphorylating TRAIL-R1/R2 or associated proteins. In addition, the mechanism by which activated PKC inhibits TRAIL-induced apoptosis was further investigated. Activation of PKC induced the phosphorylation of the intracellular domain (ICD) of TRAIL-R2. This phosphorylation, most likely on the TRAIL-R2-T298 residue, prevents aggregation of TRAIL-R2 into a high molecular weight (HMW)-TRAIL DISC. Inhibition of HMW-DISC formation prevents FADD recruitment, caspase-8 recruitment and activation, and blocks the induction of both the apoptotic and non-apoptotic arms of TRAIL signalling.

Acknowledgements

I would firstly like to thank the Medical Research Council for funding my research and professors Marion MacFarlane and Kelvin Cain for their help and guidance.

I am also grateful to all of the members of the MacFarlane and Cain labs for their continued support and advice. I thank Mrs Rebecca Jukes-Jones for the mass spectrometry work she performed and special thanks to Dr Michelle Hughes and Mr Surjinder Singh for their help in scraping the millions of cells. I would also like to thank Dr Munisha Devi for the ILZ-TRAIL and biotinylated ILZ-TRAIL she provided.

To all the great friends I have made at the MRC Toxicology Unit I say thank you for being there over the last four years. And special thanks to everyone in the “Thesis Therapy” group for getting us all through the writing stage.

Mum and Dad, I can’t ever thank you enough for always being there for me and for your constant love and care. I wouldn’t have made it without you behind me. And to the rest of my family and friends, thank you for your support.

Table of Contents

Acknowledgements	3
Table of Contents	4
List of Figures, Tables and Appendices.....	10
Abbreviations.....	14
Chapter 1: Introduction	18
1.1: Cancer.....	19
1.2: Apoptosis.....	20
1.2.1: Function and Morphology.....	20
1.2.2: Genetic Basis for Apoptosis.....	21
1.3: Caspases	23
1.4: Intrinsic Apoptosis	27
1.5: Extrinsic Apoptosis	30
1.6: Death Ligands and their Cognate Death Receptors	31
1.6.1: TNF α : TNFR1.....	31
1.6.2: CD95L : CD95	34
1.6.3: TRAIL : TRAIL-R1 and TRAIL-R2.....	36
1.7: Death-inducing Signalling Complex (DISC) Formation	40
1.7.1: Ligation of Death Receptors.....	40
1.7.2: Death Domain-mediated Recruitment of Adaptor Proteins.....	42
1.7.3: Death-Effector Domain-Mediated Recruitment of Initiator Caspases	45
1.7.4: DISC Internalisation	47
1.8: TRAIL or CD95L-induced “Secondary Complex” Formation	47
1.9: Regulation of TRAIL Signalling	49
1.9.1: Modulation of TRAIL Receptor Levels	49
1.9.2: TRAIL Receptor Aggregation.....	51

1.9.3: DISC-Interacting Proteins	52
1.9.4: PKC.....	55
1.11: Thesis Aims	57
Chapter 2: Materials and Methods	59
2.1: Chemicals.....	60
2.2: Reagents	60
2.2.1: TRAIL Generation and Biotinylation	60
2.2.3: Antibodies.....	60
2.2.4: Expression of GST-Fusion Proteins.....	60
2.3: Cell Culture	64
2.3.1: Rationale for Cell Lines Used	64
2.4: General Methods.....	65
2.4.1: Assessment of Protein Expression in Cell Lines.....	65
2.4.2: SDS-PAGE.....	65
2.4.3: Western Blot Analysis.....	66
2.4.4: Coomassie Staining.....	66
2.4.5: Bradford Protein Assay	66
2.4.6: Apoptosis Assessment of Annexin V-FITC and DRAQ7 Stained Cells by Flow Cytometry.....	66
2.4.7: Knockdown of Protein Expression by siRNA Transfection	68
2.4.8: Measurement of TRAIL-R1 and TRAIL-R2 Cell Surface Expression.....	69
2.5: Analysis of the TRAIL DISC	69
2.5.1: TRAIL DISC Isolation.....	69
2.5.2: Separation of TRAIL DISC by Sucrose Density Gradient (SDG) Centrifugation	70
2.5.3: 2-D Gel Electrophoresis of Isolated TRAIL DISC	70

2.5.4: Treatment of the Isolated TRAIL DISC with Phosphatases.....	71
2.6: Mass Spectrometry	71
2.6.1: “Shotgun Proteomics”	72
2.6.2: “Off-bead” Method	72
2.6.3: Label-Free “Top 3” Quantitation	72
2.6.4: Identification of Protein “Hits”	73
2.7: GST-TRAIL-R-ICD <i>In Vitro</i> Binding Assay	73
Chapter 3: Development of an Improved Platform to Identify Isolated TRAIL DISC Proteins, Unstimulated TRAIL receptors and Associated Proteins by Label-free Quantitative Mass Spectrometry	74
3.1: Introduction.....	75
3.2: Results	77
3.2.1: Concentration-response of BJAB Cells to TRAIL-induced Apoptosis.....	77
3.2.2: Western Blot Analysis of Isolated TRAIL DISC and Unstimulated TRAIL receptors from BJAB Cells	79
3.2.3: Detection and Quantification of TRAIL DISC Proteins using Label-free “Top 3” LC-MS/MS Shotgun Proteomics.....	81
3.2.4: Identification and Confirmation of Novel TRAIL DISC-Interacting Proteins.	85
3.2.5: By Evaluating an “Off-bead” Method to Analyse the Isolated TRAIL DISC, it was Determined that Further Reduction in the Volume of Streptavidin Beads Does not Enhance TRAIL DISC Detection.....	89
3.2.6: Detection of Unstimulated TRAIL receptors Isolated from BJAB Cells by Label-free Quantitative Mass Spectrometry using the “Off-bead” Method	95
3.3: Discussion	102
3.3.1: Summary of Chapter Findings	102
3.3.2: Optimisation of the Isolation and Detection of TRAIL DISC Proteins by Mass Spectrometry.....	102

3.3.3: Evaluation of Shotgun Proteomics and “Off-bead” Methods to Analyse Samples by Mass Spectrometry	103
3.3.4: Identification of Novel TRAIL DISC-Associated Proteins by Mass Spectrometry.....	104
3.3.5: Detection of Unstimulated TRAIL receptors and Associated Proteins by Mass Spectrometry.....	106
3.3.6: Using “Top 3” Label-free Quantitation to Determine the Amount of Detected Proteins by Mass Spectrometry	107
Chapter 4: Identification of Novel TRAIL-R1/R2 Specific Mechanisms of Regulation..	109
4.1 Introduction.....	110
4.2: Results	112
4.2.1: BJAB Cells are Sensitive to TRAIL-induced Apoptosis Mediated by TRAIL-R1	112
4.2.2: Successful Isolation of TRAIL DISC and Unstimulated TRAIL Receptors using TRAIL-R1/R2-specific biotinylated TRAIL Mutants	114
4.2.3: Identification of Novel TRAIL Receptor-Interacting Proteins by Mass Spectrometry.....	119
4.2.4: Confirmation of Novel TRAIL-R1/R2-Interacting Proteins by Western Blot Analysis	128
4.2.5: siRNA Targeting of ORP8 Increases Cell Surface Expression of TRAIL-R2 ..	132
4.2.6: siRNA Targeting of ORP8 Sensitises HeLa Cells to TRAIL-induced Apoptosis	134
4.3 Discussion	137
4.3.1 Summary of Chapter Findings	137
4.3.2: TRAIL DISC Components TRAIL-R1, TRAIL-R2, TRAIL-R4, FADD, Caspase-8, cFLIP and Caspase-10 Detected by Mass Spectrometry in the DISC Isolated Using WT and TRAIL-R1-specific bTRAIL.....	139

4.3.3: ORP8 Identified as a TRAIL-R1/R2 Interacting Protein in BJAB and HeLa cells: siRNA Targeting of ORP8 in HeLa Cells Increases TRAIL-R2 Cell Surface Expression and Sensitivity to TRAIL-Induced Apoptosis	141
4.3.4: Skp1, FBXO11, CUL1 (SCF) Complex Identified as Interacting with Unstimulated TRAIL-R1/R2 in BJAB Cells.....	144
4.3.5: PP2A Phosphatase Identified as Interacting with both TRAIL-R1 and TRAIL-R2 in BJAB Cells.....	147
Chapter 5: Investigation of the Mechanism of PKC-mediated Inhibition of Death Receptor Signalling	149
5.1: Introduction.....	150
5.2: Results	152
5.2.1: PKC Activation Inhibits TRAIL-induced Apoptosis in HeLa and Jurkat E6.1 but not BJAB cells	152
5.2.2: PKC Activation Inhibits CD95-induced Apoptosis in Jurkat A3 Cells	154
5.2.3 PMA Treatment Blocks TRAIL-induced NF κ B Activation	154
5.2.4 Characterisation of PKC Isoform Expression and PKC Activation	157
5.2.5 Knockdown of PKC β Prevents PKC-mediated Inhibition of TRAIL-Induced Apoptosis	160
5.2.6 PKC Activation Inhibits the Aggregation of TRAIL-R2 to HMW-DISC	162
5.2.7 PKC Activation Modifies TRAIL-R2 at the DISC in HeLa and Jurkat E6.1 but not BJAB cells.....	163
5.2.8 PKC Activation Modifies both TRAIL-stimulated and Unstimulated TRAIL-R2	167
5.2.9 PKC-mediated Phosphorylation of TRAIL-R2 results in Phosphorylation of a Serine/Threonine Residue	169
5.2.10 <i>In Vitro</i> GST-TRAIL-R2-ICD Binding Assay Reveals Potential Sites of PKC-mediated Phosphorylation of TRAIL-R2	173
5.3 Discussion	179

5.3.1 Sensitivity of Cell Lines to PKC-mediated Inhibition of Death Receptor Signalling.....	179
5.3.2 PKC-mediated Inhibition of Non-Apoptotic Death Receptor Signalling.....	181
5.3.3 Effect of PKC Activation on DISC Formation.....	182
5.3.4 PKC-mediated Phosphorylation of TRAIL-R2.....	183
Chapter 6: Final Overview	186
Appendices	194
Bibliography.....	203

List of Figures, Tables and Appendices

Figure 1.1: Apoptosis Controlling Genes in <i>C.Elegans</i> and their Mammalian Homologues.....	22
Figure 1.2: Human Apoptotic Caspases.....	24
Figure 1.3: Apoptosis induced by the Extrinsic Apoptosis Pathway	29
Figure 1.4: Receptors of the Death Ligands: TNF α , CD95L and TRAIL	32
Figure 1.5: Models for Ligand-induced Death Receptor Aggregation Complexes	43
Figure 1.6: Regulation of TRAIL signalling by TRAIL-R1/R2 Protein Interactions	53
Figure 2.1: Forward/Side Scatter and Annexin V/DRAQ7 Blots of Control and Apoptotic Cells.....	67
Figure 3.1: Concentration-response of BJAB cells to TRAIL-induced Cell Death	78
Figure 3.2: Isolation of the TRAIL DISC and Unstimulated TRAIL-R1/R2 from BJAB Cells	80
Figure 3.3: Confirmation of the Interaction of TRAIL DISC-associated Proteins by Western Blot Analysis.....	88
Figure 3.4: “Top 3” Label-Free Quantitation of TRAIL DISC Proteins Isolated Using the “Off-Bead” Method	94
Figure 3.5: “Top 3” Label-Free Quantitation of Unstimulated TRAIL receptors Isolated using the “Off-Bead” Method	98
Figure 3.6: “Top 3” Label-Free Quantitation of TRAIL DISC and Unstimulated TRAIL receptor-Interacting Proteins.....	100
Figure 4.1: WT and TRAIL-R1-Specific TRAIL Mutants-Induce Apoptosis in BJAB Cells....	113
Figure 4.2: Isolation of the TRAIL DISC and Unstimulated TRAIL receptors Using WT and TRAIL-R1/R2-Specific Mutant bTRAIL	115
Figure 4.3: Label-Free “Top 3” Quantitation of TRAIL DISC Components and Unstimulated TRAIL receptors using TRAIL-R1/R2-Specific bTRAIL Ligands	117

Figure 4.4: Venn Diagram of Identified TRAIL DISC and Unstimulated TRAIL-R1/R2-Interacting Proteins	120
Figure 4.5: Novel DISC-only Interacting Proteins Identified by Mass Spectrometry ...	121
Figure 4.6: Novel TRAIL-R1-Interacting Proteins Identified by Mass Spectrometry	123
Figure 4.7: Novel TRAIL-R2-Interacting Proteins Identified by Mass Spectrometry	124
Figure 4.8: Novel TRAIL-R1/R2-Interacting Proteins Identified by Mass Spectrometry	127
Figure 4.9: Confirmation of Novel TRAIL DISC and Unstimulated TRAIL-R1/R2-Interacting Proteins in BJAB Cells by Western Blot Analysis.....	129
Figure 4.10: Confirmation of the Association of ORP8 with TRAIL-R1/R2 in HeLa Cells	131
Figure 4.11: siRNA Targeting of ORP8 Increases Cell Surface TRAIL-R2 Expression	133
Figure 4.12: Knockdown of ORP8 Expression Sensitises HeLa Cells to TRAIL-Induced Apoptosis.....	135
Figure 5.1: PKC Activation Blocks TRAIL-Induced Apoptosis in HeLa and Jurkat E6.1 Cells.....	153
Figure 5.2: PKC Activation Does not Block TRAIL-Induced Apoptosis in BJAB Cells.....	155
Figure 5.3: PKC Activation Blocks Anti-CD95-Induced Apoptosis in Jurkat A3 Cells	156
Figure 5.4: PMA Treatment Blocks TRAIL-Induced NF κ B Activation in HeLa Cells.....	158
Figure 5.5: Characterisation of PKC Isoform Expression and PKC Activation	159
Figure 5.6: siRNA Targeting of PKC β Prevents PKC-Mediated Inhibition of TRAIL-Induced Apoptosis	161
Figure 5.7: PKC Activation Inhibits the Aggregation of TRAIL-R2 to HMW-DISC and Impedes FADD Recruitment	164
Figure 5.8: PKC Activation Modifies TRAIL-R2 and Inhibits FADD Recruitment to the DISC in HeLa and Jurkat E6.1 Cells but not in BJAB Cells	166
Figure 5.9: PKC Activation Modifies bothe TRAIL-Stimulated (DISC Associated) and TRAIL-Unstimulated TRAIL-R2	168

Figure 5.10: Two-Dimensional Gels of TRAIL-R2 from PMA Treated HeLa Cells Indicate Phosphorylation Event	170
Figure 5.11: PKC-Induced Phosphorylation of TRAIL-R2 Occurs on Serine/Threonine Residue	172
Figure 5.12: Potential Serine/Threonine Phosphorylation Sites in TRAIL-R2 Intracellular Domain	174
Figure 5.13: PMA Treatment Blocks FADD Recruitment to TRAIL-R2 Intracellular Domain	175
Figure 5.14: <i>In Vitro</i> Binding Assay Reveals Potential Sites of PKC-Mediated Phosphorylation of TRAIL-R2.....	177
Figure 6.1: Schematic of Novel Potential Mechanisms of Regulation of TRAIL Signalling Identified in this Thesis.....	188
Figure 6.2: Schematic for the Proposed Mechanism Underlying PKC-Mediated Inhibition of TRAIL Signalling.....	189

Table 2.1: Primary Antibodies Used for Western Blot Analysis	61
Table 2.2: Primary Fluorophore-conjugated Antibodies used for Flow Cytometry Analysis	62
Table 2.3: Agonistic Primary Antibody used to Induce Cell Death.....	62
Table 2.4: Secondary Antibodies used for Western Blot Analysis	62
Table 2.5: Primers used to Mutate TRAIL-R2 Serine/Threonine Residues to Alanine ...	63
Table 3.1: Detection of TRAIL DISC Proteins Isolated from BJAB Cells using “Shotgun Proteomics” and Mass Spectrometry.....	82
Table 3.2: Potential DISC-Associated Proteins Identified by Mass Spectrometry	86
Table 3.3: Detection of Proteins from the TRAIL DISC Isolated from BJAB Cells by Mass Spectrometry Using the “Off-Bead” Method.....	90
Table 3.4: Detection of TRAIL receptors in Unstimulated Samples from BJAB Cells by Mass Spectrometry Using the “Off-Bead” Method.....	96
Table 3.5: Novel TRAIL receptor-Interacting Proteins Identified by Mass Spectrometry Using the “Off-Bead” Method	99
Appendix Figure 3.1: Amino Acid Coverage of Detected TRAIL DISC Components	195
Appendix Figure 3.2: Amino Acid Coverage of Detected Novel DISC Interacting Proteins	196
Appendix Table 4.1: All Proteins Identified by Label-free Quantitative Mass Spectrometry in Chapter 4	197
Appendix Figure 4.1: Amino Acid Coverage of DISC Components Detected in Chapter 4	201
Appendix Figure 4.2: Amino Acid Coverage of Novel TRAIL DISC and TRAIL-R1/R2 Interacting Proteins Detected in Chapter 4	202

Abbreviations

ALPS	Autoimmune lymphoproliferative syndrome
Annexin V	Annexin V-FITC
ARAP1	Arf GAP and Rho GAP domain, Ankyrin repeat and PH domain
BCL-2	B-cell lymphocytic leukaemia proto-oncogene-2
BH	BCL-2 homology domain
BIR	Baculovirus IAP repeat
BisI	Bisindolylmaleimide I
BSA	Bovine serum albumin
bTRAIL	Soluble biotinylated TRAIL
CAD	Caspase activated DNase
CARD	Caspase recruitment domain
Caspase	Cysteine-dependent aspartyl specific protease
CD95L	CD95 ligand
c-FLIP	Cellular FLIP
c-FLIPL	Cellular FLIP long isoform
c-FLIPR	Cellular FLIP raji isoform
c-FLIPS	Cellular FLIP short isoform
CHOP	CCAAT-enhancer-binding protein homologous protein
CRD	Cysteine-rich domain
CrmA	Cytokine response modifier
CUL	Cullin
Cyt c	Cytochrome c
DD	Death domain
DED	Death effector domain
DISC	Death-inducing signalling complex
DNA	Deoxyribonucleic acid
ER	Endoplasmic reticulum
FACS	Fluorescence activated cell sorter
FADD	Fas-associated death domain protein
FBXO11	F-box only protein 11

FITC	Fluorescein isothiocyanate
GAPDH	Glyceraldehyde 3-phosphate dehydrogenase
GPI	Glycosyl-phosphatidylinositol
GSK3	Glycogen synthase 3
GST	Glutathione-S-Transferase
h	Hour(s)
HERC2	HECT and RLD domain containing probable E3-ubiquitin ligase
HMW	High molecular weight
IAP	Inhibitor of apoptosis
ICD	Intracellular domain
Ig	Immunoglobulin
IKK	I κ B kinase
JNK	Jun N-terminal kinase
LC-MS/MS	Liquid chromatography tandem mass spectrometry
Lpr	Lymphoproliferative
Lsm2	Sm-like protein
MAPK	Mitogen activated protein kinase
MARCKS	Myristoylated alanine-rich C-kinase substrate
MFI	Mean fluorescence intensity
Min	Minute(s)
MOMP	Mitochondrial outer membrane permeabilisation
NEMO	NF κ B essential modulator
NF κ B	Nuclear factor- κ -B
NSCLC	Non-small cell lung cancer
Nup62	Nuclear pore protein 62
OMM	Outer mitochondrial membrane
OPG	Osteoprotegerin
ORP	Oxysterol binding protein related protein
OSBP	Oxysterol binding protein
P20D2	Peptidase M20 domain-containing protein 2

PARP	Poly-ADP ribose polymerase
PBS	Phosphate-buffered saline
PE	Phycoerythrin
PI3K	Phosphatidylinositol 3-kinase
PKC	Protein kinase C
PLAD	Pre-ligand assembly domain
PMA	Phorbol 12-myristate 13-acetate
PP2A	Protein phosphatase 2A
Ppil1	Peptidyl-prolyl cis-trans isomerase-like 1
PS	Phosphatidylserine
PTP	Protein tyrosine phosphatase
Rbmx1-1	RNA-binding motif X-linked 1
RING	Really interesting new gene
RIPK1	Receptor-interacting protein kinase 1
RNA	Ribonucleic acid
SDG	Sucrose density gradient
SDS	Sodium dodecyl sulphate
SDS-PAGE	Sodium dodecyl sulphate-polyacrylamide gel electrophoresis
siRNA	short interfering RNA
Skp1	S-phase associated protein kinase 1
SLIRP	Stem-loop interacting RNA binding protein
SNAP-23	Synaptosomal associated protein 23
SPOTS	Signalling protein oligomerisation structures
SRP	Signal recognition particle
SRPK1	Serine/arginine-rich protein-specific kinase 1
TANK	TRAF family member-associated NFκB activator
tBid	Truncated Bid
TBS-T	Tris-buffered saline with Tween 20
TfR1	Transferrin receptor 1
THD	TNF Homology Domain
TNF	Tumour necrosis factor

TNFR	Tumour necrosis factor receptor
TNFR1	TNF receptor 1
TNFR2	TNF receptor 2
TRADD	TNFR1 associated death domain protein
TRAF	TNF receptor associated factor
TRAIL	TNF-related apoptosis-inducing factor
TRAIL-R1	TRAIL receptor 1
TRAIL-R2	TRAIL receptor 2
TRAIL-R3	TRAIL receptor 3
TRAIL-R4	TRAIL receptor 4
US	Unstimulated
V	Volt
VAMP	Vesicle associated protein
v-FLIP	Viral FLIP
Vh	Volt hour(s)
WT	Wildtype
XIAP	X-linked inhibitor of apoptosis

Chapter 1: Introduction

Chapter 1: Introduction

1.1: Cancer

Cancer is one of the leading causes of morbidity worldwide (WHO, 2014). In 2012 there were estimated to be over 14 million incidences of cancer and 8.2 million cancer-related deaths. These numbers are only expected to rise, with 22 million new global incidences of cancer per year predicted to occur within the next two decades (Ferlay et al., 2015).

Cancer describes diseases resulting from the uncontrolled division of abnormal cells which become malignant and invade other sites in the body (Hanahan and Weinberg, 2011). Although grouped under the term “cancer”, over 100 different cancers have been observed which vary significantly due to the different cells from which they originate (Hanahan and Weinberg, 2000). All cancers however share the same property of growth independent of the control under which most healthy cells are constrained. This independency from control occurs by the progressive uptake of genetic alterations which transform healthy, normal cells into highly malignant derivatives (Hanahan and Weinberg, 2000). Hanahan and Weinberg published two key papers highlighting the regulatory circuits which must be disrupted in order for a cell to gain malignancy, termed the “Hallmarks of Cancer” (Hanahan and Weinberg, 2011, 2000). These hallmarks include the ability of a cell to achieve replicative immortality, proliferate without requiring growth signals, tolerate genomic instability and metastasise to other sites.

Perhaps most importantly, cancerous cells must also be able to evade the mechanisms which kill damaged cells (Hanahan and Weinberg, 2000). One important mechanism is the detection of damaged DNA. Checkpoints exist inside each cell which prevent proliferation if damaged DNA is detected. If the damage is not resolved, the cell is then directed to die by a controlled process termed apoptosis (Whibley et al., 2009). It is this DNA damage response which is exploited by conventional radiotherapy and chemotherapies. Here cancer cells are particularly sensitive as they are rapidly dividing and hence must overcome the DNA damage checkpoints more frequently (Hanahan and Weinberg, 2000). However, this targeting of rapidly dividing cells is not only

specific to malignancies; hair and myeloid precursor cells are also rapidly dividing and hence cause the common chemotherapy side effects of hair loss and myelotoxicity (Daniel and Crawford, 2006; Yeager and Olsen, 2011). Effective treatment by conventional chemotherapy requires that cancerous cells still have a functioning DNA damage response and therefore mutations in DNA damage components can lead to resistance. For example, p53 plays a major role in maintaining genome integrity, but is mutated in more than 50% of cancers and can result in poorer treatment outcome (Whibley et al., 2009).

More recent treatments are designed to target pathways which are more active in malignant cells (Reviewed in Hanahan & Weinberg, 2011). These newer treatments promise to reduce the severity of side effects by specifically targeting cancerous cells but not normal cells. Therapies that are able to induce apoptosis in cancers are particularly attractive as these can potentially lead to tumour regression and not just disease stasis (Reviewed in Amarante-Mendes & Griffith, 2015; Davids & Letai, 2012). Of particular promise are therapeutics based upon the death ligand TNF-related apoptosis-inducing ligand (TRAIL), which has been shown to specifically induce apoptotic cell death in cancer cells (Pitti et al., 1996; Wiley et al., 1995).

1.2: Apoptosis

1.2.1: Function and Morphology

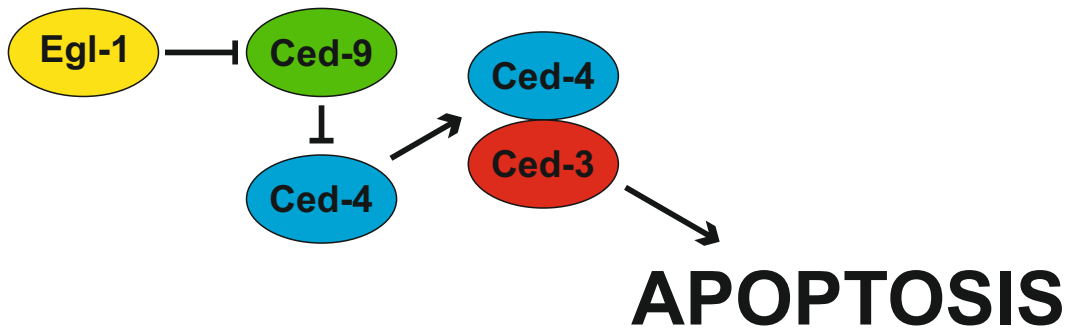
Apoptosis is derived from a Greek word to describe leaves or petals falling from a tree or flower (Kerr et al., 1972). In a biological context, it is a form of programmed cell death in which damaged, infected or superfluous cells are removed in a controlled and regulated manner. The morphology of apoptotic cells was first described by Kerr, Wylie and Currie in 1972 (Kerr et al., 1972). Cells undergoing apoptosis shrink and their nuclei condense as components of the cytoskeleton and nuclear envelope are broken down (Kerr et al., 1972). Genomic DNA is cleaved to produce internucleosomal fragments of 180 base pairs (bp) or multiples of. DNA fragmentation can be observed as “ladders” when separated by gel electrophoresis and is characteristic of apoptosis (Enari et al., 1998). As the cell shrinks, small sections of the membrane are released in a process known as “blebbing”. The cell then breaks down into multiple vesicles,

called apoptotic bodies (Kerr et al., 1972). In healthy cells, the phospholipid composition of the plasma membrane is maintained asymmetrically, such that phosphatidylserine (PS) is only present on the intracellular side. As a cell commits to apoptosis, PS is externalised by the action of a caspase-activated scramblase (Suzuki et al., 2013). Externalised PS is recognised by macrophages and other cells and serves as an “eat me” signal (Fadok et al., 2000). Apoptotic bodies are phagocytosed and removed by macrophages and neighbouring cells (Fadok et al., 2000). The apoptotic process is therefore almost entirely self-contained and hence does not mediate an inflammatory response (Reviewed in VanHook, 2014). This is in stark contrast to necrosis, a form of cell death which occurs in response to cellular damage. During necrosis, cells and organelles swell resulting in loss of plasma membrane integrity, cell lysis and the leakage of intracellular components triggering profound inflammation (Reviewed in Rock and Kono, 2008).

1.2.2: Genetic Basis for Apoptosis

In studies using *Caenorhabditis Elegans* nematodes, apoptosis was discovered to be mediated by a genetically controlled cell death programme (Ellis and Horvitz, 1986). Specific cell death genes (CED) were discovered in *C. Elegans* and subsequently shown to have homologs in mammals (Figure 1.1). Nematode embryonic development requires the regulated removal of precisely 131 cells by apoptosis (Ellis and Horvitz, 1986). However, when CED-3 and CED-4 gene expression is ablated these cells do not die (Ellis and Horvitz, 1986). In addition, alteration of the CED-9 gene to provide a gain of function mutation also results in the survival of these 131 cells (Hengartner et al., 1992). These cells are removed when CED-9 is modified with loss of function mutations, but a greater number of cells also die, resulting in embryonic lethality (Hengartner et al., 1992). Further studies demonstrate that it is the product of the CED-3 gene (Ced-3) which is actually responsible for carrying out the apoptotic response (Xue et al., 1996). Ced-3 is a cysteine protease which cleaves target proteins and is homologous to caspase-3 protein found in mammalian cells (Xue et al., 1996). Ced-4 is required for the activation of Ced-3 by oligomerising and recruiting Ced-3 monomers (Yang et al., 1998). In this regard, Ced-4 is analogous to the role Apaf-1 plays in recruiting and activating caspase-9 in the apoptosome (Yang et al., 1998).

C. Elegans



Mammals

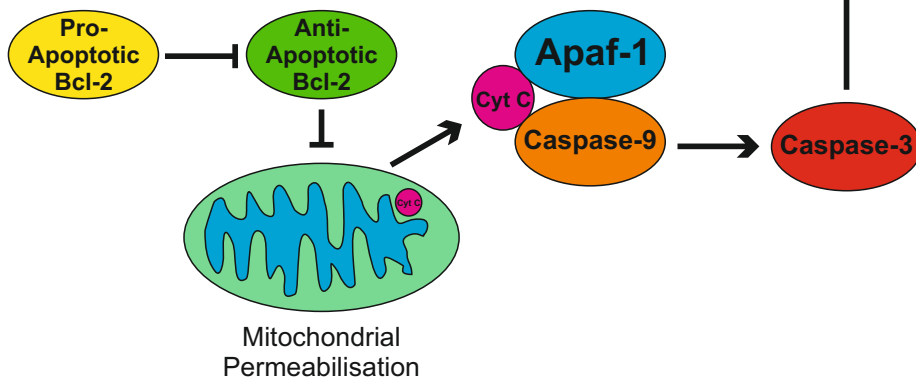


Figure 1.1: Apoptosis Controlling Genes in *C.Elegans* and their Mammalian Homologues

Genetic studies of *C.Elegans* revealed four proteins with important roles in regulating apoptosis induction. Further studies then revealed structurally similar homologues in mammals. In *C.Elegans* Egl-1 inhibits the activation of CED-9. CED-9 itself binds and prevents the activation of CED-4. Egl-1 and CED-9 are homologues of the mammalian pro-apoptotic and anti-apoptotic BCL2 family proteins respectively. CED-4 binds with and controls the activation of CED-3. In mammals, Apaf-1 plays a similar role in the activation of caspase-9 following complex formation after cytochrome C (Cyt C) has been released from the mitochondria. Ced-3 is the *C.Elegans* caspase which induces apoptosis through the cleavage of target proteins. The most similar mammalian caspase to CED-3 is the executioner caspase, caspase-3 which has a comparable role in apoptosis induction.

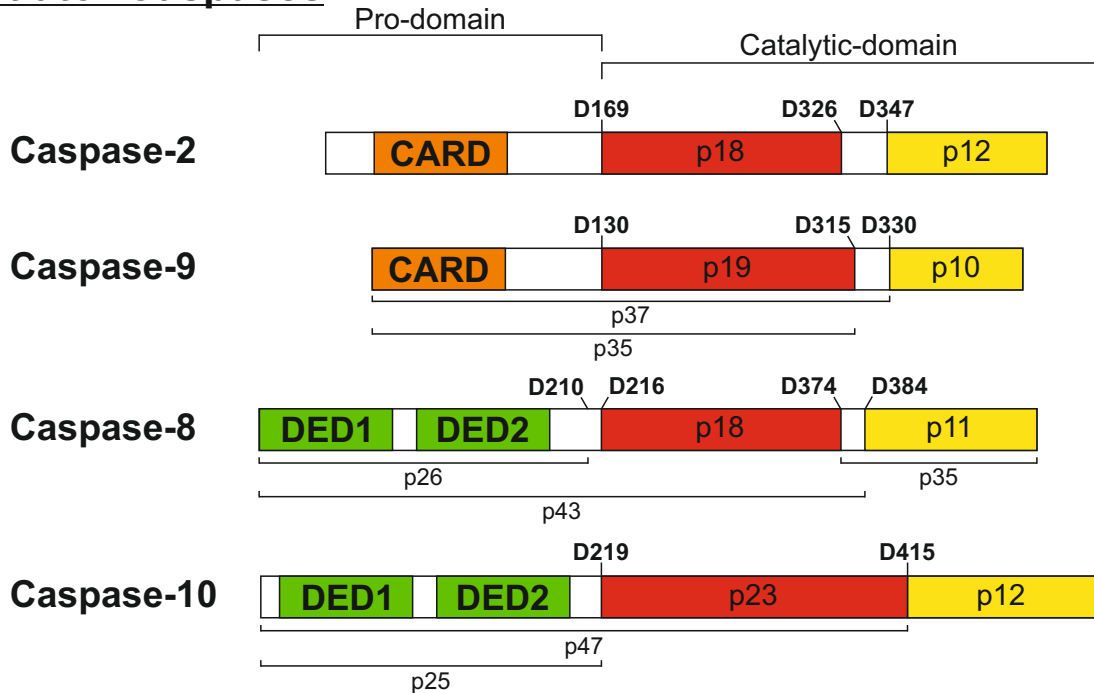
Analysis of the CED-9 gene reveals similarity with the BCL-2 family of genes in mammals, which control cell death. In nematodes, Ced-9 sequesters Ced-4 at the mitochondria and prevents its interaction with and subsequent activation of Ced-3 (Spector et al., 1997). Another gene demonstrated to control apoptosis induction is Egl-1. Loss of Egl-1 function also results in the survival of the 131 cells that normally die during development. Egl-1 contains a BCL-2 homology-3 (BH3) domain which interacts with Ced-9, preventing its interaction with and inhibition of Ced-4 (Conradt and Horvitz, 1998). In this regard, Egl-1 function is analogous to the BH3-only proteins found in mammalian cells (Lutz, 2000).

1.3: Caspases

Apoptosis is a conserved mechanism in almost all nucleated cells and is triggered in response to nutrient depletion, intracellular stress or by extracellular signals through specific death-inducing ligands (Reviewed in Ashkenazi and Salvesen, 2014). The effector molecules which carry out apoptosis are cysteine-dependent aspartate specific proteases (caspases), which function by cleaving target proteins at aspartate containing sites (Thornberry and Lazebnik, 1998).

Humans encode the genes for 11 caspases, although a further three have been observed in other mammals (Cohen, 1997). Caspases can be classified as either apoptotic inducers or non-apoptotic/inflammatory mediators. Caspases-2,-3,-6,-7, -8, -9 and 10 are implicated in the induction of apoptosis, whilst caspases -1, -4 and -5 are involved in inflammation (Reviewed in Labbé and Saleh, 2008; Pop and Salvesen, 2009). The only caspase which does not have roles in cell death is caspase-14, which mediates keratinocyte differentiation (Denecker et al., 2007). Although designated as inflammatory, caspases -1, -4 and -5 have also been shown to induce a form of inflammatory cell death through a process known as pyroptosis (Labbé and Saleh, 2008). Apoptotic caspases (Figure 1.2) can be defined as either initiator caspases (e.g. caspases-2, -8, -9 and -10) or executioner caspases (e.g. caspases-3, -6 and -7) (Reviewed in Cohen, 1997; Pop and Salvesen, 2009). Apoptosis is executed by the “caspase cascade”, in which activated initiator caspases cleave specific sites on executioner caspases resulting in their catalytic activation (Hirata et al., 1998; Slee et al., 1999). The activated executioner caspases induce apoptosis by the targeted

Initiator Caspases



Executioner Caspases

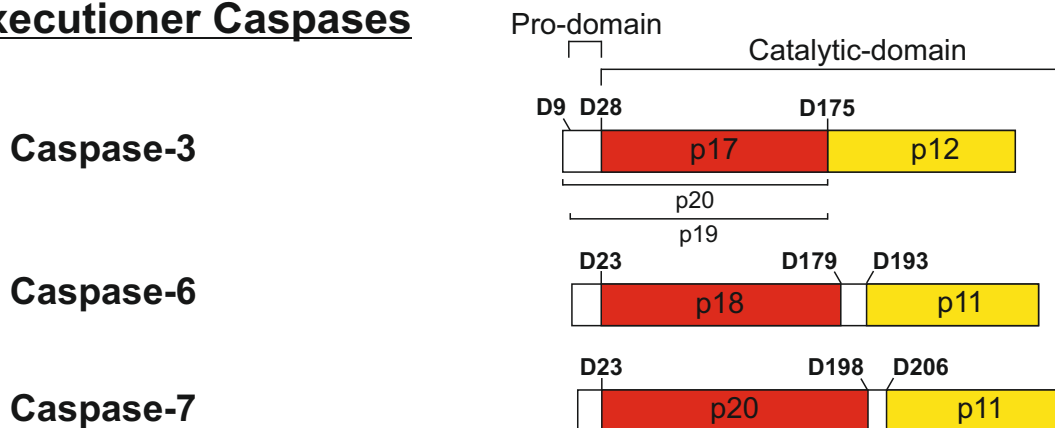


Figure 1.2: Human Apoptotic Caspases

Caspases are cysteine dependent aspartate proteases which all have a similar structure composed of an N-terminal pro domain and C-terminal catalytic domain. The pro domain of the initiator caspases contain either a caspase recruitment domain (CARD) or death effector domains (DED) which enable them to be recruited to activation complexes. The catalytic domain is composed of a large subunit of approximately 20 kDa (red box) which contains the catalytic active site, and a small subunit of approximately 10 kDa (yellow box). Caspases are themselves cleaved after aspartate residues (D) to separate the catalytic domains and to remove the pro domain. Caspase-9 is cleaved after D330 to generate a 37 kDa fragment (p37), or cleaved after D315 to generate a 35 kDa fragment (p35). Caspase-9 can also potentially be cleaved after D130, but this is not usually observed. Cleavage of caspase-8 at D374 generates a 43 kDa fragment (p43) and a 12 kDa fragment (p12). The caspase-8 pro-domain can also be removed by cleavage at D210/D216, leaving a 26 kDa fragment (p26). Caspase-10 is cleaved at D415 to generate the 47 kDa (p47) and 12 kDa (p12) catalytic subunits. The pro domain is also removed by cleavage at D219 to produce 25 kDa fragment (p25). The executioner caspases have much smaller pro-domains which are also cleaved by maturation events. Caspase-3 is initially cleaved at D175 to separate the 20 kDa (p20) and 12 kDa (p12) catalytic domains, resulting in caspase-3 activation. The pro-domain is cleaved at D9 and D29 to produce the 19 kDa (p19) and 17 kDa (p17) mature caspase-3 fragments. Sequence and domain information was acquired from the Uniprot database (www.uniprot.com) and corresponds to the canonical sequence. Accession numbers were: caspase-2: P42575-1, caspase-9: P55211-1, caspase-8: Q14790-1, caspase-10: Q92851-1, caspase-3: P42574-1, caspase-6: P55212-1, caspase-7: P55210-1. Cleavage information was taken from (Cohen, 1997).

cleavage and degradation of hundreds of structurally or functionally important proteins within the cell (Reviewed in Cohen, 1997; Pop and Salvesen, 2009). For example, caspase-3 cleaves the inhibitor of caspase activated DNase (ICAD) which inhibits the endonuclease, CAD. CAD is then able to cleave genomic DNA, generating the characteristic apoptotic nucleosomal fragments (Nagata et al., 1998).

All caspases are synthesised as single chain inactive zymogens (procaspases) which contain an N-terminal pro-domain and a C-terminal catalytic domain (Cohen, 1997; Earnshaw et al., 1999; Pop and Salvesen, 2009). Whilst initiator procaspases remain monomeric, executioner procaspases quickly assemble into inactive homodimers (Pop and Salvesen, 2009). The pro-domain of initiator procaspases is longer (approximately 100 amino acids) than executioner procaspases (less than 30 amino acids) and contains domains which enable their recruitment to activation complexes (Pop and Salvesen, 2009; Riedl and Shi, 2004). Procaspases-2, and -9 contain a single caspase activation and recruitment domain (CARD) which can interact with other CARD containing proteins (Acehan et al., 2002; Kersse et al., 2007). For instance, procaspase-9 is recruited into the apoptosome through homotypic CARD interactions with the adaptor protein Apaf-1 (Cain et al., 2000; Rodriguez and Lazebnik, 1999). Procaspases-8 and -10 contain tandem death effector domains (DED), which enable their recruitment into the death-inducing signalling complex (DISC) by homotypic DED interactions with the adaptor protein FADD (Boldin et al., 1995; Dickens et al., 2012a; Kischkel et al., 1995). The catalytic domain of caspases contains a large subunit (approximately 20 kDa), and a small subunit (approximately 10 kDa) (Reviewed in Pop and Salvesen, 2009; Walker et al., 1994; Wilson et al., 1994). The large subunit contains the catalytic cysteine and histidine residues which provide the proteolytic activity of caspases (Wilson et al., 1994). The small subunit contains several residues which are essential for the formation of the substrate binding groove (Blanchard et al., 1999; Walker et al., 1994). An unstructured flexible region links the two catalytic domains, which in executioner procaspases restrains the enzyme in an inactive conformation (Chai et al., 2001; Reviewed in Pop and Salvesen, 2009). The activity of executioner caspases is initiated by cleavage of the flexible linker by activated initiator caspases (Fuentes-Prior and Salvesen, 2004). Crystal structures of caspase-7 reveal

that cleavage of the linker allows re-arrangement of mobile loops in the catalytic domain, resulting in the formation of the active site (Chai et al., 2001; Riedl et al., 2001). The flexible linker region of initiator procaspases however is longer than in executioner procaspases and hence does not constrain the enzyme active site (Keller et al., 2009; Stennicke et al., 1999). Consequently, executioner caspases require proteolytic cleavage for activation whereas, initiator caspases undergo conformational changes that are induced by oligomerisation in order to be activated (Boatright et al., 2003; Chang et al., 2003; Reviewed in Pop and Salvesen, 2009; Shi, 2004; Shiozaki and Shi, 2004). Initiator caspase oligomerisation is induced after recruitment into an activation complex via their respective pro-domains (CARD or DEDs). The two main apoptosis-inducing signalling platforms are the apoptosome (Reviewed in Cain et al., 2002, 2000; Li et al., 1997; Zou, 1999) and the death-inducing signalling complex (DISC) (Boldin et al., 1996, 1995; Kischkel et al., 1995; Lavrik et al., 2003; Medema et al., 1997; Muzio et al., 1996), which are formed following activation of the intrinsic or extrinsic apoptotic pathways respectively. The intrinsic pathway is controlled by the actions of the BCL-2 family and is activated in response to intracellular stresses such as DNA damage or nutrient deprivation (Reviewed in Tait and Green, 2013). The extrinsic pathway is triggered following the extracellular binding of death ligands (Reviewed in Dickens et al., 2012b).

Following activation, caspases are also subject to proteolytic cleavage by other caspases or by self-processing, which are known as maturation events (Reviewed in Pop and Salvesen, 2009). Involving the removal of pro-domains and linker regions, these maturation events are not required for the initial activation of the caspases, but can impact upon their activity. The linker regions of caspases-8, -9 and -10 are severed by adjacent monomers after activation (Hughes et al., 2009; Keller et al., 2009). In addition, the activated initiator caspases are released from their activation platforms by removal of their pro-domains. The maturation of caspase-8 has been linked to increased activity, as cell death is not achieved when the cleavage events do not occur, despite initial caspase-8 activation (Hughes et al., 2009; Kang et al., 2008). The release of initiator caspases from their activation platforms has been suggested to prolong their activity in the cytosol (Martin et al., 1998; Pop et al., 2007). However, it

has also been suggested that caspase-8 is most active whilst complexed in the DISC and its release functions to turn off caspase-8 activity (Hughes et al., 2009; Lavrik et al., 2003). Caspase-9 matures either by self-processing of its pro-domain or via caspase-3 mediated cleavage of an adjacent site (Riedl and Shi, 2004). The caspase-3-mediated maturation has been shown to enable the inhibitor of apoptosis (IAP) protein, XIAP, to then inhibit caspase-9 activity (Srinivasula et al., 2001).

As caspases can be activated by proteolysis, an irreversible reaction, their activity is tightly regulated by several mechanisms. XIAP can selectively inhibit caspase-9, via its baculovirus inhibitor of apoptosis protein repeat-3 (BIR3) domain (Stennicke et al., 2002), or caspases-3 and -7 via its BIR2 domain (Chai et al., 2001; Srinivasula et al., 2001). Viruses have also been shown to produce proteins with caspase inhibiting properties. The cytokine response modifier A (CrmA) protein produced by the cowpox virus, and p35/p49 from baculoviruses, can non-specifically inhibit caspases by direct interaction (Stennicke et al., 2002). Along with many other proteins in the cell, caspases are also degraded by the proteasome. It has been observed that active caspases are more rapidly degraded than their inactive counterparts (Tawa et al., 2004), suggesting specific mechanisms to terminate activity. The inhibitors of apoptosis (IAP), including XIAP, contain RING domains in addition to their BIR domains and hence are able to target caspases for proteasome degradation by the addition of ubiquitin chains (Blankenship et al., 2009; Gyrd-Hansen et al., 2008).

1.4: Intrinsic Apoptosis

Activation of the intrinsic apoptotic pathway is controlled by members of the CED-9/BCL-2 gene family which are characterised by the presence of a single or multiple BCL-2 homology (BH) domain(s) (Reed et al., 1996). The BH3-only proteins: BAD, BID, BIK, BMF, PUMA and NOXA contain only a single BH3 domain and are mostly pro-apoptotic (Lutz, 2000). The remaining BCL-2 family members contain three or four BH domains and act to induce or inhibit apoptosis, respectively (reviewed by Chipuk et al., 2010). The pro-apoptotic members are BAX, BAK and BOK, which are counteracted by the pro-survival members: BCL-2, BCL-XL, BCL-W, A1 and MCL-1 (Chipuk et al., 2010). Whether a cell undergoes apoptosis or is maintained in a healthy state depends upon the balance and interplay between the pro-survival and pro-apoptotic BCL-2 family

members. Cellular stresses such as nutrient deprivation, DNA damage or viral infection effect the relative levels of the BCL-2 family members and tip the balance towards apoptosis (Chipuk et al., 2010). The most renowned regulator of intrinsic apoptosis in cancer cells is p53. Detection of damaged DNA leads to the activation of p53, which induces transcription of the BH3-only proteins NOXA and PUMA (Whibley et al., 2009). BH3-only proteins can induce apoptosis by activating BAX and BAK, either by directly interacting or through the sequestration of the pro-survival proteins BCL-2 or BCL-XL (Reviewed in Tait and Green, 2010). Activated BAX and BAK form homo-oligomers in the mitochondrial outer membrane, although BAX initially requires translocation to the mitochondria (Westphal et al., 2011). BAX or BAK oligomerisation induces the formation of pores which lead to mitochondrial outer membrane permeabilisation (MOMP) (Reviewed in Tait and Green, 2010). MOMP results in the release of several mitochondrial proteins, including the pro-apoptotic proteins cytochrome c and Smac (aka DIABLO). Apaf-1 is a large (130kDa) protein containing WD40 repeats, NB-ARC and CARD domains. Prior to apoptosis, Apaf-1 is maintained in a monomeric, inhibited state bound by dATP (Li et al., 1997). Following mitochondrial permeabilisation, the released cytochrome c is able to bind to the WD40 repeats of Apaf-1, causing conformational changes which release the WD40 lock on APAF-1 and hydrolyses ATP. The hydrolysed ADP is then exchanged for ATP and the Apaf-1, cytochrome c monomers combine to form a large seven-membered ring structure called the apoptosome. The apoptosome then recruits procaspase-9 via interactions between the caspase recruitment domains (CARD) of Apaf-1 and procaspase-9 (Reviewed in Cain et al. 2002). Recruitment of procaspase-9 to the apoptosome induces its activation, either by proximity induced dimerization of adjacent pro-caspase-9 monomers or by direct conformational changes induced by apoptosome binding (Chang et al., 2003; Pop et al., 2006). The activated caspase-9 subsequently cleaves and activates the executioner caspases-3 and -7, which induce apoptosis by cleaving downstream targets (described in Section 1.3). X-linked inhibitor of apoptosis (XIAP) inhibits caspases-3, -7 and -9. However, Smac, also released from the mitochondria during MOMP, sequesters XIAP and thereby facilitates apoptosis (Srinivasula et al., 2001).

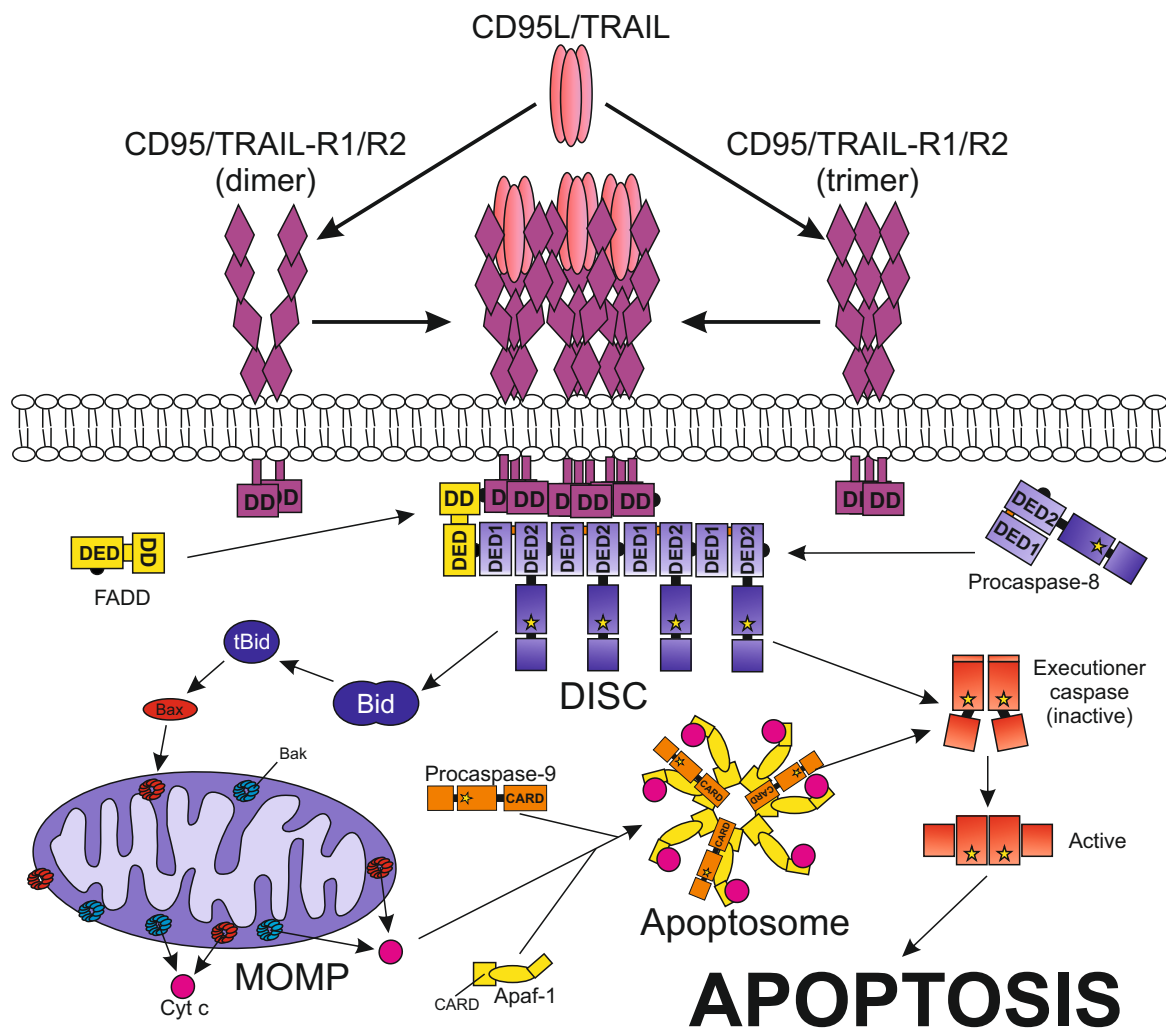


Figure 1.3: Apoptosis-Induced by the Extrinsic Pathway

Death ligands (membrane bound or soluble) bind to pre-formed death receptor dimers or trimers. The receptor-ligand structures then aggregate and recruit adaptor proteins (e.g. FADD) via death domain interactions. Procaspase-8 is recruited to FADD, causing its subsequent dimerization and activation and forming the death-inducing signalling complex (DISC). Activated caspase-8 can cleave executioner caspases (e.g. caspase-3), causing structural rearrangements resulting in their activation. In type I cells, the pool of activated executioner caspases is sufficient to drive the cell into apoptosis by the cleavage of target proteins. However, in type II cells, engagement of the intrinsic pathway is required for apoptosis induction. DISC activated caspase-8 can also cleave the BCL-2 family protein, Bid. Truncation of Bid (tBid), enables it to interact with Bax, which subsequently translocates to the mitochondria. Bax then self-associates to form pores, which lead to mitochondrial outer membrane permeabilisation (MOMP). Cytochrome C (Cyt C) is then released from the mitochondria where it interacts with the cytosolic adaptor protein Apaf-1 and caspase-9 to form the apoptosome. Caspase-9 activated in the apoptosome can then cleave executioner caspases and amplify the apoptotic signal.

1.5: Extrinsic Apoptosis

Whereas the intrinsic apoptotic pathway is stimulated by the sensing of intracellular stresses, the extrinsic pathway is initiated entirely by the propagation of extracellularly-derived signals. These initial signals are produced by the binding of members of the tumour necrosis family (TNF) of cytokines to their cognate death receptors (Reviewed in Guicciardi and Gores, 2009a), displayed in Figure 1.3. Death receptors are characterised by their intracellular death domains (DD), which once the receptors have been activated by ligation, can recruit DD-containing proteins via homotypic interactions (Boldin et al., 1995; Itoh and Nagata, 1993). Activation of TNF Receptor 1 (TNFR1) by TNF α results in the recruitment of TNFR1 associated death domain protein (TRADD) (Hsu et al., 1995). Conversely, activation of the TRAIL death receptors, TRAIL-R1 and TRAIL-R2, by TRAIL or CD95 (aka Fas) by CD95L results in the recruitment of Fas-associated protein with death domain (FADD) (Chaudhary et al., 1997; Dickens et al., 2012a; Kischkel et al., 1995; Medema et al., 1997). TRADD and FADD are adaptor proteins and contain both a death domain and a death effector domain (DED). The function of these adaptor proteins is to recruit the initiator procaspases-8 and -10 through homotypic interactions between the DEDs (Dickens et al., 2012a; Schleich et al., 2012). Once recruited, procaspase-8 (and -10) are activated by proximity-induced dimerization as described earlier (Section 1.3). In certain cells (termed Type I cells), activated caspase-8 can then trigger the induction of apoptosis by directly cleaving execution caspases-3 and -7 in sufficient quantity to commit the cell to die (Ozören and El-Deiry, 2002; Scaffidi et al., 1999, 1998). However, in type II cells, caspase-8 activation alone is insufficient to activate the required amount of caspase-3 (Ozören and El-Deiry, 2002; Scaffidi et al., 1999, 1998). Apoptosis in these cells is induced by cross-talk between the extrinsic and intrinsic pathways. Another target of activated caspase-8 is the pro-apoptotic BCL-2 family member BID, which is cleaved to produce a truncated form (tBID) (Li et al., 1998). Once generated, tBID activates BAX, inducing its translocation to the mitochondria (Reviewed in Shamas-Din et al., 2013). BAX then forms pores in the outer mitochondrial membrane, leading to MOMP (Reviewed in Tait and Green, 2010). The apoptosome is formed by released cytochrome c leading to the activation of caspase-9 and subsequent activation of

caspases-3 and-7 (as described in Sections 1.3 and 1.4). This apoptosome mediated executioner caspase activation amplifies the signal produced by caspase-8 and commits the cell to enter apoptosis. Overexpression of anti-apoptotic BCL-2 family members blocks the intrinsic pathway and therefore prevents apoptosis induced by the extrinsic pathway in Type II, but not Type I cells (Scaffidi et al., 1999).

1.6: Death Ligands and their Cognate Death Receptors

The tumour necrosis family (TNF) is made up of 19 ligands and 29 receptors and propagate signals involved in inflammation, apoptosis, proliferation and invasion (Reviewed in Aggarwal et al., 2012). All TNF family receptors are trimeric, type I transmembrane proteins which contain single or multiple cysteine-rich extracellular domains. Although they share these aspects, the primary extracellular structure of each receptor is varied enough such that they display specificity for their individual ligands (Bodmer et al., 2002; Naismith and Sprang, 1998). Ligands of the TNF family are characterised by the presence of an extracellular TNF-homology domain (THD) which promotes the formation of homo-trimers (Reviewed in Bodmer et al., 2002; Bremer, 2013). These ligands are synthesised as type II trans-membrane proteins, but can be released into the bloodstream by the action of extracellular metalloproteases (Bremer, 2013). A subset of TNF receptors are known as death receptors, due to their ability to transduce apoptotic signals through an intracellular death domain. The best characterised of these death receptors are: TNF receptor 1 (TNFR1), which is ligated by TNF α ; CD95, which binds CD95 ligand (CD95L); and TRAIL-R1 and -R2 which bind TRAIL (Reviewed in Micheau et al., 2013). The receptors which bind to TNF α , CD95L and TRAIL are shown in Figure 1.4.

1.6.1: TNF α : TNFR1

Tumour necrosis factor- α (TNF α) was first described in 1975 as an endotoxin-inducible molecule that is capable of inducing-necrotic cell death of cancer cells *in vitro* (Carswell et al., 1975). TNF α is synthesised as a 26 kDa transmembrane protein which undergoes cleavage to generate a 17 kDa trimeric soluble cytokine (Eck and Sprang, 1989). It is produced by immune cells such as natural killer cells, T cells and monocytes/macrophages as well as non-immune cells such as fibroblasts

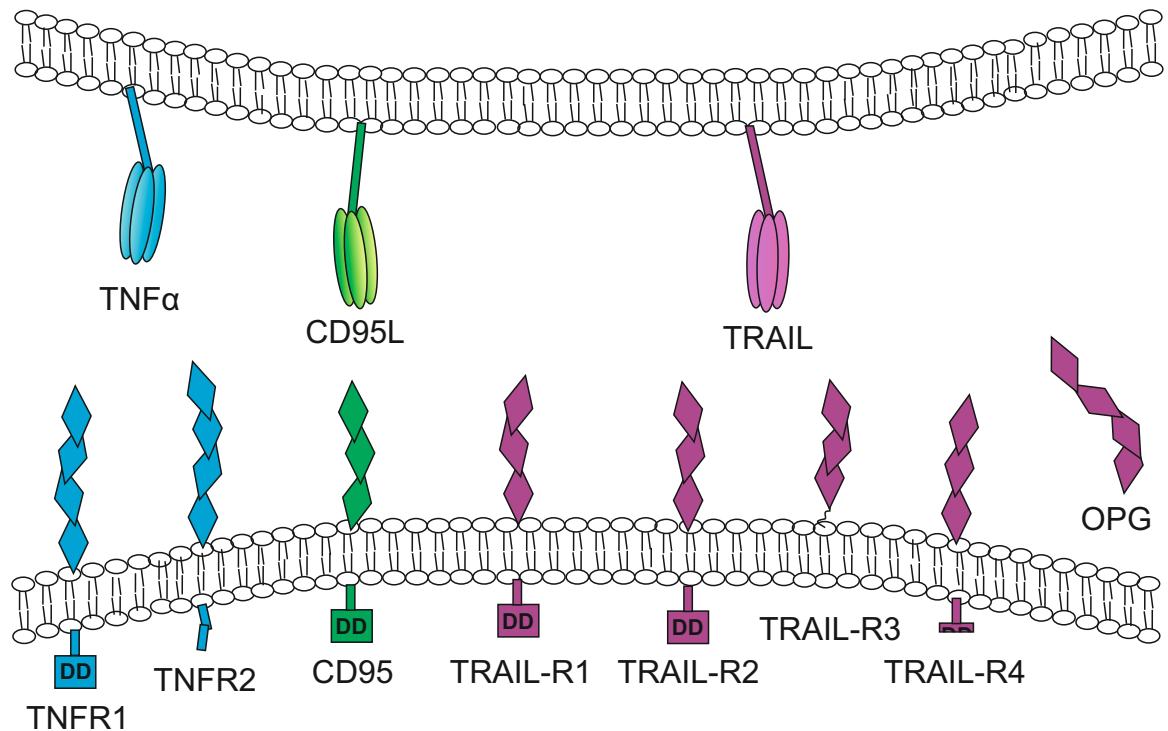


Figure 1.4: Receptors of the Death Ligands: TNF α , CD95L and TRAIL

The death ligands TNF α , CD95L and TRAIL are all synthesised as type II membrane proteins, but can be cleaved by extracellular metalloproteases to generate soluble ligands. The TNF family receptors for these ligands all contain extracellular cysteine rich domains (CRD) (represented by diamonds). TNF α can bind to two receptors, TNF receptor 1 (TNFR1) and TNFR2 (shown in blue). TNFR1 is the only TNF α death receptor as it contains an intracellular death domain (DD). CD95L binds to its only death receptor, CD95 (green). TRAIL has two death receptors, TRAIL-R1 and TRAIL-R2 (purple). TRAIL can also bind to TRAIL-R3 (purple), which lacks membrane or intracellular domains and is anchored to the membrane via a glycosphosphatidylinositol (GPI) linkage. TRAIL-R4 (purple) also binds TRAIL but is not a death receptor as it only contains a truncated death domain. Osteoprotegerin (OPG) (purple) is a soluble receptor which can bind TRAIL with low affinity.

(Reviewed in Mahmood and Shukla, 2010). TNF α can bind to two receptors, TNFR1 and TNFR2 which are both type I transmembrane proteins (Cabal-Hierro and Lazo, 2012). Whereas TNFR1 is expressed constitutively on most cell types, TNFR2 is only expressed at low levels on cells of the immune system (Choi et al., 2005). Only TNFR1 is capable of transmitting apoptotic signals, as TNFR2 does not contain an intracellular death domain (Reviewed in Cabal-Hierro and Lazo, 2012).

Interest in TNF α increased when it was observed that it could induce tumour cell death both *in vitro* and *in vivo* (Carswell et al., 1975; Wajant et al., 2003). Clinical trials were therefore conducted to determine the effectiveness of TNF α treatment as a cancer therapeutic (reviewed by Aggarwal et al., 2012). Phase I trials showed dose-dependent side effects which included fevers, hypotension, tachycardia and other symptoms of systemic inflammatory response syndrome. These side effects outweighed any potential preliminary indications of tumour cytotoxicity (Reviewed in Micheau et al., 2013). This inflammatory phenotype was explained by further study into how the TNF α signal is propagated. Although TNFR1 contains a death domain, the initial signalling complex formed (Complex I) primarily activates pro-inflammatory and immune stimulatory pathways including JNK, P-38 and NF κ B (Harper et al., 2003b; Micheau and Tschopp, 2003). Ligation of TNFR1 causes receptor aggregation, activation and the recruitment of TRADD via death domain interactions (Harper et al., 2003b; Hsu et al., 1995). Once recruited, TRADD subsequently recruits TNF receptor associated factor 2 (TRAF2), receptor interacting protein kinase 1 (RIPK1) and the cellular inhibitors of apoptosis (cIAP) 1 and 2, forming TNFR1 "Complex I" (Micheau and Tschopp, 2003). TRAF2 interacts with mitogen activated protein kinases (MAPK), leading to the activation of c-Jun N-terminal kinase (JNK) and P-38 (Lee et al., 1997, 2004). TRAF2 and cIAP1/2 also catalyse the addition of ubiquitin chains to RIPK1, resulting in the recruitment of the NF κ B essential modulator (NEMO) (Micheau and Tschopp, 2003). As a component of the I κ B kinase (IKK) complex, NEMO regulates the phosphorylation of the IKK complex, leading to its ubiquitination and subsequent degradation (Israël, 2010). IKK complex degradation releases NF κ B, which can then translocate to the nucleus and regulate the transcription of target genes (Wang et al., 1998).

It is only when TNFR1 complex 1 dissociates that apoptotic signalling by TNF α can be observed. Apoptosis is activated by the formation of initiator caspase-containing secondary complexes. TNFR1 complex IIA can either be cytoplasmic (Harper et al., 2003b; Micheau and Tschopp, 2003) or membrane-associated (Schneider-Brachert et al., 2004) and is initiated by the dissociation of RIPK1 and TRAF2 from TRADD. TRADD, either remains associated with TNFR1 at the membrane or after being released, recruits FADD which subsequently recruits and activates procaspase-8 (Hsu et al., 1996b, 1995; Micheau and Tschopp, 2003). Activated caspase-8 can then cleave executioner caspases and induce apoptosis (As described in Section 1.3). The inactive caspase-8 homologue cellular FLICE inhibitory protein long isoform (cFLIP_L), which is induced by NF κ B activation, can bind to complex IIA and inhibit caspase-8 activation (Reviewed in Dickens et al., 2012b). Complex IIB is independent of TRADD and forms when cells are treated with both TNF α and Smac Mimetics, which inhibit IAPs (Varfolomeev et al., 2008). This complex requires the deubiquitination of RIPK1 by the ubiquitinase CYLD (Wang et al., 2008). RIPK1 is subsequently released, where it can bind FADD, resulting in procaspase-8 recruitment, activation and apoptosis induction as for complex IIA (Wang et al., 2008). Therefore, although TNF α alone is not a suitable cancer therapeutic, there is promise in utilising TNF α in combination with smac mimetics to induce tumour cell death (Reviewed in Aggarwal et al., 2012).

1.6.2: CD95L : CD95

CD95 (aka Fas) is another TNF family receptor with the capacity to induce apoptosis in cancer cells. CD95 is ubiquitously expressed in the human body, although particularly high expression is found in the thymus, liver, heart and kidneys (Nagata, 1997). CD95 is bound and activated by its only ligand, CD95L (aka FasL) (Rieger et al., 1998). CD95L is predominantly expressed on activated immune cells, such as T lymphocytes and natural killer cells, but also on “immune privilege sites” such as the testis and eyes (Reviewed in Peter et al., 2015).

CD95L has been demonstrated to have important apoptotic roles in maintaining cell homeostasis and deleting autoreactive T-cells (Krammer, 2000; Nagata, 1997). In mice, mutations resulting in defective CD95 or CD95L are the cause of a lymphoproliferative (lpr) phenotype, causing lymphadenopathy, systemic lumps and erythematosus-like

autoimmune disease (Adachi et al., 1995; Karray et al., 2004; Senju et al., 1996; Takahashi et al., 1994; Watanabe-Fukunaga et al., 1992). In humans, autoimmune lymphoproliferative syndrome (ALPS), which is characterised by defective lymphocyte apoptosis, lymphocyte accumulation, and humoral autoimmunity, is the result of dominant negative mutations in CD95 (Type 1A ALPS) or CD95L (Type 1B ALPS) (Bidère et al., 2006). CD95L is also thought to be important for eliminating virus-infected or transformed cells via membrane-bound CD95L on CD8⁺ cytotoxic T lymphocytes and CD4⁺ effector T cells (Kägi et al., 1994; Kojima et al., 1994; Lowin et al., 1994; Rouvier et al., 1993). In addition, CD95L has non-apoptotic roles, which include: stimulating liver regeneration after damage (or partial removal for transplant) and the outgrowth of neurites (Desbarats et al., 2003; Desbarats and Newell, 2000).

In contrast to TNF α , the primary signalling outcome of CD95L signalling is apoptosis induction (Scaffidi et al., 1998). CD95L binds to CD95, causing activation and allowing the recruitment of the adaptor protein, FADD. FADD then recruits, dimerises and activates procaspase-8 (Kischkel et al., 1995; Medema et al., 1997), which induces apoptosis by activating downstream executioner caspases directly or via amplification by intrinsic pathway activation (Scaffidi et al., 1998).

Due to its ability to induce apoptosis, and apparent natural role in the body in removing cancerous cells, soluble CD95L was trialled as a cancer therapeutic (Reviewed in Peter et al., 2015). However, it soon became apparent that most tumour cells are resistant to even high doses of soluble CD95L (Algeciras-Schimnich et al., 2003). The use of CD95L as a cancer therapeutic was also severely hampered by the fact that CD95L treatment causes massive induction of apoptosis in hepatocytes, leading to liver failure (Ogasawara et al., 1993). In addition, CD95L treatment has actually been shown to stimulate the proliferation of tumour cells which are resistant to its apoptotic signalling (reviewed by Peter et al., 2015). In these cells, it was shown that CD95L treatment triggers the activation of non-apoptotic kinase pathways such as NF κ B and MAPK pathways (Barnhart et al., 2004; Legembre et al., 2004a, 2004b). The activation of these pathways were also shown to increase tumour motility and invasion (Barnhart et al., 2004).

CD95L expression has actually been shown to be induced when cancer cells (but not normal cells) are treated with CD95L (O'Connell et al., 1996). This expression has been described as a method of tumour "counterattack" against the immune system (Igney et al., 2000). As most immune cells themselves are sensitive to CD95L-induced apoptosis, it is thought that tumour-expressed CD95L may dampen any immune response (O'Connell et al., 1996). Although this model is not completely accepted, it has also been shown that tumour-associated epithelium (but not normal epithelium) expresses large amounts of CD95L and may also play roles in this tumour "counterattack" (Mutz et al., 2014). Also, CD95/CD95L has actually been shown to be essential for cancer cell survival. When CD95 and CD95L expression is eliminated, cancer cells die by a process known as death-induced by cancer cell elimination (DICE) (Hadji et al., 2014). This death appears to be mostly necrotic, although it also demonstrates some signs of apoptosis. The reason as to why cancer cells may require CD95/CD95L expression, is that this has been proposed as a fail-safe mechanism to ensure that transformed cells can be killed by circulating immune cells (Hadji et al., 2014).

Although immune cells have been shown to utilise CD95L to eliminate transformed cells, the role of CD95 in preventing tumour growth is still contradictory. Due to this unclear role and its severe hepatotoxic side effects, CD95L cannot be used as a cancer therapeutic (Peter et al., 2015).

1.6.3: TRAIL : TRAIL-R1 and TRAIL-R2

Analysis of proteins which share sequence homology with the extracellular domains of TNF α and CD95L led to the discovery of TRAIL by two independent groups (Pitti et al., 1996; Wiley et al., 1995). TRAIL is synthesised as a 281 amino acid type II transmembrane protein, which can be processed by extracellular proteases to produce a soluble ligand (Kim et al., 2004). Unlike TNF α and CD95L, TRAIL is ubiquitously expressed in most tissues and haematopoietic cells (Yagita et al., 2004). Human TRAIL also shows considerable conservation in mice with 65% sequence identity, enabling the two species to cross-react with the opposing TRAIL receptor(s) (Schaefer et al., 2007). Whilst TRAIL $-/-$ mice are both viable and healthy, they do

suffer from defects in both the innate and adaptive immune systems (Diehl et al. 2004; Schaefer et al. 2007).

The discovery of TRAIL generated much excitement when studies showed that TRAIL could selectively induce apoptosis in cancer cells (Ashkenazi et al., 1999; Walczak et al., 1999). Soluble TRAIL treatment has been demonstrated to effectively kill cancer-derived cell lines and also has potent tumouricidal activity *in vivo*, without being toxic to normal cells (Ashkenazi et al., 1999; Walczak et al., 1999). Stimulation of TRAIL expression on immune cells by interferon (IFN) treatment also provides anti-tumour activity (Kayagaki et al., 1999) and neutrophils are able to release large concentrations of TRAIL from intracellular granule stores following certain stimuli (Tecchio et al., 2004). TRAIL-deficient mice display increased tumour growth (Cretney et al., 2002; Finnberg et al., 2008; Zerafa et al., 2005) and enhanced metastasis (Cretney et al., 2002; Grosse-Wilde and Kemp, 2008). Taken together, these experiments point to a role for TRAIL in tumour immuno-surveillance.

TRAIL induces its apoptotic effects through the activation of two death domain (DD) containing receptors; TRAIL-R1 and TRAIL-R2 are type I transmembrane proteins which share 58% sequence identity (MacFarlane et al., 1997; Pan et al., 1997b). Like TNFR1 and CD95, they contain extracellular cysteine rich domains, and an intracellular DD (MacFarlane et al., 1997; Pan et al., 1997b). The tissue distribution of TRAIL-R1 and TRAIL-R2 is broad, with both being expressed in most normal cells (Pan et al., 1997b; Walczak et al., 1999), although humans and chimpanzees are the only species which express two TRAIL death receptors, for reasons that are not yet clear (van Roosmalen et al., 2014). For example, mice only contain one TRAIL receptor capable of inducing apoptosis, which is equally homologous to both human TRAIL-R1 and TRAIL-R2 (Wu et al., 1999). TRAIL-induced apoptosis can be achieved by the activation of the TRAIL receptors individually, or TRAIL-R1 and TRAIL-R2 can co-operate via the formation of hetero-complexes (Lemke et al., 2010; Schneider et al., 1997). TRAIL-R2 activation has been shown to require a greater amount of cross-linking than TRAIL-R1, indicating that it is preferentially activated by membrane-bound rather than soluble TRAIL (Mühlenbeck et al., 2000). Once the TRAIL receptors have been ligated, aggregated and activated, they recruit FADD via their death domains in a similar process to that

described for CD95 (Reviewed in Dickens et al., 2012a). FADD recruits and activates procaspase-8, which then activates executioner caspases directly, or through engagement of the intrinsic pathway (Ozören and El-Deiry, 2002). However, TRAIL also appears to be able to induce the activation of non-apoptotic signalling pathways such as NF κ B, MAPKs and protein kinase C (PKC) (Azijli et al., 2013; MacFarlane et al., 2002). These pathways in turn can lead to the activation of survival, proliferation and invasion promoting genes (Secchiero et al., 2003; Varfolomeev et al., 2005).

In addition to TRAIL-R1 and TRAIL-R2, humans also express three other receptors capable of binding to TRAIL. TRAIL-R3 contains the extracellular TRAIL-binding domain, but lacks an intracellular or transmembrane domain (Degli-Esposti et al., 1997b; MacFarlane et al., 1997; Mérino et al., 2006; Sheikh et al., 1999). Instead, TRAIL-R3 is anchored to the surface of the cell via a glycosyl-phosphatidylinositol linkage. The tissue distribution of TRAIL-R3 is much less ubiquitous than TRAIL-R1 and -R2 with mRNA only being detected in the heart, kidney, liver, lung placenta and spleen (Degli-Esposti et al., 1997b; Pan et al., 1997a). Due to the lack of any intracellular domain, TRAIL-R3 functions to inhibit TRAIL signalling by sequestering available ligand (Mérino et al., 2006). TRAIL-R4 is similar in structure to TRAIL-R1 and TRAIL-R2, and is expressed in mostly the same tissues (Degli-Esposti et al., 1997a; Marsters et al., 1997). However, TRAIL-R4 is unable to signal to apoptosis due to a truncated intracellular domain in which 52 of the 76 amino acids composing the death domain are missing (MacFarlane et al., 2002; Marsters et al., 1997). TRAIL-R4 can however in some contexts activate the NF κ B pathway and is therefore thought to contribute to TRAIL-resistance by both sequestering TRAIL and by activating NF κ B, which can induce the expression of anti-apoptotic proteins (Degli-Esposti et al., 1997a; Mérino et al., 2006). The fifth TRAIL receptor is osteoprotegerin (OPG), which binds TRAIL with low affinity. OPG is unlike the other TRAIL receptors in that it is a secreted protein and functions solely by sequestering extracellular TRAIL (Emery et al., 1998).

A number of TRAIL-based therapeutics are currently being developed and investigated in clinical trials, including soluble recombinant TRAIL and agonistic antibodies targeting either TRAIL-R1 or TRAIL-R2. Dulanermin is a recombinantly-produced untagged form of soluble human TRAIL, which has been tested in phase I and II clinical

trials (Reviewed by Amarante-Mendes and Griffith, 2015). All of the clinical studies have shown that Dulanermin is well tolerated by patients and most of the studies showed partial responses or stable disease across a wide range of cancer types. However, Dulanermin was judged to have poor clinical efficacy, as it was not able to generate complete responses. Explanations for the poor responses to Dulanermin treatment, included a short half-life of the ligand in the bloodstream, and potential inhibition by the binding of the non-apoptotic TRAIL receptors (TRAIL-R3, -R4 and OPG) (Reviewed in Amarante-Mendes and Griffith, 2015). Agonistic TRAIL antibodies however have been demonstrated to have a much-longer *in vivo* half-life (days compared to hours for soluble TRAIL) and can selectively bind only one TRAIL receptor (Duiker et al., 2006). This selectivity also raises another question, whether to target TRAIL-R1 or TRAIL-R2 in order to induce apoptosis. Although initially thought that most cancers were more sensitive to TRAIL-R2 induced apoptosis, it has since been shown that certain cancers, including leukemias (Li et al., 2006; MacFarlane et al., 2005; MacFarlane et al., 2002; Natoni et al., 2007) and some pancreatic adenocarcinomas (Lemke et al., 2010), are preferentially killed by TRAIL-R1 activation. Knowledge of the contribution of TRAIL-R1 or TRAIL-R2 to TRAIL-induced apoptosis in specific cancer cells is therefore critical to selecting the correct treatment. TRAIL-R2 is targeted by: Conatumamab, Drozitumab, Lexatumumab and Tigatuzumab, whereas TRAIL-R1 is targeted by Mapatumumab (Reviewed by Amarante-Mendes and Griffith, 2015). The downside to using agonistic antibodies, is that due to their bivalent nature they are unable to sufficiently engage receptor trimers (Thorburn et al., 2008). These antibodies therefore require cross-linking, which *in vivo* is achieved by binding of Fc receptor bearing immune cells (Haynes et al., 2010). The results of phase I and II therapeutic antibody trials are similar to those observed for Dulanermin, with antibodies being well tolerated with no adverse events but being unable to generate significant responses (Amarante-Mendes and Griffith, 2015). Cross-linking or the use of protein tags to increase TRAIL aggregation increases apoptotic activity, but also increases the risk of toxicity to normal, non-transformed cells (Mühlenbeck et al., 2000). Indeed, early concerns of TRAIL-mediated liver toxicity (Jo et al., 2000) were shown to be due to higher order TRAIL complexes induced by cross-linking of FLAG tagged-TRAIL (Koschny et al., 2007). Promoting TRAIL trimerisation using leucine

zipper or isoleucine zipper motifs however has been shown to increase tumour killing activity without inducing cell death in normal cells (Han et al., 2016; Walczak et al., 1999).

To date, clinical trials have shown widespread resistance to TRAIL-based therapeutics, and quickly acquired resistance in cells which are initially sensitive (Reviewed in Amarante-Mendes and Griffith, 2015). In addition, resistant cells treated with TRAIL show the activation of non-apoptotic, pro-survival signalling pathways (Reviewed in Azijli et al., 2013). A consequence of these pathways being activated is that TRAIL treatment has been shown to drive tumour cell proliferation (Ehrhardt et al., 2003; von Karstedt et al., 2015), and increased tumour cell invasion and metastasis (Cretney et al., 2002; von Karstedt et al., 2015). Therefore, despite initial promise, TRAIL-based cancer therapeutics have not proved to be effective as a monotherapy. However, the pitfalls of TRAIL treatment are based around poor efficacy and not the severe side effects observed for TNF α or CD95L therapies (Reviewed in Pennarun et al., 2010). There is therefore still hope that understanding the mechanisms which regulate TRAIL signalling can lead to the generation of more active TRAIL therapeutics or combination therapies which overcome tumour resistance.

1.7: Death-inducing Signalling Complex (DISC) Formation

As described previously, the activation of the extrinsic apoptotic pathway is determined by death ligand-induced formation of a death-inducing signalling complex (DISC) and subsequent initiator caspase activation. The death receptors: TNFR1, CD95, TRAIL-R1 and TRAIL-R2 share structural similarity in the form of extracellular cysteine rich domains and an intracellular death domain (DD). Due to these structural similarities, it is likely that the mechanisms of ligation, receptor activation and complex formation are conserved between the death receptors. Understanding how these complexes form is therefore essential to determining how apoptosis is induced by death ligands.

1.7.1: Ligation of Death Receptors

The initial step in extrinsic pathway activation, is the binding of death ligands to their cognate receptors. It has long been observed that death ligands, which are trimeric

themselves, can bind to trimeric death receptors (Banner et al., 1993; Schlessinger, 1988). Originally, it was believed that the death receptors existed as monomers on the cell surface and that ligand binding resulted in receptor trimerisation and activation (Sessler et al., 2013). This proposal was based on the much better-characterised behaviour of receptor tyrosine kinases, which are dimerised and activated in response to ligand binding (Schlessinger, 1988). An early crystal structure of TNFR1 complexed to TNF β correlated with this view, revealing a 3:3 receptor-ligand assembly (Banner et al., 1993). However, this view changed when it was observed that death receptors actually exist as pre-ligand assembled receptor complexes (Siegel et al., 2000). It was shown that interactions between the first cysteine rich domain (CRD), which was later termed the pre-ligand assembly domain (PLAD), mediate the association of receptor monomers (Chan et al., 2000). The importance of these interactions was realised by the observation that mutations in the CD95 PLAD had also been shown to cause symptoms of ALPS in patients (Siegel et al., 2000). It had also been noticed that ALPS causing mutations in CD95 had a more dominant phenotype than expected. This is explained by the presence of pre-formed receptor complexes, as the incorporation of a single defective receptor can hamper ligand binding to the other associated receptors (Sessler et al., 2013). Similarly, pre-assembled receptor complexes have been observed for CD95, TNFR1, TRAIL-R1 and TRAIL-R2 (Chan, 2007; Siegel et al., 2000; Thomas et al., 2002).

Although it is accepted that death receptors exist as pre-assembled complexes, it is less clear whether these structures take the form of dimers or trimers. Cross-linking of the extracellular domains of TNFR1 was demonstrated to produce trimers (Naismith et al., 1996). However, crystal structures show the presence of dimers and surface plasmon resonance studies of TRAIL-R2 also observe pre-formed dimers (Lee et al., 2005). Using a TRAIL:TRAIL-R2 crystal structure, Wassenaar et al., (2008) performed molecular dynamic simulations of TRAIL-R2. They demonstrated that TRAIL-R2 has a strong tendency to self-associate and will rapidly form dimers. However, they also showed that a third TRAIL-R2 monomer can then be recruited to the dimer, although with low affinity, forming an asymmetric trimer. TRAIL binding induces a conformation change in the trimer, rearranging it into a symmetric form. Receptor pre-assembly

may be essential for rapid signalling, as the requirement for a ligand to find three neighbouring monomeric receptors would be eliminated. Pre-assembly could also be important for sorting different receptors which share the same ligand, such as TNFR1 and TNFR2 which both bind TNF α or TRAIL-R1 and TRAIL-R2, which both bind TRAIL (Sessler et al., 2013).

In addition to the formation of the ligand-receptor complex, activated death receptors have also been demonstrated to form higher-order clusters (Guicciardi and Gores, 2009b). The first evidence for these clusters came from observations that CD95L binding changes the, normally diffuse, membrane distribution of CD95 to form bead-like structures at one point on the cell surface, a process known as capping (Cifone et al., 1994). Plasma membrane receptor clustering has also been observed for TNFR1, TRAIL-R1 and TRAIL-R2 (Sessler et al., 2013). Several models have been proposed to explain how the aggregated clusters may form. Once ligand-receptor trimers have formed, inter-receptor interactions are then thought to drive the formation of a signalling network (Valley et al., 2012). These receptor interactions may take the form of dimers, forming a hexagonal mosaic of ligated receptors (Ozsoy et al., 2008) (Figure 1.5: top panel). Alternatively, trimer receptor interactions would lead to the formation of complexes showing tri-fold symmetry (Chan, 2007) (Figure 1.5: bottom panel). Valley *et al* (2012) showed that after TRAIL ligation, TRAIL-R2 forms stable dimers favouring the hexagonal mosaic model. Whilst both the long and short isoforms of TRAIL-R2 were shown to form dimers, the long isoforms were additionally stabilised by formation of a di-sulphide bond. The formation of receptor networks is thought to stabilise the activation and opening of the death domains and therefore increase formation of the DISC (Sessler et al., 2013).

1.7.2: Death Domain-mediated Recruitment of Adaptor Proteins

Once the death receptors have been activated, they recruit adaptor proteins via interactions between death domains (DD) present on both the receptor and adaptor protein (Dickens et al., 2012a). In the case of TRAIL and CD95L signalling, FADD is the adaptor protein recruited, whereas TRADD is recruited to TNFR1 (Chaudhary et al., 1997; Hsu et al., 1995; Kischkel et al., 1995). Analysis of the X-ray crystal structure of *Drosophila* Tube DD, complexed to the DD of the Pelle kinase, reveals specific

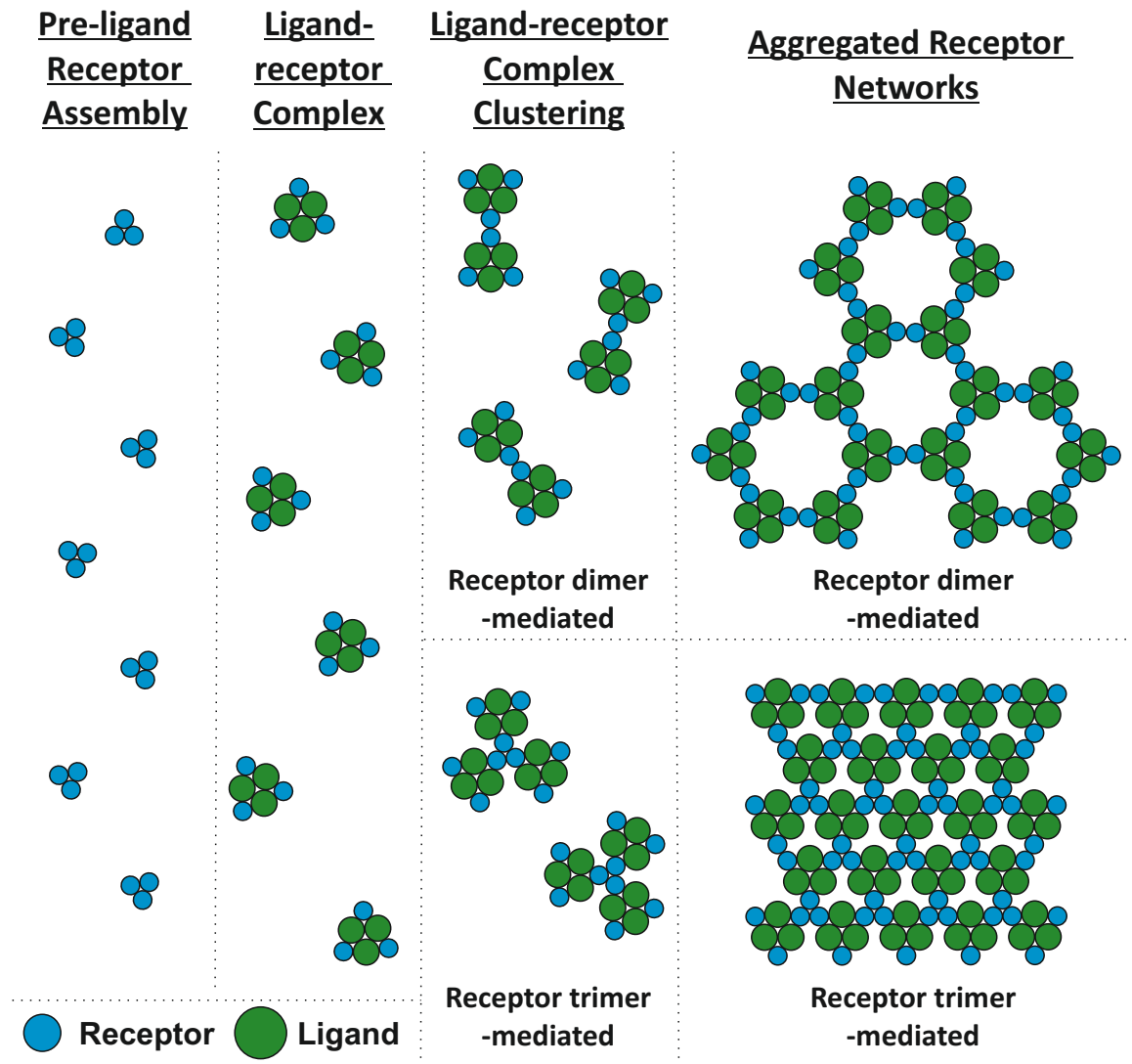


Figure 1.5: Models for Ligand-Induced Death Receptor Aggregation Complexes

Ligand binding to death receptors has been demonstrated to induce the formation of large aggregated receptor-ligand complexes. The formation of these complexes are likely produced by interactions between the ligand bound receptors. Models have therefore been produced of TRAIL-R2 aggregation based upon either dimeric or trimeric receptor interactions. Dimeric receptor interactions (top panel) lead to the formation of hexameric receptor-ligand networks. Whereas trimeric receptor interactions (bottom panel) lead to networks with tri-fold symmetry. Adapted from Valley et al., (2012).

interaction surfaces (Xiao et al., 1999). Comparison of the structure of FADD reveals that it interacts with CD95 (and presumably TRAIL-R1 and TRAIL-R2) or TRADD through a Tube-like interaction (Hill et al., 2004). TRADD however utilises a Pelle-like surface to engage with its receptor, TNFR1 or to FADD (Xiao et al., 1999). These differences in interaction surfaces used by FADD and TRADD explain how death receptors can recruit specific adaptor proteins (Sandu et al., 2005).

Exactly how adaptor proteins are recruited to the death receptors however is not fully understood and several models based on available structures have been proposed. A 2.7 Å crystal structure of CD95 and FADD DDs reveals interactions of dimeric units of CD95 and FADD with each unit composed of two CD95-DDs and two FADD-DDs (Scott et al., 2009). This structure also reveals conformational changes in the CD95-DD when compared to a non-FADD bound CD95-DD (Scott et al., 2009). The authors propose that CD95L binding induces conformational changes which open the CD95-DD. The helices $\alpha 5$ and $\alpha 6$ in the CD95-DD are shown to fuse to form the stem helix. The open conformation produced by formation of the stem helix exposes the $\alpha 1$ and $\alpha 2$ helices, of the CD95-DD, which enable hydrophobic interactions to form between adjacent CD95-DDs (Scott et al., 2009). It was proposed that in un-ligated receptors, the absence of these inter-CD95-DD interactions results in the CD95-DD flipping back to the more stable closed conformation (Scott et al., 2009). Superposition of the structure for full length FADD onto the FADD-DD in this model also reveals a conformational change in the FADD-DD. In the CD95-bound structure, the $\alpha 6$ helix in the FADD-DD adopts a new position to avoid a structural collision with the C-helix of CD95 (Scott et al., 2009). The $\alpha 6$ helix is located just upstream of a linker sequence between the FADD-DD and DED and its movement imposes a conformational change on the FADD-DED. This conformational change results in the opening and “activation” of the DED, which increases its ability to bind other DEDs, such as the ones present on procaspase-8 (Scott et al., 2009). This model elegantly describes how CD95L binding to CD95 can trigger a series of conformational changes which result in the activation of death receptors and complex formation. This model can also explain the reason for higher order complex formation, as adjacent CD95 receptors stabilise the active open conformation of the DD. However, the interaction sites between receptors and FADD

described in this model do not conform to ALPS mutation data and cannot explain why the known CD95-DD mutations lead to loss of CD95 function (Sessler et al., 2013).

Another structural model of CD95-FADD determined by electron microscopy describes a complex made up of a ring of five FADD-DDs layered onto a ring of five CD95-DDs (Wang et al., 2010). This complex is stabilised both by intra-ring interactions between the FADD or CD95-DDs and inter-ring interactions between the two ring structures (Wang et al., 2010). The benefit of this model, is that the majority of the CD95-DD ALPS causing mutations occur at the predicted interaction sites described (Sessler et al., 2013). This model does not however provide a mechanism for higher order receptor clustering but does provide a basis for recruitment of multiple caspase-8 monomers, which are required for their activation by proximity induced-dimerisation (Boatright et al., 2003; Hughes et al., 2009).

Although these models differ in their structure of the ligand-receptor complex, they all share a similar stoichiometry of one receptor to one molecule of FADD (Esposito et al., 2010; Scott et al., 2009; Wang et al., 2010). However, a caveat of these models is that they are all formed from structures containing truncated proteins and therefore may not reflect the true interactions of full length proteins (Scott et al., 2009; Wang et al., 2010). This is highlighted by a study by Dickens et al., (2012a) in which quantitative mass spectrometry was used to study the TRAIL DISC. Isolated active TRAIL DISCs were separated from unstimulated TRAIL receptors and shown to exist in large complexes, typically over 700 kDa in size. The isolated DISC displays a stoichiometry in which three times less FADD than TRAIL receptors is detected, disputing the earlier models (Dickens et al., 2012a). This increased level of receptors correlates with previous studies which show a requirement for higher order receptor clustering to achieve sufficient DISC activity (Mühlenbeck et al., 2000).

1.7.3: Death-Effector Domain-Mediated Recruitment of Initiator Caspases

Dickens et al., (2012a) also demonstrated an even greater discrepancy in the stoichiometry of procaspase-8 recruited to the DISC. This study from our laboratory showed that nine times more procaspase-8 than FADD is recruited to the DISC, which

diverges massively from the previously accepted view of each FADD molecule recruiting a single caspase-8 monomer (P Schneider et al., 1997). As no structures of the caspase-8 DEDs were available, a model was generated based upon the known structure of the homologous viral FLIP (MC159) (Yang et al., 2005). Whilst FADD only contains one DED, procaspase-8 contains tandem DEDs. The model produced by Dickens et al., (2012a) shows that procaspase-8 interacts with FADD via hydrophobic interactions between a conserved FL motif on the DED of FADD and a hydrophobic patch on DED1 of procaspase-8. This is consistent with previous studies which demonstrate that mutation of the FL motif in FADD abrogates procaspase-8 recruitment (Eberstadt et al., 1998). It was always unclear why caspase-8 (as well as caspase-10 and cFLIP) require the presence of two death effector domains (DED), when one would seem sufficient to mediate recruitment to FADD. Dickens et al., (2012a) argue that an FL motif conserved on DED2 of procaspase-8 is able to recruit a subsequent procaspase-8 monomer in a similar mechanism to that described for FADD. This mechanism also provides for the sequential addition of procaspase-8 monomers, enabling chains of procaspase-8 to be recruited to a single FADD molecule (Dickens et al., 2012a). This model correlates with another study which analysed CD95 DISC formation and which also postulated the formation of caspase-8 chains (Schleich et al., 2012). Not only does this “chain model” explain the abundance of procaspase-8 relative to FADD, but it also correlates with the observation that overexpression of procaspase-8 DEDs alone results in the formation of DED filaments (Dickens et al., 2012a; Siegel et al., 1998). These filaments are not observed when full length procaspase-8 is overexpressed, suggesting that the catalytic domain of caspase-8 prevents spontaneous chain formation (MacFarlane et al., 2000). The proposed model was validated by point mutations of the FL motifs of the DEDs procaspase-8. In an in vitro binding assay, (Dickens et al., 2012a) mutation of the procaspase-8 DED2 FL motif reduced procaspase-8 recruitment but did not completely abolish it (Dickens et al., 2012a). This is consistent with procaspase-8 being recruited to FADD via DED1 and subsequent procaspase-8 molecules being recruited via interactions between the DED2-FL motif of the bound monomer and the hydrophobic pocket of DED1 on the incoming procaspase-8 (Dickens et al., 2012a; Hughes et al., 2016).

1.7.4: DISC Internalisation

Once the DISC has been formed, there appear to be opposing requirements for the complex to be internalised in order for effective apoptotic signals to be transduced. After ligand binding, the CD95 DISC is internalised, forming CD95-containing receptosomes (Miaczynska et al., 2004). Although the CD95 DISC is initiated at the membrane, caspase-8 activation occurs mainly in the receptosomes (Lee et al., 2006). When clathrin-dependent endocytosis is blocked, internalisation does not occur and apoptotic signalling is blocked (Miaczynska et al., 2004). However, CD95L-induced activation of NF κ B and ERK can occur in the absence of internalisation (Lee et al., 2006). TRAIL-induced apoptosis however does not require internalisation of the DISC, and blockade of endocytosis enhances, rather than abrogates, apoptosis (Kohlhaas et al., 2007). Activation of the TRAIL DISC has actually been shown to induce cleavage of components of the endocytic machinery, leading to its shutdown (Kohlhaas et al., 2007).

1.8: TRAIL or CD95L-induced “Secondary Complex” Formation

It is becoming increasingly clear that TRAIL and CD95L can also induce the activation of non-canonical kinase pathways through the formation of a secondary complex (Azijli et al., 2013). This complex is thought to function in a similar way to Complex I formed by TNF α binding to TNFR1 (Hsu et al., 1996a). The structure and components of this secondary complex are however poorly understood. There have been reports that the membrane environment in which the DISC forms could influence the formation of the secondary complex (Song et al., 2007). It has also been reported that TRAIL receptors activated in lipid rafts form a fully active DISC and successfully signal to apoptosis (Ouyang et al., 2013). However, non-lipid raft associated TRAIL receptors were demonstrated to recruit mainly cFLIP and RIPK1, and instead transmit pro-survival signals (Ouyang et al., 2013).

Co-immunoprecipitation experiments have been used to determine which proteins are recruited to the secondary complex. In TRAIL treated cells, RIPK1, TRAF2, FADD and activated caspase-8 have been shown to interact (Varfolomeev et al., 2005). TRADD has also been shown to interact with the TRAIL receptors (Chaudhary et al.,

1997; P Schneider et al., 1997; Sheridan et al., 1997), and is proposed to increase secondary complex formation by decreasing FADD recruitment, thereby facilitating increased RIPK1 binding (Cao et al., 2011). Through this complex, it is believed that NFκB essential modulator (NEMO), also known as inhibitor of nuclear factor kappa-B kinase subunit gamma (IKKγ), is recruited (Varfolomeev et al., 2005). NEMO forms a complex with IKKα and IKKβ, which may also be recruited (Chaudhary et al., 1997; P Schneider et al., 1997; Sheridan et al., 1997), leading to phosphorylation, subsequent degradation and the release of NFκB. The degradation of IKKβ is essential for the activation of the classical NFκB pathway, enabling NFκB dimers composed of RelA and p50 subunits to translocate to the nucleus and regulate transcription of target genes (Delhase et al., 1999). An alternative NFκB pathway exists in which upstream NFκB-inducing kinase (NIK) activates an IKKα homodimer, which induces the phosphorylation and subsequent ubiquitination of the NFκB p100 subunit. This ubiquitination targets the inhibitory C-terminus for proteasomal degradation, producing p52 which can then regulate the transcription of target genes (Senftleben et al., 2001). To date, the activation of the alternative NFκB pathway by TRAIL has not been reported (Azijli et al., 2013).

The activation of the classical NFκB pathway was one of the first reported non-canonical signals shown to be induced by TRAIL (MacFarlane et al., 2002). Once released, NFκB translocates to the nucleus where it promotes the transcription of a large cohort of mostly pro-survival genes (Israël, 2010). These include: cFLIP, BCL-XL, MCL-1 and cIAPs, which may contribute to TRAIL resistance (Reviewed in Azijli et al., 2013). Conversely, expression of TRAIL-R1 and TRAIL-R2 can also be induced by NFκB activation (Azijli et al., 2013; Ravi et al., 2001) and explains why in some cases, activation of NFκB can enhance TRAIL-induced apoptosis (Ravi et al., 2001).

The activation of NFκB has been proposed as a major cause of the survival/proliferation signals triggered by TRAIL in TRAIL-resistant cancer cells (Zhang and Fang, 2005). However, formation of the TRAIL secondary complex has also been implicated in the activation of other kinase pathways, including: the JNK, p38 and ERK1/2 MAPKs, protein kinase C (PKC), phosphatidylinositide 3-kinase (PI3K) and Akt (protein kinase B, PKB) (reviewed by Azijli et al., 2013).

The activation of these kinase pathways by TRAIL has also been described in healthy tissues that are resistant to TRAIL-induced apoptosis. For example, TRAIL-induced Akt and ERK1/2 activation triggers proliferation in endothelial cells (Secchiero et al., 2003). TRAIL activated NF κ B, in addition to Akt and ERK1/2, has also been shown to stimulate the production of pro-inflammatory cytokines, TNF α , interleukin-1 β (IL-1 β) and interferon- γ (IFN- γ) (Reviewed in Azijli et al., 2013).

1.9: Regulation of TRAIL Signalling

The excitement surrounding the possible cancer-killing use of TRAIL has been dampened somewhat by the widespread inherent or acquired resistance of many cancers to TRAIL-induced apoptosis (Reviewed in Amarante-Mendes and Griffith, 2015). Added to this is the stimulatory effect of TRAIL on proliferation and metastasis observed in TRAIL-resistant cells (Cretney et al., 2002; Ehrhardt et al., 2003; von Karstedt et al., 2015). Therefore, if TRAIL is to be used as an effective cancer therapy the mechanisms which govern the sensitivity of cancer cells to TRAIL-induced apoptosis must be fully understood. In addition, through a greater knowledge of TRAIL signalling regulation, new targets can be assessed for co-treatments which will augment TRAIL killing of malignant cells (Reviewed in Abdulghani and El-Deiry, 2010). TRAIL signalling has been shown to be regulated at multiple levels, from the TRAIL receptors themselves to DISC formation as well as downstream caspase activation (Mahalingam et al., 2009).

1.9.1: Modulation of TRAIL Receptor Levels

Downregulation of TRAIL-R1 and TRAIL-R2 would seem an obvious mechanism to mediate resistance to TRAIL signalling. Indeed, TRAIL sensitivity has been shown to correlate with TRAIL-R1 (Ozören et al., 2000) and TRAIL-R2 (Mitsiades et al., 2001; Rieger et al., 1998; Zhang et al., 1999) expression. Loss of TRAIL-R1 and TRAIL-R2 was shown to contribute to TRAIL resistance in melanoma cells (Zhang et al., 1999). In addition, mutations in TRAIL-R1 and TRAIL-R2 are increased in metastatic breast cancer (Shin et al., 2001). TRAIL-R2, but not TRAIL-R1, expression can also be induced following DNA damage through p53-mediated upregulation of TRAIL-R2 (Burns et al., 2001; Wu et al., 2000, 1997). This means that DNA damaging agents can sensitise

cancer cells to TRAIL-induced apoptosis through the increase of TRAIL-R2 levels. TRAIL-decoy receptor (TRAIL-R3 and TRAIL-R4) levels inversely correlate with TRAIL sensitivity (Rieger et al., 1998). TRAIL-R3 prevents the assembly of the DISC by binding and sequestering TRAIL (Mérino et al., 2006), whereas TRAIL-R4 is co-recruited to the DISC with TRAIL-R2 and reduces caspase activation by reducing FADD binding (Mérino et al., 2006; Sheridan et al., 1997).

Sensitivity of cancer cells to TRAIL also correlates with the surface levels of TRAIL-R1 and TRAIL-R2 (Zhang et al., 1999). A number of different proteins have been shown to be able to regulate the surface levels of the TRAIL receptors. The signal recognition particle (SRP) is important for protein sorting and targets secretory and membrane proteins to the ER. SRP components, SRP54 and SRP72, were shown to regulate TRAIL-R1 surface levels. Downregulation of SRP54/SRP72 decreases the amount of TRAIL-R1 at the cell surface and confers resistance to TRAIL-R1-targeting monoclonal antibodies (Ren et al., 2004). SRP component modulation was not shown to effect TRAIL-R2 trafficking and therefore appears to be a TRAIL-R1-specific mechanism (Ren et al., 2004). A splice variant of the adaptor protein Arf GAP with Rho GAP domain, Ankyrin repeat and PH domain (ARAP1), has been shown to interact with the TRAIL-R1 DD, and at lower levels with the TRAIL-R2 DD. Loss of ARAP1 leads to a decrease in TRAIL-R1 surface levels and reduces TRAIL-induced apoptosis (Símová et al., 2008). Again, this mechanism appears specific to TRAIL-R1, suggesting that control of receptor trafficking to the cell surface may be a major regulatory method for TRAIL-R1, but not TRAIL-R2, signalling. Endoplasmic reticulum (ER) stress has also been demonstrated to induce the upregulation of TRAIL-R2 cell surface expression (Lu et al., 2014a; Yamaguchi and Wang, 2004). ER stress can be triggered by accumulation of unfolded proteins in the ER (unfolded protein response) (Lu et al., 2014a) or chemically, by treatment with thapsigargin, which inhibits the sarco/endoplasmic reticulum Ca^{2+} -ATPase (SERCA). Prolonged ER stress activates C/EBP homologous protein (CHOP), which mediates an increase in TRAIL-R2 expression (Lu et al., 2014a).

The protein levels of the TRAIL death receptors have also been shown to be controlled by ubiquitination. The proteasome inhibitor, PS-341, induces an increase in TRAIL-R2 and to a smaller extent, TRAIL-R1 protein levels. This is shown to be associated with

levels of TRAIL-R2 ubiquitination (Johnson et al., 2003). Ubiquitination can also directly regulate TRAIL-R1 surface expression levels, since the RING domain containing protein, MARCH-8, was shown to ubiquitinate TRAIL-R1. Overexpression of MARCH-8 results in increased TRAIL-R1 cell surface levels; conversely knockdown of MARCH-8 decreases the amount of TRAIL-R1 on the cell surface (van de Kooij et al., 2013).

1.9.2: TRAIL Receptor Aggregation

To form a fully-active DISC, the ligated TRAIL receptors must be further aggregated to form large signalling networks (Valley et al., 2012). Mechanisms which effect the ability of the TRAIL receptors to aggregate can therefore have a profound effect on TRAIL signalling.

In multiple cancers, the expression levels of GALNT14, a glycotransferase enzyme, correlates with TRAIL sensitivity. GALNT14 mediated O-glycosylation of TRAIL-R1/R2 is suggested to control TRAIL-induced receptor aggregation and therefore DISC recruitment. Sites on TRAIL-R2 have been identified as possible glycosylation sites (Wagner et al., 2007). S-palmitoylation involves the covalent attachment of palmitate to cysteine residues. Rossin et al., (2009) showed that TRAIL-R1 can be partially palmitoylated at a cysteine residue near the transmembrane domain. Overexpression studies, demonstrated that palmitoylation is required for TRAIL-R1/TRAIL-R2 hetero-oligomerisation, and homo-oligomerisation of TRAIL-R1. TRAIL-R1 palmitoylation is also required for constitutive localisation of TRAIL-R1 into lipid rafts (Rossin et al., 2009).

Lipid rafts are membrane micro-domains rich in cholesterol and sphingolipids which can function as signalling platforms for many receptors (Simons and Toomre, 2000). By preventing palmitoylation, with the palmitate analogue 13-oxypalmitate, or disrupting lipid rafts, by depleting cholesterol with cholesterol oxidase, TRAIL-R1 lipid raft localisation, DISC formation and TRAIL induced apoptosis are disrupted (Rossin et al., 2009). Lipid raft localisation provides a convenient mechanism to stabilise the aggregation of activated receptors. However, the role of lipid rafts in TRAIL signalling is disputed due to conflicting reports on the requirement for receptor-lipid raft localisation. Song et al., (2007) reported that in TRAIL-sensitive non-small cell lung

cancer (NSCLC) cells, DISC formation, driven by FADD and caspase-8 recruitment, occurs in lipid rafts. Conversely, in TRAIL-resistant NSCLC cells, TRAIL receptors are not localised into lipid rafts and DISC formation occurs in non-raft fractions. These non-raft “DISCs” are formed by the recruitment of RIPK1 and cFLIP, and induce the formation of non-apoptotic signalling pathways. Ouyang et al., (2013) reported that in a TRAIL-sensitive NSCLC cell line, ligand binding induces translocation of the TRAIL receptors into lipid rafts. The absence of lipid raft localisation of TRAIL receptors is described as being responsible for TRAIL resistance in a generated NSCLC (H460) cell line (Ouyang et al. 2013). Constitutive localisation of TRAIL-R1 to lipid rafts was shown by Marconi et al., (2013) who observed that TRAIL-R1 is bound to GM3, a glycosphingolipid component of lipid rafts, only in TRAIL-sensitive B cells. TRAIL-R2 however was not shown to be constitutively located to lipid rafts. Dickens *et al* (2012a) however demonstrated that TRAIL-R1/R2 are not localised to lipid rafts in BJAB cells, and that the TRAIL DISC forms in non-raft fractions. This is itself in contrast to a previous paper showing the lipid raft localised association of the TRAIL DISC in HeLa cells (Jin et al., 2009), leading to the hypothesis that DISC formation (and the requirement for lipid raft localisation) may be fundamentally different between cells of haematopoietic or epithelial lineage (Dickens et al. 2012a).

1.9.3: DISC-Interacting Proteins

A key event in TRAIL signalling is the recruitment of initiator caspases to the TRAIL receptors and the formation of an active DISC (Pennarun et al., 2010). Certain proteins have been described to regulate DISC formation and caspase activation by their recruitment into the DISC or via binding to the TRAIL receptors (Figure 1.6).

Cellular FLICE-inhibitory protein (cFLIP) is a catalytically-inactive homologue of caspase-8, which exists in the cell mainly as the three isoforms: long, short and raji (cFLIP_L, cFLIP_S, cFLIP_R respectively) (Rasper et al., 1998). The cFLIP_S and cFLIP_R isoforms contain two DED domains but then only a short carboxyl terminus sequence of amino acids. cFLIP_L however contains two DEDs and a longer carboxyl terminus sequence, containing caspase-like domains which are catalytically inactive (Yu et al. 2009). Overexpression of all cFLIP isoforms have been shown to be anti-apoptotic, as the cFLIP proteins compete with procaspase-8/10 for FADD binding (Bagnoli et al., 2010).

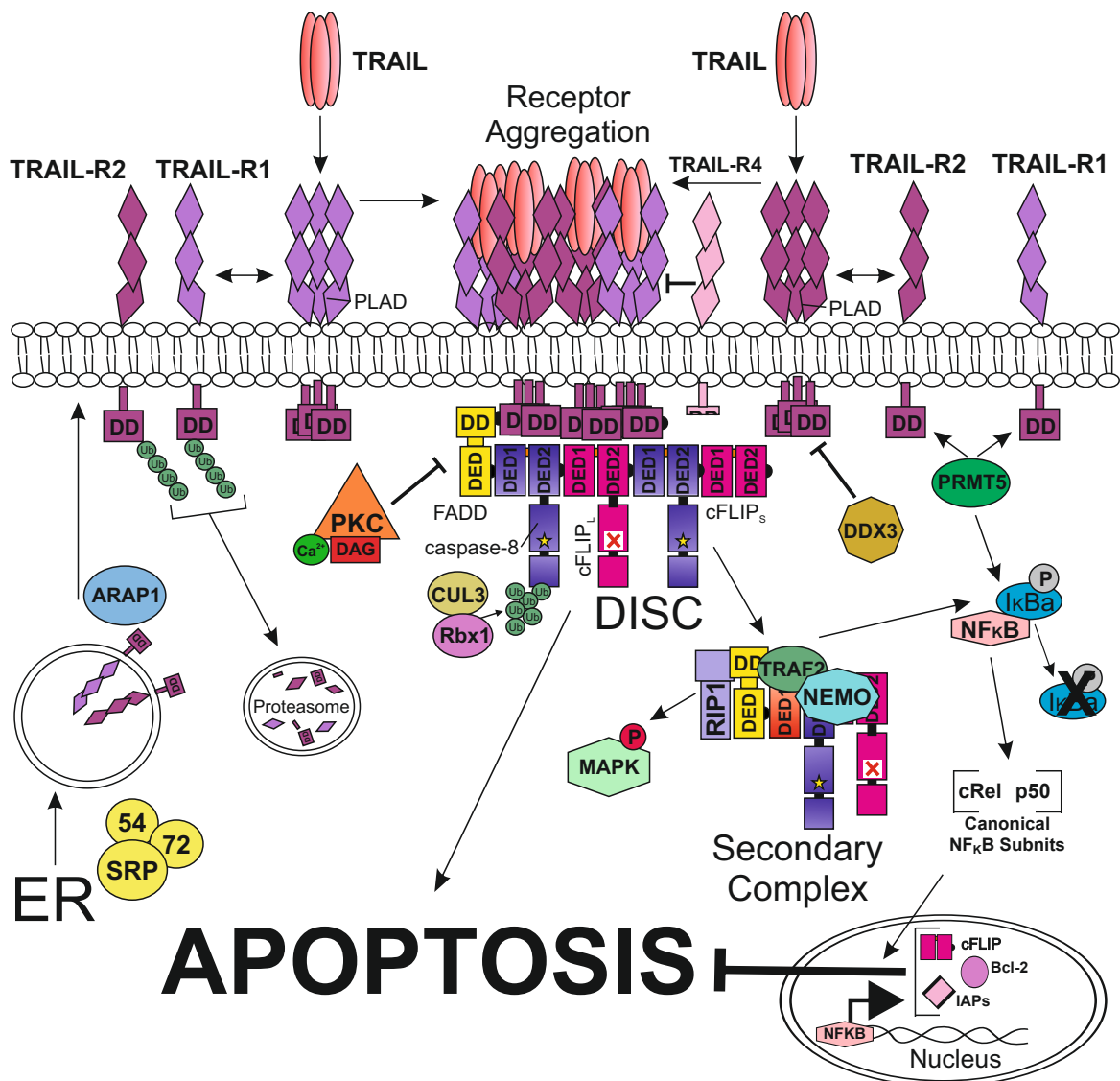


Figure 1.6: Regulation of TRAIL-Signalling by TRAIL-R1/R2 Protein Interactions

TRAIL signals to apoptosis through the ligation of its death receptors TRAIL-R1 and TRAIL-R2. Ligation of the two receptors causing their aggregation to large complexes which allow the recruitment of FADD by death domain (DD) interactions. FADD then recruits procaspase-8 by the formation of death effector domain (DED) filaments, forming the death-inducing signalling complex (DISC). DDX3 has been demonstrated to selectively inhibit TRAIL-R2 recruitment to the DISC. The caspase-8 homologue, cFLIP_L facilitates the formation of caspase-8 chains. However, cFLIP_S inhibits DISC formation by terminating filament formation. A CUL3/Rbx1 complex has been demonstrated to poly-ubiquitinate caspase-8, increasing its activity. Active caspase-8 induces apoptosis by activating downstream executioner caspases. However, the DISC has also been shown to form an intracellular secondary complex which through the recruitment of RIPK1, TRAF2, TRADD and NEMO can activate kinase pathways such as MAPKs and NFκB. PRMT5 has been demonstrated to bind to DDs of TRAIL-R1 and TRAIL-R2, inhibiting DISC formation and promoting canonical NFκB activation. TRAIL-R4 has also been shown to inhibit DISC formation by sequestering TRAIL and by inducing NFκB activation. PKC activation also inhibits FADD recruitment and DISC formation by currently unknown mechanisms. Controlling the surface levels of TRAIL-R1 and TRAIL-R2 also regulates TRAIL signalling. SRP components SRP54 and SRP72 have been shown to directly bind TRAIL-R1 and TRAIL-R2, and facilitate their sorting and release from the ER. ARAP1 has also been shown to aid the trafficking of TRAIL-R1 to the plasma membrane. TRAIL-R1 and TRAIL-R2 levels have been demonstrated to be recycled from the membrane and degraded by the proteasome.

However, at lower expression levels, cFLIP_L has been shown to contribute to the formation of DED oligomers at the DISC (Hughes et al., 2016). These DED oligomers, made up of recruited procaspase-8 and cFLIP, are essential for the activation of caspase-8 (Hughes et al., 2016). cFLIP is regulated both at the transcriptional and protein level. Activation of transcription factors such as NFκB, c-myc and p53 have been shown to induce cFLIP expression, whilst c-Fos and cJun repress cFLIP expression (Li et al., 2007). JNK-mediated activation of the ubiquitin E3-ligase ITCH results in decreased cFLIP levels by poly-ubiquitination and subsequent proteasome mediated degradation (Chang et al., 2006). The half-life of cFLIP can be increased by mTOR-induced activation of the de-ubiquitinase USP2, which removes the degradative poly-ubiquitination of cFLIP (Safa et al., 2008). Phosphorylation of cFLIP has also been observed, resulting in reduced affinity for FADD and the subsequent increase in procaspase-8 and procaspase-10 recruitment to the DISC (Higuchi et al., 2003).

Jin et al (2009) recently described a role for caspase-8 poly-ubiquitination at the DISC, which increases the activity of caspase-8. TRAIL stimulation induces DISC formation and translocation to lipid rafts where a CUL3-RBX1 complex induces the poly-ubiquitination of pro-caspase-8. The ubiquitin-binding protein p62 then binds the poly-ubiquitin chains and causes the recruitment of caspase-8 to ubiquitin rich foci, promoting cleavage and activation of caspase-8 (Jin et al., 2009). Also identified at the DISC by proteomic screening, was the de-ubiquitinase A20. Over-expression of A20 can ablate the CUL3-dependent increase in caspase-8 activation (Jin et al., 2009). In addition, TRAF2 was subsequently shown to bind to the poly-ubiquitinated caspase-8 (Jin et al., 2009). TRAF2 binding triggers the degradation of caspase-8 through the addition of K48-linked poly-ubiquitin chains. The effect of TRAF2 binding is described as an intrinsic shut-off timer for caspase-8 activation (Gonzalvez et al. 2012). This role of CUL3 in TRAIL signalling may be limited only to epithelial-derived cell lines, as it could not be detected in the TRAIL DISC isolated from haematopoietic cells (Dickens et al. 2012a).

Protein arginine methyltransferase 5 (PRMT5) was identified by proteomic screening to specifically interact with TRAIL-R1 and TRAIL-R2, but not TNFR1 or CD95 (Tanaka et al., 2009). Silencing of PRMT5 can sensitise various cancer cell lines to TRAIL-induced

apoptosis, but does not affect non-transformed cells. PRMT5 contributes to TRAIL-induced activation of IKK and therefore the NF κ B pathway, leading to increased expression of NF κ B target genes (Tanaka et al., 2009). The effect of knockdown of PRMT5 can be rescued by simultaneous expression of active IKK β , showcasing a role in NF κ B activation. The effect of PRMT5 was specific to TRAIL however, as silencing had no effect on TNF α mediated NF κ B activity (Tanaka et al., 2009).

The ATP-dependent RNA helicase, DDX3, has been shown to specifically bind to TRAIL-R2 and can inhibit TRAIL-induced apoptosis by blocking DISC formation in breast cancer cells (Li et al., 2006). DDX3 was also shown to form a complex with glycogen synthase kinase 3 (GSK3) and cIAP1. Inhibition of GSK3 activity, or knockdown of DDX3, can sensitise cancer cell lines to TRAIL-induced apoptosis (Oliver et al., 2012; Sun et al., 2008).

In the presence of overexpressed FADD, both TRADD and RIPK1 have been shown to interact with TRAIL-R1/R2 (Chaudhary et al., 1997; Lin et al., 2000; Pascal Schneider et al., 1997). However, evidence for endogenous level interactions has been inconsistent. RIPK1 but not FADD was shown to interact with the receptors (Lin et al., 2000), whereas RIPK1 was found to only bind FADD in a secondary complex and not with the TRAIL receptors (Jin and El-Deiry, 2006; Varfolomeev et al., 2005). TRADD has also been shown to interact directly with the TRAIL receptors and mediate the recruitment of RIPK1 (Cao et al., 2011). RIPK1 has been shown to be important for TRAIL-induced non-apoptotic pathway activation (Varfolomeev et al., 2005). Knockdown of RIPK1 and TRAF2 can sensitise cells to TRAIL-induced apoptosis by preventing the activation of NF κ B, p38 and JNK (Lin et al., 2000; Varfolomeev et al., 2005). Knockdown of TRADD also sensitises cancer cells to TRAIL-induced apoptosis, due to a reduction in TRAIL-induced NF κ B activation (Cao et al., 2011; Kim et al., 2011).

1.9.4: PKC

The Protein kinase C (PKC) family is a large group of serine/threonine kinases which are activated by intracellular Ca²⁺ or diacylglycerol (DAG) (Steinberg, 2008). Activated G-protein coupled receptors (GPCRs) induce phospholipase C activity, which generate DAG and Inositol 1,4,5 triphosphate (IP₃) by the hydrolysis of the phospholipid,

phosphatidylinositol 4,5-bisphosphate (PIP₂). IP₃ binds to its receptors on the ER and stimulates the release of Ca²⁺ into the cytosol (Berridge, 2009). PKCs can also be activated by phorbol esters, such as phorbol 12-myristate 13-acetate (PMA), which are analogues of DAG (Wu-Zhang and Newton, 2013). Phorbol esters have long been used to induce cancer formation and have been shown to inhibit apoptosis (Koivunen et al., 2006). The discovery of PKCs as the target of phorbol esters highlighted a role for PKC activation in the inhibition of apoptosis (Koivunen et al., 2006). Activation of PKC has specifically been shown to inhibit apoptotic induction by TRAIL, as well as CD95L and TNF α (Byun et al., 2006; Harper et al., 2003a; Meng et al., 2010).

Early studies presented multiple mechanisms for how PKC could affect the extrinsic apoptotic pathway. These included the phosphorylation and inhibition of pro-survival BCL-2 family proteins: BCL-2 (Ito et al., 1997), MCL-1 (Domina et al., 2004) and BAD (Holmström et al., 2000). Activation of the NF κ B pathway by PKC (Busuttill et al., 2002), and induction of the expression of apoptotic inhibitors such as cFLIP, was also suggested. However, it became apparent that the critical event occurs earlier as several groups demonstrated that PKC activation blocks an event upstream of caspase activation (Gómez-Angelats et al., 2000; Harper et al., 2003a; Sarker et al., 2001). PMA treatment blocks caspase activation and caspase-3-dependent cleavage of PKC isoforms in Jurkat cells treated with anti-CD95 antibodies. This leads to a decrease in CD95-induced cell shrinkage, MOMP and K⁺ loss (Gómez-Angelats et al., 2000). The blockade of TRAIL-induced apoptosis by PKC activation was demonstrated to inhibit the cleavage of caspase-8. This prevented induction of MOMP and cytochrome c release in TRAIL-treated Jurkat cells (Sarker et al., 2001). In a study from our laboratory, Harper et al (2003) also demonstrated that PKC activation can block the release of Smac and cytochrome c from mitochondria following TRAIL treatment of HeLa cells. Importantly, PMA treatment can only inhibit apoptosis induction if added before TRAIL or CD95 agonistic antibodies (Trauzold et al., 2001). This implies that PKC activation is targeting an early apoptotic event. PKC activation was demonstrated to block the initial stage of CD95 DISC assembly, as PMA treatment inhibited recruitment of FADD in Jurkat cells (Gómez-Angelats and Cidlowski, 2001; Meng et al., 2002). Conversely, treatment with the PKC inhibitor Go6976 sensitised the cells to CD95-

induced apoptosis and enhanced recruitment of FADD to the DISC (Gómez-Angelats and Cidlowski, 2001). CD95-induced apoptosis was not blocked by PMA pre-treatment in SKW6.4 cells, a lymphoblastoid B cell derived line, having effect no FADD recruitment. The authors argued that the lack of inhibition in the SKW6.4 cells points to a difference in PKC sensitivity being due to cells being Type I or Type II in regard to extrinsic apoptotic signalling. SKW6.4 cells are Type I cells and are not sensitive to PKC-mediated inhibition, whereas Jurkats are Type II cells, and require amplification of caspase activation by the intrinsic pathway, and are sensitive to PKC-mediated inhibition (Meng et al., 2002). As previously observed for CD95L signalling (Gómez-Angelats and Cidlowski, 2001; Meng et al., 2002), FADD recruitment to the TRAIL DISC was impeded following PKC activation. Importantly, FADD recruitment to recombinant GST:TRAIL-R1/R2 constructs could also be prevented by PMA treatment (Harper et al., 2003a). This implies that blockade of adaptor protein recruitment to death receptor signalling complexes is a conserved mechanism for PKC-inhibition of death ligand apoptotic signalling. Moreover, an early study showed that phorbol ester treatment could block the appearance of CD95 bands at approximately 120 and 200 kDa on non-reducing gels, suggesting that PKC activation can block CD95 aggregation (Ruiz-Ruiz et al., 1999). PMA treatment however, has no effect on the ability of TRAIL-R1 or TRAIL-R2 to form dimers or trimers (Harper et al., 2003a). Importantly, FADD itself does not appear to be a direct target for PKC, as treatment with PMA does not change the phosphorylation status of FADD in HeLa (Harper et al., 2003a) or Jurkat cells (Meng et al., 2010). Therefore, although PKC activation has been demonstrated to block TRAIL (and other death ligand)-induced apoptosis, the mechanism(s) underlying this phenomenon are not yet understood.

1.11: Thesis Aims

The ability of death ligands to induce apoptosis in cancer cells raised the possibility of targeted cancer treatments with reduced side effects. Whereas TNF α and CD95L-based approaches suffered from serious side effects in patients, TRAIL treatment is well tolerated. However, the use of TRAIL as a therapeutic has been hampered by intrinsic or acquired resistance in many cancers. Increasing our understanding of the mechanisms which regulate TRAIL-induced apoptosis will enable new strategies to

overcome TRAIL resistance in cancer. This thesis describes work to identify novel proteins involved in the regulation of TRAIL signalling and characterises a mechanism of TRAIL:TRAIL-Receptor regulation which until now has been unclear.

The first results chapter of this project describes the development of an improved platform to enable the detection of isolated TRAIL receptors and the TRAIL-DISC by label-free quantitative mass spectrometry. The development of this platform enabled novel TRAIL DISC and TRAIL receptor-interacting proteins to be identified.

In the second results chapter, the mass spectrometry platform was utilised to determine differences in mechanisms of regulation between TRAIL-R1 and TRAIL-R2 signalling. The reason for humans to express two functional death receptors (TRAIL-R1 and TRAIL-R2) is currently unclear. With numerous TRAIL-based therapeutics currently being tested clinically which specifically interact with TRAIL-R1 or TRAIL-R2, it is imperative to understand the mechanisms which determine sensitivity to apoptosis-induced by each receptor. Novel proteins were identified which interacted with the TRAIL DISC and with TRAIL-R1 or TRAIL-R2. The role of these proteins in regulating TRAIL signalling was then further characterised.

The third data chapter describes an investigation of the mechanism by which activation of PKC can inhibit TRAIL-induced apoptosis. It has long been observed that activation of PKC can block apoptosis induction by TRAIL, CD95L and TNF α . How PKC inhibits death receptor-mediated apoptosis, however, is currently not fully understood. Elucidating the mechanism of PKC-mediated inhibition of apoptosis may lead to new therapeutic targets to enhance efficacy of death receptor-based therapeutics for cancer therapy.

Chapter 2: Materials and Methods

Chapter 2: Materials and Methods

2.1: Chemicals

All chemicals were of the highest quality and were purchased from Sigma (Gillingham, UK) unless otherwise stated. Bisindolylmaleimide I (GF 109203X was purchased from Calbiochem Nottingham, UK).

2.2: Reagents

2.2.1: TRAIL Generation and Biotinylation

Recombinant His-tagged TRAIL was generated in-house following expression in *E.coli* cells and subsequent purification using nickel beads as previously described (MacFarlane et al. 1997). Recombinant His-tagged TRAIL was biotinylated using 20 mg/ml D-Biotinoyl- ϵ -Amidocaproic Acid-N-Hydroxysuccinimide ester (Roche) according to the manufacturer's instructions and as previously described (Harper and MacFarlane, 2008)

TRAIL mutants, which specifically bind to TRAIL-R1 or TRAIL-R2, were generated and biotinylated as described above using vector constructs generated previously (MacFarlane et al., 2005a)

2.2.3: Antibodies

Primary antibodies used for western blot and flow cytometry analysis or induction of cell death are detailed in Table 2.1, Table 2.2 and Table 2.3 respectively. Secondary antibodies used for western blot analysis are detailed in Table 2.4.

2.2.4: Expression of GST-Fusion Proteins

GST-fusion proteins were created by fusing glutathione S-transferase (GST) to the N-terminus of the intracellular domains (ICDs) of TRAIL-R1 (residues 269–468) and TRAIL-R2 (residues 209–411). The vectors containing the TRAIL-R1 and TRAIL-R2-ICDs fused to GST were previously produced in our lab (Harper et al., 2003a; Hughes et al., 2013). (Receptor fusion proteins were overexpressed in XA-90 cells, kindly provided by Prof. D. Riches, National Jewish Medical and Research Center, Colorado), by inducing with 1 mM

Protein	~ Size (kDa)	Type	Company	Dilution
Caspase-8	55/53, 43/41, 18, 10	Rabbit Polyclonal	Kind gift from Dr X Sun, MRC Toxicology Unit, Leicester, UK	1 : 2000
Caspase-9	45, 37, 35	Rabbit Polyclonal	Kind gift from Dr X Sun, MRC Toxicology Unit, Leicester, UK	1 : 2000
Caspase-3	32, 20, 19, 17	Rabbit Polyclonal	Kind gift from Dr X Sun, MRC Toxicology Unit, Leicester, UK	1 : 2000
PARP	113, 89	Mouse Monoclonal	EnzoBML	1 : 2500
TRAIL-R1 (CT)	57	Rabbit Polyclonal	Prosci Incorporated	1 : 1000
TRAIL-R2 (CT)	48, 40	Rabbit Polyclonal	Prosci Incorporated	1 : 1000
FADD	24	Mouse Monoclonal	BD Transduction Laboratories	1 : 250
c-FLIP	55, 43, 26	Rabbit Polyclonal	Merck Frost Centre (Rasper et al., 1998)	1 : 3000
Transferrin Receptor 1	85	Mouse Monoclonal	BD Transduction Laboratories	1 : 1000
PP2A-C	36	Rabbit Monoclonal	Cell Signalling Technology	1 : 1000
RIPK1	76	Mouse Monoclonal	BD Pharmingen	1 : 500
TRADD	34	Mouse Monoclonal	BD Transduction Laboratories	1 : 500
TANK	48	Rabbit Polyclonal	Cell Signalling Technology	1 : 1000
ORP8	101	Rabbit Polyclonal	Abcam	1 : 1000
Skp1	19	Rabbit Monoclonal	Cell Signalling Technology	1 : 250
Cullin-1	90	Rabbit Polyclonal	Cell Signalling Technology	1 : 500
Fbxo11	106/103	Rabbit Polyclonal	Bethyl Laboratories Incorporated	1 : 1000
PP2A-A	65	Rabbit Monoclonal	Cell Signalling Technology	1 : 1000
PP2A-B_{55α}	52	Rabbit Monoclonal	Cell Signalling Technology	1 : 1000
GAPDH	36	Mouse Monoclonal	Abcam	1 : 2000
Phosphorylated IκBα	36	Mouse Monoclonal	Cell Signalling Technology	1 : 1000

Table 2:1 continues onto the next page

IκBα	36	Rabbit Polyclonal	Cell Signalling Technology	1 : 1000
PKCα	77	Rabbit Polyclonal	Cell Signalling Technology	1 : 1000
PKCβ_I	77	Rabbit Polyclonal	Abcam	1 : 1000
PKCβ_{II}	77	Rabbit Monoclonal	Abcam	1 : 1000
PKCγ	78	Rabbit Polyclonal	Santa Cruz Biotechnology	1 : 500
PKCδ	78	Rabbit Polyclonal	Cell Signalling Technology	1 : 1000
PKCϵ	84	Rabbit Monoclonal	Cell Signalling Technology	1 : 1000
PKCη	78	Rabbit Polyclonal	Bethyl Laboratories Incorporated	1 : 1000
PKCθ	82	Rabbit Polyclonal	Cell Signalling Technology	1 : 1000
Phosphorylated MARCKS	80	Rabbit Monoclonal	Cell Signalling Technology	1 : 1000
GST	26	Mouse Monoclonal	Novagen	1 : 10000

Protein	Type	Company	Concentration (μg/ml)
TRAIL-R1	Mouse IgG ₁ K - phycoerythrin (PE)	eBioscience	5
TRAIL-R2	Mouse IgG ₁ K - PE	eBioscience	1.25
IgG control	Mouse IgG ₁ K - PE	eBioscience	5

Agonistic Antibody	Company	Concentration (ng/ml)
Anti-CD95 (CH11)	Millipore	100

Secondary Antibody	Company	Dilution
Goat anti-mouse IgG peroxidase	Sigma	1 : 2000
Goat anti-rabbit IgG peroxidase	DAKO	1 : 2000
IRDye [®] 800CW Goat anti-Mouse IgG	Odyssey	1 : 6000
IRDye [®] 800CW Goat anti-Rabbit IgG	Odyssey	1 : 6000
IRDye [®] 680CW Goat anti-Mouse IgG	Odyssey	1 : 6000
IRDye [®] 680CW Goat anti-Rabbit IgG	Odyssey	1 : 6000

Residue	Primer	Primer Nucleic Acid Sequence
S249	Sense	CCCACCACCACCTGCGCAGATGCCTTTCA
	Antisense	TGAAAGGCATCTGCGCAGGTGGTGGTGGG
S261	Sense	CCCCAGGTCGTTGTGCGGCTCTGTCCACACGCTC
S262	Antisense	GAGCGTGTGGACAGAGCCGCACAACGACCTGGGG
S277	Sense	GGTGGGCTGCAAGATAGCCACGATCTCATTGAGGA
	Antisense	TCCTCAATGAGATCGTGGCTATCTTGCAGCCCACCC
T282	Sense	CTCAGGGACCTGGGCGGGCTGCAAGATAC
	Antisense	GTATCTTGCAGCCCGCCAGGTCCTGAG
T298	Sense	ACATGTTGACACCTGCTGGCTCTGCTGGCTC
	Antisense	GAGCCAGCAGAGCCAGCAGGTGTCAACATGT
S304	Sense	CTCCCCGGGGCCAACATGTTGACACC
	Antisense	GGTGTCAACATGTTGGCCCCGGGGAG
S308	Sense	GCAGATGCTCTGCCTCCCCGGGGGA
	Antisense	TCCCCGGGGAGGCAGAGCATCTGC
S320	Sense	GCCTCCTCCTGAGCCCTTTCAGCTTCTGC
	Antisense	GCAGAAGCTGAAAGGGCTCAGAGGAGGAGGC
T335	Sense	GAAGCACTGTCTCAGAGCCTCAGCGGGATCACCTTCATTTG
T337	Antisense	CAAATGAAGGTGATCCCGCTGAGGCTCTGAGACAGTGCTTC
S353	Sense	GCGGCTCCCAGGCGTCAAAGGGCAC
	Antisense	GTGCCCTTTGACGCTGGGAGCCGC
T381	Sense	CTTTATCAGCATCGCGTACAAGGCGTCCCTGTGGCCCG
T384	Antisense	CGGGCCACAGGGACGCCTTGACGCGATGCTGATAAAG
T393	Sense	CATCTCGCCCGCTTTGTTGACCCACTTTATCAGCA
	Antisense	TGCTGATAAAGTGGGTCAACAAAGCCGGGCGAGATG
S398	Sense	CAGCAGGGCGTGACAGCAGCATCTCGCCCGGT
T401	Antisense	ACCGGGCGAGATGCTGCTGTCCACGCCCTGCTG
T408	Sense	CTCTCTCCAGCGCCTCCAAGGCATCC
	Antisense	GGATGCCTTGAGGCGCTGGGAGAGAG
S424	Sense	TCTAGATACATGAACTTTCAGCGGCCAACAAGTGGTCCTCAATCTTC
S425	Antisense	GAAGATTGAGGACCACTTGTTGGCCGCTGGAAAGTTCATGTATCTAG
S437	Sense	CCGCTCGAGTTAGGCCATGGCAGCGTCTGCATTACCTT
S440	Antisense	AAGGTAATGCAGACGCTGCCATGGCCTAACTCGAGCGG

isopropyl-d-thiogalactoside for 3 h, and cells were then lysed by sonication in 1.5% (w/v) Sarkosyl, containing 5 mM dithiothreitol and Complete™ protease inhibitors (Roche Applied Science). The lysate was bound to 1.5 ml of washed glutathione-Sepharose beads (50% slurry in PBS) for 1 h at 4°C; the beads were washed twice in ice-cold PBS, and the amount of purified GST-fusion protein quantified by Coomassie Blue staining and comparison with bovine serum albumin (BSA) standards.

Mutations of TRAIL-R2 ICD serine and threonine residues to alanine residues were made using the Stratagene QuikChange® Site-Directed Mutagenesis kit (Agilent Technologies) and confirmed by DNA sequencing. Double mutations were carried out if two S/T residues were within four amino acids. The primers used for each mutation are detailed in Table 2.5. TRAIL-R2-ICD mutants were then expressed and bound to glutathione beads using the method described above.

2.3: Cell Culture

All cell culture reagents were acquired from Invitrogen (Paisley, UK) apart from the plastic ware, which was from Grenier Bioone (Frickhausen, Germany). The Burkitt's lymphoma cell line, BJAB was kindly provided by Dr Andrew Thorburn (University of Colorado Health Sciences Center, Aurora, USA (Thomas et al., 2004)). Two Jurkat T cell lines were cultured. Clone E6.1 was obtained from the European collection of animal cell cultures (ECCAC, Wiltshire, UK), and the parental clone A3 (wildtype) was a kind gift from Dr J Blenis (Harvard Medical School, Boston, USA). The cervical carcinoma cell line, HeLa was also obtained from the ECCAC (Wiltshire, UK). BJAB and Jurkat cell lines were cultured in Roswell Park Memorial Institute (RPMI) media supplemented with 10% foetal calf serum (FCS) and 2mM Glutamax™. HeLa cells were maintained in Dulbecco's Modified Eagle Medium (DMEM), containing 2mM Glutamax™ which was supplemented with 10% FCS. Cells were incubated at 37°C with 5% CO₂ in a humidified atmosphere and passaged every 3-4 days.

2.3.1: Rationale for Cell Lines Used

BJAB cells have been used extensively in our lab and are known to be sensitive to TRAIL-induced apoptosis and form a large TRAIL DISC (Dickens et al., 2012a). For this reason and due to a suspension cell line being easier to culture large cell numbers,

they were chosen to perform the mass spectrometry screens for TRAIL-receptor interacting proteins. HeLa cells are also known to be sensitive to TRAIL-induced apoptosis and are easier to transfect than BJAB cells. Therefore, HeLa cells were used to validate potential TRAIL-receptor interacting proteins by siRNA transfection. HeLa cells have also been used extensively in the field to study the effect of PKC activation on TRAIL-induced apoptosis (Harper et al., 2003a). Jurkats are another cell line that has been used to investigate PKC modulation of TRAIL signalling (Meng et al., 2010) and were therefore used in conjunction with HeLa and BJAB cells.

2.4: General Methods

2.4.1: Assessment of Protein Expression in Cell Lines

Cell pellets were re-suspended in 1 x sample buffer (62 mM Tris, 0.05% w/v bromophenol blue, 15% v/v glycerol, 2% w/v SDS, 5% v/v β -mercaptoethanol) and sonicated for 4 cycles (5s on, 5s off). Samples were heated at 95°C for 3 min and analysed by sodium dodecyl sulphate-polyacrylamide gel electrophoresis (SDS-PAGE).

2.4.2: SDS-PAGE

SDS-PAGE gels were run using the Mini-PROTEAN® II electrophoresis cell (BioRad, Hemel Hempstead, UK). Mini gels were prepared with a 4% stacking gel (125 mM Tris-HCl (Roche, Newhaven, UK) pH 6.8, 0.1% w/v SDS, 4% acrylamide (Protogel®, National Diagnostics, Geneflow Ltd, Fadley, UK) cast onto a running gel (375 mM Tris-HCl pH 8.8, 0.1% w/v SDS, variable acrylamide) of varied percentage, depending on the protein of interest. Typically 10% or 12% running gels were used. For experiments with more than 13 samples, the Criterion™ electrophoresis cell (BioRad) was used to run pre-cast 1.0 mm 4-20% 18-well or 26-well (Biorad) gels. Samples to be analysed by mass spectrometry by shotgun proteomics were separated using 1.0 mm 4-20% Bolt™ Bis/Tris gels (Invitrogen).

Proteins were always separated alongside SeeBlue® and SeeBlue® Plus2 pre-stained protein standards (Invitrogen). Gels were run in electrode buffer (25 mM Tris, 192 mM glycine (Fisher Scientific, Loughborough, UK), 0.1 % w/v SDS) at 60-120 V until the protein markers had resolved to the desired level. After SDS-PAGE, gels were either

blotted onto Polyvinylidene fluoride (PVDF) or stained with Coomassie (See section 2.4.4).

2.4.3: Western Blot Analysis

Following SDS-PAGE, proteins were transferred to Immobilon® polyvinylidene fluoride (PVDF) membrane (MerckMillipore). The membrane was blocked for 1 h at room temperature with 5% w/v milk (Marvel, Nestlé, Surrey, UK) in Tris-buffered saline with Tween-20 (TBS-T, 2 mM Tris-HCL pH 7.6, 13.7 mM NaCl (Fisher Scientific), 0.1% v/v Tween-20). Proteins of interest were visualised by incubation with specific primary (2 h at room temperature or overnight at 4°C) and secondary antibodies (1 h at room temperature).

2.4.4: Coomassie Staining

Gels were washed with distilled water before overnight incubation with ProtoBlue™ Safe Colloidal Coomassie G-250 stain (National Diagnostics). Background staining was removed by de-staining in distilled water. The Coomassie stain was prepared by diluting 7 parts stain with 3 parts ethanol (Fischer Scientific).

2.4.5: Bradford Protein Assay

The protein concentration of samples was determined using the Bradford protein assay (Bradford, 1976). Bradford assay solution was prepared by dilution of 1 part protein assay concentrate (Biorad) with 4 parts distilled water. Defined amounts of protein containing sample or BSA were added to 1 ml of the Bradford solution in cuvettes (Sarstedt, Numbrecht, Germany) and mixed by inversion. The absorbance at 595 nm was measured using a Lambda 2 UV/VIS spectrophotometer (Perkin Elmer, Wellesley, USA). The protein concentration of the samples were calculated using the BSA values to construct a standard curve (1 – 10 mg/ml).

2.4.6: Apoptosis Assessment of Annexin V-FITC and DRAQ7 Stained Cells by Flow Cytometry

Apoptosis was assessed by annexin V-FITC (Kind gift from Dr X Sun, MRC Toxicology Unit, Leicester, UK), which binds to externalised phosphatidylserine (PS) (Nagata et al., 2016), and the membrane impermeable, far-red fluorescent dye, DRAQ7™ (Abcam,

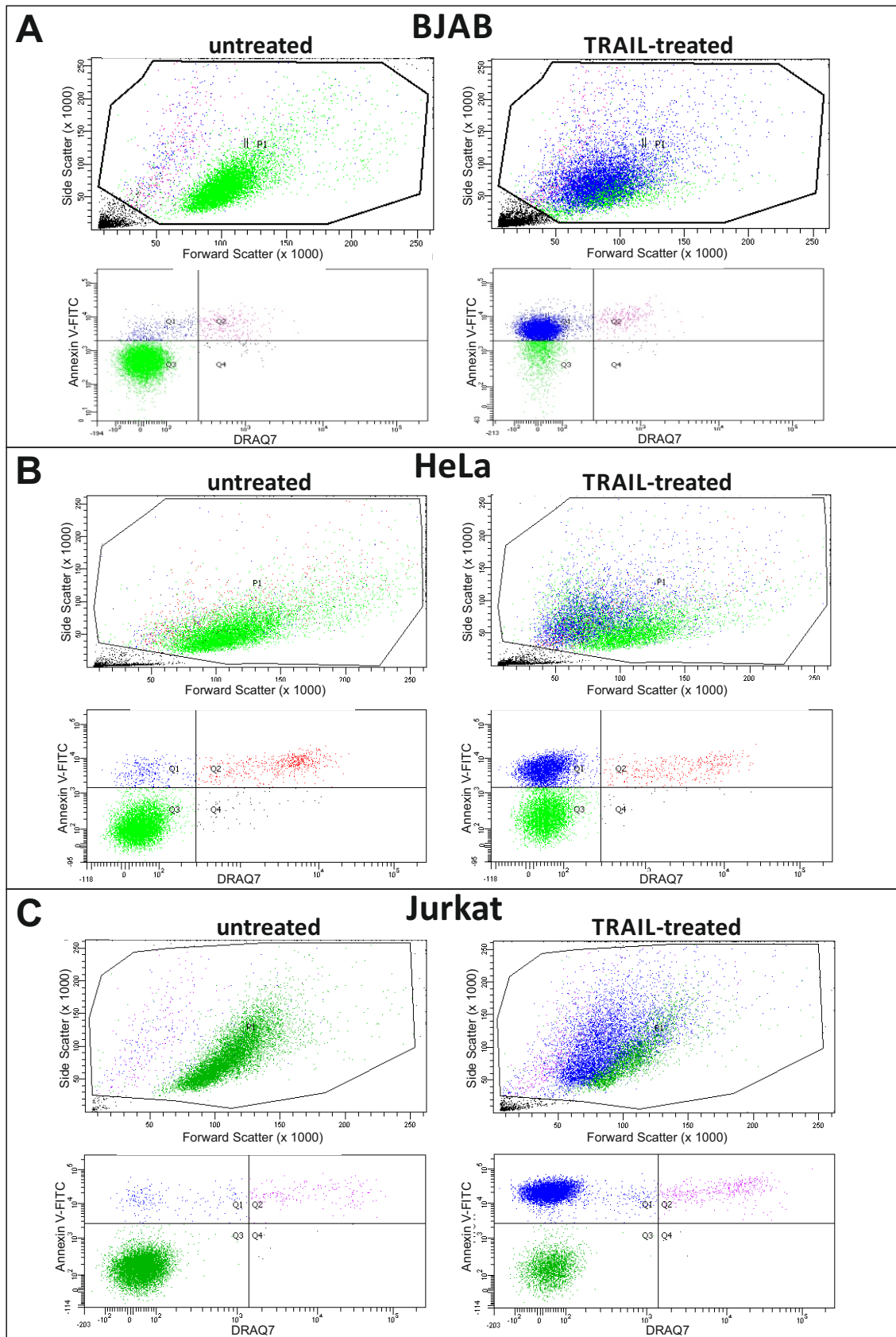


Figure 2.1: Forward/Side Scatter and Annexin V/DRAQ7 Blots of Control and Apoptotic Cells
 Dot blots generated from the BD FACSDiva software for the measurement of apoptosis in untreated or TRAIL treated BJAB, HeLa and Jurkat E6.1 cells. The cells were either left untreated (control) or treated with 500 ng/ml of TRAIL for 4 h at 37°C. Apoptosis was assessed through annexin V-FITC/DRAQ7 staining as described in Section 2.4.6.

Cambridge, UK). Suspension cells (200 μ l) were added to 0.8 ml of annexin buffer (10 mM HEPES-NaOH (Fischer Scientific) pH 7.4, 150 mM NaCl, 5 mM KCl (Fischer Scientific), 1 mM MgCl₂, 1.8 mM CaCl₂). Adherent cells (HeLa) were washed once with phosphate-buffered saline (PBS), trypsin added and cells incubated at 37°C until they detached. Cells were again washed with PBS before being re-suspended in 1 ml warm media and incubated at 37°C for 30 min to recover. The cells (200 μ l) were then added to annexin buffer as for suspension cells. 0.2 μ l (HeLa and Jurkat cells) or 0.8 μ l (BJAB cells) of annexin V-FITC (batch-dependent concentration) was then added and the samples incubated in the dark at room temperature for 8 min (HeLa and Jurkat) or 15 min (BJAB). Subsequently, 1 μ l 0.3 mM DRAQ7 (Abcam) was added and samples incubated on ice for 2 min. The level of annexin V-FITC and DRAQ7™ staining was assessed by flow cytometry using a BD FACSCanto™II (BD FACSDiva software). Figure 2.1 demonstrates typical results following TRAIL treatment of BJAB, HeLa and Jurkat E6.1 cells.

2.4.7: Knockdown of Protein Expression by siRNA Transfection

Expression of target proteins was knocked down by transfection of targeting small interfering RNA (siRNA) using lipofectamine RNAiMax® (Invitrogen). Specific siRNA constructs were acquired from ThermoFischer Scientific which targeted ORP8 (Product ID s41692), PKC α (Product ID s11092) and PKC β (Product ID s11095). The optimal concentration of each siRNA, volume of lipofectamine RNAiMax® and time after transfection for efficient protein expression knockdown was determined by small scale experiments. For the siRNA constructs used in this project, HeLa cells were transfected for 24 or 48 h with 10 nM (final concentration) siRNA, using 4 μ l lipofectamine RNAiMax® per transfection. One day prior to transfection, 1.25 x 10⁵ (for 24 h transfection) or 2.5 x 10⁵ (for 48h transfection) HeLa cells were plated in 6 well plates. For the transfection, the siRNA was diluted in 250 μ l Opti-MEM® I reduced serum medium (Invitrogen) to give a final concentration of 10 mM (in 3ml). Lipofectamine RNAiMax® (4 μ l) was then diluted in 250 μ l Opti-MEM® reduced serum medium before the siRNA and lipofectamine RNAiMax® solutions were combined and incubated at room temperature for 15 min. The siRNA/RNAiMax® mix was then added to the cells to give a final volume of 3 ml. The cells were then incubated for 24 or 48 h at 37°C

with 5% CO₂ in a humidified incubator. Knockdown of the target protein expression was determined following SDS-PAGE separation and subsequent western blot analysis.

2.4.8: Measurement of TRAIL-R1 and TRAIL-R2 Cell Surface Expression

HeLa cells ($\sim 1 \times 10^6$) were washed once with PBS, trypsin added and cells incubated at 37°C until they detached. Cells were again washed with PBS before being re-suspended in 1 ml warm media and incubated at 37°C for 30 min to recover. Cells were pelleted, media removed and cells re-suspended in 10% v/v goat serum in PBS and incubated with the appropriate phycoerythrin (PE)-conjugated antibody (eBioscience, Insight Biotechnology Ltd, Wembley, UK) for 1 h on ice in the dark. Cells were incubated with either anti-human TRAIL-R1, anti-human TRAIL-R2 or mouse IgG1 kappa (isotype control) antibody. Following incubation, cells were washed in PBS and the level of cell surface receptor expression analysed using the BD FACSCanto™II (BD FACSDiva software).

2.5: Analysis of the TRAIL DISC

2.5.1: TRAIL DISC Isolation

Isolation of TRAIL signalling complexes was performed essentially as previously described (Harper et al., 2001; Harper and MacFarlane, 2008; Hughes et al., 2013). Cells were pre-treated with 500 ng/ml biotinylated TRAIL (bTRAIL) for 1 h on ice followed by incubation at 37 °C for 10 min (BJAB) 15 min (HeLa) or 20 min (Jurkat). Untreated (control) samples were generated using the same approach but without the treatment with bTRAIL. Suspension cells were then washed three times with ice-cold PBS and lysed in DISC lysis buffer (30 mM TRIS-HCl (pH 7.5), 150 mM NaCl, 10% glycerol, 1% Triton X-100), containing Complete™ protease inhibitor. For experiments analysing the effect of PKC activation on DISC formation (Chapter 5), PhosSTOP™ phosphatase inhibitors (Sigma-Aldrich) were also included in the DISC lysis buffer. Adherent cells (HeLa) were washed once with PBS and then scraped into fresh (cold) PBS. Cells were then centrifuged and washed two times with cold PBS before being lysed in the same buffer used for suspension cells. Cell lysates were cleared by centrifugation (15,000 x g for 30 min at 4°C) and a sample of the supernatant mixed with 10 x SDS-sample buffer (0.5 M Tris-HCl pH 6.8, 0.4% bromophenol blue, 15% v/v

glycerol, 16% w/v SDS, 5% v/v β -mercaptoethanol). To isolate unstimulated TRAIL receptors, 0.5 μ g/ml bTRAIL was added to the supernatants from cells not previously treated with bTRAIL. The supernatants were incubated for 17 h at 4°C on an end-to-end rotator with 50 μ l magnetic M-280 streptavidin Dynabeads® (Dyna, Invitrogen). Beads were isolated from the supernatant using a magnet, washed and proteins eluted by boiling at 95°C for 5 min in 1 x SDS-sample buffer. Proteins in the supernatant fractions (inputs) and bead eluates were separated by SDS-PAGE and analysed by western blot. For large-scale experiments for mass spectrometry analysis, the protocol was scaled up and the number of cells and volume of Dynabeads® used are detailed in the respective figure legends.

Additional treatments prior to the isolation of the DISC are described in the respective figure legends.

2.5.2: Separation of TRAIL DISC by Sucrose Density Gradient (SDG) Centrifugation

Cells were treated as described above to induce formation of the DISC. The washed cell pellet was lysed in 2 ml of DISC lysis buffer and the lysate cleared by centrifugation. The cleared lysate was loaded onto a continuous 10 – 45% sucrose gradient (10 – 45% w/v sucrose, 50 mM Tris-HCl pH 7.4, 150 mM NaCl, 0.1% v/v Triton X-100) and centrifuged at 180,000 g for 17h at 4°C. Following centrifugation, the gradients were fractionated into 1 ml samples. To each of the fractions, 30 μ l of magnetic M-280 streptavidin Dynabeads® was added, before incubation overnight at 4°C on an end-to-end rotator. The beads were then washed and proteins eluted by boiling in 1 x SDS-sample buffer. Eluted proteins were separated by SDS-PAGE and analysed by western blotting.

2.5.3: 2-D Gel Electrophoresis of Isolated TRAIL DISC

The TRAIL DISC was isolated as described above, but instead eluted from the beads by incubation in urea buffer (8M Urea, 2% v/v Triton X-100, 5% v/v glycerol) for 30 min at 37°C. 20 μ l of this sample was added to 230 μ l rehydration buffer (8M Urea, 2% v/v Triton X-100, 5% v/v glycerol, 65 mM DTT, 0.2% pH 3-10 ampholytes (Biorad)) and applied to a 11cm pH 4-7 non-linear ReadyStrip™ IPG strip (Biorad). The strip was

covered with DryStrip cover fluid (GE Healthcare) and actively rehydrated at 50 V with the sample overnight in the PROTEAN IEF cell (Biorad). Electrode wicks were inserted under the strip before running at 250 V for 15 min, the voltage slowly ramped up to 8000 V and run for 35,000 Vh. Before the second SDS-PAGE dimension the strip was incubated with DTT-containing (130 mM) equilibration buffer (6M Urea, 2% v/v SDS, 0.375M Tris-HCl pH 8.8, 20% v/v glycerol) for 15 min, and then a further 15 min with iodoacetamide (GE Healthcare)-containing (135 mM) equilibration buffer. Following SDS-PAGE separation, the proteins were transferred onto PVDF membrane for western blot analysis.

2.5.4: Treatment of the Isolated TRAIL DISC with Phosphatases

To analyse the effect of phosphatase treatment on the TRAIL DISC, the isolated DISC was treated with λ phosphatase (New England Biolabs (NEB), Cambridge, UK) or protein tyrosine phosphatase (PTP) (R & D systems, Abingdon, Oxford, UK). The TRAIL DISC was isolated as described above, in the presence of phosphatase inhibitors. However, after incubation of the magnetic M-280 streptavidin DynaBeads[®] with the cell lysate overnight, the beads were washed three times in DISC lysis buffer, containing Complete[™] protease inhibitors but not PhosSTOP[®] phosphatase inhibitors. After washing, the beads were incubated with either phosphatase buffer (10% v/v 1 x NEB PMP buffer (New England Biolabs) diluted in d.H₂O), λ phosphatase (phosphatase buffer, 1 mM MnCl₂ (New England Biolabs), 100 units λ phosphatase) or PTP (phosphatase buffer, 100 units PTP) for 30 min at 37°C. Proteins were then eluted into 1 x SDS-sample buffer by boiling at 95°C for 5 min, separated by SDS-PAGE and analysed by western blotting.

2.6: Mass Spectrometry

The TRAIL DISC and unstimulated TRAIL receptors were isolated from BJAB cells as described above by scaling up the protocol six to ten fold. The number of cells and volume of magnetic M-280 streptavidin beads used is described in the respective figure legends. The isolated proteins were either eluted and separated by SDS-PAGE, using Bolt[™] gels (“Shotgun proteomics” method) or eluted from the beads and immediately analysed by mass spectrometry (“Off-Bead” method).

2.6.1: “Shotgun Proteomics”

SDS-PAGE gels were sliced into 24 slices, de-stained, dehydrated and digested with trypsin (Promega) overnight at 30°C. The samples from every two adjacent gel slice were combined, to give a total of 12 samples from each lane. Tryptic peptides were extracted with trifluoroacetic acid (TFA; 0.2%), dried in a speedvac then solubilized in 20 µl injection solvent (97% FA (5%) 3% MeCN). For Top 3 label-free analysis, the injection solvent is spiked with 20 fmol / µl yeast alcohol dehydrogenase (ADH) and bovine serum albumin (BSA). Injection volumes varied, depending on the protein amounts, but were typically 4.5 µl. Samples were analysed by a nanoaquity LC system (Waters), interfaced to a Synapt G2S; operated in HDMSE (ion mobility) mode. Each sample was loaded on the Synapt G2S; and analysed concurrently. The HDMSE data was processed and searched using the Protein Lynx Global Server (PLGS), version 3, and protein identifications made using the Uniprot database (human reviewed). Scaffold (Proteome Software, Portland, Oregon, USA) was used to validate protein identifications derived from MS/MS sequencing results, visualised using the ProteinProphet computer algorithms (Searle 2010). In Scaffold, the results from each individual paired gel slice sample were collated to give total protein identifications from each gel lane.

2.6.2: “Off-bead” Method

Alternatively, purified TRAIL-DISC complexes were analysed using an Off-bead method in which the magnetic M-280 Dynabeads® were re-suspended in Rapigest (Waters), and protein eluted by heating to 80°C for 45 min. The samples were then digested with trypsin (Promega) overnight at 30°C, before addition of neat TFA to remove the Rapigest. 20 µl of each sample was mixed with injection solvent (97% FA (5%), 3% MeCN) and injected onto the Synapt-G2S; and analysed as described above. Using the on-bead method, only one sample was loaded onto the mass spectrometer resulting in a much reduced time for sample analysis when compared to “shotgun proteomics”.

2.6.3: Label-Free “Top 3” Quantitation

Label-free quantitation was carried out using the “Top 3” method as described (Silva et al., 2006). In brief, the abundances of the three most abundant peptides for each

protein were compared to the abundances of a known amount of ADH included (80 fmol) in each sample analysed. Quantified amounts (fmol) for each identified protein, in each sample (each paired slice for shotgun method) were generated by PLGS and outputted as csv files. Using a programme written in-house by Dr Ian Powley, the total amounts of each protein of interest for the whole sample were extracted.

2.6.4: Identification of Protein “Hits”

For each mass spectrometry experiment, proteins were determined to be interacting with the DISC or unstimulated receptors, if peptides were detected in the treated or unstimulated samples but not in the untreated samples. Peptide detection thresholds were set at 90% peptide probability. Specifically-interacting proteins were identified in Scaffold and a list of proteins of interest was generated. “Top 3” quantitative data for each of the proteins of interest were then calculated as described above.

2.7: GST-TRAIL-R-ICD *In Vitro* Binding Assay

To assess GST-TRAIL-R-ICD protein binding (Harper et al., 2003a; Hughes et al., 2013), HeLa cells were either left untreated or treated with PMA (20 ng/ml) for 30 min at 37°C, then washed once with PBS and harvested by trypsinisation. Alternatively, Jurkat cells were re-suspended in fresh media and left untreated or treated with PMA for 30 min at 37°C. Cell pellets were re-suspended in 3 ml of DISC lysis buffer (see above) and incubated on ice for 45 min. Lysates were cleared by centrifugation, and aliquots of the supernatant containing 5 mg of protein (10 mg/ml) were incubated for 16 h at 16 °C with 10 µg of purified GST-ICD fusion proteins bound to glutathione-Sepharose beads. Bound proteins were pelleted by centrifugation at 200 × *g* for 3 min, washed five times in PBS containing protease inhibitors, and released from beads by boiling for 5 min in SDS sample buffer. The interaction of FADD with GST-TRAIL-R-ICDs was assessed by western blotting, following separation of the proteins by SDS-PAGE.

***Chapter 3: Development of an Improved Platform
to Identify Isolated TRAIL DISC Proteins,
Unstimulated TRAIL receptors and Associated
Proteins by Label-free Quantitative Mass
Spectrometry***

Chapter 3: Development of an Improved Platform to Identify Isolated TRAIL DISC Proteins, Unstimulated TRAIL receptors and Associated Proteins by Quantitative Label-free Mass Spectrometry

3.1: Introduction

Death ligands induce apoptosis through the ligation, aggregation and activation of death receptor signalling complexes (reviewed by Dickens et al., 2012b). The death ligand TRAIL induces apoptosis by activating its death receptors TRAIL-R1 and TRAIL-R2, causing their aggregation and subsequent formation of the death-inducing signalling complex (DISC) (Kischkel et al., 2000; Sprick et al., 2000; Tschopp et al., 2000). In the DISC, procaspase-8 is activated following the formation of death effector domain (DED) filaments/chains and subsequently cleaves downstream effector caspases which induce apoptosis (Dickens et al., 2012a). The discovery of TRAIL generated substantial interest since it was reported that TRAIL is highly selective at inducing apoptosis in malignant cells but not normal cells (Pitti et al., 1996; Wiley et al., 1995). However, subsequent studies have shown that many tumour cells, including primary cells from patients, display inherent resistance to TRAIL treatment, or rapidly develop resistance upon treatment (MacFarlane et al., 2002; Stegehuis et al., 2010; van Dijk et al., 2013; Zhu et al., 2004).

TRAIL signalling can be directly regulated via modulation of the core DISC components and by the binding of proteins which inhibit or promote DISC activity. For example, TRAIL-R4 can bind TRAIL and is recruited to the DISC but prevents caspase-8 activation by preventing the recruitment of FADD due to the absence of a functional death domain (DD) (Mérino et al., 2006). Cellular FLICE-inhibitory protein (cFLIP) can either inhibit or enhance the activation of caspase-8 depending on the isoform and the extent of cFLIP binding to the DISC. The long isoform of cFLIP (cFLIP_L) is a homologue of caspase-8 which lacks the catalytic active site but can be cleaved and promotes

caspase-8 chain assembly, thereby enhancing activity. Higher concentrations of cFLIP_L can also be inhibitory by preventing caspase-8 filament assembly (Hughes et al., 2016). The short isoform of cFLIP (cFLIP_S) however, only contains the N-terminal DEDs and acts as a chain terminator, inhibiting caspase-8 activation (Hughes et al., 2016). In addition, cullin-3 (Cul3) was demonstrated to bind to the TRAIL DISC in HeLa cells, and in a complex with the E3-ligase, RING box protein-1 (Rbx1), catalyses the poly-ubiquitination of caspase-8 (Jin et al., 2009). The ubiquitin binding protein p62 then binds the poly-ubiquitin chains and causes the recruitment of caspase-8 to ubiquitin rich foci, promoting cleavage and activation of caspase-8 (Jin et al., 2009). This process is regulated by the binding of the de-ubiquitinating enzyme, A20 which removes the ubiquitin chains (Jin et al., 2009), or by TRAF2 which targets the ubiquitinated caspase-8 for degradation (Gonzalvez et al., 2012). This process however may be limited only to epithelial-derived cell lines as Cul3 could not be detected in DISC isolated from cell lines of haematopoietic origin (Dickens et al., 2012a).

By identifying and understanding novel mechanisms which regulate the sensitivity of cells to TRAIL-induced apoptosis, new strategies may be developed to overcome resistance to TRAIL-based therapeutics. This chapter describes the development of an improved platform to analyse isolated TRAIL receptors and activated DISCs by label-free quantitative mass spectrometry. After demonstrating that the known membrane-bound TRAIL receptors (TRAIL-R1-R4) and DISC components could be reliably detected, novel DISC associated proteins were identified which may have novel roles in the regulation of TRAIL signalling.

3.2: Results

3.2.1: Concentration-response of BJAB Cells to TRAIL-induced Apoptosis

To determine the sensitivity of BJAB cells to TRAIL-induced apoptosis, 1×10^6 cells were treated with increasing concentrations of TRAIL, ranging from 0 to 2 $\mu\text{g/ml}$ (Figure 3.1). After a 4 h treatment, cells were stained with annexin-V-FITC and DRAQ7 and cell death quantified by flow cytometry (Figure 3.1 A). TRAIL concentrations lower than 0.1 $\mu\text{g/ml}$ did not induce significant cell death above background levels. However, as the concentration of TRAIL increased further the percentage of cell death rapidly rose to a maximum of 88.5% annexin-V positive cells at 1.0 $\mu\text{g/ml}$. Further analysis of this dose response revealed that in BJAB cells the EC₅₀ for TRAIL is 0.21 $\mu\text{g/ml}$.

The effect of TRAIL treatment was further analysed by western blotting of whole cell lysates of treated cells for caspase-8, caspase-9, caspase-3 and PARP (Figure 3.1 B). The western blot for caspase-8 detected the p43/p41 and subsequent p18 fragments in cells treated with 0.5, 1.0 or 2.0 $\mu\text{g/ml}$ TRAIL (Figure 3.1 B, Lanes 5-7), demonstrating caspase-8 activation and auto-processing. The p43/p41 and p18 fragments were also detected in cells treated with 0.25 $\mu\text{g/ml}$ TRAIL (Lane 4), however at a lower level than for the higher TRAIL concentrations, correlating with the FACs data (Figure 3.1 A). Cells treated with 0.05 or 0.1 $\mu\text{g/ml}$ TRAIL (Lanes 2-3) did not show the formation of caspase-8 fragments over background levels (Lane 1), demonstrating that caspase-8 had not been activated by TRAIL treatment at these lower concentrations. Caspase-9 was cleaved to the p37 and p35 fragments in cells treated with 0.25 $\mu\text{g/ml}$ or greater TRAIL concentrations (Lanes 4-7). P37 was the pre-dominant fragment detected, indicating that caspase-9 had been cleaved by activated caspase-3 and not auto-processed within the apoptosome. In untreated cells or cells treated with 0.05 or 0.1 $\mu\text{g/ml}$ TRAIL (Lanes 1-3), caspase-9 fragments were not detected. The fully active, mature, p17 caspase-3 fragment was detected in cells treated with 0.25, 0.5, 1.0 and 2.0 $\mu\text{g/ml}$ TRAIL (Lanes 4-7). Increasing amounts of the mature p17 fragment were detected in comparison to the p20 and p19 fragments with increasing TRAIL concentrations. Again, cells treated with 0.05 or 0.1 $\mu\text{g/ml}$ TRAIL (Lanes 2-3) show no induction of cell death, and the active caspase-3 fragments were not

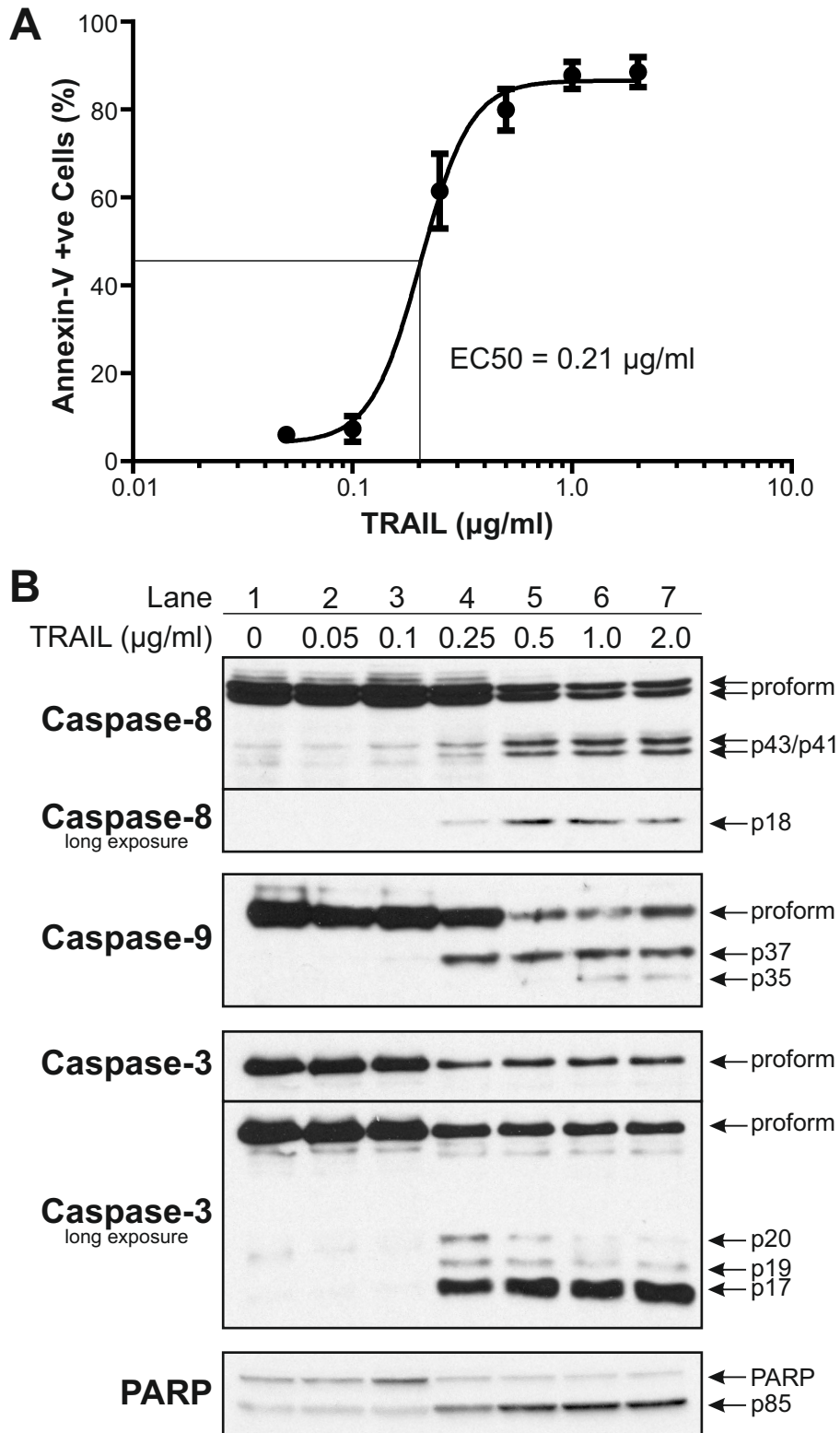


Figure 3.1: Concentration-response of BJAB Cells to TRAIL-induced Cell Death

1×10^6 BJAB cells were treated with 0, 0.05, 0.1, 0.25, 0.5, 1.0 or 2.0 µg/ml TRAIL for 4 h. Cells were then stained with annexin-V-FITC and DRAQ7 and cell death analysed by flow cytometry (A). The percentage of annexin-V positive cells was plotted against [TRAIL] and modelled using a four-parameter logistic curve which determined the EC50 to be 0.21 µg/ml. B Western blots were performed from the remaining cells and probed for caspase-8, caspase-9, caspase-3 and PARP.

detected. Consistent with this, full length PARP predominated in the untreated or 0.05, 0.1 µg/ml TRAIL-treated samples (Lanes 1-3). Whereas, the PARP p85 fragment predominated in the samples treated with 0.25 µg/ml TRAIL (Lane 4) and the amounts of the p85 band increased with increasing concentrations of TRAIL to 0.5, 1.0 and 2.0 µg/ml (Lanes 5-7). Taken together, the FACS data and western blots show that BJAB cells are sensitive to TRAIL-induced apoptosis. Moreover, TRAIL concentrations of 0.5-1 µg/ml are sufficient to induce maximal cell death after 4 h treatment.

3.2.2: Western Blot Analysis of Isolated TRAIL DISC and Unstimulated TRAIL receptors from BJAB Cells

After demonstrating the sensitivity of BJAB cells to TRAIL-induced apoptosis, the ability of biotinylated TRAIL (bTRAIL) to precipitate the TRAIL DISC was determined. A concentration of 0.5 µg/ml bTRAIL was utilised as it has previously been shown to sufficiently activate the apoptotic pathway in BJAB cells (Dickens et al., 2012a). BJAB cells were treated with 0.5 µg/ml TRAIL and incubated on ice for 1 h to enable increased DISC formation by slowing the kinetics of receptor internalisation and complex dissociation (Dickens et al., 2012a; Hughes et al., 2013). Cells were then incubated at 37°C for 10 mins, lysed and the DISC isolated by incubation with 50 µl streptavidin beads (Dynabeads) before elution into sample buffer. In addition, unstimulated TRAIL receptors were isolated by the addition of 0.5 µg/ml bTRAIL after the cell lysis. Western blot analysis of the isolated DISC and unstimulated samples (Figure 3.2) show the detection of a band corresponding to TRAIL-R1. The TRAIL-R1 western blot also shows a band at a higher molecular weight (*) in both the unstimulated (Lane 5) and DISC (Lane 6) samples. This band could indicate the presence of a glycosylated or other post-translational modification of TRAIL-R1. Both the long and short isoforms of TRAIL-R2 were successfully detected in the unstimulated (Lane 5) and DISC (Lane 6) samples. The detection of both TRAIL-R1 and TRAIL-R2 confirms their presence in both the unstimulated and DISC samples. Neither TRAIL-R1 nor TRAIL-R2 were detected in the input samples (Lanes 1-3) and first therefore require precipitation to enable detection. The TRAIL DISC was shown to be successfully isolated as FADD, caspase-8 and cFLIP were detected in the DISC sample (Lane 6) but not in the unstimulated sample (Lane 5). The detection of caspase-8

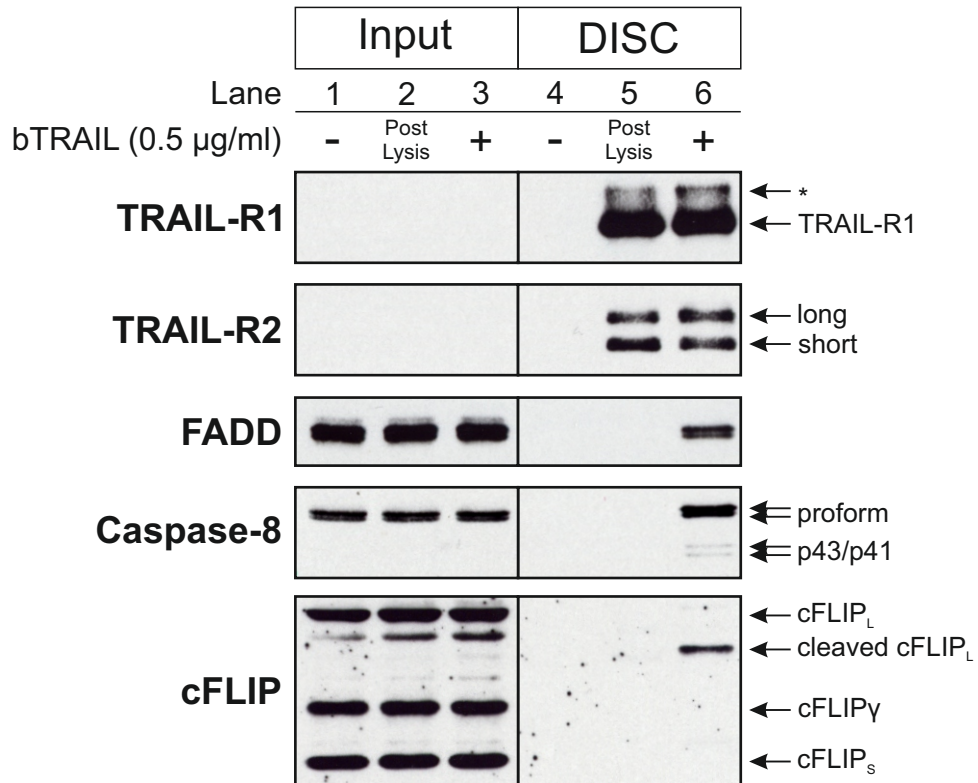


Figure 3.2: Isolation of the TRAIL DISC and Unstimulated TRAIL-R1/R2 from BJAB Cells
 50×10^6 BJAB cells were treated with 0.5 μ g/ml biotinylated TRAIL (bTRAIL), lysed and TRAIL DISC isolated by incubation with 50 μ l streptavidin beads (Dynabeads) overnight before elution into sample buffer. Unstimulated TRAIL-receptors were isolated by the addition of 0.5 μ g/ml bTRAIL after cell lysis and an untreated control was performed by incubating 50 μ l streptavidin beads with the lysate without addition of bTRAIL. Input samples were taken immediately before addition of streptavidin beads. Western blots were performed from the eluted samples and probed for TRAIL-R1, TRAIL-R2, FADD, caspase-8 and cFLIP. * Represents a post-translationally modified form of TRAIL-R1 (Robinson et al., 2012)

p43/p41 fragments demonstrated that the isolated DISC had activated and cleaved caspase-8. In addition, only the cleaved form of cFLIP_L was detected, whilst the cFLIP_S isoform was not detected. Importantly, none of the DISC proteins were detected in the untreated sample (Lane 4), demonstrating that they do not bind non-specifically to the streptavidin beads.

3.2.3: Detection and Quantification of TRAIL DISC Proteins using Label-free “Top 3” LC-MS/MS Shotgun Proteomics

The protocol used to isolate the TRAIL DISC from BJAB cells was scaled up to enable detection of DISC proteins by mass spectrometry. Initially, 300×10^6 BJAB cells were treated with 0.5 µg/ml bTRAIL (as previously described, Section 3.3.2), lysed, and the DISC isolated by incubation with 300 µl streptavidin beads (DynaBeads) and then eluted into sample buffer. An untreated control was also analysed from 300×10^6 BJAB cells which were not treated with bTRAIL but were lysed and incubated with streptavidin beads alone as in the DISC sample. The eluted samples were separated by SDS-PAGE, coomassie stained and analysed by mass spectrometry using the “shotgun proteomics” method (Boyd et al., 2009). Briefly, the gels were sliced and proteins from each individual gel slice extracted, processed and sequentially analysed. The generated data was processed and searched using the Protein Lynx Global Server (PLGS), and protein identifications made using the Uniprot database (human reviewed). The data from each individual slice was collated and identified proteins visualised in Scaffold using the ProteinProphet computer algorithms (Searle 2010). Peptides detected for each protein were displayed if the peptide probability scores were greater than 90%.

The data obtained show that TRAIL-R1 and TRAIL-R2 were successfully isolated, as 9 unique peptides of each protein were detected with an amino acid coverage of 24 and 20%, respectively (Table 3.1, DISC 1: red highlighted rows). A further TRAIL receptor, TRAIL-R4 was also detected, although with a lower amino acid coverage of 13% from 5 unique peptides. The TRAIL DISC was successfully isolated, as the known DISC proteins, caspase-8, cFLIP and caspase-10 were detected. Caspase-8 was detected with the most success, by an amino acid coverage of 50% from 29 unique peptides. Although detected with lower coverage of 16% and 8% respectively, cFLIP and

Protein	Sample	No. Cells (x 10 ⁶)	Volume Beads (μl)	Amino Acid Coverage (%)	Total Unique Peptides	Unique Spectra	Assigned Protein Probability (%)
TRAIL-R1	DISC 1	300	300	24	9	9	100
	DISC 2	500	500	4	2	2	100
	DISC 3	500	300	23	9	13	100
	DISC 4	500	300	29	13	18	100
	UT 1	300	300	0	0	0	0
	UT 2	500	500	0	0	0	0
TRAIL-R2	DISC 1	300	300	20	9	9	100
	DISC 2	500	500	18	7	9	100
	DISC 3	500	300	24	9	16	100
	DISC 4	500	300	34	17	31	100
	UT 1	300	300	0	0	0	0
	UT 2	500	500	0	0	0	0
TRAIL-R4	DISC 1	300	300	13	5	5	100
	DISC 2	500	500	3	1	1	100
	DISC 3	500	300	23	8	8	100
	DISC 4	500	300	16	5	6	100
	UT 1	300	300	0	0	0	0
	UT 2	500	500	0	0	0	0
FADD	DISC 1	300	300	0	0	0	0
	DISC 2	500	500	3	1	1	100
	DISC 3	500	300	7	3	2	100
	DISC 4	500	300	19	5	6	100
	UT 1	300	300	0	0	0	0
	UT 2	500	500	0	0	0	0
Caspase-8	DISC 1	300	300	50	29	37	100
	DISC 2	500	500	44	19	20	100
	DISC 3	500	300	59	37	63	100
	DISC 4	500	300	62	35	53	100
	UT 1	300	300	0	0	0	0
	UT 2	500	500	0	0	0	0
cFLIP	DISC 1	300	300	16	7	7	100
	DISC 2	500	500	3	1	1	42
	DISC 3	500	300	31	13	17	100
	DISC 4	500	300	31	15	19	100
	UT 1	300	300	0	0	0	0
	UT 2	500	500	0	0	0	0
Caspase-10	DISC 1	300	300	8	3	5	100
	DISC 2	500	500	0	0	0	0
	DISC 3	500	300	21	7	7	100
	DISC 4	500	300	20	7	7	100
	UT 1	300	300	0	0	0	0
	UT 2	500	500	0	0	0	0

Table 3.1: Detection of TRAIL-DISC Proteins from BJAB Cells by Mass Spectrometry by Shotgun Proteomics

BJAB cells (300 or 500 x 10⁶) were treated with 0.5 µg/ml bTRAIL, lysed and the TRAIL DISC isolated by incubation with streptavidin beads (300 µl or 500 µl) overnight before elution into sample buffer. In addition, untreated control samples were isolated using the same method but without the addition of bTRAIL. Samples were then ran on SDS-PAGE gels, coomassie stained and analysed by mass spectrometry using the shotgun proteomics method. Mass spectrometry results were visualised using Scaffold with proteins and peptides displaying 95% and 90% probability respectively being displayed. The results for the known DISC proteins: TRAIL-R1, TRAIL-R2, TRAIL-R4, FADD, caspase-8, cFLIP and caspase-10 are displayed.

caspase-10 identification were also assigned a protein probability of 100%. Importantly, no peptides from known DISC components were detected in the untreated sample (Table 3.1, UT 1) demonstrating that core DISC proteins were not binding to the streptavidin beads non-specifically. However, despite the detection of the other DISC binding proteins, FADD was not identified in this DISC isolation. As the proportion of FADD in the DISC relative to the TRAIL receptors and the DED-only proteins (caspase-8, cFLIP and caspase-10) has previously been shown to be sub-stoichiometric (Dickens et al., 2012a), the lower level of FADD present in the DISC may therefore explain why it was not detected. To increase precipitation of DISC-associated FADD, the experiment was repeated using an increased number of cells by scaling up the protocol. 500×10^6 BJAB cells were treated with $0.5 \mu\text{g/ml}$ bTRAIL (as described previously, Section 3.2.2), lysed and the DISC isolated using $500 \mu\text{l}$ streptavidin beads and eluted into sample buffer. Again, the DISC sample was separated by SDS-PAGE, coomassie stained and analysed by mass spectrometry using the shotgun proteomics method. The results show that TRAIL-R1, TRAIL-R2, TRAIL-R4, caspase-8, cFLIP and importantly, FADD were detected (Table 3.1, DISC 2: green highlighted rows). However, despite FADD now being detected, the overall DISC protein identifications were lower than in DISC 1. The coverage of TRAIL-R1 fell from 24% to 4%, with only 2 peptides being detected. The detection of TRAIL-R4 and cFLIP also deteriorated with amino acid coverage falling to 3% from 13% and 16% respectively and the protein probability for cFLIP falling to 42%. Caspase-10 was not detected in DISC 2, while the detection of TRAIL-R2 and caspase-8 was also reduced.

Therefore, although FADD was detected, the overall coverage of known DISC proteins decreased, despite the number of cells being increased to 500×10^6 . This poorer detection may have been due to the volume of beads also being increased. A greater volume of streptavidin beads may result in a greater number of proteins binding non-specifically and therefore the proportion of DISC proteins isolated may actually be lower. To determine if reducing the volume of beads would increase the detection of core DISC proteins, the DISC was isolated using $300 \mu\text{l}$ streptavidin beads from 500×10^6 cells, and analysed as before. The results show that TRAIL-R1, TRAIL-R2, TRAIL-R4, FADD, caspase-8, cFLIP and caspase-10 were all detected with 100% protein

probability (Table 3.1, DISC 3: blue highlighted rows). The number of peptides for TRAIL-R1 and TRAIL-R2 returned to those observed in DISC 1, with 9 peptides each giving 23% and 24% coverage, respectively. TRAIL-R4 detection increased to 23% coverage from 8 peptides, and 3 peptides were now detected for FADD. The detection of caspase-8, cFLIP and caspase-10 was also increased following the reduction in streptavidin bead volume to 300 μ l.

To confirm that the reduced bead volume of 300 μ l used to isolate DISC from 500×10^6 BJAB cells gives a better detection of core DISC proteins, the experiment was repeated. The results again show the detection of TRAIL-R1, TRAIL-R2, TRAIL-R4, FADD, caspase-8, cFLIP and caspase-10 (Table 3.1, DISC 4: blue highlighted rows) with a greater number of peptides and amino acid coverage than DISC 1 and 2 (red and green rows respectively). The number of peptides detected for TRAIL-R1 and TRAIL-R2 increased to 13 and 17 respectively, whereas the 5 peptides detected for TRAIL-R4 were equal to that in DISC 1 but gave a higher amino acid coverage of 16%. FADD was detected at its highest level of 5 peptides and caspase-8 detection was also consistently higher than in DISC 1 and 2 with 37 and 35 peptides detected in DISCs 3 and 4, respectively. The detection of cFLIP and caspase-10 was also consistently higher with 15 and 7 peptides respectively, matching the increase previously observed in DISC 3.

3.2.4: Identification and Confirmation of Novel TRAIL DISC-Interacting Proteins

Having demonstrated that the all of the canonical components of the TRAIL DISC could be consistently detected by mass spectrometry (Table 3.1), the ability to detect hitherto unknown novel DISC-associated proteins could be explored. Across the four TRAIL DISC samples and two untreated (UT) samples, 569 different proteins were identified. Of these proteins, 79 were detected in the TRAIL DISC samples but not the untreated samples, including core DISC proteins already discussed. Table 3.2 displays the total number of unique peptides detected for potential novel DISC-interacting proteins. Transferrin receptor protein-1 (TfR1) was consistently detected across all four DISC samples, with the highest number of unique peptides, in agreement with previous studies (Dickens et al, unpublished data). However, other proteins were

Accession Number	Protein	Total Unique Peptides			
		DISC 1	DISC 2	DISC 3	DISC 4
CA057_HUMAN	Nucleoside-triphosphatase C1orf57	0	0	1	2
SRP09_HUMAN	Signal recognition particle 9 kDa protein	0	0	0	2
CS043_HUMAN	Uncharacterized protein C19orf43	0	0	0	2
TRADD_HUMAN	Tumour necrosis factor receptor type 1-associated DEATH domain protein	0	0	0	2
RIPK1	Receptor interacting Serine/Threonine-protein kinase 1	0	0	3	2
RAB14_HUMAN	Ras-related protein Rab-14	0	0	0	1
NDUAA_HUMAN	NADH dehydrogenase [ubiquinone] 1 alpha subcomplex subunit 10	0	0	3	1
RAC2_HUMAN	Ras-related C3 botulinum toxin substrate 2	0	0	2	1
HVCN1_HUMAN	Voltage-gated hydrogen channel 1	2	0	0	1
CP080_HUMAN	Uncharacterised protein C16orf80	3	0	2	1
BZW2_HUMAN	Basic leucine zipper and W2 domain-containing protein 2	0	0	4	0
PSB2_HUMAN	Proteasome subunit beta type-2	0	0	2	0
AGK_HUMAN	Acylglycerol kinase	0	0	3	0
SQSTM_HUMAN	Sequestosome-1	0	0	3	0
OAS2_HUMAN	2'-5'-oligoadenylate synthetase 2	0	0	3	0
TRAF1_HUMAN	TNF receptor-associated factor 1	0	0	3	0
DDHD1_HUMAN	Phospholipase DDHD1	0	0	1	0
DOCK5_HUMAN	Dedicator of cytokinesis protein 5	2	0	1	0
MX1_HUMAN	Interferon-induced GTP-binding protein Mx1	0	0	7	0
F184B_HUMAN	Protein FAM184B	0	1	2	0
LYSC_HUMAN	Lysozyme C	3	0	0	0
ANR12_HUMAN	Ankyrin repeat domain-containing protein 12	0	0	2	0
NUDC_HUMAN	Nuclear migration protein nudC	0	0	2	0
LCN1_HUMAN	Lipocalin-1	2	0	0	0
SH3G1_HUMAN	Endophilin-A2	0	0	2	0
AGR2_HUMAN	Anterior gradient protein 2 homolog	2	0	0	0
NR4A2_HUMAN	Nuclear receptor subfamily 4 group A member 2	0	0	2	0
RS28_HUMAN	40S ribosomal protein S28	0	2	0	0
CRO30_HUMAN	Transmembrane protein C18orf30	0	0	2	0
UBP35_HUMAN	Ubiquitin carboxyl-terminal hydrolase 35	2	0	0	0

Table 3.2: Potential DISC-associated Proteins Identified by Mass Spectrometry

The number of unique peptides of proteins detected in the DISC samples (1-4) but not the untreated samples (UT 1 and 2) from the mass spectrometry results detailed in Table 3.1 are displayed.

detected at lower levels and with less consistency, almost exclusively in TRAIL DISC 3 and 4.

To determine if the potential DISC-associated proteins identified by mass spectrometry (Table 3.2) could be confirmed by western blot analysis, TRAIL DISC and unstimulated TRAIL receptors were isolated from 50×10^6 BJAB cells as described above. In addition, an untreated sample was included to provide control for non-specific interaction of target proteins with streptavidin beads. Western blots of the isolated samples were probed for TRAIL-R1, TRAIL-R2, FADD and caspase-8 to confirm the TRAIL DISC had been successfully isolated. To investigate whether the proteins identified by mass spectrometry could be further confirmed, western blot analysis was used to probe for TfR1, protein phosphatase 2A catalytic subunit (PP2A-C), RIPK1, TRADD and TRAF family member-associated NF κ B activator (TANK) (Figure 3.3). TRAIL-R1 and TRAIL-R2 were detected in both the unstimulated (Lane 5) and DISC (Lane 6) samples, confirming their successful precipitation. The TRAIL DISC was successfully isolated, as both FADD and caspase-8 were detected only in the DISC sample (Lane 6). Caspase-8 was also shown to be activated/cleaved, as the p43/p41 fragments were detected (Lane 6).

TfR1 was detected in the DISC sample (Lane 6), confirming its interaction with the TRAIL DISC. TfR1 was also however detected in the unstimulated sample (Lane 5), implying that it interacts with the TRAIL-R1/R2 irrespective of TRAIL stimulation. This association was also observed for PP2A-C, which was detected in both the unstimulated receptors (Lane 5) and DISC (Lane 6) samples. The intensity of the band corresponding to PP2A-C was stronger in the unstimulated sample (Lane 5), implying that the pre-dominant interaction was with non-DISC associated TRAIL-R1/R2. Both RIPK1 and TRADD were only detected in the DISC sample (Lane 6) and not the unstimulated (Lane 5) or untreated (Lane 4) samples, showing a specific interaction with the TRAIL DISC. TANK however was detected in both the untreated (Lane 4) and DISC (Lane 6) samples, showing that its identification is the result of a non-specific interaction with streptavidin beads. TANK was not however detected in the unstimulated sample (Lane 5), possibly because the bTRAIL added post-lysis is present in excess (compared to the DISC samples, in which the excess bTRAIL is washed off

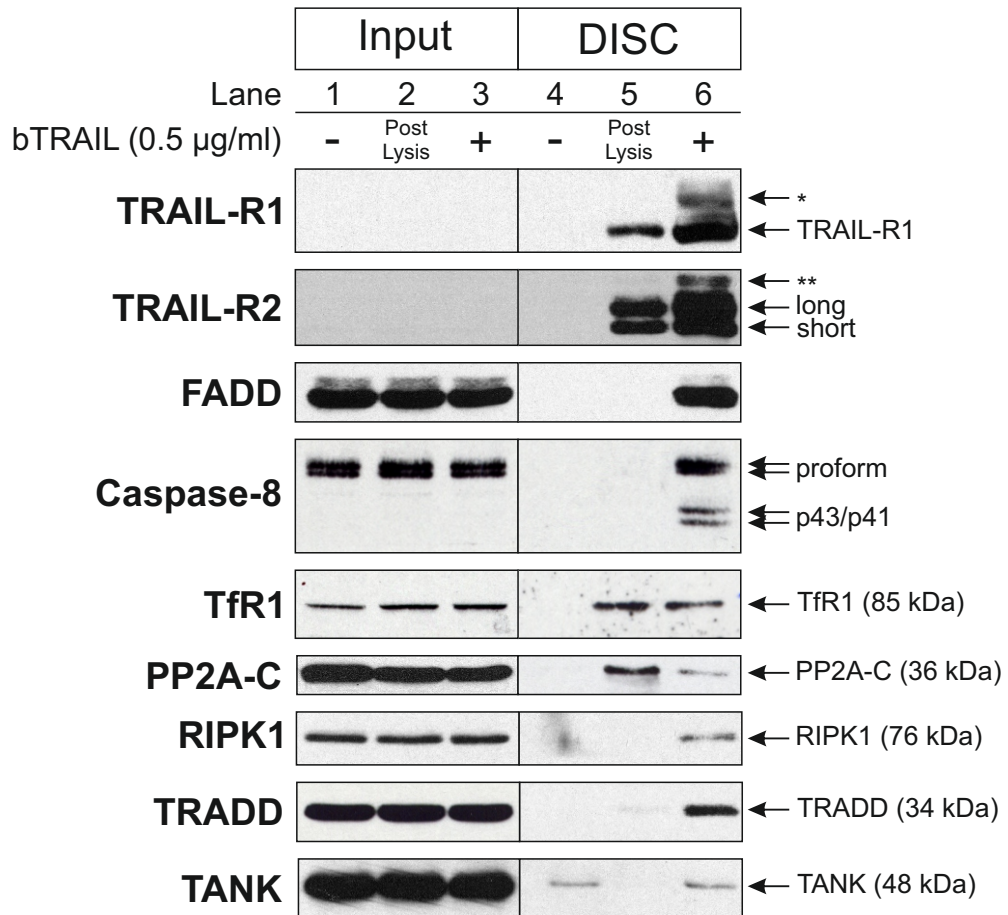


Figure 3.3: Confirmation of the Interaction of TRAIL DISC-associated Proteins by Western Blot Analysis

50 x 10⁶ BJAB cells were treated with 0.5 µg/ml bTRAIL, lysed and TRAIL DISC isolated by overnight incubation with 50 µl streptavidin beads before elution into sample buffer. In addition, unstimulated TRAIL-receptors were isolated by the addition of 0.5 µg/ml bTRAIL after cell lysis. Untreated control samples were isolated using the same method but without the addition of bTRAIL. Input samples were taken immediately before addition of streptavidin beads. Western blots were performed from the isolated samples and probed for TRAIL-R1, TRAIL-R2, FADD, caspase-8, transferrin receptor 1 (TfR1), serine/threonine phosphatase 2A-catalytic subunit (PP2A-C), receptor interacting protein kinase-1 (RIPK1), tumour necrosis factor receptor type 1-associated death domain protein (TRADD) and TRAF family member-associated NFκB activator (TANK). * Represents a post-translationally modified form of TRAIL-R1 (Robinson et al., 2012). ** Represents another form of TRAIL-R2, which may contain post-translational modifications.

before incubation with streptavidin beads) and therefore likely blocks the bead sites where TANK is binding non-specifically.

3.2.5: By Evaluating an “Off-bead” Method to Analyse the Isolated TRAIL DISC, it was Determined that Further Reduction in the Volume of Streptavidin Beads Does not Enhance TRAIL DISC Detection

Having showed that reducing the volume of streptavidin beads to 300 μl (from 500 μl) increased the detection of the DISC by mass spectrometry (Table 3.1), the effect of reducing the volume of streptavidin beads further was investigated. 500 x 10⁶ BJAB cells were treated with 0.5 $\mu\text{g/ml}$ bTRAIL (as described previously, Section 3.2.2), lysed and incubated with either 300 μl , 200 μl , 150 μl or 100 μl streptavidin beads to isolate the TRAIL DISC. To control for non-specific interactions with the beads, cell lysates were incubated with 300 μl streptavidin beads but without the addition of bTRAIL. To analyse the samples, a new method was utilised in which the precipitated proteins were eluted and processed directly from the beads (“off-bead” method) rather than running on a gel first as in the “shotgun proteomics” method (Sections 3.2.3 - 3.2.4). The “off-bead” method ideally works with less-complex samples and therefore should be ideal for analysing the isolated TRAIL DISC. The benefit of the “off-bead” method is that each isolation is loaded onto the mass spectrometer as one sample, instead of a series of sequential samples from the sliced gel as in the shotgun method. Using the “off-bead” method therefore increases throughput, as less time is taken loading the samples onto the mass spectrometer, and therefore enables multiple experimental parameters to be used (Turriziani et al., 2014).

The results show that TRAIL-R1, TRAIL-R2, TRAIL-R4, FADD, caspase-8, cFLIP and caspase-10 were all detected in the TRAIL DISC isolated with 300 μl beads using the “off-bead” method (Table 3.3, blue highlighted rows). The number of peptides detected for TRAIL-R1, TRAIL-R2, TRAIL-R4 and FADD were similar to those detected using the shotgun proteomics method (Table 3.1, DISCs 3 + 4). However, using the “off-bead” method, the number of peptides detected for caspase-8 (Table 3.3, DISC 1 + 2) was lower than detected using the “shotgun proteomics” method (Table 3.1, DISC 3 + 4). The detection of cFLIP and caspase-10 was less reproducible using the “off-

Protein	Sample	No. Cells (x 10 ⁶)	Volume Beads (μl)	Amino Acid Coverage (%)	Unique Peptides	Unique Spectra	Assigned Protein Probability (%)	Protein (fmol)
TRAIL-R1	DISC 1	500	300	21	10	10	100	347.6
	DISC 2	500		17	7	7	100	234.5
	DISC 3	500	200	23	8	8	100	191.4
	DISC 4	500		15	4	4	100	158.6
	DISC 5	500	150	6	3	3	100	121.0
	DISC 6	500	100	8	4	4	100	72.1
TRAIL-R2	DISC 1	500	300	56	16	19	100	368.1
	DISC 2	500		55	15	16	100	320.4
	DISC 3	500	200	55	15	16	10	86.2
	DISC 4	500		17	6	6	100	81.1
	DISC 5	500	150	19	7	7	100	140.7
	DISC 6	500	100	17	6	6	100	43.4
TRAIL-R4	DISC 1	500	300	21	6	6	100	123.6
	DISC 2	500		18	4	4	100	69.2
	DISC 3	500	200	24	6	6	100	29.3
	DISC 4	500		3	1	1	63	0.0
	DISC 5	500	150	2	1	1	99	0.0
	DISC 6	500	100	0	0	0	0	0.0
FADD	DISC 1	500	300	34	6	7	100	92.1
	DISC 2	500		49	7	8	100	52.0
	DISC 3	500	200	36	6	6	100	33.2
	DISC 4	500		6	1	1	52	0.0
	DISC 5	500	150	8	2	2	100	31.8
	DISC 6	500	100	10	2	2	99	19.4
Caspase-8	DISC 1	500	300	50	18	19	100	314.6
	DISC 2	500		54	20	20	100	206.4
	DISC 3	500	200	56	22	22	100	137.7
	DISC 4	500		22	10	10	100	108.2
	DISC 5	500	150	9	4	4	100	135.1
	DISC 6	500	100	22	8	8	100	63.3
cFLIP	DISC 1	500	300	8	4	4	100	61.2
	DISC 2	500		27	12	12	100	47.8
	DISC 3	500	200	20	9	9	100	17.3
	DISC 4	500		9	4	4	100	15.6
	DISC 5	500	150	7	3	3	100	20.9
	DISC 6	500	100	2	1	1	100	10.7
Caspase-10	DISC 1	500	300	0	0	0	0	0.0
	DISC 2	500		22	8	8	82	26.8
	DISC 3	500	200	2	1	1	19	0.0
	DISC 4	500		3	2	2	19	0.0
	DISC 5	500	150	3	2	2	69	0.0
	DISC 6	500	100	0	0	0	0	0.0

Table 3.3: Detection of Proteins from the TRAIL DISC Isolated from BJAB Cells by Mass Spectrometry using the "Off-bead" Method

500 x 10⁶ cells BJAB cells were treated with 0.5 µg/ml bTRAIL, lysed and TRAIL DISC isolated by incubation with 300 µl (highlighted in blue), 200 µl (green), 150 µl (red) or 100 µl (orange) streptavidin beads overnight. Samples were eluted and analysed directly by mass spectrometry using the "off-bead" method. Mass spectrometry results were visualised using Scaffold, with proteins and peptides displaying 95% and 90% probability being displayed. The results for the known DISC proteins: TRAIL-R1, TRAIL-R2, TRAIL-R4, FADD, caspase-8, cFLIP and caspase-10 are shown. "Top Three" label-free quantitated values were calculated by comparison of the amounts of the three most abundant peptides of each protein with the three most abundant proteins detected from 80 fmol yeast alcohol dehydrogenase that was spiked into each sample.

bead” method (Table 3.3, DISCs 1 + 2), although the maximum number of peptides detected for each protein was similar to that detected using “shotgun proteomics” (Table 3.1, DISCs 3 + 4). Following the detection of core DISC proteins using the “off-bead” method, the impact of reducing the volume streptavidin beads used to isolate the DISC could be evaluated. Further reductions to the volume of streptavidin beads did not enhance identification of core DISC proteins, but actually resulted in the number of peptides observed to decrease (Table 3.3). The number of peptides detected for TRAIL-R1 was 10 (Table 3.3: DISC 1) and 7 (DISC 2) when using 300 µl beads (blue), however when the volume of beads decrease to 200 µl the peptide detections dropped to 8 (DISC 3) and 4 (DISC 4). This decreased further to 3 (DISC 5) and 4 (DISC 6) peptides as the bead volumes were lowered to 150 µl and 100 µl, respectively. The same pattern was observed for TRAIL-R2; a maximum of 16 peptides (DISC 1) were detected from the DISC isolated with 300 µl beads. DISC 3, isolated using 200 µl streptavidin beads produced 15 peptides of TRAIL-R1, whereas in the repeat experiment (DISC 4) only detected 6 peptides. As the volume of beads used was lowered further to 150 µl and 100 µl however, only the lower numbers of 7 (DISC 5) and 6 (DISC 6) peptides were detected. TRAIL-R4 was detected with 6 (DISC 1) and 4 (DISC 2) peptides from the DISC isolated using 300 µl beads, whereas the two DISC isolations using 200 µl beads resulted in 6 (DISC 3) and 1 (DISC 4) peptides being detected. Taken together with the TRAIL-R2 and TRAIL-R1 results, this shows that the isolation of DISC 4 was less effective in comparison with DISC, 3 despite both being isolated using 200 µl of beads. Further reductions to 150 µl and 100 µl had a markedly greater effect as only one peptide was detected in the 150 µl bead isolation (DISC 5) and TRAIL-R4 was not detected at all in the 100 µl bead sample (DISC 6). FADD, which was not detected previously using the lower number of BJAB cells (Table 3.1, DISC 1), was detected with all volumes of beads used (Table 3.3). However, in a similar pattern to the TRAIL receptors, the number of peptides detected decreased from 6/7 (Table 3.3: DISC 1/2) to 2 (DISC 5) and 2 (DISC 6), as the bead volumes were reduced from 300 µl to 150 and 100 µl, respectively. The reduction of beads from 300 µl to 200 µl had no negative effect on caspase-8 identification (if we accept that the values for DISC 4 are lower) and actually increased slightly from 19/20 (DISC 1/2) peptides to 22 (DISC 3) peptides. However, as observed for the other DISC proteins, further

reductions of the bead volumes drastically reduced the number of caspase-8 peptides detected, with only 4 detected (DISC 5) using 150 μ l beads and 8 (DISC 6) with 100 μ l beads. The number of peptides detected for cFLIP using 300 μ l beads (blue) was inconsistent, with a high of 12 detected in DISC 2 but only 4 in DISC 1. When the bead volume was reduced to 200 μ l, 9 peptides were detected in DISC 3 and 4 peptides in DISC 4. Taken together, the number of peptides detected appears to decrease as the volume of beads was reduced. This is certainly true as the volume of beads was decreased further to 150 μ l and 100 μ l as only 3 (DISC 5) and 1 (DISC 6) peptide(s) were detected respectively, correlating with the pattern observed for the other proteins. Caspase-10 was identified through the detection of 8 peptides in DISC 2, but in DISC 1 (also isolated using 300 μ l beads) no peptides were detected. When the bead volume was reduced to 200 μ l, the number of peptides detected also decreased to 1 (DISC 3) and 2 (DISC 4). Further bead volume reductions to 150 μ l resulted in 2 peptides (DISC 5) being detected, whilst caspase-10 was not identified in DISC 6, isolated using 100 μ l streptavidin beads.

By analysing the number of unique peptides detected, it is apparent that reducing the volume of streptavidin beads to isolate the DISC below 300 μ l impedes the identification of TRAIL DISC proteins, rather than enhancing it as was hoped (Table 3.3). However, despite the number of unique peptides detected being a good indicator of the amount of protein being identified, it does not give a quantifiable value. To resolve this issue, the amount of protein detected was analysed using “Top 3” label-free quantitation. To each of the samples loaded onto the mass spectrometer, 80 fmol of *yeast* Alcohol Dehydrogenase (ADH) was spiked in. The amount of the three most abundant peptides for each protein were then compared to the amount of the three most abundant peptides of ADH detected. By comparing these values, and knowing the amount of ADH in each sample, the amount of each protein detected could be calculated.

The “Top 3” quantified values for the amount of each DISC protein detected are shown in the last column of Table 3.3 and also expressed graphically in Figure 3.4. The “Top 3” data confirms that reducing the volume of beads used to isolate the DISC results in lower amounts of TRAIL DISC proteins being detected. The amount of

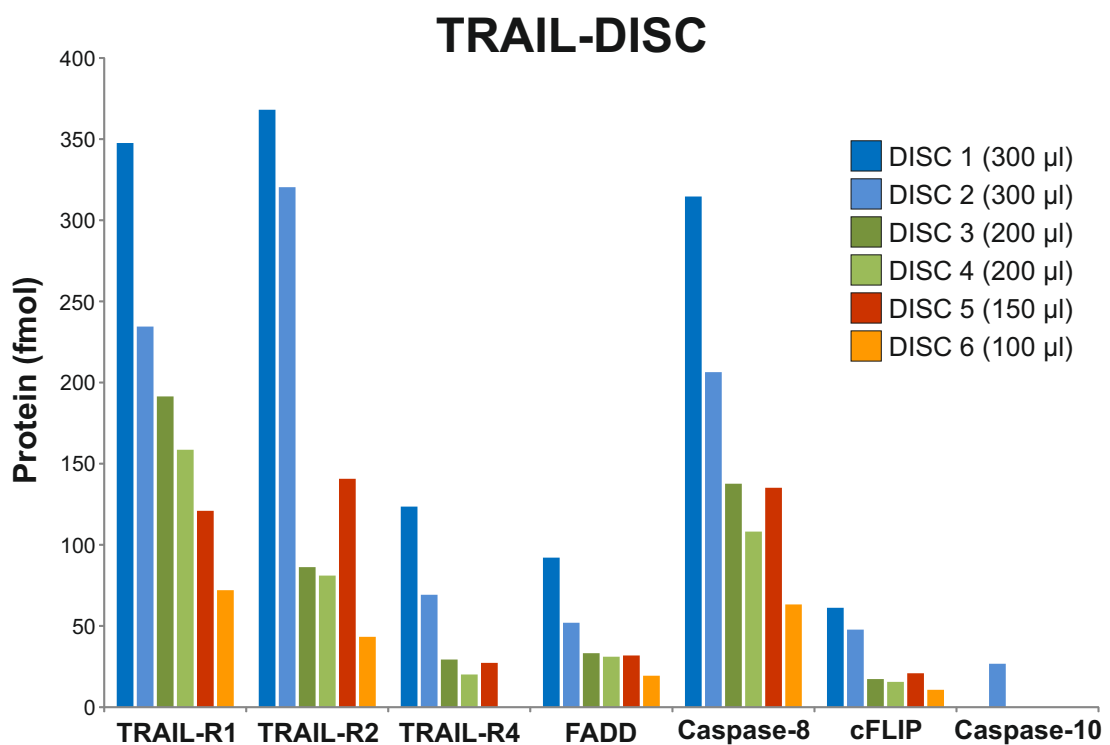


Figure 3.4: “Top Three” Label-free Quantitation of TRAIL DISC Proteins Isolated using the “Off-bead” Method

The “Top Three” label free quantitated values for the canonical DISC proteins: TRAIL-R1, TRAIL-R2, TRAIL-R4, FADD, caspase-8, cFLIP and caspase-10 from the mass spectrometry results described for the isolated TRAIL-DISCs (Table 3.3).

protein roughly correlates with the number of peptides detected for each protein, however there are examples in which the two values differ. In DISC 5, 140.7 fmol of TRAIL-R2 is detected, whereas in DISC 3 only 86.2 fmol is detected, despite only 7 unique peptides of TRAIL-R2 being identified in DISC 5 and 16 being identified in DISC 3. Similarly, 61.2 fmol of cFLIP was detected from 4 peptides in DISC 1 but only 47.8 fmol of cFLIP was detected from 12 peptides in DISC 2. This discrepancy is due to the fact that the “Top 3” method measures the abundance of peptides rather than the range of different peptides detected and therefore a small number of peptides detected repeatedly would represent a larger amount of protein than a large number of diverse peptides being detected in low abundance. “Top 3” values for some of the proteins in which only 1 peptide was detected were not calculated as the software requires abundance values from at least three of the most abundant independent peptides. Values were however calculated for the amount of FADD in DISC 5 and 6, despite only two peptides being detected. This is due to the detection of other peptides which did not meet the criteria to be displayed in Scaffold but met the detection criteria in the ProteinLynx Global Server (PLGS) software, from which the “Top 3” values are generated.

3.2.6: Detection of Unstimulated TRAIL receptors Isolated from BJAB Cells by Label-free Quantitative Mass Spectrometry using the “Off-bead” Method

Western blots (Figure 3.3) from small scale DISC isolations showed that proteins identified by mass spectrometry (Table 3.2), even those detected with low numbers of peptides (PP2A-C, RIPK1, TRADD), could be confirmed as interacting with the TRAIL DISC. However, they also revealed that some of the proteins detected may actually be interacting with TRAIL-R1/R2 irrespective of TRAIL stimulation. However, the proteins interacting with the unstimulated TRAIL receptors could also have a regulatory effect on TRAIL signalling. The unstimulated receptor precipitations were therefore analysed to determine if these proteins could be detected by mass spectrometry. Therefore, 500×10^6 BJAB cells were lysed, 0.5 $\mu\text{g/ml}$ bTRAIL added post-cell lysis and unstimulated receptors isolated by incubation with 300 μl , 200 μl , 150 μl or 100 μl of

Protein	Sample	No. Cells (x 10 ⁶)	Volume Beads (μl)	Amino Acid Coverage (%)	Unique Peptides	Unique Spectra	Assigned Protein Probability (%)	Protein (fmol)
TRAIL-R1	US 1	500	300	20	7	7	100	91.81
	US 2	500		19	6	6	100	47.50
	US 3	500	200	15	5	5	100	46.58
	US 4	500		8	3	3	100	53.71
	US 5	500	150	7	3	3	94	53.27
	US 6	500	100	0	0	0	0	0.00
TRAIL-R2	US 1	500	300	56	16	16	100	124.01
	US 2	500		44	14	14	100	74.46
	US 3	500	200	37	11	11	100	56.76
	US 4	500		27	8	8	100	26.31
	US 5	500	150	0	0	0	0	0.00
	US 6	500	100	0	0	0	0	0.00
TRAIL-R4	US 1	500	300	14	3	3	100	49.25
	US 2	500		14	3	3	100	19.80
	US 3	500	200	0	0	0	0	0.00
	US 4	500		0	0	0	0	0.00
	US 5	500	150	0	0	0	0	0.00
	US 6	500	100	0	0	0	0	0.00

Table 3.4: Detection of TRAIL-Receptors in Unstimulated Samples from BJAB Cells by Mass Spectrometry using the "Off-bead" Method

500 x 10⁶ cells BJAB cells were lysed, followed by addition of 0.5 μg/ml bTRAIL and unstimulated TRAIL-receptors isolated by incubation with 300 μl (highlighted in blue), 200 μl (green), 150 μl (red) or 100 μl (orange) streptavidin beads overnight. Samples were eluted and analysed directly by mass spectrometry using the off-bead method. Mass spectrometry results were visualised using Scaffold with proteins and peptides displaying 95% and 90% probability being displayed. The results for the TRAIL-receptors: TRAIL-R1, TRAIL-R2 and TRAIL-R4. "Top Three" label free quantitated values were calculated by comparison of the amounts of the three most abundant peptides of each protein with the three most abundant proteins detected from 80 fmol yeast alcohol dehydrogenase that was spiked into each sample.

streptavidin beads. Samples were then analysed by mass spectrometry using the “off-bead” method.

Table 3.4 shows the results for the detection of TRAIL-R1, TRAIL-R2 and TRAIL-R4 from the unstimulated cell lysates. As with the DISC isolations, the reduction in volume of beads used to isolate the samples reduced the number of peptides detected for each protein. A maximum of 7 peptides were detected for TRAIL-R1 using 300 μ l beads, which decreased to 3 using 150 μ l beads and zero detection with 100 μ l beads. Similarly TRAIL-R2 was detected with a maximum of 16 peptides using 300 μ l beads, decreasing to 11 peptides with 200 μ l and no detection observed with either 150 μ l or 100 μ l beads. TRAIL-R4 was only detected in the 300 μ l bead sample, with three peptides being observed. “Top 3” values were again calculated as described above for the DISC isolations and are displayed in Figure 3.5 and confirmed the reduction in the efficiency of TRAIL receptor isolation as the volume of beads used was decreased (Figure 3.5). As observed for the DISC isolations (Figure 3.4), the amount of TRAIL-R1 and TRAIL-R2 detected in DISC 2 was lower than detected in DISC 1, using the same volume of beads, although still higher than the receptors isolated using 200 μ l beads. The amount of the TRAIL receptors detected was lower than the corresponding amounts in the DISC samples (Figure 3.4), with approximately 350 fmol of TRAIL-R1 and TRAIL-R2 being detected in the TRAIL DISC, whereas around 100 fmol was detected in the unstimulated samples. This implies that activation of the receptors and their associated aggregation to form the DISC results in a greater detection efficiency, possibly by the recruitment of additional receptors that weren’t directly bound by bTRAIL added post-cell lysis. Alternatively the binding of bTRAIL may be less efficient once the cells have been lysed and the cell membrane structure is disrupted.

In addition to the canonical TRAIL DISC components described, 10 other proteins were identified in the unstimulated receptor isolation samples but not in the untreated control samples (Table 3.5). None of these proteins detected and confirmed as interacting with the TRAIL DISC using the “shotgun proteomics” method were detected in the “off-bead” processed samples. The loss of detection of these DISC-interacting proteins indicates that the “off-bead” method may be less sensitive compared to the “shotgun proteomics” method. Despite this, 10 additional proteins

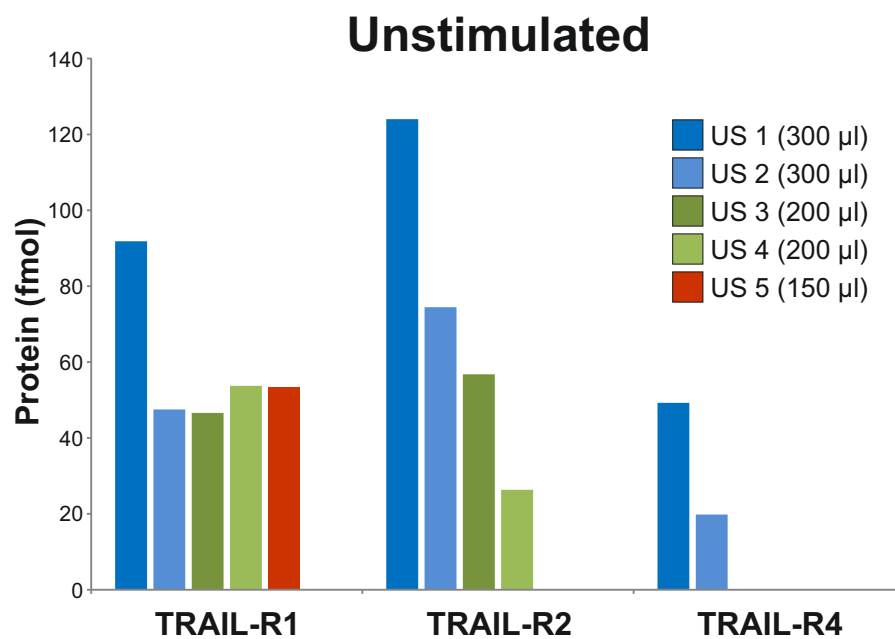


Figure 3.5: “Top Three” Label-free Quantitation of Unstimulated TRAIL-Receptors Isolated using the “Off-bead” Method

The “Top Three” label free quantitated values for TRAIL-R1, TRAIL-R2 and TRAIL-R4 from the mass spectrometry results described for the isolated unstimulated TRAIL-receptors (Table 3.4).

		Total Unique Peptides															
		DISC						US						UT			
Accession Number	Protein	1	2	3	4	5	6	1	2	3	4	5	6	1	2	3	4
OSBL8_HUMAN	Oxysterol-binding protein-related protein 8 (ORP8)	0	0	0	0	0	0	2	2	2	9	0	0	0	0	0	0
OSBL9_HUMAN	Oxysterol-binding protein-related protein 9 (ORP9)	0	0	0	0	0	0	8	1	1	6	0	0	0	0	0	0
HERC2_HUMAN	Probable E3 ubiquitin-protein ligase HERC2	0	0	0	0	0	0	6	7	1	1	0	0	0	0	0	0
OSB11_HUMAN	Oxysterol-binding protein-related protein 11 (ORP11)	0	0	0	0	0	0	6	5	5	4	0	0	0	0	0	0
FBXW5_HUMAN	F-box/WD repeat-containing protein 5	0	0	0	0	0	0	7	5	5	3	0	0	0	0	0	0
OSB10_HUMAN	Oxysterol-binding protein-related protein 10 (ORP10)	0	0	0	0	0	0	5	2	6	3	0	0	0	0	0	0
P20D2_HUMAN	Peptidase M20 domain-containing protein 2	0	0	0	0	0	0	5	2	0	0	0	0	0	0	0	0
KRT82_HUMAN	Keratin, type II cuticular Hb2	0	0	0	0	0	0	0	0	1	0	0	0	0	0	0	0
RLA2_HUMAN	60S acidic ribosomal protein P2	0	0	0	0	0	0	3	5	0	1	0	0	0	0	0	0
SKP1_HUMAN	S-phase kinase-associated protein 1	0	0	0	0	0	0	0	3	2	0	0	0	0	0	0	0

Table 3.5: Novel TRAIL-receptor-interacting Proteins Identified by Mass Spectrometry using the "Off-bead" Method

The total number of unique peptides of other proteins detected in the DISC samples (1-6) or unstimulated samples (US 1-6) but not the untreated samples (UT 1-4) from the mass spectrometry results detailed in Tables 3.3 and 3.4 are displayed.

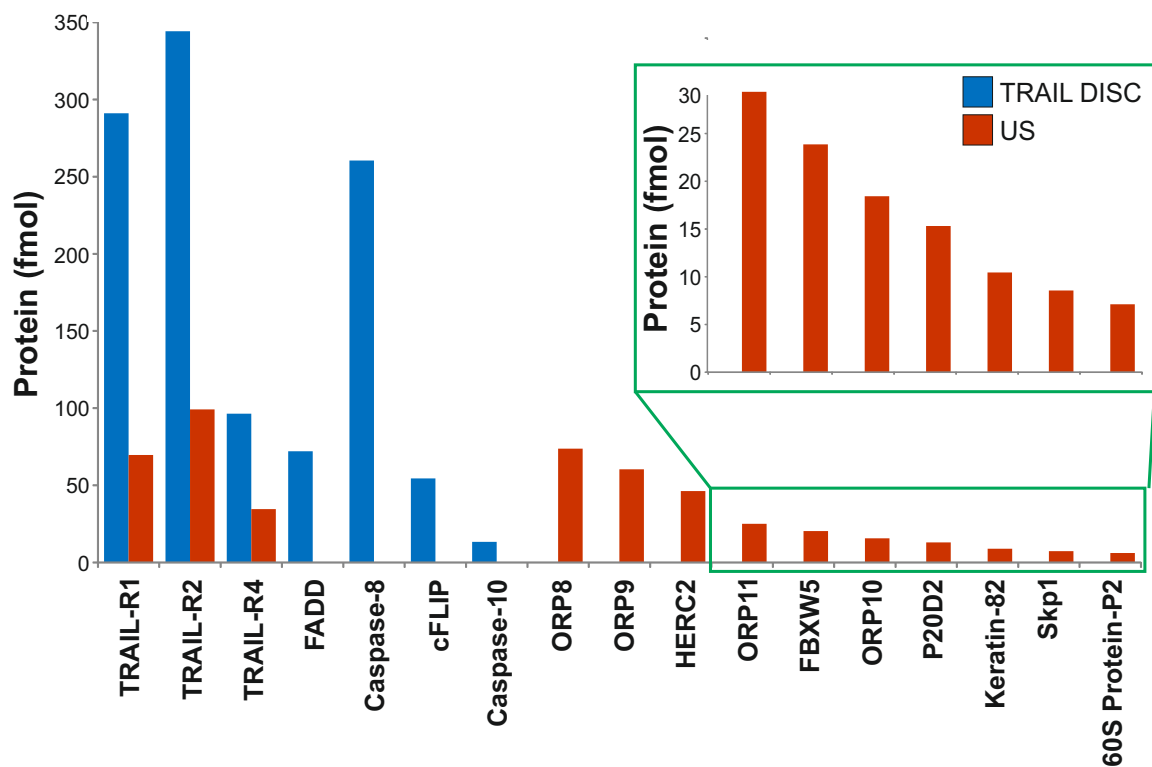


Figure 3.6: “Top Three” Label-free Quantitation of TRAIL DISC and Unstimulated TRAIL-R1/R2 Interacting Proteins

The “Top Three” label-free quantitated values from the mass spectrometry results for all proteins detected in the DISC 1 and DISC 2 samples from the experiment described in Table 3.5 are displayed. The “Top Three” values presented are the total amount of each protein detected in DISC 1 and DISC 2, divided by 2. The values for the known DISC components: TRAIL-R1, TRAIL-R2, TRAIL-R4, FADD, caspase-8, cFLIP and caspase-10 are indicated on the left.

were detected in the unstimulated samples but not in untreated control samples (Table 3.5). Among these proteins were four of the oxysterol binding protein (ORP) family, of which peptides were detected in the 300 μ l and 200 μ l isolations. HECT and RLD domain containing E3-ubiquitin ligase (HERC2) was also detected with a maximum of 73 peptides, a greater amount seen for any of the DISC proteins. "Top 3" values for the total amount of each potential TRAIL receptor-interacting protein (Figure 3.6) show that ORP8 and ORP9 were the most abundantly detected with 283.5 fmol and 252.2 fmol respectively. Despite the huge number of peptides detected for HERC2, only 124.7 fmol was present across all the samples. Further analysis of HERC2 reveals that it is a large protein at 527 kDa, composed of 4834 amino acids. Therefore the large number of peptides detected is not surprising, as there are simply a larger number of possible peptides to detect. The use of "Top 3" quantitation mitigates against the apparent high level detection of larger proteins, as only the three most abundant peptides are analysed. Other proteins detected, include ORP10 and ORP11, P20D2, Keratin, 60S ribosomal protein-P2 and S-phase kinase associated protein-1 (Skp-1)

3.3: Discussion

3.3.1: Summary of Chapter Findings

This Chapter has described experiments to optimise methods to analyse the precipitated TRAIL DISC and unstimulated TRAIL receptors by mass spectrometry. The experiments described have:

1. Shown that BJAB cells are sensitive to TRAIL-induced apoptosis and can form an active TRAIL DISC
2. Demonstrated that TRAIL-R1, TRAIL-R2, TRAIL-R4, FADD, caspase-8, cFLIP and caspase-10 can be optimally detected by mass spectrometry from the TRAIL DISC isolated from 500×10^6 BJAB cells, using 300 μ l streptavidin beads.
3. Identified novel TRAIL DISC-associated proteins by mass spectrometry.
4. Confirmed the detection of RIPK1 and TRADD with the TRAIL isolated DISC, whilst Tfr1 and PP2A-C were detected associated with both the TRAIL DISC and unstimulated TRAIL receptors.
5. Evaluated the use of both the “shotgun proteomics” and “off-bead” methods to analyse samples by mass spectrometry, showing that the “off-bead” method was less sensitive in detecting low abundance DISC interacting proteins.
6. Demonstrated that unstimulated TRAIL-R1, TRAIL-R2 and TRAIL-4 can be optimally detected by mass spectrometry from the TRAIL DISC isolated from 500×10^6 BJAB cells using 300 μ l streptavidin beads.
7. Identified proteins which are associated with the unstimulated TRAIL receptors
8. Utilised “Top 3” label-free quantitation to determine the amounts of each protein detected.

3.3.2: Optimisation of the Isolation and Detection of TRAIL DISC Proteins by Mass Spectrometry

The results demonstrate that TRAIL-R1, TRAIL-R2, TRAIL-R4, FADD, caspase-8, cFLIP and caspase-10 can be reliably detected by mass spectrometry (Tables 3.1 and 3.3). The optimal detection of the core DISC proteins was only achieved however when the volume of streptavidin beads used to isolate the DISC was revised. Isolating the TRAIL DISC using 300 μ l of beads resulted in detection of all canonical DISC proteins with a

much greater number of peptides and coverage than when 500 μl of beads were used (Table 3.1). In fact, the use of 500 μl of streptavidin beads to isolate the TRAIL DISC from 500×10^6 cells actually resulted in a worse detection of the majority of core DISC proteins than a previous isolation using 300 μl beads from only 300×10^6 cells. The detection of the bona fide DISC proteins could not be subsequently improved by further reduction of the volume of beads used (Table 3.3).

The requirement for the volume of beads to be optimised is due to a balance between the capacity of the streptavidin beads to bind bTRAIL and the surface area of the beads available for non-specific protein interactions. As shown, when the volume of beads used to isolate the DISC was reduced to 200 μl and below (Figure 3.4), there is a limit to how much a certain amount of streptavidin beads can bind to bTRAIL (and associated proteins). However, if the volume of beads used is too high then a greater amount of non-specific interactions can occur. As only a certain concentration of peptides can be loaded onto the mass spectrometer at once, a greater concentration of non-specific interacting proteins reduces the relative concentration and therefore specific detection of isolated proteins of interest.

3.3.3: Evaluation of Shotgun Proteomics and “Off-bead” Methods to Analyse Samples by Mass Spectrometry

Shotgun proteomic mass spectrometry analysis typically involves the initial separation of a sample by SDS-PAGE and loading of the sample onto the mass spectrometer as a series of sequential samples from the cut and digested gel. This method means that a single sample can take over 20 hours of machine time to be analysed (depending on the number of gel slices). The “off-bead” method however dispenses with the initial acrylamide gel separations and digests the sample in solution after elution from the beads. These tryptic peptides are then loaded onto the mass spectrometer as a single sample, therefore dramatically reducing the amount of time required for analysis. This “off-bead” method ideally works with less-complex samples and the affinity-based method of isolating TRAIL DISC interacting proteins should in principle be ideal.

TRAIL-R1, TRAIL-R2, TRAIL-R4, FADD, caspase-8, cFLIP and caspase-10 were all detected using both the shotgun (Table 3.1) and “off-bead” (Table 3.3) methods. The

number of peptides for each protein and the percentage amino acid coverage were roughly similar between the two methods (Table 3.1, DISC 3 and 4 vs Table 3.3, DISC 1 and 2). When the isolated TRAIL DISC was analysed using the shotgun method, 72 additional proteins were also identified in the DISC but not the control samples (Table 3.2). However, when the “off-bead” method was used to analyse the isolated TRAIL DISC, additional proteins to the core DISC components were not detected. The data show that although the “off-bead” method can be used to detect higher abundance proteins, it may not be sufficiently sensitive to identify unknown novel TRAIL DISC interacting proteins, which are most likely present in low abundance.

3.3.4: Identification of Novel TRAIL DISC-Associated Proteins by Mass Spectrometry

As discussed previously, analysis of the TRAIL DISC using the “shotgun proteomics” method identified 72 proteins which were present in the DISC samples but not in the untreated control samples. This is a marked improvement on a previous study from our lab, using a less sensitive mass spectrometer, which only detected one novel DISC associated protein, Transferrin Receptor 1 (TfR1) (Dickens, 2009). However, care must be exercised in labelling these proteins detected as interacting with the TRAIL-DISC. Many of these “hits” were detected with only one or two peptides in only one of the samples analysed by mass spectrometry. Therefore, novel interacting proteins detected in low abundance should be detected across multiple samples before they are considered as possible DISC-interacting proteins. The use of a secondary interaction assay, such as a yeast two-hybrid screen, could be used to confirm the interactions observed by mass spectrometry.

Excluding the known DISC components: TRAIL-R1, TRAIL-R2, TRAIL-R4, FADD, caspase-8, cFLIP and caspase-10, TfR1 was the most abundantly detected protein with a maximum of 18 unique peptides. Western blot analysis confirmed the interaction of TfR1 with the TRAIL DISC (Figure 3.3) and also detected the interaction of TfR1 with the unstimulated TRAIL receptors. This is in accordance with previous data from our lab which showed that TfR1 interacts with TRAIL-R1/R2 prior to TRAIL stimulation (Dickens et al, unpublished data). The role of TfR1 in TRAIL signalling was also previously investigated and was shown to have a small effect on TRAIL-R2 cell surface

levels (Dickens et al, unpublished data). As the role of Tfr1 has already been investigated, it was not followed up further in this study. In accordance with our previous study (Dickens et al., 2012a), CUL3 was not detected in the TRAIL DISC isolated from BJAB cells. This further supports the idea that the role of CUL3 in the regulation of TRAIL signalling (Jin et al., 2009) is specific to epithelial and not haematopoietic-derived cell lines (Dickens et al., 2012a).

Of the other identified DISC interacting proteins, a small selection for which there were available antibodies were confirmed by western blot analysis. RIPK1 and TRADD were confirmed as interacting with the TRAIL DISC but not the unstimulated TRAIL receptors (Figure 3.3). Although not components of the canonical active TRAIL DISC, both RIPK1 and TRADD have been observed in the DISC isolated from TRAIL-resistant cells (Kim et al., 2011; Ouyang et al., 2013). As BJAB cells are exquisitely sensitive to TRAIL-induced apoptosis (Figure 3.1), it is likely that the RIPK1 and TRADD detected here are associated with a small proportion of TRAIL DISC which is not actively signalling to apoptosis (Kim et al., 2011). Signalling through a non-apoptotic TRAIL DISC is likely able to activate pro-survival pathways associated with TRAIL signalling. TRAIL DISC activation of the NF κ B, p38 or JNK pathways could therefore be further analysed to determine if TRAIL is inducing pro-survival signalling in BJAB cells (Azijli et al., 2013). It would be interesting to know if the proportion of RIPK1 and TRADD detected through DISC isolations would increase if the TRAIL DISC was isolated from TRAIL-resistant cells. Cell lines can be made resistant to apoptotic induction through prolonged treatment with low concentrations of cell death agonists (Flusberg et al., 2013). Therefore, a BJAB cell line could be made TRAIL-resistant and the effect of this on the RIPK1/TRADD composition of the isolated TRAIL DISC analysed.

PP2A-C is the catalytic subunit of the serine/threonine phosphatase PP2A. Western blot analysis showed that PP2A-C was interacting both with the TRAIL DISC and unstimulated TRAIL receptors (Figure 3.3). In addition to PP2A-C, the scaffold A subunit of PP2A was also identified by mass spectrometry (Table 3.2). As PP2A is a phosphatase, any likely activity will revolve around the removal of phosphates from target proteins. As PP2A-C was shown to interact with the unstimulated receptors, this implies that the phosphatase may be removing phosphorylations from the TRAIL-

R1/R2 directly. Alternatively, PP2A could be acting upon one of the other proteins shown to be isolated along with the TRAIL DISC.

3.3.5: Detection of Unstimulated TRAIL receptors and Associated Proteins by Mass Spectrometry

Whilst western blot analysis for TfR1, PP2A-C, RIPK1 and TRADD confirmed their interactions with the TRAIL DISC (Figure 3.3), they also showed that TfR1 and PP2A-C could additionally be detected in the unstimulated TRAIL receptor samples. Their presence implies that these proteins are interacting with the TRAIL receptors prior to TRAIL stimulation. There have already been reports in the literature of the regulation of TRAIL signalling by proteins which interact with these TRAIL receptors not associated with the DISC (Ren et al., 2004; Tanaka et al., 2009; van de Kooij et al., 2013).

TRAIL-R1, TRAIL-R2 and TRAIL-4 were successfully detected by the addition of bTRAIL to lysates produced from BJAB cells (Table 3.4). Again, optimal detection of the TRAIL receptors occurred using 300 μ l of streptavidin beads and 500×10^6 cells. In addition, 10 proteins were detected in the unstimulated samples but not in the control samples. These included 4 members of the oxysterol binding protein family: ORP8, ORP9, ORP10 and ORP11 which are pre-dominantly described as regulators of cholesterol and lipid transport, although signalling roles are beginning to be identified (Raychaudhuri and Prinz, 2010; Wang et al., 2005). The probable E3 ubiquitin ligase HERC2 was detected with a maximum of 73 peptides, higher than that observed for any of the DISC proteins (Table 3.4). In addition, F-box/WD repeat containing protein 5 (FBXW5) was detected which could possibly interact with HERC2 and form an ubiquitin ligase complex. Skp1 has also been shown to appear in ubiquitin-ligase complexes and was detected, albeit at low levels. These proteins were detected using the “off-bead” method, which as discussed above is less sensitive than the “shotgun proteomics” method. Indeed, TfR1 and PP2A-C were demonstrated by western blot analysis to interact with the unstimulated TRAIL receptors but were not detected using the “off-bead” method. Therefore, it is likely that even more TRAIL receptor-associated proteins could be detected if the experiment were to be repeated using the shotgun method.

As demonstrated by the unstimulated TRAIL receptor isolations, bTRAIL treatment efficiently isolated both TRAIL-R1 and TRAIL-R2. As the two death receptors are not thought to interact prior to stimulation by TRAIL, it is therefore likely that the TRAIL receptor-associated proteins detected could be specifically interacting with either TRAIL-R1 or TRAIL-R2. The detection of such specific interactions could lead to the discovery of regulatory mechanisms which function solely through TRAIL-R1 or TRAIL-R2 and should be investigated further.

3.3.6: Using “Top 3” Label-free Quantitation to Determine the Amount of Detected Proteins by Mass Spectrometry

Although mass spectrometry is inherently non-quantitative, due to differences in ionisation efficiency or detectability of the different peptides in a sample, methods have been developed to enable the amount of a protein detected to be quantified (Reviewed by Nikolov et al., 2012). The method employed in this study is “Top 3” label-free quantitation, which involves the comparison of the amount of the “Top 3” most abundant peptides of each protein with those of a standard protein of known amount spiked into the sample. “Top 3” quantitation has been demonstrated to give a more accurate estimation than other methods which seek to compare the number of different spectra detected for each protein (Fabre et al., 2014).

The “Top 3” values calculated were able to show the quantity of each of the DISC proteins: TRAIL-R1, TRAIL-R2, TRAIL-R4, FADD, caspase-8, cFLIP and caspase-10 (Figure 3.4). The results confirmed that FADD was present at a much lower level than TRAIL-R1, TRAIL-R2 or caspase-8. This correlates with a previous study from our lab (Dickens et al., 2012a) which demonstrated that FADD binding to aggregated TRAIL receptors recruits multiple caspase-8 molecules, thus explaining FADD sub-stoichiometry. The results also showed that the amounts of TRAIL-R1, TRAIL-R2, TRAIL-R4, FADD, caspase-8, cFLIP and caspase-10 detected decreased as the volume of streptavidin beads used to isolate the TRAIL DISC decreased below 200 μ l (Figure 3.4). This reduction in the amount of each protein correlated with a reduction in the number of unique peptides detected for each protein (Table 3.3). In addition, the amount of each TRAIL receptor detected in the unstimulated samples also reduced with the reducing bead volume (Figure 3.5). In these samples, 10 proteins were identified, which were not observed in

the bead only controls. “Top 3” quantitation of these proteins revealed that ORP8 and ORP9 were detected in similar amounts to TRAIL-R1 and TRAIL-R2, indicating a significant interaction. The use of the “Top 3” data meant that HERC2, which had four times more peptides detected than TRAIL-R2, was actually shown to be present at a lower abundance. The increased number of peptides detected was purely due to the greater molecular weight (527 kDa) of HERC2.

In conclusion, this chapter has led to the development of an improved platform to investigate isolated TRAIL DISC composition and stoichiometry as well as unstimulated TRAIL-R1/R2 by quantitative label-free mass spectrometry. The TRAIL DISC and TRAIL-R1/R2 can be optimally isolated from 500×10^6 BJAB cells, using 0.5 $\mu\text{g/ml}$ bTRAIL and 300 μl streptavidin beads. To investigate the role of novel TRAIL-R1/R2 or DISC-interacting proteins, samples should be further analysed using “shotgun proteomics” and the amount of protein determined by “Top 3” label-free quantification.

***Chapter 4: Identification of Novel TRAIL-R1/R2
Specific Mechanisms of Regulation***

Chapter 4: Identification of Novel TRAIL-R1/R2 Specific Mechanisms of Regulation

4.1 Introduction

TRAIL is unique among the TNF-cytokine family of death ligands as humans (and chimpanzees) express two functional death receptors, TRAIL-R1 and TRAIL-R2, which can form the DISC and signal to apoptosis. The significance of having both TRAIL-R1 and TRAIL-R2 is unclear, as most other organisms (including rodents) express only one TRAIL death receptor (van Roosmalen et al., 2014). It has not yet been conclusively shown whether the two receptors perform identical roles or whether functional differences exist between them.

There have been reports however of differences in sensitivity to cell death induced by TRAIL-R1 or TRAIL-R2 in different cancer cell lines. Haematopoietic tumour-derived cells appear to be sensitive only to TRAIL-R1-induced apoptosis (Kohlhaas et al., 2007; MacFarlane et al., 2005a; MacFarlane et al., 2005b; Natoni et al., 2007; Szegezdi et al., 2011; Tur et al., 2008), despite the expression of both TRAIL-R1 and TRAIL-R2. The Jurkat T cell line is however a notable exception, in that it does not express TRAIL-R1 and therefore can only be sensitive to TRAIL-R2-induced apoptosis (Gasparian et al., 2009). Cell lines derived from solid malignancies show mixed sensitivity to TRAIL-R1 and/or TRAIL-R2-induced apoptosis (reviewed in detail by van Roosmalen et al., 2014). The reasons for cells being sensitive to either TRAIL-R1 or TRAIL-R2-mediated cell death are not completely understood. Multiple mechanisms have been described which may impact on TRAIL sensitivity. Loss of TRAIL receptor expression is an obvious factor determining TRAIL sensitivity. Deleterious mutations of TRAIL-R1/R2 genes has only rarely been reported (van Roosmalen et al., 2014), however epigenetic silencing of TRAIL-R1 has been observed (Horak et al., 2005). Cells undergoing ER-stress selectively increase TRAIL-R2 expression (Lu et al., 2014a). Control of TRAIL receptor surface expression and activity by direct protein binding has also been demonstrated. Signal recognition particle (SRP) SRP72 and SRP54 (Ren et al., 2004), and Arf and Rho GAP adaptor protein (ARAP1), (Símová et al., 2008) were all demonstrated to control TRAIL-R1 cell surface levels by effecting intracellular trafficking. O-glycosylation of

TRAIL-R1 and TRAIL-R2 was demonstrated to increase TRAIL sensitivity (Wagner et al., 2007), palmitoylation of TRAIL-R1 was shown to increase recruitment to lipid rafts and subsequently increase TRAIL signalling (Rossin et al., 2009). The selective binding of DDX3 to TRAIL-R2 and subsequent disruption of DISC formation was shown to selectively inhibit apoptosis by a TRAIL-R2 agonist (Li et al., 2006). The detection of these regulatory mechanisms, and in particular those caused by TRAIL-R1/R2 modulation via protein binding, raises the possibility that currently unknown mechanisms also exist.

Understanding the mechanisms which determine whether cells are sensitive to TRAIL-R1 or TRAIL-R2 may be critical in developing new strategies to overcoming resistance to TRAIL based therapeutics. To identify novel TRAIL-R1/R2 regulatory mechanisms, the TRAIL DISC and unstimulated TRAIL-R1/R2 were isolated using TRAIL-R1 and TRAIL-R2-selective mutants previously generated in our (MacFarlane et al., 2005b; Natoni et al., 2007). Utilising the platform developed in Chapter 3 enabled proteins which specifically interact with TRAIL-R1 or TRAIL-R2 to be identified by mass spectrometry. Those proteins were then assayed for their role in regulating sensitivity to TRAIL-induced apoptosis mediated by TRAIL-R1 or TRAIL-R2.

4.2: Results

4.2.1: BJAB Cells are Sensitive to TRAIL-induced Apoptosis Mediated by TRAIL-R1

To determine the effect of selectively targeting either TRAIL-R1 or TRAIL-R2 cells, 1×10^6 BJAB cells were treated with $1 \mu\text{g/ml}$ of wild-type (WT) TRAIL or a mutant form of TRAIL specific for TRAIL-R1 (R1) or TRAIL-R2 (R2) for 5 h (Figure 4.1). Apoptosis was measured by the percentage of cells displaying annexin-V binding to externalised phosphatidylserine (PS) (Figure 4.1 A). WT TRAIL induced 83.0% cell death as compared to 12.9% cell death in untreated cells. Selectively targeting TRAIL-R1 with the TRAIL-R1-specific mutant also induced a high level of cell death with 61.6% of cells displaying annexin-V positive staining. However, when BJAB cells were treated with the TRAIL-R2-specific TRAIL mutant only 21.7% of cells displayed annexin-V staining, which was shown not to be significantly different from the untreated cells. Western blots probed for caspase-8, caspase-9, caspase-3 and PARP (Figure 4.1 B) correlated with the FACs data (Figure 4.1 A). WT TRAIL treatment (Lane 2) induced the cleavage of caspase-8 to its p43/p41 and p18 signature fragments, demonstrating that caspase-8 had been activated and self-processed. WT TRAIL treatment induced the cleavage of caspase-9 to its p37 and p35 fragments, with the p37 fragment predominating. The abundance of the p37 fragment indicates that caspase-9 had been processed by activated caspase-3 rather than by caspase-9 self-processing in the apoptosome. This is in accordance with BJAB cells being classed as Type I cells (Scaffidi et al., 1998) and therefore not requiring intrinsic pathway activation for TRAIL to induce apoptosis. Caspase-3 was demonstrated to be fully activated by the complete processing and maturation to its p17 fragment. From the western blot analysis it is also clear that the TRAIL-R1-targeting TRAIL mutant (Lane 3) is also activating the apoptotic pathway, as caspase-8, caspase-9, caspase-3 and PARP are all shown to be cleaved. Cleavage fragment generation is similar to that observed with WT TRAIL, although with slightly reduced loss of the proforms/appearance of corresponding cleavage fragments. In addition, incomplete maturation of the caspase-3 p20 fragment to p17 agrees with the reduced apoptosis induction highlighted by FACs analysis (Figure 4.1 A). Caspase-8 cleavage was undetectable in samples from TRAIL-R2-specific mutant TRAIL-treated

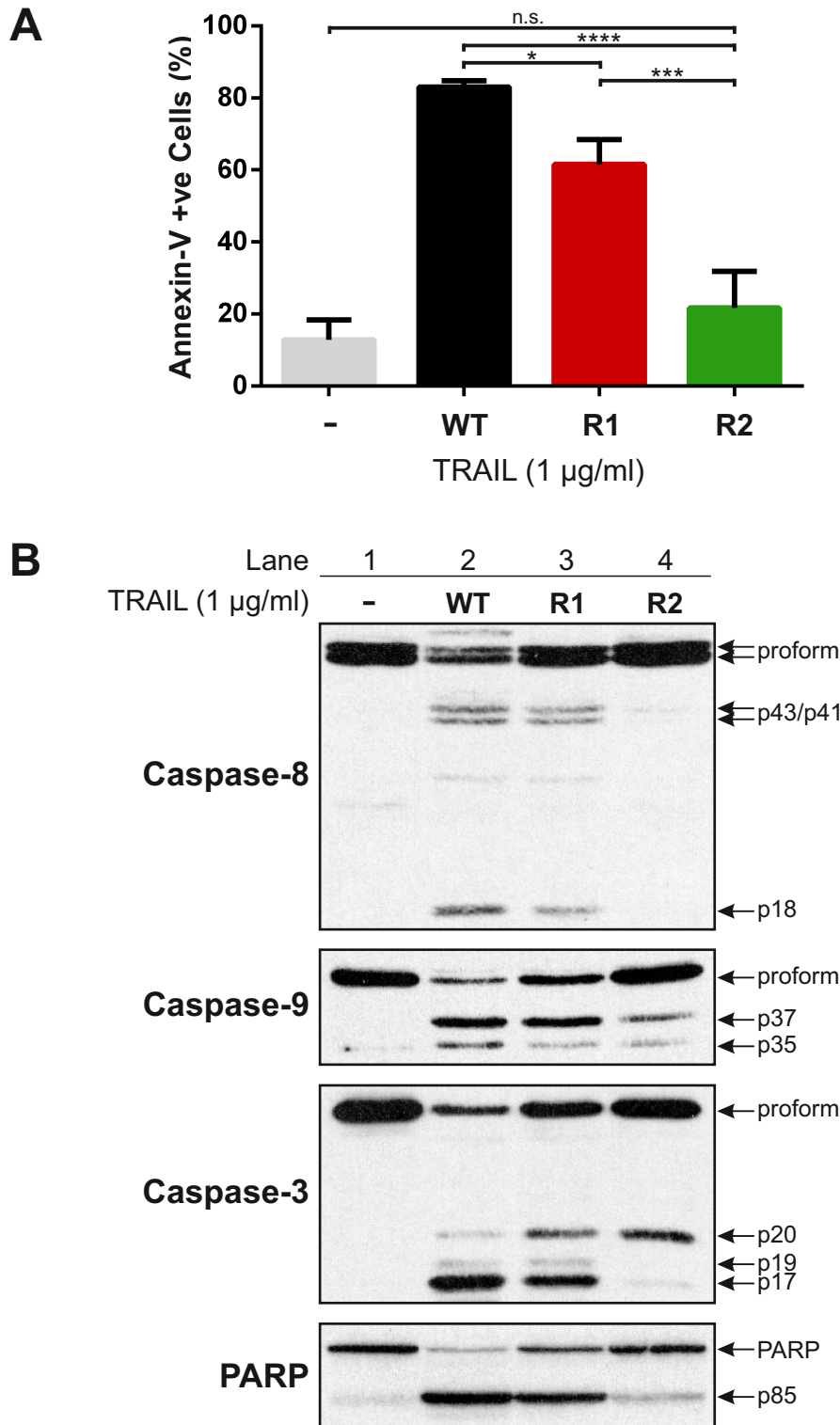


Figure 4.1: WT and TRAIL-R1-Specific TRAIL Mutants-Induce Apoptosis in BJAB Cells
 1×10^6 BJAB cells were treated with either 1 µg/ml wild-type (WT) TRAIL or 1 µg/ml TRAIL-R1 or TRAIL-R2-specific mutant TRAIL for 5 hours. Cells were stained with Annexin-V-FITC and DRAQ7 and cell death analysed by flow cytometry (A). Western blots performed from cell pellets were probed for caspase-8, caspase-9, caspase-3 and PARP (B). Data shown in A is % Annexin-V-FITC positive cells from 3 independent experiments +/- standard deviation (SD). Differences between the group means were shown to be statistically different by one-way ANOVA. Significant differences were determined by a post-hoc tukey test and are highlighted by * ($P < 0.05 = *$, $P < 0.01 = **$, $P < 0.001 = ***$, $P < 0.001 = ****$).

cells (Lane 4) and was indistinguishable from the untreated sample (Lane 1). Cleavage of caspase-9 to p37 and p35 (Lane 4) was detected at higher levels than in the untreated cells (Lane 1), although at much lower levels than observed in the WT (Lane 2) or TRAIL-R1-specific TRAIL (Lane 3) samples. Similarly, caspase-3 cleavage was detected in the TRAIL-R2-specific TRAIL-treated cells (Lane 4), however there is almost no processing of the p20 fragment to the fully active p17 fragment. This showed that the TRAIL-R2-specific TRAIL can activate the TRAIL apoptotic machinery but at too low a level to induce apoptosis in BJAB cells. This is mirrored when you consider the PARP western blots. Whereas WT (Lane 2) and TRAIL-R1-targeting TRAIL (Lane 3) induce significant cleavage of PARP to the p85 fragment, TRAIL-R2-targeting TRAIL (Lane 4) induces only slightly more PARP cleavage than observed in untreated cells (Lane 1). Taken together, these results show that BJAB cells signal to apoptosis almost exclusively via the activation of TRAIL-R1.

4.2.2: Successful Isolation of TRAIL DISC and Unstimulated TRAIL Receptors using TRAIL-R1/R2-specific biotinylated TRAIL Mutants

It was then determined if the TRAIL-R1 and TRAIL-R2-selective mutants could be used to induce formation of a TRAIL-R1/R2 DISC for subsequent isolation and analysis by mass spectrometry. Accordingly, 500×10^6 BJAB cells were treated with either 0.5 $\mu\text{g/ml}$ WT, TRAIL-R1-specific or TRAIL-R2-specific biotinylated TRAIL (bTRAIL) and incubated on ice for 1 h followed by incubation at 37°C for 10 min. Cells were then lysed and the DISC isolated using 300 μl of streptavidin beads (Dynabeads). In addition, 0.5 $\mu\text{g/ml}$ of each of the bTRAIL variants were added to lysates obtained from untreated cells, post-lysis and unstimulated TRAIL-R1/R2 isolated using 300 μl streptavidin beads. After elution into sample buffer, western blots were performed from a small fraction of each sample (7.5 μl of 70 μl sample) to confirm the DISC had been successfully isolated (Figure 4.2). The input samples confirmed the same amount of FADD and caspase-8 was present in the lysates from which each of the samples was isolated. TRAIL-R1 and TRAIL-R2 could not be detected in the input samples and instead require bead precipitation to be detected by western blot analysis. In the WT bTRAIL-treated samples TRAIL-R1 and TRAIL-R2 were detected in both the unstimulated (Lane 9) and WT DISC (Lane 12) isolations. In the TRAIL-R1-specific

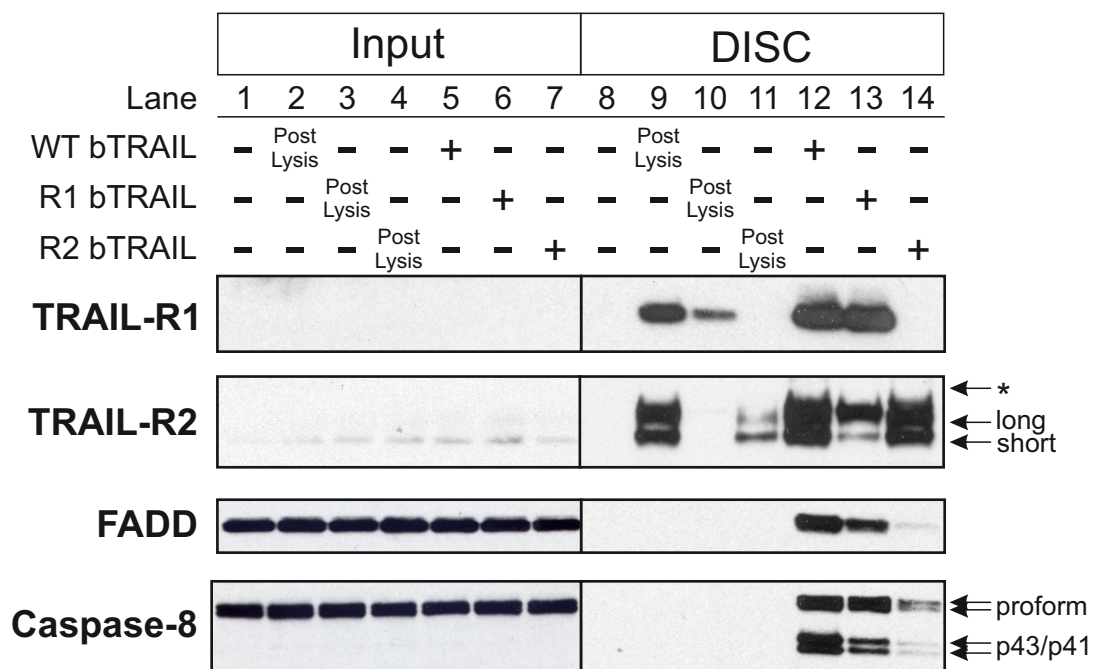


Figure 4.2: Isolation of the TRAIL DISC and Unstimulated TRAIL-Receptors using WT and TRAIL-R1/R2-specific Mutant bTRAIL

500 x 10⁶ BJAB cells were treated with 0.5 µg/ml wild-type (WT) or TRAIL-R1 (R1) or TRAIL-R2 (R2)-specific bTRAIL mutants. Cells were then lysed and the DISC isolated by incubation with 300 µl streptavidin beads. WT, TRAIL-R1-specific and TRAIL-R2-specific bTRAIL was also added to untreated cells post-lysis and unstimulated TRAIL-receptors isolated by incubation with 300 µl streptavidin beads. DISC and Unstimulated TRAIL-Receptor isolations were eluted into 70 µl sample buffer. Input samples were taken immediately before addition of streptavidin beads. Western blots were performed from 7.5 µl of each sample and probed for TRAIL-R1, TRAIL-R2, FADD and caspase-8.

bTRAIL-treated samples, TRAIL-R1 and TRAIL-R2 were both detected in the DISC isolation (Lane 13) but only TRAIL-R1 was detected in the unstimulated sample (Lane 10), displaying TRAIL-R1 mutant specificity. The detection of TRAIL-R2 in the TRAIL-R1-selective bTRAIL-treated DISC isolations is explained by the fact that the TRAIL receptors have been shown to hetero-trimerise upon ligand binding (Kischkel et al., 2000; MacFarlane et al., 2005b; Schneider et al., 1997). The amount of TRAIL-R2 detected in the TRAIL-R1-specific bTRAIL DISC isolations is however lower than in the WT, demonstrating that the ability of WT TRAIL to bind to both TRAIL-R1 and TRAIL-R2 results in more TRAIL-R2 being detected in the DISC. In the TRAIL-R2-specific bTRAIL-treated samples, TRAIL-R2 but not TRAIL-R1 is detected in the DISC isolation (Lane 14). Again, only TRAIL-R2 is detected in the unstimulated (Lane 11) sample, although at a much lower level than the WT bTRAIL unstimulated sample (Lane 9). Both WT and TRAIL-R1-selective bTRAIL treatment successfully induced both FADD and caspase-8 recruitment to the DISC (Lanes 12 and 13), with their levels being slightly reduced with the TRAIL-R1-specific bTRAIL. FADD and caspase-8 were detected in the TRAIL-R2-selective bTRAIL DISC isolation (Lane 14), however at a much lower level than observed for the WT or TRAIL-R1-selective bTRAIL samples (Lanes 12 and 13). These results demonstrated that the TRAIL receptors and TRAIL DISC were successfully isolated using WT, TRAIL-R1-selective and TRAIL-R2-selective bTRAIL. The greater amount of DISC proteins detected using the TRAIL-R1-selective bTRAIL compared to the TRAIL-R2-selective bTRAIL again confirms that TRAIL signalling in BJAB cells is primarily mediated through TRAIL-R1 activation.

The remainder of the samples were analysed by mass spectrometry using the “shotgun proteomics” method (Chapter 3). The data confirmed TRAIL-R1, TRAIL-R2, FADD and caspase-8 detection, in addition to TRAIL-R4 and the other canonical DISC-interacting proteins cFLIP and caspase-10 (Figure 4.3) using WT and TRAIL-R1-specific bTRAIL. All of the proteins except for FADD, TRAIL-R4 and caspase-10 were also detected using TRAIL-R2-specific bTRAIL. “Top 3” label-free quantitation of the DISC proteins shows that TRAIL-R1 and TRAIL-R2 were detected at similar levels (315.0 fmol and 257.1 fmol respectively) in the DISC isolated with WT bTRAIL (Figure 4.3 A). This contrasts with the TRAIL receptor selective bTRAIL DISC isolations. TRAIL-R1-specific

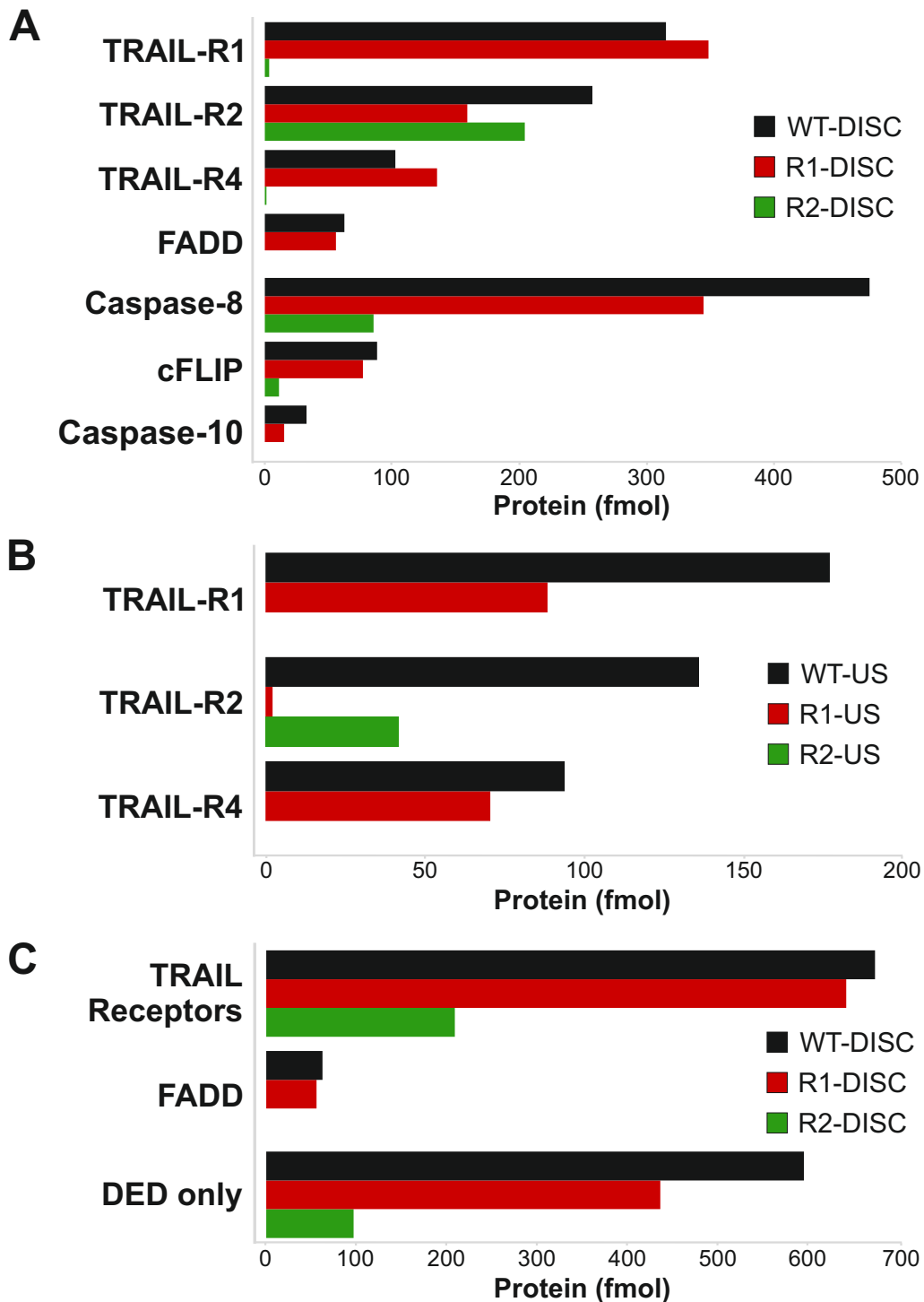


Figure 4.3: Label-free “Top 3” Quantitation of TRAIL DISC Components and Unstimulated TRAIL-Receptors using TRAIL-R1/R2-Specific bTRAIL Ligands

The remaining samples from Figure 4.2 were separated by SDS-PAGE and analysed by mass spectrometry using the “shotgun proteomics” method. “Top Three” label-free quantitative values for the TRAIL DISC components were calculated: TRAIL-R1, TRAIL-R2, TRAIL-R4, FADD, caspase-8, cFLIP and caspase-10 in the wild-type (WT), TRAIL-R1-specific (R1) or TRAIL-R2-specific (R2) bTRAIL-treated samples are shown in **A**. Quantitation of TRAIL-R1, TRAIL-R2 and TRAIL-R4 in the WT, R1 and R2-unstimulated (US) samples are shown in **B**. Peptides were not detected from FADD, caspase-8, cFLIP or caspase-10 in the US samples. The total amount of TRAIL-R1, -R2 and -R4 (TRAIL Receptors), FADD and the DED-only containing proteins: caspase-8, cFLIP and caspase-10 detected in each of the DISC samples is shown in **C**.

bTRAIL recruited substantially more TRAIL-R1 than TRAIL-R2 (348.3 fmol and 159.1 fmol respectively), whereas the R2 specific bTRAIL almost exclusively recruited TRAIL-R2 rather than TRAIL-R1 (204.3 fmol and 3.4 fmol respectively). In addition to the TRAIL death receptors, TRAIL-R4 was detected in both the WT and TRAIL-R1-specific bTRAIL DISC isolations, but not in the TRAIL-R2-specific bTRAIL DISC.

Slightly more FADD was detected in the WT bTRAIL DISC sample than the TRAIL-R1-specific bTRAIL, with 62.4 fmol and 55.8 fmol, respectively (Figure 4.3 A), which is comparable to that observed in the western blot analysis (Figure 4.2). No FADD was detected in the TRAIL-R2-specific bTRAIL DISC sample (Figure 4.3 A). This contrasts with the western blot analysis (Figure 4.2), which showed low levels of FADD recruitment, and is most likely due to the level of FADD not reaching the threshold required for its detection by mass spectrometry. The presence of low levels of FADD in the TRAIL-R2-specific bTRAIL DISC sample can however be inferred as caspase-8, which is only recruited to the DISC via binding to FADD (Sprick et al., 2000), was detected (Figure 4.3 A). The levels of caspase-8 were greatest in the WT bTRAIL DISC sample with 474.8 fmol detected as compared to 344.5 fmol for the TRAIL-R1-specific bTRAIL DISC, and only 85.5 fmol in the TRAIL-R2-specific bTRAIL DISC. The reduced recruitment of caspase-8 to the R2-specific DISC is likely to be due to loss of FADD binding, as less cFLIP, which is also recruited via caspase-8/FADD chain assembly (Hughes et al., 2016), was detected. For the TRAIL-R2-specific DISC, 11.2 fmol was detected, which was substantially lower than for the WT or TRAIL-R1-specific DISC with 88.2 fmol and 77.1 fmol, respectively. In addition, caspase-10 was not detected in the TRAIL-R2-specific DISC, which may indicate a difference between TRAIL-R1 and TRAIL-R2-selective DISC formation, but is most likely also due to lower levels of FADD recruitment. Also, caspase-10 was only detected in low amounts in the WT and TRAIL-R1-specific TRAIL DISC at 32.7 fmol and 15.1 fmol, respectively.

TRAIL-R1 was detected in both the WT and TRAIL-R1-specific bTRAIL unstimulated samples, with 176.8 fmol and 88.3 fmol, respectively (Figure 4.3 B). The lower amount of TRAIL-R1 detected with TRAIL-R1-specific bTRAIL may reflect a reduced affinity caused by mutating the protein to achieve specificity (MacFarlane et al., 2005b). Importantly though, TRAIL-R1 was not detected with the TRAIL-R2-specific bTRAIL,

which correlates with the western blot analysis (Figure 4.2) and confirms the specificity of the ligands. TRAIL-R2 was predominantly detected in both the WT and TRAIL-R2-specific unstimulated samples, with 135.8 fmol and 41.8 fmol, respectively (Figure 4.3 B). TRAIL-R2 was detected with the TRAIL-R1-specific bTRAIL, although at a significantly lower level of only 2.2 fmol which supports the strong TRAIL-R1 specificity. Similarly to that seen in DISC samples (Figure 4.3 A), TRAIL-R4 was also detected in the WT and TRAIL-R1-specific bTRAIL unstimulated samples (Figure 4.3 B) at 93.7 fmol and 70.4 fmol, respectively. TRAIL-R4 was not detected in the TRAIL-R2-specific bTRAIL samples (Figure 4.3 A and B), which contradicts previous reports of a TRAIL-R2-specific association of TRAIL-R4 (Mérino et al., 2006).

When comparing the combined total of TRAIL receptors to FADD and the DED-only proteins (caspase-8, cFLIP and caspase-10) (Figure 4.3 C), it is apparent that the amount of FADD is sub-stoichiometric and thus correlates with previous studies from our laboratory (Dickens et al., 2012a). In the WT bTRAIL DISC the ratio of TRAIL receptors : FADD : DED-only proteins is 10.8 : 1 : 9.5, which compares with a ratio of 11.5 : 1 : 7.8 for the TRAIL-R1-specific bTRAIL DISC. Comparing the ratios in this manner makes it apparent that slightly less DED-only proteins were recruited to the TRAIL-R1-specific bTRAIL DISC, possibly indicating shorter DED-mediated filaments of caspase-8, caspase-10 and cFLIP (Dickens et al., 2012a). The above ratio cannot be deduced for the TRAIL-R2-specific bTRAIL as FADD was not detected, but the amount of DED proteins detected compared to TRAIL receptors was much lower in comparison to that observed in the WT and TRAIL-R1-specific bTRAIL DISC.

4.2.3: Identification of Novel TRAIL Receptor-Interacting Proteins by Mass Spectrometry

The mass spectrometry experiments detected 2018 different proteins in the untreated (UT), unstimulated (US) and isolated DISC samples (Figure 4.4). Of these, 102 proteins were not detected in any of the untreated control samples. These proteins can be subdivided into those detected: only in the isolated DISC (18); Detected only in the unstimulated samples (6); and proteins which were detected in both DISC and unstimulated samples (78) (Figure 4.4 A). The core DISC components (FADD, caspase-8, cFLIP and caspase-10) were only recruited to the DISC after TRAIL receptor

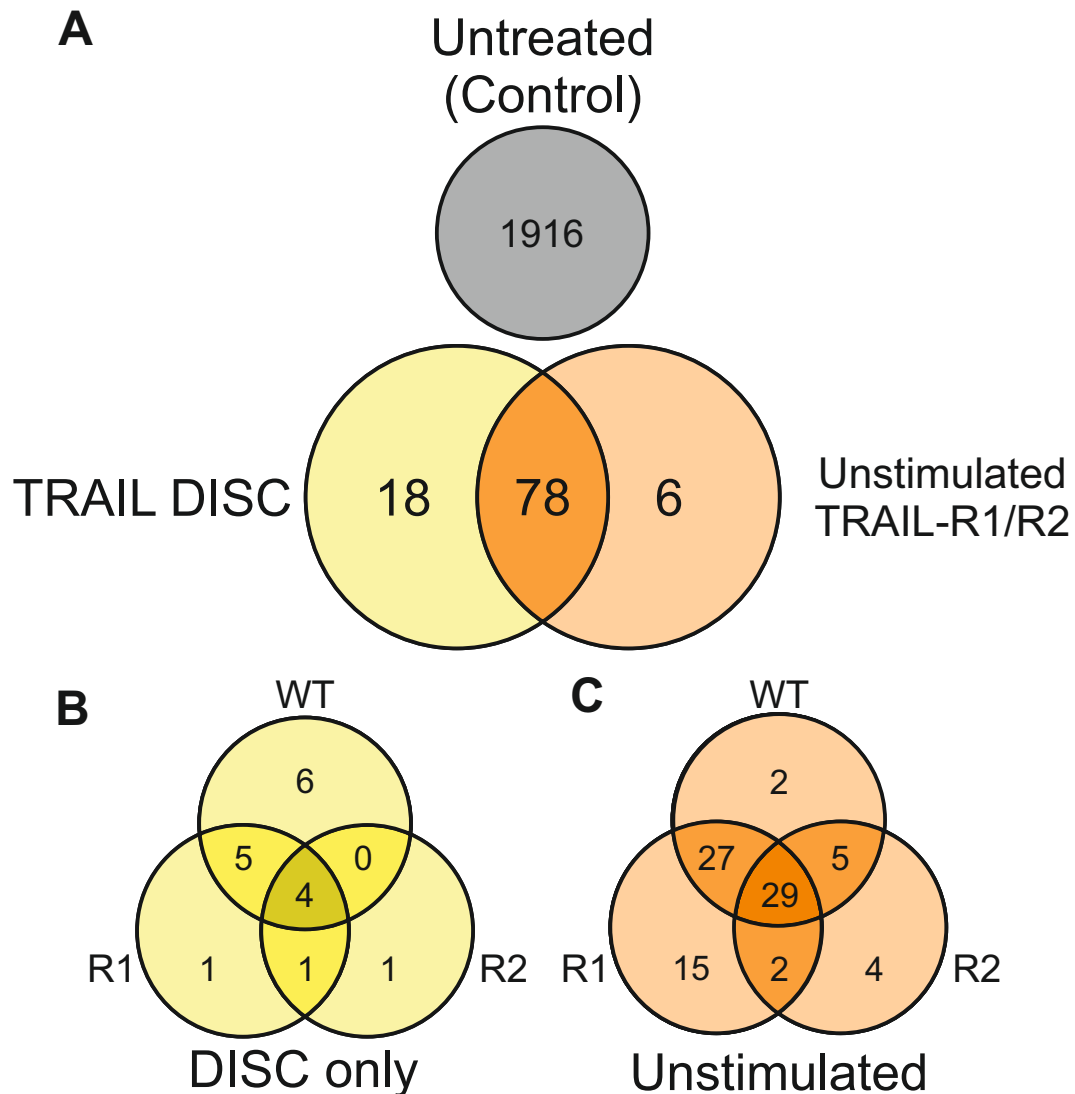


Figure 4.4: Venn Diagram of Identified TRAIL DISC and Unstimulated TRAIL-R1/R2-Interacting Proteins

2018 proteins were detected across the 3 DISC samples, 3 unstimulated (US) samples and 4 untreated (3/4 detailed in Chapter 3) samples analysed. Using Scaffold to identify the proteins detected, proteins were identified, which were not detected, in any of the untreated samples. “Top Three” quantitated values for the amounts of these 102 proteins were then extracted from the PLGS files. The “Top Three” quantitated protein amounts were used to determine the distribution of the proteins across the DISC and US samples from the wild-type (WT) bTRAIL or TRAIL-R1 (R1) or TRAIL-R2 (R2) specific bTRAIL samples. Proteins were defined as being in one category if over 95% of the detected protein amount was observed in that category. **A** Venn diagram showing the number of proteins detected in the DISC and US samples and those proteins discarded as they were detected in the untreated control samples. **B** Venn diagram showing proteins detected exclusively in the DISC samples, categorised according to those detected in the wild-type (WT) bTRAIL or TRAIL-R1 (R1) or TRAIL-R2 (R2)-specific bTRAIL-treated samples. **C** Venn diagram showing proteins detected in any of the US samples, categorised according to those detected in the wild-type (WT) bTRAIL or TRAIL-R1 (R1) or TRAIL-R2 (R2)-specific bTRAIL unstimulated samples.

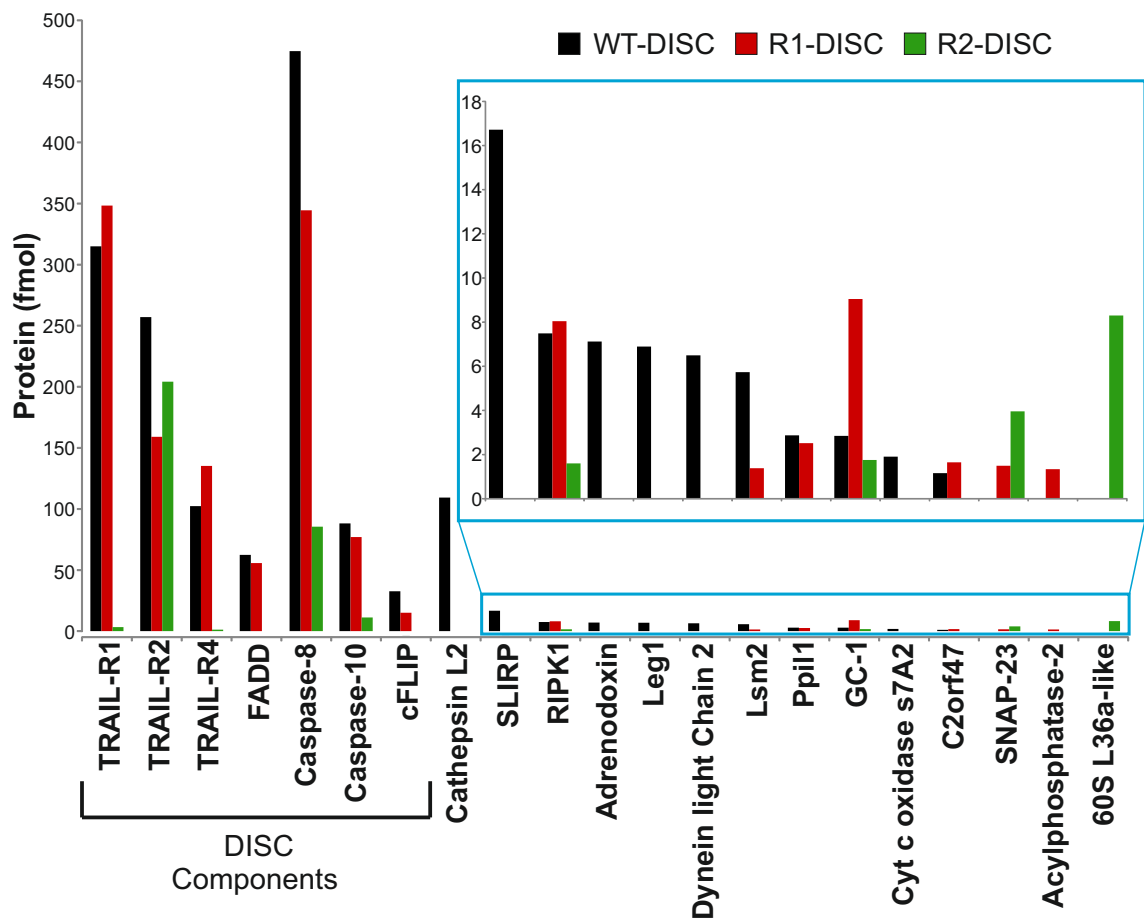


Figure 4.5: Novel DISC-only Interacting Proteins Identified by Mass Spectrometry

“Top Three” quantitated values for the proteins only detected the DISC samples (Figure 4.4 B), in addition to TRAIL-R1, TRAIL-R2 and TRAIL-R4, are displayed. The known DISC components: TRAIL-R1, TRAIL-R2, TRAIL-R4, FADD, caspase-8, caspase-10 and cFLIP are shown on the left, followed by the novel DISC-interacting proteins identified.

stimulation. Hence, novel DISC-interacting proteins should only be detected in the isolated DISC and not in the unstimulated samples. There were 18 DISC-only proteins detected, which could then be sub-divided into those detected in the WT, TRAIL-R1-specific and TRAIL-R2-specific bTRAIL DISC samples (Figure 4.4 B). TRAIL receptors are detected in both the DISC and unstimulated (US) samples (Figure 4.3 A and B), and therefore, proteins which specifically interact with the TRAIL receptors, independent of ligand stimulation are likely to be present in both DISC and US samples. To determine specific TRAIL-R1 and TRAIL-R2-interacting proteins, proteins were identified which were detected in the TRAIL-R1-specific bTRAIL unstimulated sample, but not with TRAIL-R2-specific bTRAIL. In addition, proteins were identified which were detected in the TRAIL-R2-specific bTRAIL unstimulated sample but not with TRAIL-R1-specific bTRAIL (Figure 4.4 C).

Figure 4.5 shows those proteins detected in the isolated DISC (Figure 4.4 B), in addition to the TRAIL receptors, TRAIL-R1, TRAIL-R2 and TRAIL-R4. Cathepsin L2, was detected at a level comparable to that of FADD and caspase-10 in the WT bTRAIL DISC sample. Of those proteins detected at a lower level, two were detected in all three of the DISC samples: RIPK1 and mitochondrial glutamate carrier 1 (GC-1). RIPK1 has previously been shown to be detected in the TRAIL DISC in TRAIL resistant cells (Bellail et al., 2010; Cao et al., 2011; Harper et al., 2001) and its detection highlights the ability of the method to detect even low level DISC interacting proteins. Stem-loop interacting RNA binding protein (SLIRP), adrenodoxin, Leg1, dynein light chain 2 and cytochrome c oxidase s7a2 were detected at low levels only in the WT bTRAIL DISC. Sm-like protein (Lsm2), peptidyl-prolyl cis-trans isomerase-like 1 (Ppil1) and uncharacterised protein C2orf47 were detected at low levels in both the WT and TRAIL-R1-specific bTRAIL DISC. Synaptosomal associated protein 23 (SNAP-23) was the only protein to be detected in the TRAIL-R1 and TRAIL-R2-specific bTRAIL DISC but not the WT bTRAIL DISC. Acylphosphatase-2 and 60S ribosomal L36a-like protein were only detected at low levels in the TRAIL-R1-specific and TRAIL-R2-specific bTRAIL DISC respectively.

Of the 42 proteins shown to be enriched in the TRAIL-R1-specific bTRAIL unstimulated samples (Figure 4.6) versus TRAIL-R2-specific, two are notable in that they are

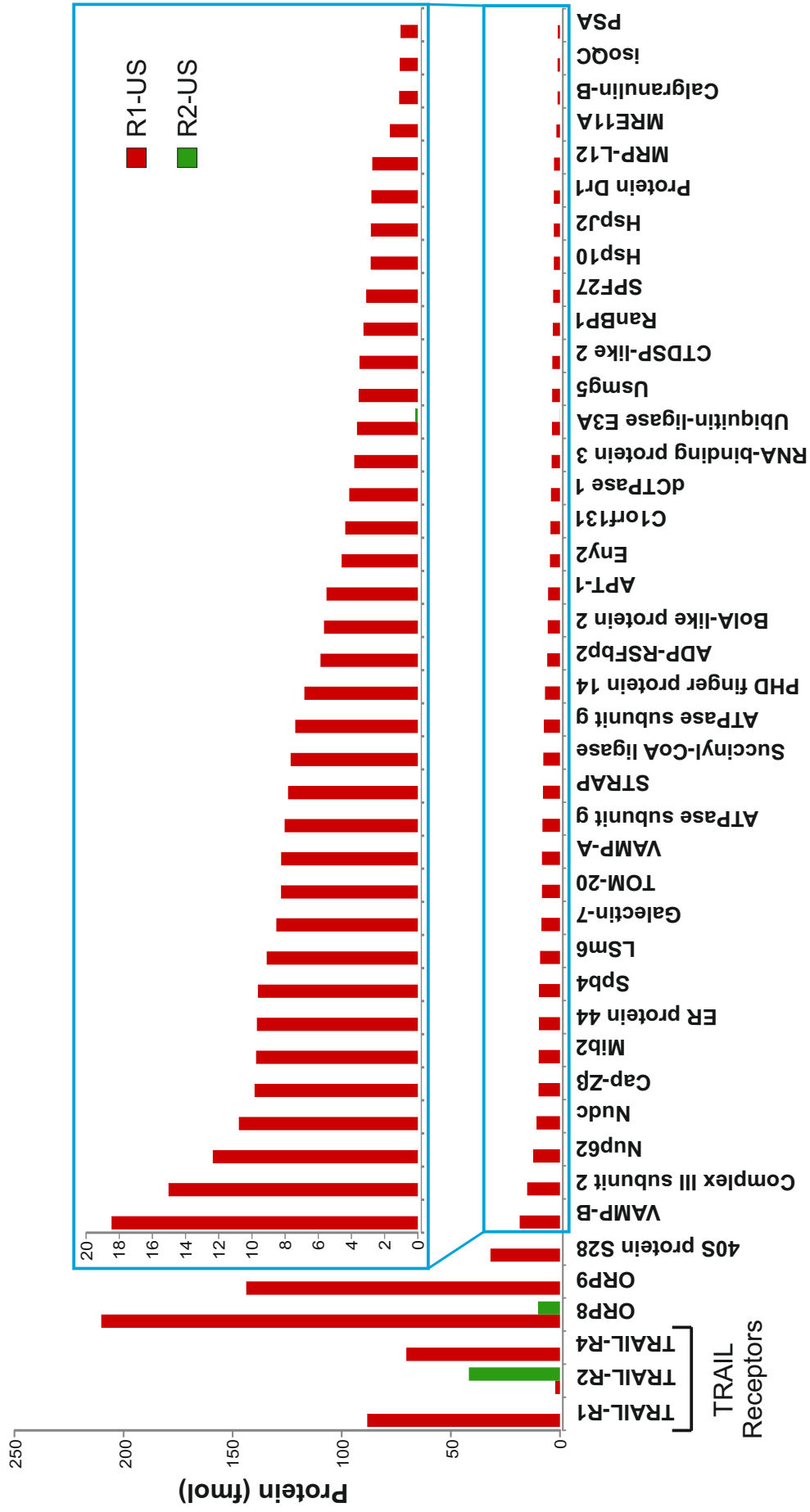


Figure 4.6: Novel TRAIL-R1-Interacting Proteins Identified by Mass Spectrometry

“Top Three” quantitated values for the 42 proteins detected in the TRAIL-R1 (R1)-specific bTRAIL unstimulated (US) samples and not the TRAIL-R2 (R2)-specific bTRAIL US samples (Figure 4.4 C) in addition to TRAIL-R2 are displayed. The TRAIL receptors: TRAIL-R1, TRAIL-R2 and TRAIL-R4 are shown on the left, followed by the novel TRAIL-R1-interacting proteins identified. Values are displayed from the R1 and R2 US samples to show the specificity of the proteins detected for TRAIL-R1.

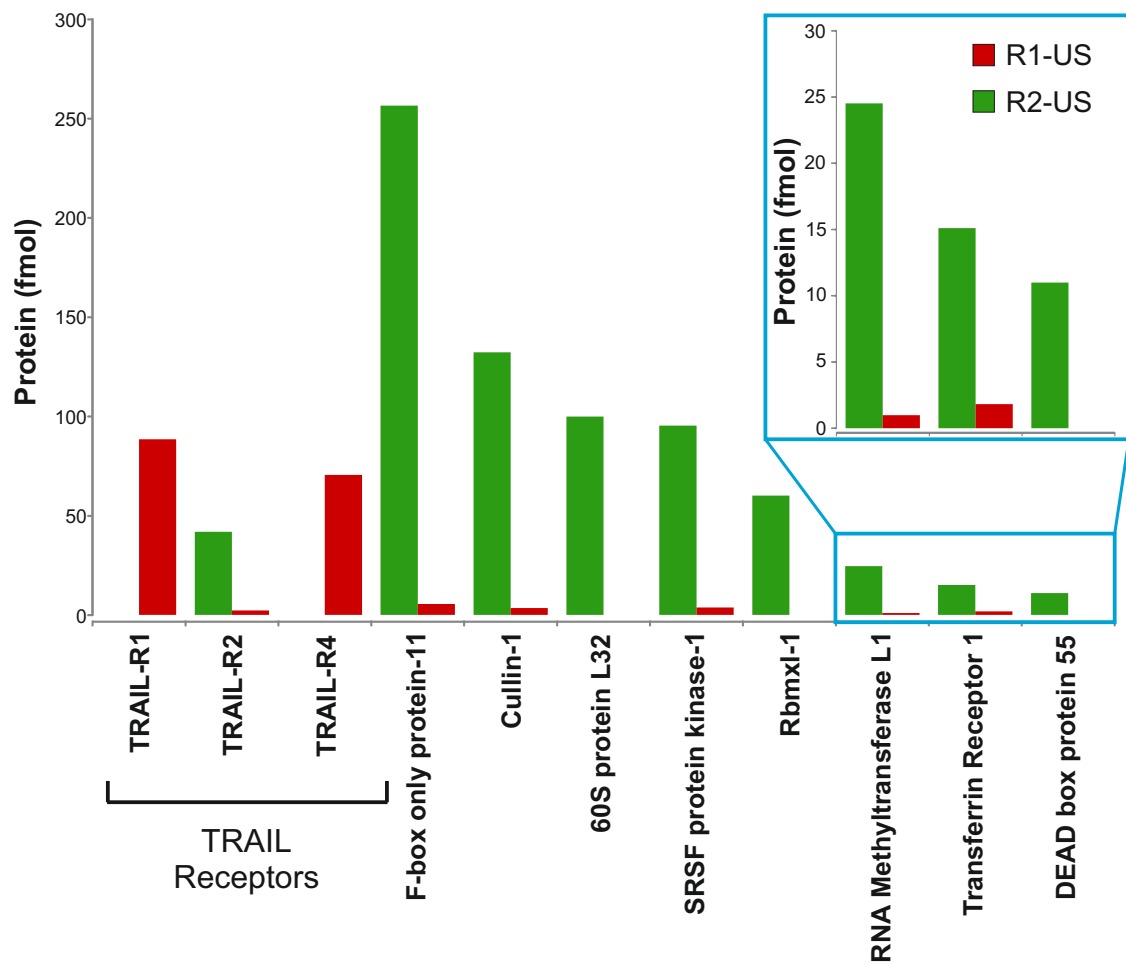


Figure 4.7: Novel TRAIL-R2-Interacting Proteins Identified by Mass Spectrometry

“Top Three” quantitated values for the 8 proteins detected in the TRAIL-R2 (R2)-specific bTRAIL unstimulated (US) samples and not the TRAIL-R1-(R1) specific bTRAIL US samples (Figure 4.4 D), in addition to TRAIL-R1 and TRAIL-R4, are displayed. The TRAIL receptors: TRAIL-R1, TRAIL-R2 and TRAIL-R4 are shown on the left, followed by the novel TRAIL-R1-interacting proteins identified. Values are also displayed from the R2 and R1 US samples to show the specificity of the proteins detected for TRAIL-R2.

detected at a higher level than TRAIL-R1. Oxysterol binding protein related proteins (ORP) 8 and 9 were detected in the TRAIL-R1-specific bTRAIL unstimulated sample at 210.2 and 143.8 fmol respectively, compared to the detection of 88.3 fmol of TRAIL-R1. ORP9 was not detected in the TRAIL-R2-specific bTRAIL unstimulated sample, although low amounts of ORP8 (10.1 fmol) were detected, indicating a TRAIL-R1-specific association. The other TRAIL-R1 interacting proteins identified were detected at a much lower levels than TRAIL-R1, ORP8 and ORP9. The next most abundant protein detected is the 40S ribosomal S28 protein at 31.8 fmol. Other proteins of note were vesicle associated protein (VAMP) B, nuclear pore protein 62 (Nup62) and VAMP-A, detected at 18.5 fmol, 12.4 fmol and 8.2 fmol, respectively; which are known interaction partners of ORP8 and ORP9 (Béaslas et al., 2012; Wyles and Ridgway, 2004).

Analysis of the mass spectrometry results also showed nine proteins which were enriched in the TRAIL-R2-specific bTRAIL unstimulated sample compared to the TRAIL-R1-specific sample (Figure 4.7). The most abundant protein detected was F-box only protein 11 (FBXO11), with 256.2 fmol detected in the TRAIL-R2-specific bTRAIL unstimulated sample compared to 5.5 fmol in the TRAIL-R1-specific bTRAIL unstimulated sample. The second most abundant hit was Cullin-1 (CUL1) with 132.1 fmol detected in the TRAIL-R2-specific bTRAIL sample and only 8.4 fmol detected in the TRAIL-R1 sample. These two proteins were detected at much higher levels than TRAIL-R2 (41.8 fmol), indicating a significant interaction. The detection of both FBXO11 and CUL1 in the TRAIL-R2-specific bTRAIL unstimulated sample is noteworthy, as they are known to interact in Skp, Cullin, F-box (SCF) ubiquitin ligase complexes (Xie et al., 2013). 60S ribosomal L32 protein, serine/arginine rich protein kinase 1 and RNA-binding motif X-linked 1 (Rbmxl-1) were also detected in higher amounts than TRAIL-R2, with values of 99.8 fmol, 95.2 fmol and 60.0 fmol, respectively. Transferrin receptor 1 (TfR1), which was shown to interact with the TRAIL DISC and unstimulated TRAIL receptors in Chapter 3, was shown to be enriched in the TRAIL-R2 US sample (15.1 fmol) compared to the TRAIL-R1 US sample (1.8 fmol). This TRAIL-R2-specific interaction correlates with previous studies from our laboratory, which show that TfR1 can specifically modulate TRAIL-R2 cell surface levels (Dickens et al, unpublished

data). The remaining two identified TRAIL-R2-interacting proteins were RNA methyltransferase-L1 and DEAD box protein-55 with 24.5 fmol and 11.0 fmol detected respectively.

In Chapter 3, ORP8, ORP9, FBXO11 and CUL1 were also detected in the unstimulated samples from WT bTRAIL-treated cells. Skp1, a known interaction partner of FBXO11 and CUL1 was identified in both the DISC and unstimulated samples from WT, TRAIL-R1-specific and TRAIL-R2-specific bTRAIL (Figure 3.6). RIPK1 was also detected previously in the WT bTRAIL isolated DISC and confirmed by western blot analysis (Figure 3.3). The previous mass spectrometry data also showed the presence of PP2A-C associated with the TRAIL DISC, which was confirmed by western blot analysis (Figure 3.3). Upon further analysis of the mass spectrometry data from the WT, TRAIL-R1-specific and TRAIL-R2-specific bTRAIL isolated samples, PP2A-C, along with the PP2A-A and PP2A-B_{55α} subunits were also detected. As these proteins had been detected in two independent TRAIL DISC samples analysed by mass spectrometry, it was decided to further investigate their role in TRAIL signalling.

Figure 4.8 shows the amounts of selected proteins from the WT, TRAIL-R1-specific and TRAIL-R2-specific bTRAIL unstimulated and DISC samples. ORP8 (Figure 4.8 A) and ORP9 (B) were detected at high levels in both the TRAIL-R1-specific bTRAIL unstimulated (Figure 4.6) and DISC samples, in addition to the WT bTRAIL unstimulated sample. The known ORP8/ORP9 interaction partner, VAMP-B was detected at lower levels (Figure 4.8 C) but its detection in the WT and TRAIL-R1-specific bTRAIL unstimulated samples and TRAIL-R1-specific bTRAIL DISC mirrored that of ORP8 and ORP9. Skp1 was detected in all of the WT, TRAIL-R1-specific and TRAIL-R2-specific bTRAIL unstimulated and DISC samples (D). CUL1 (E) and FBXO11 (F) were pre-dominantly detected in the TRAIL-R2-specific bTRAIL unstimulated and DISC samples. RIPK1, as previously shown (Figure 4.5), was only detected in the DISC samples (Figure 4.8 G). Serine/arginine-rich protein-specific kinase 1 (SRPK1), which was identified as a TRAIL-R2-interacting protein (Figure 4.7), was pre-dominantly detected in the TRAIL-R2-specific bTRAIL US sample, but with low level detection in all of the other samples (Figure 4.8 H). Tfr1 was detected in all of the DISC samples, but was pre-dominantly detected in only the WT and TRAIL-R2-specific bTRAIL US samples

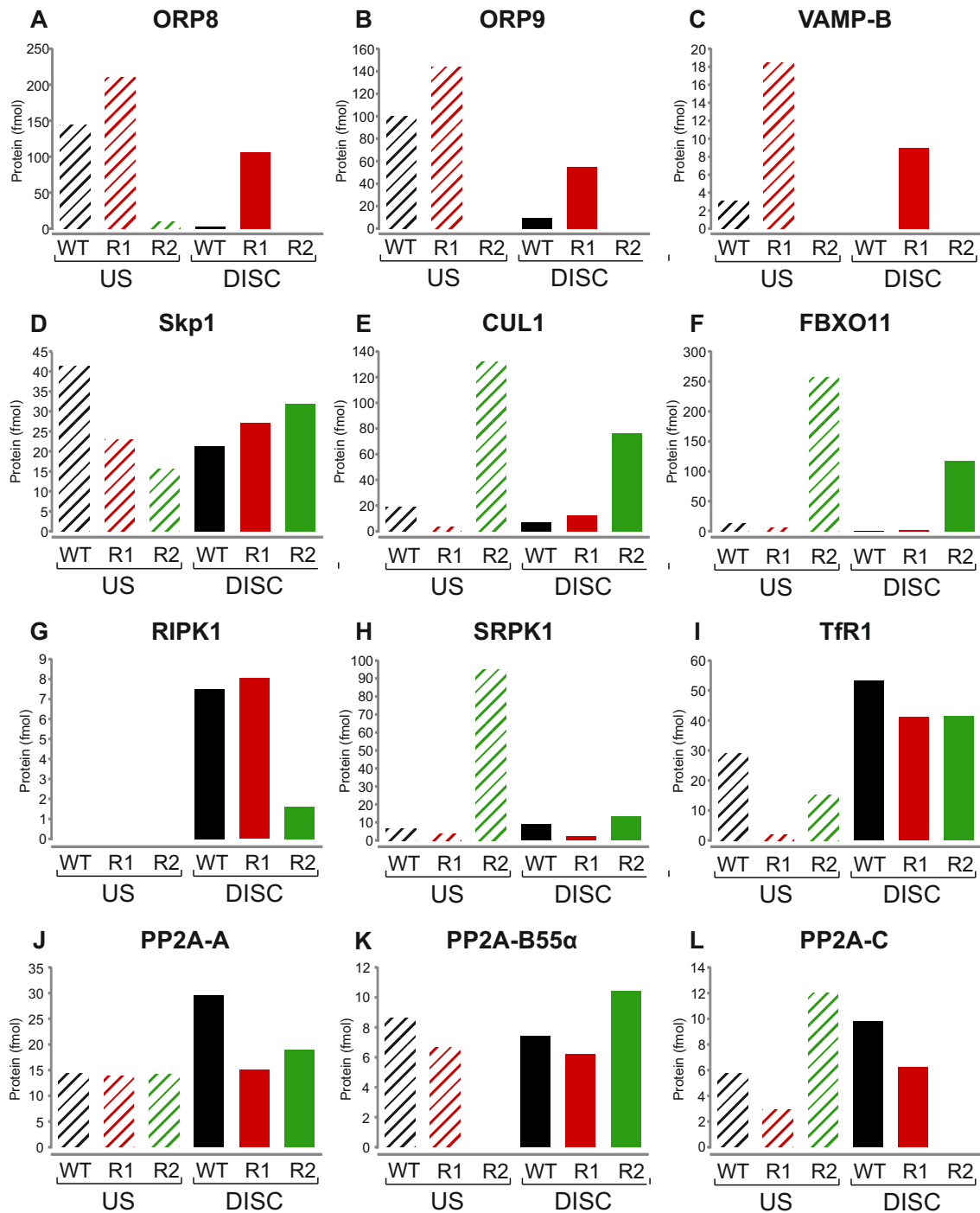


Figure 4.8: Novel TRAIL-R1/R2-Interacting Proteins Identified by Mass Spectrometry

Quantitative values from each of the wild-type, TRAIL-R1-specific and TRAIL-R2-specific bTRAIL unstimulated (US) and DISC samples are shown in: **A** Oxysterol binding protein related protein 8 (ORP8); **B** ORP9; **C** Vesicle-associated Membrane Protein-associated protein B (VAMP-B); **D** S-phase kinase associated protein 1 (Skp1); **E** Cullin 1 (CUL1); **F** F-box only protein 11 (FBXO11); **G** Receptor Interacting Protein Kinase 1 (RIPK1); **H** Serine/arginine-rich Protein-specific Kinase 1 (SRPK1); **I** Transferrin Receptor 1 (TfR1); **J** Protein Phosphatase 2A- scaffold A subunit (PP2A-A), **K** PP2A-B55 α regulatory subunit (PP2A-B55 α); **L** PP2A catalytic subunit (PP2A-C).

This confirms that Tfr1 can interact with the TRAIL DISC and specifically with unstimulated TRAIL-R2 (Chapter 3 and Dickens et al unpublished data). PP2A-A was detected in the WT, TRAIL-R1-specific and TRAIL-R2-specific bTRAIL unstimulated and DISC samples (Figure 4.8 J), whereas PP2A-B55 α and PP2A-C were detected in all the samples, except for the TRAIL-R2-specific bTRAIL unstimulated and DISC samples, respectively (Figure 4.8 K & L).

4.2.4: Confirmation of Novel TRAIL-R1/R2-Interacting Proteins by Western Blot Analysis

To confirm the interactions detected using mass spectrometry by western blot analysis, BJAB cells were treated with 0.5 μ g/ml WT or TRAIL-R1 or TRAIL-R2-specific bTRAIL, lysed and the DISC and unstimulated TRAIL-R1/R2 isolated as described above. Western blot analysis shows ORP8 was detected in the WT and TRAIL-R1-specific bTRAIL unstimulated samples but was absent from the other samples (Figure 4.9: Lanes 9 & 10). The TRAIL-R1-selective interaction agrees with the mass spectrometry data (Figure 4.8 A) and taken together points to a specific interaction between ORP8 and TRAIL-R1. The mass spectrometry data (Figure 4.8 A) also revealed a lower level interaction of ORP8 in the TRAIL-R1-specific bTRAIL DISC sample which was not evident by western blot (Figure 4.9: Lane 13). As even the higher level of interaction detected with WT and TRAIL-R1-specific bTRAIL unstimulated sample of detection required long exposures to detect the ORP8 bands, it is possible that the ORP8 TRAIL-R1 DISC interaction was present but couldn't be detected. The presence of ORP9 could not be confirmed by western blot as no suitable antibodies were available.

The mass spectrometry data revealed a low level abundance of RIPK1 in all of the TRAIL DISC samples (Figure 4.8 G). Western blot analysis confirmed the presence of RIPK1 in the WT and TRAIL-R1-specific bTRAIL DISC samples (Figure 4.9 lanes 12-13). RIPK1 could not be detected in the TRAIL-R2-specific bTRAIL DISC sample, however both FADD and caspase-8 levels were also very low in this sample. Therefore, the lack of RIPK1 detection in the TRAIL-R2 DISC may be due to low levels of DISC being precipitated. RIPK1 was not detected in the unstimulated samples using mass spectrometry or western blot analysis, demonstrating that RIPK1 interacts specifically with the TRAIL DISC.

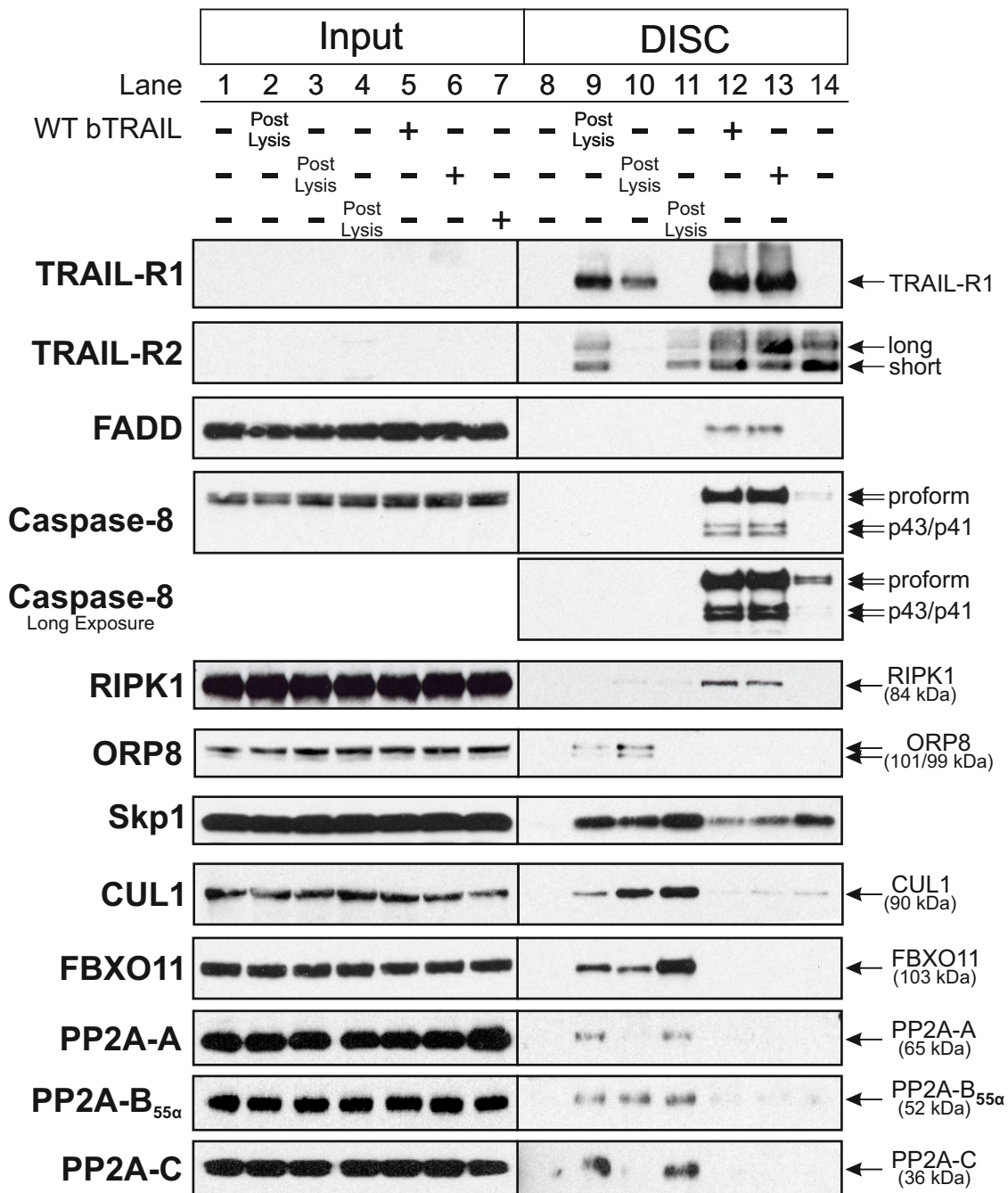


Figure 4.9: Confirmation of Novel TRAIL DISC and Unstimulated TRAIL-R1/R2-Interacting Proteins in BJAB Cells by Western Blot Analysis.

50 x 10⁶ BJAB cells were treated with 0.5 µg/ml wild-type (WT) or TRAIL-R1 (R1) or TRAIL-R2 (R2)-specific bTRAIL mutants. Cells were then lysed and the TRAIL DISC isolated by incubation with 50 µl streptavidin beads. WT, TRAIL-R1-specific and TRAIL-R2-specific bTRAIL was also added to untreated cells post-lysis and unstimulated TRAIL-R1/R2 isolated by incubation with 50 µl streptavidin beads. An untreated sample was also included in which no bTRAIL was added to control for non-specific interactions with the streptavidin beads. Input samples were taken immediately before addition of streptavidin beads. Western blot analysis was performed for TRAIL-R1, TRAIL-R2, FADD and caspase-8 to confirm TRAIL-receptor and DISC isolations. Western blots were also probed for RIPK1, ORP8, FBXO11, CUL1, Skp1, PP2A-A, PP2A-B_{55α} and PP2A-C.

CUL1 and FBXO11 had been identified as possible TRAIL-R2-interacting proteins, and by mass spectrometry they were pre-dominantly detected in the TRAIL-R2-specific bTRAIL unstimulated and DISC samples (Figure 4.8 E & F). Western blot analysis confirmed the detection of CUL1 in the TRAIL-R2-specific bTRAIL unstimulated sample (Lane 11), however CUL1 was also detected in the TRAIL-R1-specific (Lane 10) and to a lower extent in the WT bTRAIL (Lane 9) unstimulated samples. A similar pattern was observed for FBXO11, which was detected in both the TRAIL-R2 (Lane 11) and TRAIL-R1-specific bTRAIL (Lane 10) unstimulated samples. It is important to note CUL1 and FBXO11 were not detected in the untreated control sample (Lane 8). Therefore, despite their detection in multiple samples, which differs from the observed TRAIL-R2-specificity indicated by mass spectrometry, these proteins are not interacting non-specifically with the streptavidin beads. The known FBXO11 and CUL1 interaction partner Skp1 was detected in all of the WT, TRAIL-R1 and TRAIL-R2-specific bTRAIL unstimulated and DISC samples. This finding is in accordance with the ubiquitous detection of Skp1 in the mass spectrometry data (Figure 4.8 D).

Three components of the PP2A phosphatase, PP2A-A, PP2A-B_{55α} and PP2A-C were detected by mass spectrometry associated with TRAIL-R1/R2 and the TRAIL DISC at low abundance (Figure 4.8: J, K & L). Western blot analysis for PP2A-A (Figure 4.9) confirmed a very low level of protein in the WT (Lane 9) and TRAIL-R2-specific bTRAIL (Lane 11) unstimulated samples. This pattern was also observed for PP2A-C, however PP2A-B_{55α} was detected in the unstimulated samples from WT, TRAIL-R1 and TRAIL-R2-specific bTRAIL, although also at very low levels. Although the interaction of three different PP2A phosphatase subunits was evident and associated with TRAIL-R1/R2, the level of detection was very low. Considering the ubiquitous expression and multiple roles of the PP2A phosphatase and the extremely low levels of detection it would be difficult to investigate the role of PP2A in the TRAIL DISC further.

The interaction of the potential TRAIL DISC-interacting proteins was then further analysed in another cell line. The TRAIL DISC and unstimulated TRAIL-R1/R2 were isolated from HeLa cells treated with 0.5 µg/ml WT, TRAIL-R1-specific or TRAIL-R2-specific bTRAIL (Figure 4.10). Following treatment, the cells were incubated on ice for 1 h before incubation at 37°C for 15 min. The cells were then lysed and the DISC and

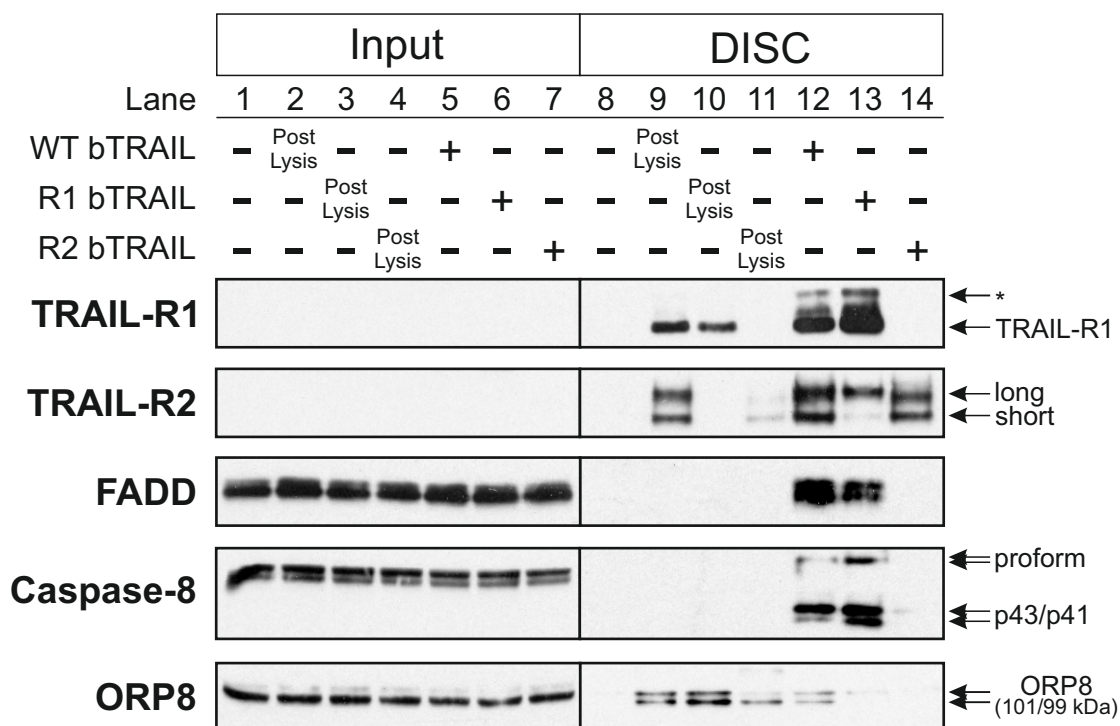


Figure 4.10: Confirmation of the Association of ORP8 with TRAIL-R1/R2 in HeLa Cells

HeLa cells (1 x T175 flask at 70-80% confluency, 12×10^6 cells approx.) were treated with 0.5 $\mu\text{g}/\text{ml}$ wild-type (WT) bTRAIL or TRAIL-R1 (R1) or TRAIL-R2 (R2)-specific mutant bTRAIL. Cells were then lysed and DISCs isolated by incubation with 50 μl streptavidin beads. WT, TRAIL-R1-specific and TRAIL-R2-specific bTRAIL was also added to untreated cells post-lysis and unstimulated TRAIL-R1/R2 isolated by incubation with 50 μl streptavidin beads. An untreated sample was also included in which no bTRAIL was added to control for non-specific interactions with the streptavidin beads. Input samples were taken immediately before addition of streptavidin beads. Western blot analysis was performed for TRAIL-R1, TRAIL-R2, FADD, caspase-8 and ORP8. * Represents a post-translationally modified form of TRAIL-R1 (Robinson et al., 2012).

unstimulated receptors isolated as described previously. The TRAIL DISC was successfully isolated as TRAIL-R1, TRAIL-R2 and FADD were all detected in the samples isolated using the WT (Lane 12) and TRAIL-R1-specific (Lane 13) bTRAIL. As observed in the BJAB cells, in the TRAIL-R2-specific bTRAIL-treated sample (Lane 14), TRAIL-R2 was detected but TRAIL-R1 was not. FADD was not detected using the TRAIL-R2-specific bTRAIL, indicating that the DISC had not been formed. The specificity of the TRAIL-receptor selective bTRAIL mutants was again demonstrated, as in the unstimulated samples TRAIL-R1 was detected only in the WT (Lane 9) and TRAIL-R1-specific (Lane 10) bTRAIL samples. TRAIL-R2 was only detected in the WT (Lane 9) and TRAIL-R2-specific (Lane 11) bTRAIL samples, with a greater amount detected in the WT sample. Western blot analysis revealed ORP8 was present in the WT (Lane 9) and TRAIL-R1-specific (Lane 10) bTRAIL unstimulated samples, as with the BJAB cells. However, in HeLa cells ORP8 was also detected in the TRAIL-R2-specific bTRAIL unstimulated sample (Lane 11) and in the WT DISC sample (Lane 12). The detection of ORP8 in both the TRAIL-R1 and TRAIL-R2-specific bTRAIL samples implies that in HeLa cells, ORP8 interacts with both unstimulated TRAIL-R1 and TRAIL-R2, whereas in BJAB cells, ORP8 interacts specifically with TRAIL-R1. The other proteins identified as interacting with TRAIL-R1/R2 in BJAB cells: CUL1, FBXO11, Skp1 and PP2A could not be detected in the unstimulated or TRAIL DISC samples isolated from HeLa cells.

4.2.5: siRNA Targeting of ORP8 Increases Cell Surface Expression of TRAIL-R2

As ORP8 had been confirmed to interact with the TRAIL-R1 in BJAB cells (Figure 4.9) and TRAIL-R1 and TRAIL-R2 in HeLa (Figure 4.10) cells, its role in the regulation of TRAIL signalling was investigated further. The effect of siRNA targeting ORP8 was examined in HeLa cells, as HeLa cells have been shown to be more amenable to transfection of siRNA oligonucleotides.

As modulation of ORP8 expression has been reported to effect the cell surface expression of CD95 (Zhong et al., 2015), its role on the cell surface expression of TRAIL-R1/R2 was investigated. HeLa cells were transfected with 5 nM ORP8 targeting siRNA, 5 nM non-targeting control siRNA or no RNA for 24 or 48 h. The cells were then incubated with PE-conjugated antibodies specific to TRAIL-R1, TRAIL-R2 or IgG control

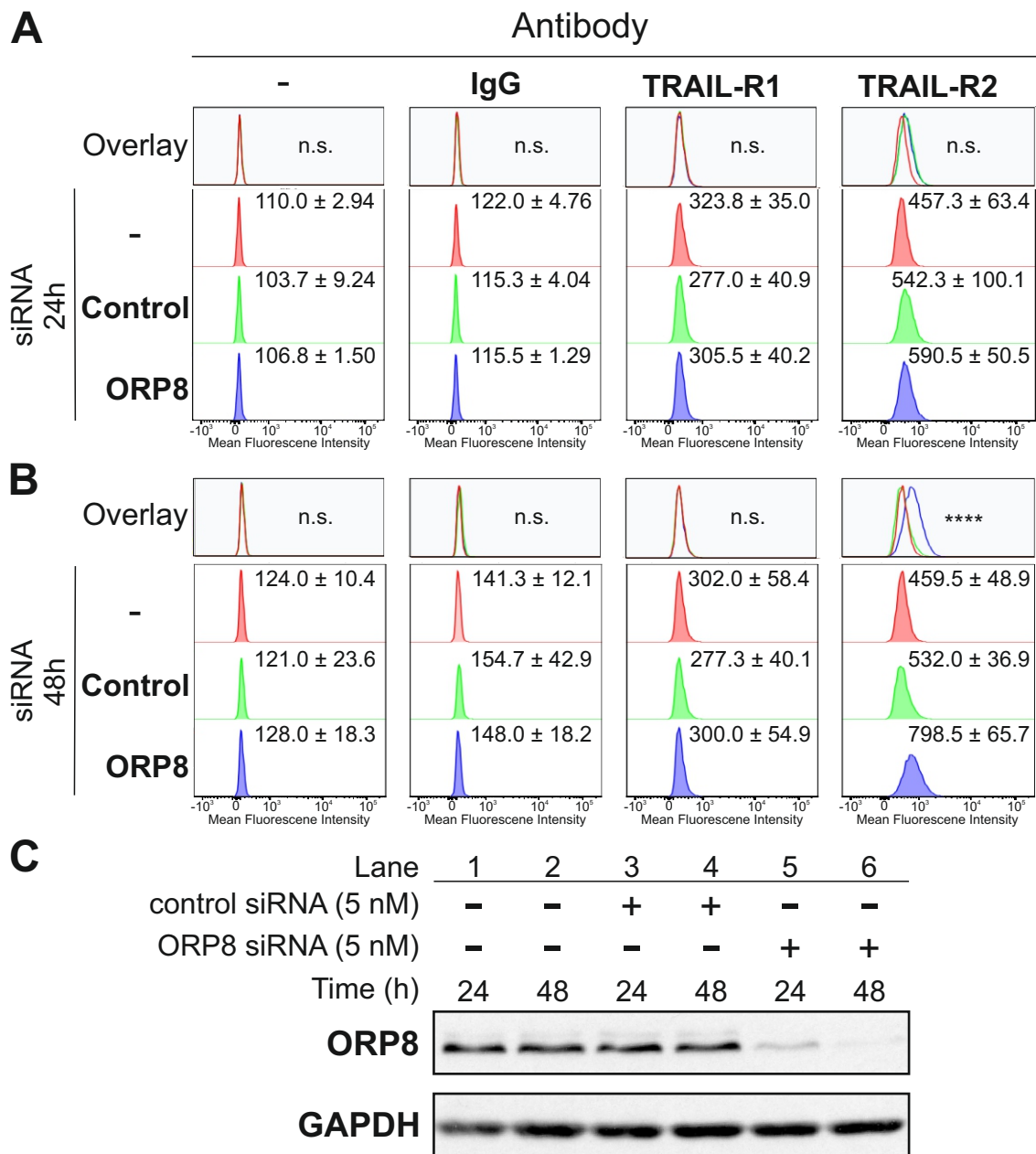


Figure 4.11: siRNA Targeting of ORP8 Increases Cell Surface TRAIL-R2 Expression

1.25 x 10⁵ or 2.5 x 10⁵ HeLa cells were transfected for 24 h (A) or 48 h (B), respectively with 5 nM ORP8 targeting siRNA, control siRNA or no siRNA. A,B Cells were blocked in goat serum, separated into 4 groups and incubated with no antibody (-) or PE-conjugated IgG control, TRAIL-R1 or TRAIL-R2 antibodies. TRAIL-R1/R2 cell surface levels were determined by flow cytometry and fluorescence intensity histograms aligned using ImageFlow. Values displayed are the geometric mean +/- standard deviation. Differences between the means were shown to be statistically different by two-way ANOVA for the 48 h siRNA targeted cells but not the 24 h transfected cells. Significant differences were determined by a post-hoc Burkitts test and are highlighted by * (P<0.05 = *, P<0.01 = **, P<0.001 = ***, P<0.001 = ****). C Western blot analysis was performed a for ORP8, with GAPDH used as a loading control.

and the cell surface expression of TRAIL-R1/R2 determined by flow cytometry. Cells treated with the ORP8 and control siRNA for 24 h showed no significant difference in the surface expression of TRAIL-R1 or TRAIL-R2 (Figure 4.11 A). However, after 48 h siRNA treatment the ORP8 siRNA transfected cells showed a significant increase in the level of TRAIL-R2 on the cell surface, from 459.5 or 532.0 mean fluorescence intensity units (MFI) in the no siRNA or control siRNA-transfected cells to 798.5 MFI in the ORP8 siRNA-transfected cells (Figure 4.11 B). ORP8 siRNA transfection was shown by western blot analysis to have reduced the expression of ORP8 in cells transfected for 24 and 48 h (Figure 4.11 C). The amount of ORP8 in the 48 h transfected cells was lower than that for the 24 h transfected cells and could explain why only the 48 h knockdown of ORP8 induced the upregulation of TRAIL-R2 on the cell surface.

4.2.6: siRNA Targeting of ORP8 Sensitises HeLa Cells to TRAIL-induced Apoptosis

As siRNA targeting of ORP8 for 48 h induced an increase in TRAIL-R2 surface expression (Figure 4.11), the effect of ORP8 knockdown on TRAIL-induced apoptosis was evaluated. HeLa cells were transfected with 5 nM ORP8 siRNA, 5 nM control siRNA or no siRNA for 48 h followed by 5 h treatment with 1 µg/ml WT TRAIL, TRAIL-R1-specific or TRAIL-R2-specific mutants. Cells were stained with annexin-V-FITC and DRAQ7 and cell death analysed by flow cytometry (Figure 4.12 A).

Incubation with transfection reagent (RNAiMax) alone induced very little cell death, with only 7.5% of cells being detected as positive for annexin-V staining following transfection/treatment. Addition of either the control or ORP8 siRNA did slightly increase the percentage of annexin-V positive cells (9.7% and 11.7%, respectively) but not significantly. Treatment with WT TRAIL induced 46.5% cell death in the no siRNA control, which did not increase significantly with the control siRNA (48.7%). ORP8 transfected cells however displayed an increased sensitivity to WT TRAIL-induced apoptosis as cell death increased to 61.4%. Similar results were observed for cells treated with the TRAIL-R1-specific TRAIL. The cells transfected with no siRNA or control siRNA showed 39.3% and 42.1% annexin-V positive cells, which increased to 54.7% in the ORP8 siRNA-transfected cells. Despite HeLa cells being previously described as being sensitive to both TRAIL-R1 and TRAIL-R2-mediated apoptosis

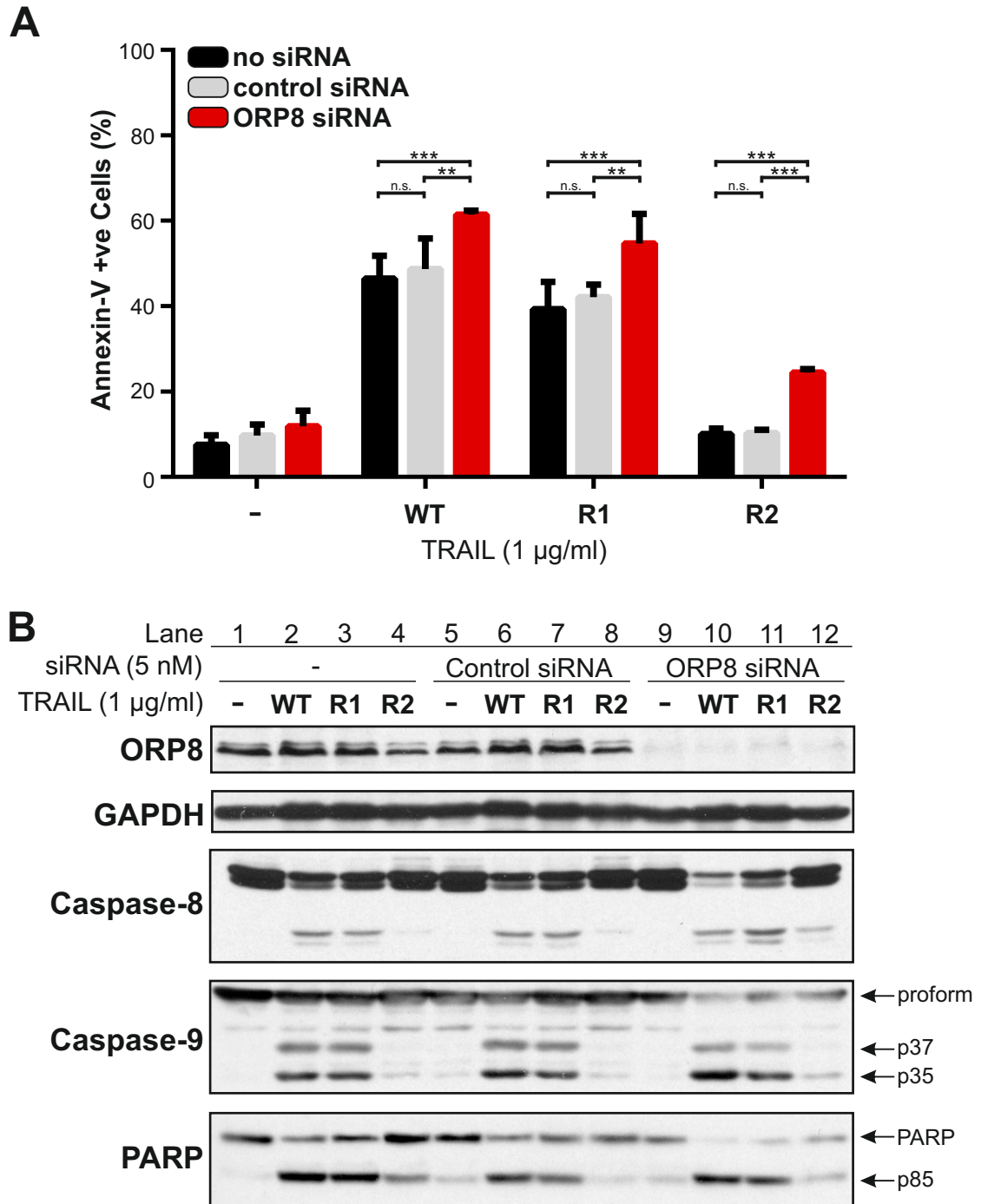


Figure 4.12: Knockdown of ORP8 Expression Sensitises HeLa Cells to TRAIL-Induced Apoptosis

1.25×10^5 HeLa cells were transfected with 5 nM ORP8 targeting siRNA, control siRNA or no siRNA for 48 h. Cells were then treated with either 1 µg/ml wild-type (WT) TRAIL or 1 µg/ml TRAIL-R1 or TRAIL-R2-specific mutant TRAIL for 5 h. Cells were stained with Annexin-V-FITC and DRAQ7 and cell death analysed by flow cytometry (A). Western blots of cell pellets were probed for ORP8, caspase-8, caspase-9, caspase-3 and PARP. Blots were also probed for GAPDH as a loading control (B). Data shown in A is % Annexin-V-FITC positive cells from 3 independent experiments +/- standard deviation (SD). Differences between the group Means were shown to be statistically different by two-way ANOVA. Significant differences were determined by a post-hoc Burkitt's test and are highlighted by * ($P < 0.05 = *$, $P < 0.01 = **$, $P < 0.001 = ***$, $P < 0.001 = ****$).

(Gasparian et al., 2009; Ohtsuka et al., 2003), treatment with the TRAIL-R2-specific TRAIL mutant did not induce cell death above background. However, ORP8 siRNA treatment increased cell death from 10.0% and 10.3% in the no siRNA and control siRNA transfected cells, respectively, to 24.4%. Western blots probed for ORP8 (Figure 4.12 B) showed that ORP8 expression had been reduced by the ORP8 siRNA (Lanes 9-12) but not the control siRNA (Lanes 5-8). Probing for GAPDH confirmed that this decrease was not due to reduced protein loading. The increased cell death in the ORP8 siRNA transfected siRNA was confirmed by western analysis for caspase-8, caspase-9 and PARP (Figure 4.12 B). Caspase-9 was shown to be cleaved to the p37 and p35 fragments by treatment with WT TRAIL (Lanes 2, 6 and 10) and the TRAIL-R1-specific mutant (Lanes 3, 7 & 11). The appearance of the p35 band is more pronounced in the ORP8 siRNA transfected cells (Lanes 10-11). For the TRAIL-R2-specific mutant treated cells (Lanes 4, 8 & 12), a faint band was detected in the no siRNA (Lane 4) and control siRNA (Lane 8) transfected cells, which was more pronounced for the ORP8 siRNA transfected cells (Lane 12). PARP was shown to be cleaved, generating its p85 fragment by WT TRAIL (Lanes 2, 6 & 10), the TRAIL-R1-specific (Lanes 3, 7 & 11) and to a lesser extent the TRAIL-R2-specific (Lanes 4, 8 & 12) mutant. The loss of full length PARP was more evident in those cells transfected with ORP8 siRNA and subsequently treated with TRAIL (Lanes 10-12) in comparison with the no siRNA (Lanes 2-4) and control siRNA (Lanes 6-8) transfected cells.

4.3 Discussion

4.3.1 Summary of Chapter Findings

This chapter has described the isolation of the TRAIL DISC and unstimulated TRAIL-R1/R2 using WT TRAIL and TRAIL mutants which bind specifically to TRAIL-R1 or TRAIL-R2 (Marion MacFarlane et al., 2005) and subsequent analysis by mass spectrometry and western blotting. These experiments have:

1. Demonstrated that TRAIL-R1, TRAIL-R2, FADD, caspase-8 (by mass spectrometry and western blot analysis), cFLIP and caspase-10 (by mass spectrometry) are present in DISC isolated using WT TRAIL and a TRAIL-R1-specific mutant in BJAB cells.
2. Demonstrated that TRAIL-R2, caspase-8 (by mass spectrometry and western blot analysis), cFLIP (by mass spectrometry) and FADD (by western blot analysis) are present in the TRAIL DISC isolated using a TRAIL-R2-specific TRAIL mutant in BJAB cells.
3. Confirmed that BJAB cells signal preferentially through TRAIL-R1, as shown by the greater amount of DISC formation using a TRAIL-R1-specific mutant compared to a TRAIL-R2-specific mutant.
4. Identified and confirmed the interaction of ORP8, pre-associated with TRAIL-R1 and not TRAIL-R2 in BJAB cells, but pre-associated with both TRAIL-R1 and TRAIL-R2 in HeLa cells (Table 4.1).
5. Demonstrated that siRNA targeting of ORP8 in HeLa cells induces increased expression of TRAIL-R2 at the cell surface and increases sensitivity to apoptosis induced by WT TRAIL and TRAIL-R1/R2 specific TRAIL mutants.
6. Identified and confirmed the interaction of FBXO11, CUL1 and Skp1 pre-associated with TRAIL-R1/R2 and in the DISC in BJAB cells (Table 4.1).
7. Identified and confirmed the interaction of PP2A, pre-associated with TRAIL-R1/R2 and in the TRAIL DISC in BJAB cells (Table 4.1).

		Sample					
		Unstimulated			DISC		
Cell Line	Protein	WT	R1	R2	WT	R1	R2
BJAB	ORP8	+	+	-	-	-	-
	Skp1	+	+	+	+	+	+
	CUL1	+	+	+	-	-	-
	FBXO11	+	+	+	-	-	-
	PP2A-A	+	-	+	-	-	-
	PP2A-B55 α	+	+	+	-	-	-
	PP2A-C	+	-	+	-	-	-
HeLa	ORP8	+	+	+	+	-	-

Table summarising the detection of ORP8, Skp1, CUL1, FBXO11, PP2A-A, PP2A-B55 α and PP2A-C by western blot analysis from the samples described in Figure 4.9 (BJAB) and 4.10 (HeLa). Sample in which the specified protein was detected are marked by + and samples in which the protein was not detected are marked by - . In the HeLa cell line, Skp1, CUL1, FBXO11, PP2A-A, PP2A-B55 α and PP2A-C were not detected and are therefore not displayed.

4.3.2: TRAIL DISC Components TRAIL-R1, TRAIL-R2, TRAIL-R4, FADD, Caspase-8, cFLIP and Caspase-10 Detected by Mass Spectrometry in the DISC Isolated Using WT and TRAIL-R1-specific bTRAIL

The results demonstrated that TRAIL-induced apoptosis in BJAB cells is mediated via the activation of TRAIL-R1. WT and TRAIL-R1-selective TRAIL significantly induced cell death, whereas targeting of TRAIL-R2 using a TRAIL-R2-specific TRAIL mutant did not (Figure 4.1). This is in accordance with multiple reports of haematopoietic-derived cells being more sensitive to TRAIL-R1-targeted ligands (MacFarlane et al., 2005a; MacFarlane et al., 2005b; Natoni et al., 2007; Szegezdi et al., 2011; Tur et al., 2008). The TRAIL-R1 sensitivity of BJAB cells was also apparent by isolation of an active TRAIL DISC using the TRAIL-R1/R2 selective mutants. WT and TRAIL-R1-specific bTRAIL successfully precipitated: TRAIL-R1, TRAIL-R2, TRAIL-R4, FADD, caspase-8, cFLIP and caspase-10, which were detected by mass spectrometry. In contrast, using the TRAIL-R2-specific bTRAIL, only TRAIL-R2, caspase-8 and FADD could be detected in the DISC isolated (Figure 4.3 A). HeLa cells were also shown to be insensitive to TRAIL-R2-specific TRAIL-induced apoptosis (Figure 4.12) and very little DISC was formed by the TRAIL-R2-specific bTRAIL (Figure 4.10). HeLa cells have however been reported to be sensitive to either TRAIL-R1 or TRAIL-R2 targeted ligands (Gasparian et al., 2009; Ohtsuka et al., 2003; Ren et al., 2004). TRAIL-R2 requires a greater degree of ligand cross-linking to be sufficiently activated (Mühlenbeck et al., 2000). Therefore targeting of TRAIL-R2-specifically may still be able to induce apoptosis in BJAB and HeLa cells if the TRAIL-R2 targeting ligand is more efficiently able to aggregate the receptors. Strategies such as cross-linking of agonistic antibodies or the development of leucine zipper TRAIL have been used to increase receptor aggregation (Mühlenbeck et al., 2000; Walczak et al., 1999). The TRAIL-R2-specific bTRAIL used in this study could be modified using such strategies to enable effective, specific targeting of TRAIL-R2. This approach could be useful in selectively killing cancer cells which are sensitive to TRAIL-R2, but not TRAIL-R1-induced apoptosis.

The specificity of the TRAIL receptor selective TRAIL mutants was confirmed by their ability to isolate the unstimulated TRAIL receptors, TRAIL-R1 and TRAIL-R2. The TRAIL-R1-selective bTRAIL mutant precipitated TRAIL-R1 and not TRAIL-R2 in both BJAB

(Figure 4.3 B) and HeLa (Figure 4.10) cells. Conversely, the TRAIL-R2-selective bTRAIL mutant precipitated TRAIL-R2 and not TRAIL-R1 in BJAB (Figure 4.3) and HeLa (Figure 4.10) cells, however at a much lower level than WT TRAIL. The specificity of the TRAIL-R1/R2 mutants was less clear in the DISC isolations. The TRAIL-R1-selective bTRAIL mutant precipitated both TRAIL-R1 and a smaller amount of TRAIL-R2 in the DISC samples from BJAB (Figure 4.3) and HeLa (Figure 4.10) cells. Considering the selectivity of the mutants to bind their specific TRAIL receptor in the unstimulated samples, these data confirm that TRAIL-R1/R2 form hetero-complexes upon ligand binding (Lemke et al., 2010).

TRAIL-R4 was also detected in the DISC samples isolated using both WT and TRAIL-R1-specific bTRAIL but not with the TRAIL-R2-specific bTRAIL mutant. This observation appears to contradict a previous report which suggested that TRAIL-R4 specifically associates with TRAIL-R2 and not TRAIL-R1 (Mérino et al., 2006). However, due to the hetero-complexes formed by the TRAIL-R1-specific bTRAIL, TRAIL-R2 was also present in this DISC sample. In addition, as the TRAIL-R1-specific bTRAIL was demonstrated to only interact with TRAIL-R1 (Figure 4.3), all of the TRAIL-R2 recruited will be that which has been recruited via TRAIL-R1 to enable DISC formation. The absence of TRAIL-R4 detection in the TRAIL-R2-specific bTRAIL DISC sample may be because the TRAIL-R2 isolated is insufficiently aggregated to induce TRAIL-R4 recruitment. Unlike TRAIL-R1-associated TRAIL-R2 in the DISC, TRAIL-R2 isolated using the TRAIL-R2-specific bTRAIL, may be mostly un-complexed receptors not capable of recruiting additional proteins to the DISC.

TRAIL-R4 is also detected in the unstimulated TRAIL receptor isolations and again appears in the WT and TRAIL-R1-specific, but not TRAIL-R2-specific bTRAIL samples (Figure 4.3). The selective detection of TRAIL-R4 in the TRAIL-R1-specific bTRAIL samples could also be because the ligand can bind TRAIL-R4 directly (as WT TRAIL does) whereas the mutation to generate TRAIL-R2-specificity abolished this interaction.

4.3.3: ORP8 Identified as a TRAIL-R1/R2 Interacting Protein in BJAB and HeLa cells: siRNA Targeting of ORP8 in HeLa Cells Increases TRAIL-R2 Cell Surface Expression and Sensitivity to TRAIL-Induced Apoptosis

Mass spectrometry revealed that ORP8 and ORP9 are selectively recruited to unstimulated TRAIL-R1 and not TRAIL-R2 (Figure 4.8). Western blots then confirmed the specific association of ORP8 (Table 4.1) with unstimulated TRAIL-R1 in BJAB cells (Figure 4.9). In unstimulated receptors and TRAIL DISC isolated from HeLa cells, ORP8 was detected associated with both unstimulated TRAIL-R1 and TRAIL-R2 (Figure 4.10). ORP8 detection was also observed in the WT bTRAIL DISC (Figure 4.10). Although detected in the DISC sample, care must be taken before listing ORP8 as a TRAIL DISC-interacting protein. In the method used to isolate the DISC, the activated DISC is not separated from non-aggregated TRAIL receptors, which although bound by TRAIL have not formed a DISC. Separation of the activated DISC by sucrose density centrifugation, which would separate the high molecular weight (HMW) DISC from the less dense unstimulated TRAIL receptors (Dickens et al., 2012a) would confirm whether the ORP8 DISC interaction observed is real.

Oxysterol binding proteins (OSB) and oxysterol binding protein related proteins (ORP) are a family of proteins which can bind cholesterol and oxysterols. Their roles were initially thought to be limited to cellular lipid metabolism or sterol transport but recently they have been identified as having key functions in signalling pathway regulation (Olkkonen and Li, 2013). OSBP, the founding member of the ORP family, is able to bind to cholesterol in the cell membrane (Wang et al., 2005). In addition to cholesterol, it was also shown to recruit two phosphatases, the tyrosine phosphatase PTPBS and the serine/threonine phosphatase PP2A (Wang et al., 2005). Once recruited to OSBP, these two phosphatases then regulate ERK activity by the coordinated de-phosphorylation of specific tyrosine and threonine residues on ERK. When cholesterol levels decrease, the complex falls apart. Via its formation of an activation platform, OSBP is therefore able to regulate ERK activity (Wang et al., 2005). The potential role(s) of ORP8 and ORP9 associated with TRAIL-R1/R2 may therefore play a similar role in regulating TRAIL signalling. The ability of members of the OSBP family to bind to PP2A is intriguing, as PP2A was also detected pre-associated with the

TRAIL receptors. Therefore, the recruitment of PP2A may be mediated through a direct interaction with either ORP8 or ORP9. ORP9 was also demonstrated to interact with PKC β and mTOR. This interaction negatively regulates Akt activity and thus effects cell survival, cell cycle control and glucose metabolism. PKC β has also been strongly implicated in the regulation of death receptor signalling (Meng et al., 2010), and could possibly be interacting with the TRAIL receptors by interacting with ORP9. Although PKC β was not detected in this study, this may be because kinase interactions are often transient and therefore may require cross-linking to enable protein identification.

ORP8 is closely related to ORP5, and both proteins contain C-terminal regions which anchor them to the ER membrane (Olkkonen and Li, 2013). They also contain an N-terminal pleckstrin homology (PH) domain which targets the proteins to the plasma membrane (Zhong et al., 2015). This dual membrane targeting has implicated these ORPs in activity at membrane contact sites (MCS), areas where the membrane of two different organelles or the plasma membrane are very closely (10-20 nm) situated, which are important for signalling processes (Olkkonen and Li, 2013). It would be interesting to determine if the interaction between ORP8/ORP9 and TRAIL-R1 occurs throughout the cellular membrane or is concentrated to the ER or MCS. This could reveal if the ORP proteins are involved in membrane trafficking of TRAIL-R1 or regulating cross-talk between membrane compartments which could then have effects on TRAIL signalling. VAMP-A and VAMP-B, ER-resident proteins were also identified associated with TRAIL-R1 and could also have roles in regulating TRAIL-R1 trafficking. An important organelle in apoptotic signalling is the mitochondria, which once permeabilised releases cytochrome c, leading to apoptosome formation. Caspase-8, activated at a DISC in close proximity to the mitochondria (at MCS), could increase MOMP formation via cleaved Bid if all of the components were localised to a small area thus increasing apoptotic signalling in Type II cells.

ORP8-deficient macrophages have increased migration mediated by alterations in the macrophage transcriptome which effected centrosome and microtubule cytoskeleton organisation (Béaslas et al., 2012). TRAIL signalling has been shown to be augmented by interacting with the cytoskeleton via E-cadherin (Lu et al., 2014b). Loss of this

interaction attenuated TRAIL-induced apoptosis and thus if ORP8 can regulate cytoskeleton organisation it may also effect TRAIL signalling.

The results showed that siRNA targeting of ORP8 induces an increase in the cell surface expression of TRAIL-R2, but not TRAIL-R1 (Figure 4.11). The selectivity of the effect to TRAIL-R2 is surprising as in BJAB cells ORP8 was only shown to interact with TRAIL-R1. However, ORP8 was shown to interact with both TRAIL-R1 and TRAIL-R2 in HeLa cells and as such there may be differences in the role of ORP8 between cell types. HeLa cells in which ORP8 expression had been reduced were also shown to be more sensitive to apoptosis induced by either WT TRAIL or TRAIL-R1 or TRAIL-R2 targeted mutants. The increased surface expression of TRAIL-R2 induced by targeting ORP8 with siRNA can readily explain the increased susceptibility to WT and TRAIL-R2-induced death. Although it was initially puzzling why increased TRAIL-R2 surface expression would increase TRAIL-R1 mediated cell death, this correlates with the observed hetero-complex formation of TRAIL-R1 and TRAIL-R2 in the DISC even when stimulated a TRAIL-R1-selective form of TRAIL.

Modulation of ORP8 expression levels has previously been demonstrated to effect cell death induced by CD95L. Zhong et al., (2015) showed that overexpression of ORP8 could induce apoptosis in human hepatoma cells. The induced cell death was demonstrated to be due to an increase in CD95 cell surface levels and an upregulation of CD95L. It was then shown that ORP8 overexpression had induced the activation of the ER stress response and in a p53-dependent mechanism, induced the increased surface expression of CD95 (Zhong et al., 2015). ER stress response activation has also been implicated in upregulation and increased sensitivity towards TRAIL-R2 (He et al., 2013; Liu et al., 2015; Lu et al., 2014a). Activation of the ER stress response was demonstrated to activate CHOP, which subsequently induced the upregulation of TRAIL-R2 expression. To determine if the increased TRAIL-R2 cell surface expression and TRAIL sensitivity following ORP8 knockdown observed here is mediated by the ER stress response, CHOP could be co-silenced. If removal of CHOP expression abrogated the observed effects of ORP8 knockdown then it is likely the effect is being mediated by the ER stress response.

Overexpression of ORP9S or depletion of ORP9L has been demonstrated to perturb ER-Golgi protein transport (Ngo and Ridgway, 2009). TRAIL receptors on the cell surface have been shown to be continuously recycled even without stimulation by TRAIL (Kohlhaas et al., 2007). Therefore, in light of the effect of ORP8 knockdown on TRAIL-R2 surface levels, it is possible that ORP8 plays a role in the recycling of TRAIL-R2 from the cell surface. Perturbation of this ORP8-mediated recycling results in the accumulation of TRAIL-R2 at the cell surface and leads to an increase in sensitivity to TRAIL-induced apoptosis. This alternative explanation would explain the interaction observed between ORP8 and TRAIL-R2, but does not explain why there is no effect on TRAIL-R1 cell surface levels by ORP8 knockdown. To address, the experiment should be repeated in BJAB cells, which showed only a TRAIL-R1:ORP8 interaction, to determine if the observed effect on TRAIL-R2 cell surface expression is still evident.

The ability of altered ORP expression to sensitise cells to apoptosis induced by CD95L (Zhong et al., 2015) and TRAIL (Figure 4.12) highlights a possible new avenue to treat CD95L or TRAIL-resistant cells. A new class of drugs called ORPphilins has been demonstrated to selectively inhibit the function of certain ORPs by preventing binding of oxysterols. Many of these ORPphilins are anti-proliferative natural products (including Cephalostatin-1, OSW-1 and Ritterazine-B) and have been identified as possible new anti-cancer therapeutics (Burgett et al., 2011). Although an inhibitory effect of ORPphilins on ORP8 has not yet been detected, it is possible that a combined ORPphilin-TRAIL/CD95L treatment could target previously TRAIL or CD95L-resistant tumour cells.

4.3.4: Skp1, FBXO11, CUL1 (SCF) Complex Identified as Interacting with Unstimulated TRAIL-R1/R2 in BJAB Cells

FBXO11 and CUL1 were identified in the mass spectrometry screen as being proteins that may interact specifically with unstimulated TRAIL-R2 and not TRAIL-R1 (Figure 4.8). Subsequent smaller scale isolations and western blot analysis however showed that both proteins were found pre-associated with TRAIL-R1 and TRAIL-R2 (Figure 4.9 & Table 4.1). F-box proteins are known to form interactions with Cullin proteins to recruit ubiquitin ligases and ubiquitinate target proteins (Lydeard et al., 2013). These complexes contain an F-box protein, such as FBXO11, a Cullin protein, such as CUL1, a

Skp protein and an E3 ligase. The mass spectrometry data also showed the presence of Skp1 (Figure 4.8) and western blot analysis confirmed that Skp1 pre-associates with TRAIL-R1/R2 and is also present in DISC-associated receptor complexes (Figure 4.9 & Table 4.1).

Skp-CUL-F-box (SCF) complexes are the most studied of the Cullin ring ligase (CRL) family of ubiquitin ligase complexes (Petroski and Deshaies, 2005). In these complexes, CUL1 and Skp1 function as scaffolds to recruit and position RING domain-containing proteins and F-box containing proteins which determine target specificity (Skaar et al., 2013). SCF complexes can mediate the ubiquitination of target proteins which can then lead to signalling outcomes or protein degradation depending on the ubiquitin chain linkage. In SCF complexes, it is the F-box containing protein which determines target specificity (Skaar et al., 2013). The F-box protein detected in this study is F-box only protein 11 (FBXO11).

FBXO11 has been demonstrated to be a tumour suppressor (Yang et al., 2015) whose function is mainly due to its role in a Skp1-CUL1-FBXO11 complex. Patients with glioblastoma, skin and prostate cancer who displayed high FBXO11 expression were shown to have greater survival and lower tumour grades (Yang et al., 2015). FBXO11 was shown to be especially important in B-cell lymphomas. BCL-6 is an important oncogene in B cells which controls multiple genes involved in B-cell development, differentiation and activation and is overexpressed in the majority of diffuse large cell B-cell lymphomas (DLBCL). FBXO11, in complex with Skp1 and CUL1, targets BCL6 for ubiquitination and subsequent proteasomal degradation. Mutation of FBXO11 was shown to lead to an increase in BCL6 levels and hence increased tumourigenicity (Duan et al., 2012). The FBXO11-containing SCF complex was also shown to block epithelial-mesenchymal transition (EMT), tumour initiation and metastasis in breast cancer cells. FBXO11 was discovered to mediate the ubiquitination of the transcription factor SNAIL, leading to its downregulation by proteasomal degradation. SNAIL is important in activating genes which initiate EMT and lead to increased tumour metastasis and invasion (Zheng et al., 2014). A Skp1-CUL1-FBXO11 complex also mediated the ubiquitination and degradation of cdc10-dependent transcript 2 (Cdt2). This

degradation leads to the increase in downstream p21 and set8 which downregulate TGF β signalling (Abbas et al., 2013).

Therefore, all of the known roles so far for FBXO11, CUL1 and Skp1 involve the targeted ubiquitination and proteasome degradation of target proteins (Abbas et al., 2013; Duan et al., 2012; Yang et al., 2015; Zheng et al., 2014). It can therefore be inferred that the detection of FBXO11, CUL1 and Skp1 associated with unstimulated TRAIL-R1/R2 and in the TRAIL DISC suggests that components of the TRAIL DISC are targets for ubiquitination.

Several reports have already demonstrated that ubiquitination of DISC-associated proteins can have profound effects on TRAIL signalling. A complex containing cullin-3 (CUL3) and RBX1 was shown to mediate the poly-ubiquitination of DISC-associated caspase-8. These poly-ubiquitin chains enhance/lead to the recruitment of p62 and subsequent migration of caspase-8 to ubiquitin dense speckles (Jin et al., 2009), termed the “aggresome” (Békés and Salvesen, 2009). Prevention of CUL3-mediated caspase-8 ubiquitination and “aggresome” formation was shown to decrease TRAIL-induced apoptosis. A20 de-ubiquitinates caspase-8 to reverse the CUL3-mediated effect, displaying dynamic regulation of “aggresome” formation (Jin et al., 2009). Conversely, caspase-8 ubiquitination has also been shown to negatively regulate TRAIL-induced apoptosis. TRAF2 mediates the RING dependent K48-linked poly-ubiquitination of caspase-8 downstream of CUL3. This poly-ubiquitination rapidly leads to degradation of caspase-8 by the proteasome and functions as a shut-off timer for apoptotic signalling. Ubiquitination of TRAIL-R1, but not TRAIL-R2, was demonstrated to inhibit TRAIL-induced apoptosis. Here, MARCH-8 ubiquitinates TRAIL-R1 on lysine 273 leading to down-regulation of TRAIL-R1 at the cell surface by lysosomal mediated degradation (van de Kooij et al., 2013).

In this study, Skp1, CUL1 and FBXO11 were detected in both TRAIL DISC samples and with unstimulated TRAIL-R1/R2 (Figure 4.9). This implies that the SCF complex could be targeting TRAIL-R1/R2 regardless of TRAIL stimulation. Although the initial mass spectrometry data indicated that the SCF complex may be associated only with TRAIL-R2 (Figure 4.8), subsequent experiments and western blot analysis showed very little difference in levels of these proteins between the TRAIL-R1 and TRAIL-R2-containing

samples (Figure 4.10). The effect of knocking down the expression of FBXO11, CUL1 and Skp1 on TRAIL-R1/R2 levels and TRAIL signalling should therefore be investigated. The combination of TRAIL DISC isolations with de-ubiquitinase (DUB) inhibitors may also reveal the accumulation of ubiquitin chains on TRAIL-R1/R2.

However, although FBXO11, CUL1 and Skp1 were identified in TRAIL-R1/R2 isolated complexes it does not necessarily mean that TRAIL-R1 and TRAIL-R2 are the targets for ubiquitination. The SCF complex may have been recruited via indirect interactions with another protein that is associated with TRAIL-R1/R2. This may explain why the detection of FBXO11 and CUL1 was inconsistent between the mass spectrometry screens (Figure 4.8) and subsequent western blot analysis (Figure 4.9).

4.3.5: PP2A Phosphatase Identified as Interacting with both TRAIL-R1 and TRAIL-R2 in BJAB Cells

PP2A is a serine/threonine phosphatase with regulatory roles in a large number of signalling pathways (Eichhorn et al., 2007). PP2A exists as a holoenzyme consisting of three subunits: the catalytic (C) subunit containing the active site, the scaffold (A) subunit and the regulatory (B) subunit, responsible for substrate specificity and subcellular localisation. Initially, a core enzyme composed of the catalytic and scaffold subunits forms and recruits the regulatory subunit (Eichhorn et al., 2009). The ability of PP2A to phosphorylate and regulate a large array of substrates is mostly due to a large repertoire of over 20 different regulatory subunits which can bind the core enzyme (Slupe et al., 2011).

PP2A has already been implicated in regulating apoptosis induction by death receptor signalling (Härmälä-Braskén et al., 2003). Inhibition of PP2A by calyculin A treatment or PP2a inhibitor protein (I2PP2A) expression was shown to block apoptosis induction by CD95L, TNF- α or TRAIL (Härmälä-Braskén et al., 2003). However, PP2A inhibition or siRNA knockdown of PP2A has also been shown to sensitise resistant cells to TRAIL-induced apoptosis (Yang et al., 2014). The catalytic domain of PP2A (PP2A-C) was previously detected associated with TRAIL-R1/R2 after TRAIL stimulation in a complex with Src and caspase-8 (Xu et al., 2013). Here it was demonstrated that PP2A dephosphorylated and activated Src, which inhibited caspase-8 activity by

phosphorylating it on the tyrosine 380 residue (Xu et al., 2013). However, TRAIL activity was then shown to induce the CUL3 mediated ubiquitination and proteasomal degradation of PP2A-C, restoring caspase-8 activity (Xu et al., 2014).

The PP2A subunits, PP2A-A, PP2A-B_{55α} and PP2A-C were detected by mass spectrometry pre-associated with the TRAIL-R1/R2 and also in the TRAIL DISC (Figure 4.8) Western blot analysis confirmed their interactions, summarised in Table 4.1. As the results show that PP2A interacts with TRAIL-R1/R2 independent of TRAIL stimulation, this implies that the effect of PP2A is occurring prior to DISC formation. PP2A could therefore be directly de-phosphorylating TRAIL-R1/R2 suggesting a mechanism by which PP2A enables TRAIL-R1/R2 to be activated by keeping them in a dephosphorylated state.

Considering the very low amount of PP2A detected in the unstimulated TRAIL-R1/R2 samples and the ubiquitous nature of PP2A signalling, it may be difficult to discern the role of PP2A by knocking down the catalytic and scaffold functioning subunits, as these are used in most PP2A functions. However, the role of the regulatory subunit varies depending on the targets (Eichhorn et al., 2009), therefore knockdown of PP2A B_{55α} by siRNA, or knockout using CRISPR/cas9 could reveal the role of PP2A in TRAIL signalling.

Chapter 5: Investigation of the Mechanism of PKC-mediated Inhibition of Death Receptor Signalling

Chapter 5: Investigation of the Mechanism of PKC-mediated Inhibition of Death Receptor Signalling

5.1: Introduction

As discussed throughout, it is important to fully understand how death receptor signalling is regulated in order to develop new strategies to overcome resistance of cancer cells to TRAIL and other death ligand-inducers of apoptosis. The previous chapters have described efforts to identify hitherto unknown mechanisms of death receptor regulation that are not yet known. However, there are also several known pathways which can affect death receptor signalling but are still not completely understood. Activation of protein kinase C (PKC) inhibits apoptosis induced by TRAIL, CD95L and TNF α (Gómez-Angelats et al., 2000; Harper et al., 2003a; Meng et al., 2002; Ruiz-Ruiz et al., 1999; Sarker et al., 2001; Trauzold et al., 2001). The PKC family is a large group of serine threonine kinases, classified by sensitivity to diacyl glycerol (DAG) and Ca²⁺ activation. Conventional PKC isotypes (α , β , β_{II} and γ) are activated by both DAG and Ca²⁺, whereas novel PKC isotypes (δ , ϵ , η , θ and μ) are insensitive to Ca²⁺ but respond to DAG. Atypical PKCs (λ , ζ and ι) are insensitive to both DAG and Ca²⁺ (Bononi et al., 2011).

Both conventional and novel PKC isotypes can be activated by treatment with phorbol ester DAG analogues. PKC activation by these agents inhibits apoptosis induced by TRAIL (Sarker et al., 2001) and CD95 (Ruiz-Ruiz et al., 1999), upstream of caspase-8 activation (Gómez-Angelats et al., 2000). Subsequently, PKC activation was demonstrated to block FADD recruitment to both the CD95 and TRAIL DISC (Gómez-Angelats and Cidlowski, 2001; Harper et al., 2003a). Previously, in our laboratory, Harper et al. (2003) demonstrated that HeLa cells pre-treated with phorbol 12-myristate 13-acetate (PMA) are resistant to TRAIL induced death. This resistance was prevented when PMA-mediated PKC activation was blocked using the PKC inhibitor, Bisindolylmaleimide I (BisI). PKC activation was shown to inhibit FADD recruitment to TRAIL-R1/R2 receptors by DISC analysis. TRADD recruitment to TNFR1 is also blocked by PKC, demonstrating that this is a general death receptor phenomenon (Harper et al., 2003a). However, while PKC activation was clearly affecting FADD recruitment to

the DISC, this was not apparently due to changes in FADD phosphorylation (Harper et al., 2003a).

Therefore, it has been convincingly demonstrated that PKC activation can block the extrinsic apoptotic pathway and that this inhibition occurs upstream of caspase activation and inhibits FADD recruitment to the DISC. However, the studies conducted so far have left a number of unanswered questions. Most importantly, how does PKC activation block the recruitment of FADD to the DISC and subsequently block apoptosis induction, and what is the target for PKC? In addition, what effect does PKC activation have on non-apoptotic death receptor signalling? This study was undertaken to address these outstanding questions.

5.2: Results

5.2.1: PKC Activation Inhibits TRAIL-induced Apoptosis in HeLa and Jurkat E6.1 but not BJAB cells

To study the effect of PKC activation on TRAIL-induced apoptosis, HeLa cells were pre-treated with 20 ng/ml PMA prior to 5 h TRAIL treatment (Figure 5.1A). In addition, a Bisindolymaleimide I (Bisl) pre-treatment was utilised to inhibit PMA induced PKC activation, showing that the effects of PMA were indeed PKC-mediated. PMA treatment almost completely abrogated TRAIL-induced apoptosis, with the percentage of cells showing phosphatidylserine (PS) externalisation reducing from 47.5 to 3.7% (Figure 5.1A). This inhibition was reversed by pre-treating with Bisl (38.6%). The inhibition of TRAIL-induced apoptosis by PKC activation was also confirmed by the disappearance of the p43/p41 and subsequent p18 cleavage fragments of caspase-8, showing that caspase-8 activation at the DISC was inhibited (Figure 5.1B). Furthermore, the downstream cleavage of caspases-9 (p37/p35) and -3 (p20/p19) following PMA pre-treatment was blocked. There was also a loss of cleavage of PARP to the p85 fragment (Figure 5.1B), a signature of apoptosis induction (Duriez and Shah, 1997).

I next examined the effect of PKC activation on TRAIL signalling in the T cell line, Jurkat E6.1. Jurkat cells do not express TRAIL-R1 and thus are relatively insensitive to soluble, non-oligomerised TRAIL-induced death (Sprick et al., 2000). Instead, Jurkat cells were treated with ILZ-TRAIL, a recombinantly generated TRAIL construct containing an isoleucine zipper (ILZ) motif to encourage greater oligomerisation of TRAIL-R2 and DISC activity (Han et al., 2016). Again, PMA pre-treatment inhibited ILZ-TRAIL-induced apoptosis with the percentage of Jurkat cells showing PS externalisation reducing from 80.2 to 49.7% (Figure 5.1C). The loss of PS externalisation also correlated with a reduction in the cleavage of caspase-8 to its p41/43 and p18 fragments. Downstream cleavage of caspase-9, caspase-3 and PARP was also reduced following PMA pre-treatment (Figure 5.1D). Although not as dramatic as in HeLa cells (Figure 5.1A), where TRAIL-induced apoptosis was almost completely abolished, PKC activation did

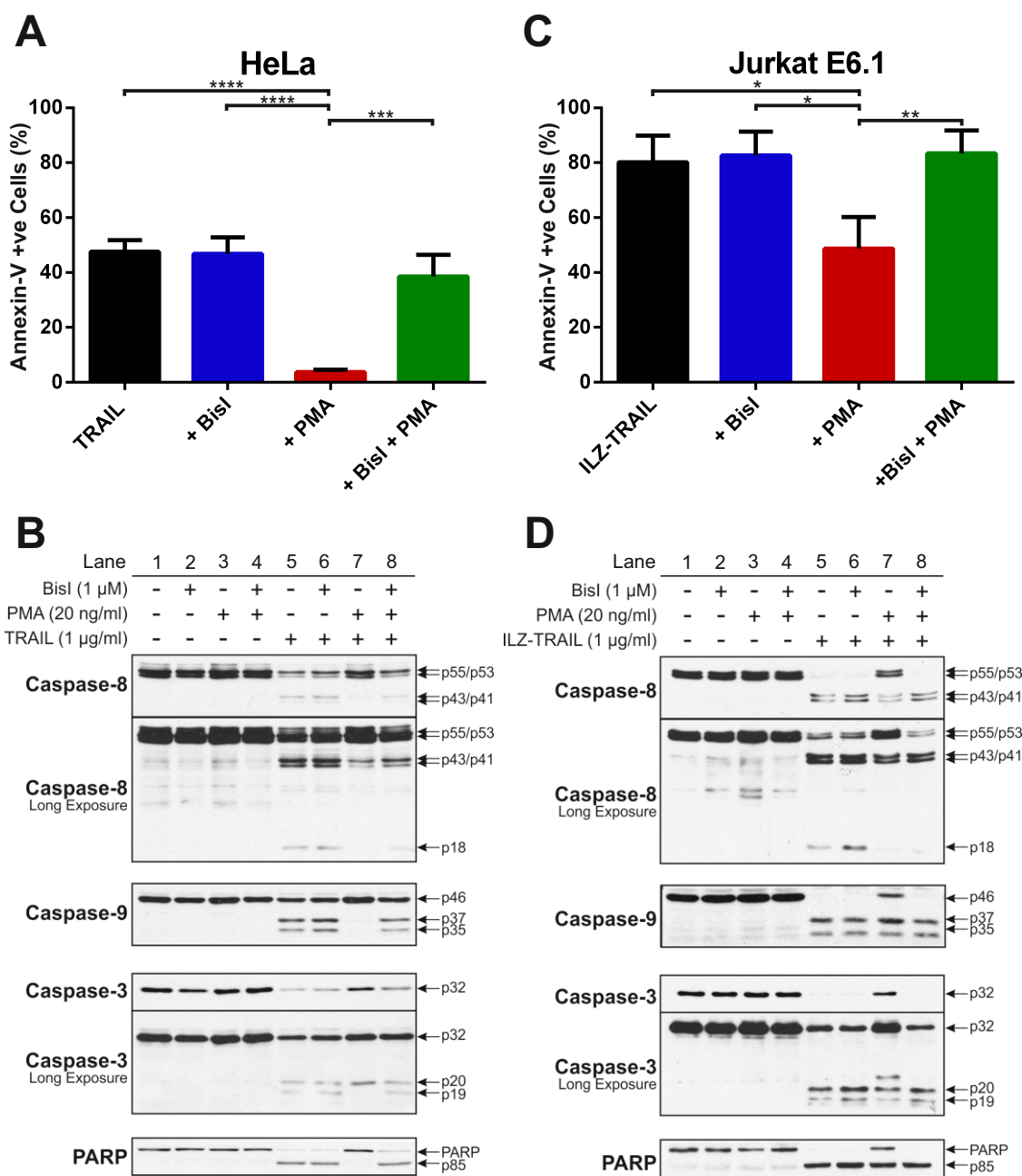


Figure 5.1: PKC Activation Blocks TRAIL-Induced Apoptosis in HeLa and Jurkat E6.1 Cells

HeLa (A + B), Jurkat E6.1 (C + D) cells were pre-treated with either: 1 μ M BisI, 20 ng/ml PMA or 1 μ M BisI and 20 ng/ml PMA. Initially cells were treated with BisI for 30 min before addition of PMA for 30 min. After pre-treatment, cells were treated with 1 μ g/ml TRAIL (A + B) or ILZ-TRAIL (C + D) for 5 hours. Cells were harvested, stained with Annexin V-FITC and DRAQ7 and analysed by flow cytometry (A + C). Cell pellets were also taken for western blots (B + D). Western blots (B + D) of cell pellets were probed for caspase-8, caspase-9, caspase-3 and PARP. Data shown in (A + C) is % Annexin-V positive cells minus background from 3 independent experiments +/- standard deviation (SD). Background cell death for the HeLa cells was 5.1% +/- 0.38 (A) and for the Jurkat E6.1 cells (C) was 4.6% +/- 0.74. Differences between the group means were shown to be statistically different by one-way ANOVA. Significant differences were determined by a post-hoc tukey test and are highlighted by * (P<0.05 = *, P<0.01 = **, P<0.001 = ***, P<0.001 = ****).

significantly reduce TRAIL-induced apoptosis in Jurkat cells (Figure 1b), demonstrating that the effect observed is not specific to HeLa cells.

In contrast, when the Burkitt's lymphoma cell line, BJAB (Figure 5.2) was pre-treated with PMA prior to TRAIL treatment, there was no inhibitory effect on PS externalisation (Figure 5.2A). Cleavage of caspase-8, caspase-9, caspase-3 and PARP showed no difference following PMA treatment (Figure 5.2B), differing from that seen in both HeLa and Jurkat cells (Figure 5.1). This demonstrates that the inhibitory effect of PKC activation on TRAIL-induced apoptosis may not occur in all cell types. Discerning the reason for this cell-specific difference may therefore be important in determining how PKC activation can inhibit TRAIL signalling.

5.2.2: PKC Activation Inhibits CD95-induced Apoptosis in Jurkat A3 Cells

The effect of PKC activation on CD95L signalling in Jurkat cells was studied further. CD95L-induced apoptosis has also previously been reported to be inhibited by phorbol ester treatment (Meng et al., 2002). Jurkat A3 cells were pre-treated with 20 ng/ml PMA prior to 5 h treatment with the agonistic CD95 antibody, CH11 (Figure 5.3). Similar to the effects observed for TRAIL-induced apoptosis (Figure 5.1), PMA inhibited PS externalisation induced by CH11 (Figure 5.3a), from 60.7 to 31.5%. This loss was accompanied by a reduction in the proteolytic cleavage of caspase-8, caspase-9, caspase-3 and PARP (Figure 5.3B). Pre-treatment with BisI reversed the effect of PMA treatment, with 62% of cells PS +ve (Figure 5.3A) along with increased amounts of caspase-8, caspase-9, caspase 3 and PARP fragments generated. This demonstrates that PKC activation can block CD95L-induced apoptosis as well as TRAIL-induced apoptosis and is likely to share a common underlying mechanism.

5.2.3 PMA Treatment Blocks TRAIL-induced NF κ B Activation

In addition to its pro-apoptotic, caspase-activating signalling arm, TRAIL has also been shown to induce pro-survival signalling pathways after formation of a secondary signalling complex following DISC dissociation (Varfolomeev et al., 2005).

It is currently unknown whether PKC activation can block TRAIL-induced secondary signalling complex formation and subsequent pro-survival pathway activation. Accordingly, HeLa cells were treated with 0.5 μ g/ml TRAIL for increasing lengths of

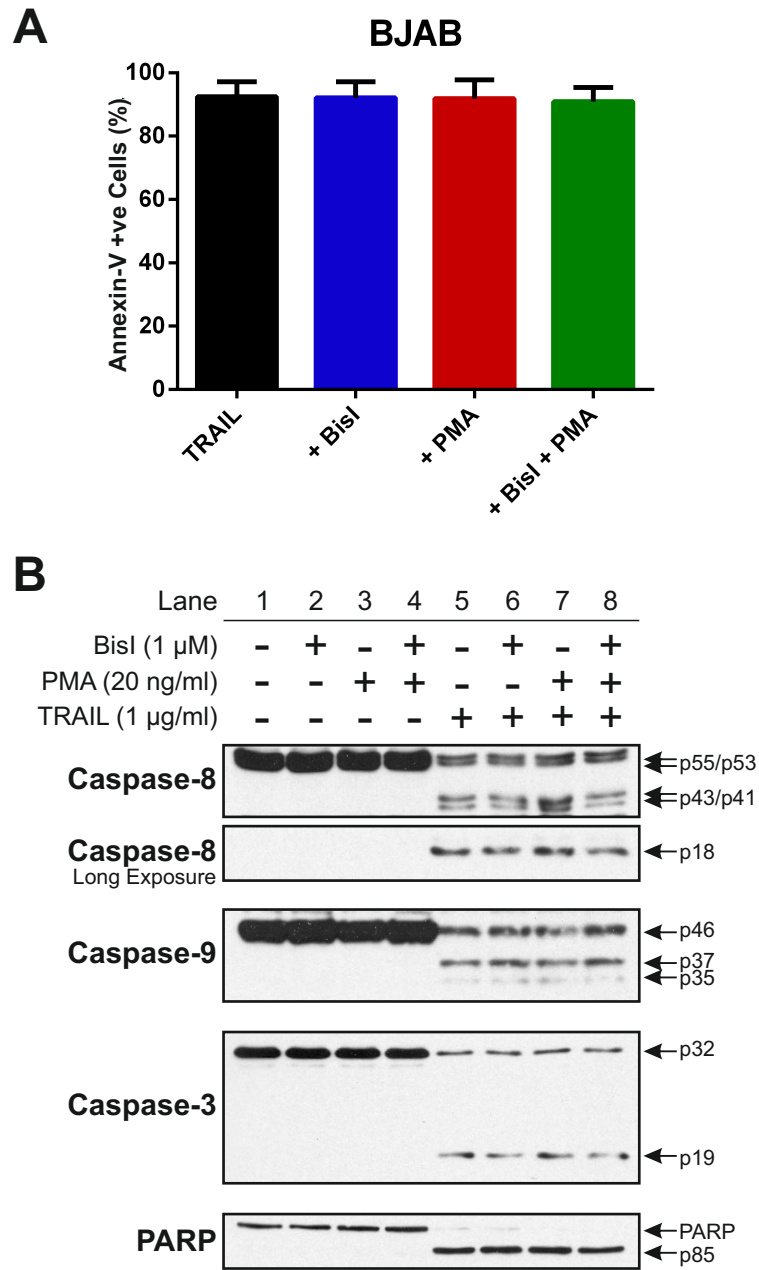


Figure 5.2: PKC Activation Does not Block TRAIL-Induced Apoptosis in BJAB Cells

BJAB cells were pre-treated with either: 1 μ M Bis1, 20 ng/ml PMA or 1 μ M Bis1 and 20 ng/ml PMA. Initially cells were treated with Bis1 for 30 min before addition of PMA for 30 min. After pre-treatment, cells were treated with 1 μ g/ml TRAIL for 5 hours. Cells were harvested, stained with Annexin V-FITC and DRAQ7 and analysed by flow cytometry (A). Cell pellets were also taken for western blots (B). Western blots (A) of cell pellets were probed for caspase-8, caspase-9, caspase-3 and PARP. Data shown in (A) is % Annexin-V positive cells minus background from 3 independent experiments +/- standard deviation (SD). Background cell death was 10.8% +/- 0.81. Differences between the group means were shown to be statistically different by one-way ANOVA. Significant differences were determined by a post-hoc tukey test and are highlighted by * ($P < 0.05 = *$, $P < 0.01 = **$, $P < 0.001 = ***$, $P < 0.001 = ****$).

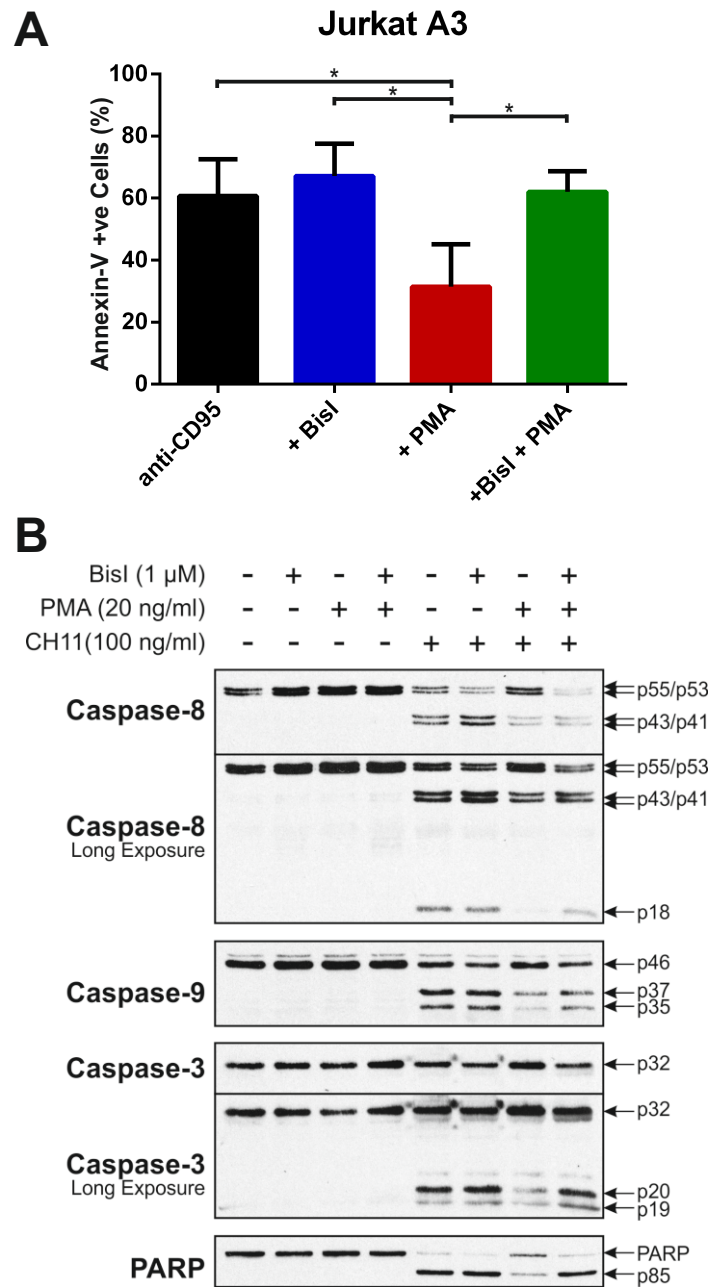


Figure 5.3: PKC Activation Blocks Anti-CD95-Induced Apoptosis in Jurkat A3 Cells

Jurkat A3 cells (1×10^6) were pre-treated with either: 1 μ M BisI, 20 ng/ml PMA or 1 μ M BisI and 20 ng/ml PMA. Initially cells were treated with BisI for 30 min before addition of PMA for 30 min. After pre-treatment, cells were treated with 100 ng/ml anti-CD95 (CH11) for 5 h, stained with Annexin V-FITC and DRAQ7 or pelleted. Western blots (b) of the cell pellets were probed for caspase-8, caspase-9, caspase-3 and PARP. Data shown in a) is % Annexin V positive cells minus background from 3 independent experiments +/- standard deviation (SD). Background cell death was 6.2% +/- 1.35. Differences between the group means were shown to be statistically different by one-way ANOVA. Significant differences were determined by a post-hoc tukey test and are highlighted by * ($P < 0.05 = *$, $P < 0.01 = **$, $P < 0.001 = ***$, $P < 0.001 = ****$).

time with or without pre-treatment with PMA (Figure 5.4). Addition of TRAIL resulted in phosphorylation of the NF κ B inhibiting protein, I κ B α after 30-60 min. Conversely, HeLa cells pre-treated with PMA prior to TRAIL, failed to induce phosphorylation of I κ B α above basal levels. This indicates that PMA pre-treatment is blocking both the apoptotic (Figure 5.1) and non-apoptotic (Figure 5.4) arms of TRAIL signalling.

5.2.4 Characterisation of PKC Isoform Expression and PKC Activation

Both HeLa and Jurkat cells show the propensity for TRAIL (Figure 5.1) (and anti-CD95 (Figure 5.3)) signalling to be inhibited by PKC activation, whereas BJAB cells do not (Figure 5.2). To determine if the difference in sensitivity is due to differences in the level of PKC proteins, the expression of each of the PKC isoforms in HeLa, BJAB and Jurkat cell lines was characterised (Figure 5.5). PKC α expression was detected in HeLa and Jurkat cells but much lower expression was observed in BJAB cells. PKC β_1 expression was detected in all three cell lines at similar levels. HeLa cells were shown to not express the PKC β_{II} isoform, which agrees with reports in the literature (Kaneki et al., 1999), but contrasts with its expression in BJAB and Jurkat cells. PKC γ levels appeared to be low but broadly consistent across the three cell lines. PKC δ expression was higher in BJAB cells when compared to HeLa and Jurkat. This was also the case for PKC ϵ expression, in which the expression was significantly higher in BJAB cells. PKC η was detected in all three cell lines whereas PKC θ was only detected in Jurkat cells.

Prolonged activation or inhibition of PKC isoforms has also been demonstrated to effect the protein levels of the PKC isoforms (Basu and Sivaprasad, 2007). In addition to native differences between the cell lines, there also appeared to be differences in the effect of PMA or BisI on the protein levels of the PKC isoforms. In HeLa cells, BisI treatment led to a drop in PKC β_1 and PKC γ levels. Conversely, expression of PKC θ and PKC η isoforms appeared to increase. This pattern was different for the BJAB and Jurkat cells in which PMA and BisI treatment caused the expression of PKC γ to increase but had little effect on the other isoforms.

To determine if PMA treatment could indeed activate PKC in each cell line, western blots were probed for the phosphorylation of MARCKS (Figure 5.5B), a downstream PKC substrate (Vääräniemi et al., 1999). In all three cell lines, PMA treatment induced

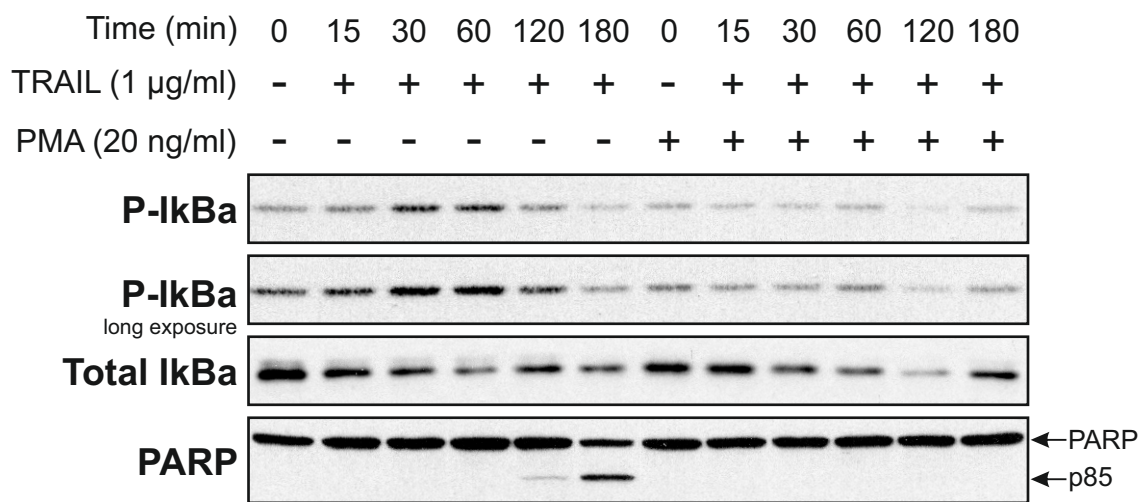


Figure 5.4: PMA Treatment Blocks TRAIL-Induced NFκB Activation in HeLa Cells

HeLa cells were treated with 0.5 µg/ml TRAIL for 15, 30, 60, 120 or 180 min. In addition cells were pre-treated with 20 ng/ml PMA 30 min prior to TRAIL treatment. Following treatment, cells were harvested, lysed in DISC lysis buffer and protein concentration determined by Bradford assay. SDS-PAGE gels were loaded with 30 µg of each sample. Western blots were probed for P-IκBα, IκBα and PARP.

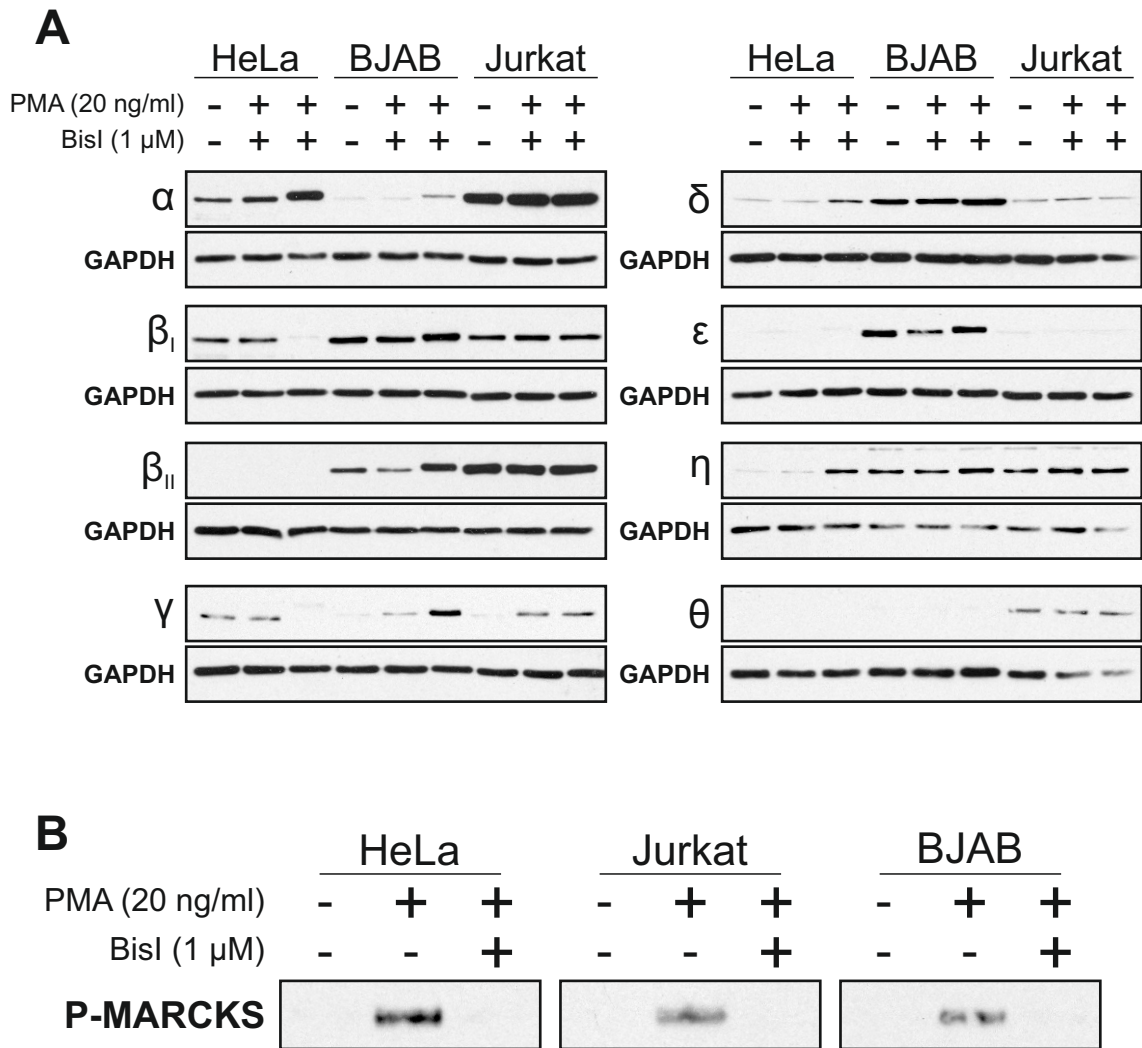


Figure 5.5: Characterisation of PKC isoform Expression and PKC activation

HeLa, BJAB or Jurkat E6.1 cells were treated with 1 μ M Bisl for 30 min, followed by 20 ng/ml PMA for 30 min, or only 20 ng/ml PMA for 30 min, or left untreated. Cells were lysed in DISC lysis buffer and protein concentration determined by Bradford assay. 30 μ g of each sample was loaded onto SDS-PAGE gels, western blotted and probed for PKC isoforms and GAPDH (A) or Phosphorylated-MARCKS (B).

the phosphorylation of MARCKS. Moreover, MARCKS phosphorylation could be prevented by pre-treatment with BisI. This demonstrates that in all three cell lines PMA can activate PKC and that this activation can be blocked by BisI. MARCKS can be phosphorylated by multiple PKC isoforms however, so this information alone does not reveal which PKC isoform is responsible for the inhibition of death receptor signalling.

5.2.5 Knockdown of PKC β Prevents PKC-mediated Inhibition of TRAIL-Induced Apoptosis

The inhibitory effect on TRAIL signalling was observed following PMA treatment, which like other phorbol esters can only activate the conventional and novel PKC isoforms (Wu-Zhang and Newton, 2013). At the concentration used here (1 μ M) BisI would also only inhibit the conventional and novel PKC isoforms. Thus, PKC β II is unlikely to be responsible for the effects observed, as HeLa cells (in which TRAIL signalling is inhibited) do not express PKC β II (Figure 5.5A). It is also unlikely PKC ϵ is responsible as only the BJAB cells (in which TRAIL signalling is not inhibited) express PKC ϵ . The lower expression of PKC α in BJAB cells could explain the lack of TRAIL inhibition by PMA observed in these cells. However, there have also been reports that PKC β isoforms can inhibit signalling by death receptors (Meng et al., 2010).

To explore this further, the roles of PKC α and PKC β in inhibiting TRAIL-induced apoptosis were evaluated in HeLa cells (Figure 5.6). PKC isoform expression was knocked down by 48 h treatment with siRNA and cells were then treated with PMA or BisI and PMA followed by TRAIL. TRAIL-induced apoptosis (42.4 and 43.2%), as measured by annexin V binding (Figure 5.6A), was reduced by PMA pre-treatment to 13.5% and 14.3% in the no siRNA (-) and control siRNA (Neg) transfected cells, respectively (Figure 5.6A). BisI pre-treatment again prevented this inhibition with 40.8 and 39.7% annexin V +ve cells detected, respectively. The reduction in annexin V binding by PMA was shown to be statistically significant ($P < 0.05$), correlating well with previous data (Figure 5.1). Western blots probed for caspase-8 (Figure 5.6B) correlated with the FACs data, showing that PMA pre-treatment prevents the cleavage of caspase-8 to its p43/41 and p18 fragments in the no siRNA (-) and control siRNA (Neg) transfected samples (Lanes 3 and 7) and fragmentation returning following BisI pre-treatment (Lanes 4 and 8).

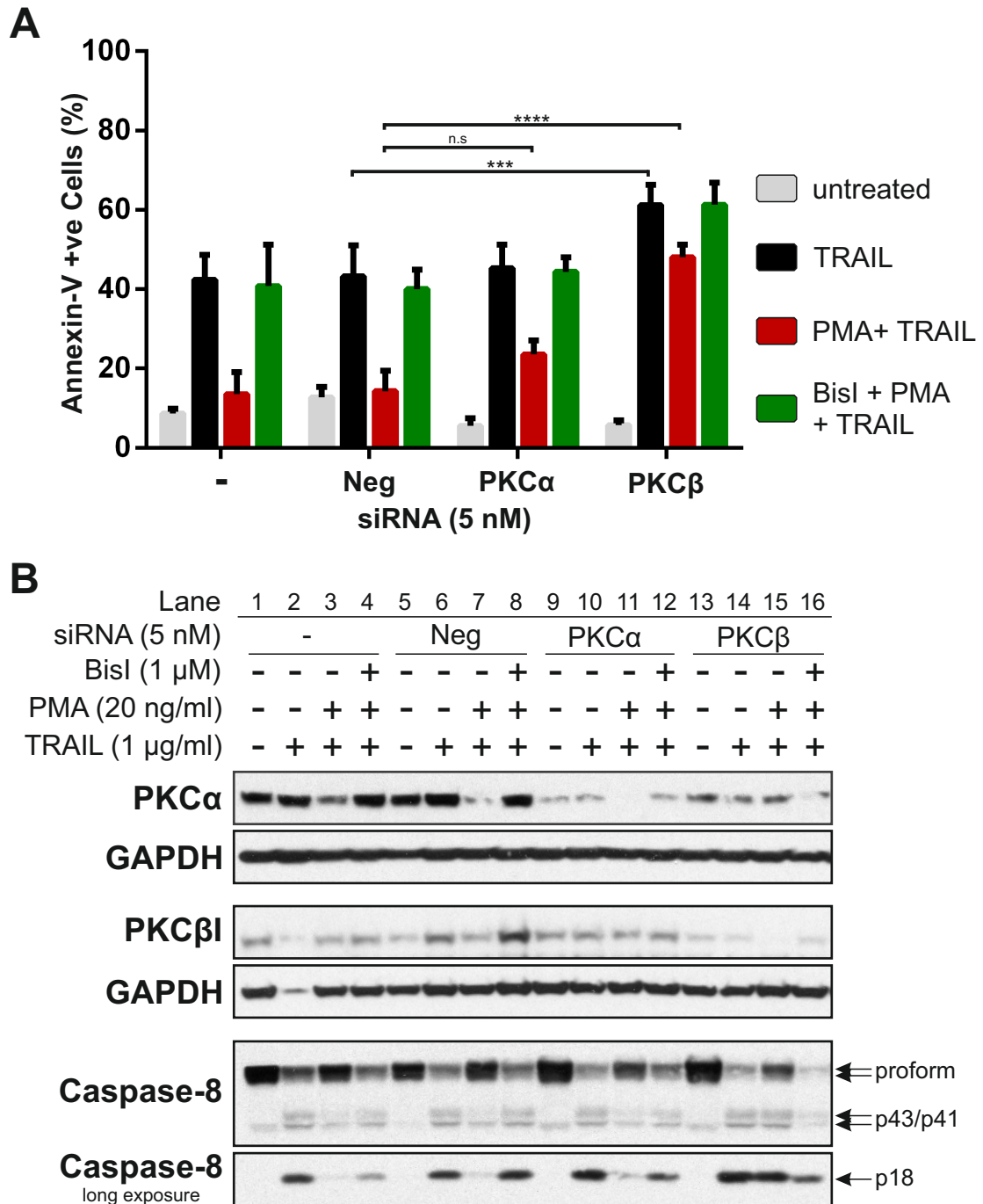


Figure 5.6: siRNA Targeting of PKCβ Prevents PKC-Mediated Inhibition of TRAIL-Induced Apoptosis

HeLa cells were transfected with either no siRNA (-) or 5 nM of control (Neg) or PKCα or PKCβ targeting siRNA for 24 h. Cells were then pre-treated with either 20 ng/ml PMA or 1 μM BisI and 20 ng/ml PMA. Initially cells were treated with BisI for 30 min before addition of PMA for 30 min. After pre-treatment, cells were treated with 1 μg/ml TRAIL for 5 h. Cells were harvested, stained with Annexin V-FITC and DRAQ7 and analysed by flow cytometry (A). Cell pellets were also taken for western blots (B). Western blots (B) were performed from the cell pellets and probed for PKCα, PKCβ or caspase-8, caspase-9. Data shown in (A) is % Annexin-V positive cells minus background from 3 independent experiments +/- standard deviation (SD). Differences between the group means were shown to be statistically different by two-way ANOVA. Significant differences were determined by a post-hoc Dunnett test and are highlighted by * (P<0.05 = *, P<0.01 = **, P<0.001 = ***, P<0.0001 = ****).

Knockdown of PKC α , as confirmed by western blot (Figure 5.6B, Lanes 9-12), had no effect on TRAIL-induced PS externalisation in HeLa cells (45.3%, Figure 5.6A). Pre-treatment with PMA reduced the amount of PS externalisation to 23.5%, which although not as low as observed in the control siRNA transfected cells (14.3%), was not statistically significant. Bisl pre-treatment returned TRAIL-induced PS externalisation to 44.4%. Again, PMA treatment (Lane 11) prevented the cleavage of caspase-8 to its p43/p41 and p18 subunits and Bisl pre-treatment (Lane 12) reversed this inhibition (Figure 5.6B).

Knockdown of PKC β (Figure 5.6B, Lanes 13-16) was shown to increase the percentage of cells displaying PS externalisation after TRAIL treatment to 61.2% (Figure 5.6A) when compared to no siRNA (-) or control siRNA (Neg) transfected cells, 42.4 and 43.2% respectively. In addition, the number of annexin V +ve cells with the PMA pre-treatment was only marginally reduced to 48.0%. This is markedly different to the control treatments, in which PMA treatment almost completely abrogates TRAIL-induced apoptosis (Figure 5.6A). Bisl pre-treatment restored PS externalisation to 61.3%, again higher than the no siRNA (-) and control (Neg) transfected cells. Western blots for caspase-8 (Figure 6b) show that PMA treatment (Lane 15) in the PKC β siRNA treated cells did not reduce the cleavage of caspase-8 to the p43/41 and p18 bands (compare to lane 14). The amount of caspase-8 p43/41 and p18 subunits generated were similar in all of the PKC β siRNA samples which were treated with TRAIL (Lanes 14-16). The intensity of the bands corresponding to the p43/41 and p18 bands appeared lower in the Bisl treated sample (Lane 16), however the reduction in caspase-8 proform was still apparent and was similar to that seen in cells treated with TRAIL alone (Lane 13). This demonstrates that the knockdown of PKC β is able to prevent the inhibition of TRAIL-induced apoptosis by PMA and this may be the major isoform responsible for PKC-mediated inhibition of TRAIL signalling.

5.2.6 PKC Activation Inhibits the Aggregation of TRAIL-R2 to HMW-DISC

It has been reported that after TRAIL binds to its cognate receptors, TRAIL-R1 and TRAIL-R2, the resultant DISC formed is of a greater size that can be accounted for by the minimal components of the trimerised receptors, FADD and caspase-8 chains. This high molecular weight (HMW) DISC has been suggested to be essential for effective

apoptotic signalling by TRAIL (Dickens et al., 2012a). To observe the effects of PMA on HMW DISC formation, lysates from HeLa cells treated with biotinylated TRAIL (bTRAIL) alone, cells pre-treated with PMA and bTRAIL, and cells pre-treated with BisI, PMA and bTRAIL were separated using equilibrium sucrose density gradients (SDG). In the sucrose gradients, the TRAIL-DISCs migrate to the density of sucrose which approximately corresponds to the density of the DISC. The gradients were then fractionated and DISCs isolated from each fraction using streptavidin beads. The isolated DISCs were then analysed by SDS-PAGE and western blotting for known DISC components. The SDG western blots (Figure 5.7) show that TRAIL-R1 (peak between fractions 7-10) and TRAIL-R2 (peak between fractions 8-10) predominantly localise to high molecular weight fractions. It is only in these TRAIL receptor containing HMW fractions (Fractions 8-11) that FADD and caspase-8 can be detected, highlighting the importance of HMW-DISC formation in TRAIL signalling. In the cells pre-treated with PMA (PMA + TRAIL), the amount of FADD and caspase-8 recruited to the DISC is significantly decreased compared to cells treated with TRAIL alone (TRAIL). In addition, the position of the TRAIL-R2 peak shifts from fractions 9-10 in cells treated with TRAIL alone (TRAIL) to a peak at fractions 7-8 in those cells pre-treated with PMA (PMA + TRAIL). When cells were incubated with BisI prior to PMA and TRAIL treatment (BisI + PMA + TRAIL), the observed effects of PMA were reversed. Thus, the amount of FADD and caspase-8 recruited to the HMW-DISC increased and TRAIL-R2 peaked in fractions 9-10. The effect of PMA pre-treatment on the position of TRAIL-R1 was much less dramatic than for TRAIL-R2, and a much smaller size shift was observed. Therefore, PKC activation selectively decreases the size of TRAIL-R2 containing HMW-DISCs and reduces the recruitment of both FADD and caspase-8.

5.2.7 PKC Activation Modifies TRAIL-R2 at the DISC in HeLa and Jurkat E6.1 but not BJAB cells

Since PKC is a kinase, it is likely that the effects of PKC activation on TRAIL-DISC formation are mediated by protein phosphorylation. In respect of this, the DISC isolation protocol was modified to include phosphatase inhibitors in the lysis buffer. In this way, phosphorylation(s) of isolated DISC proteins could be observed. HeLa cells were pre-treated with PMA, BisI and PMA or not pre-treated, followed by incubation

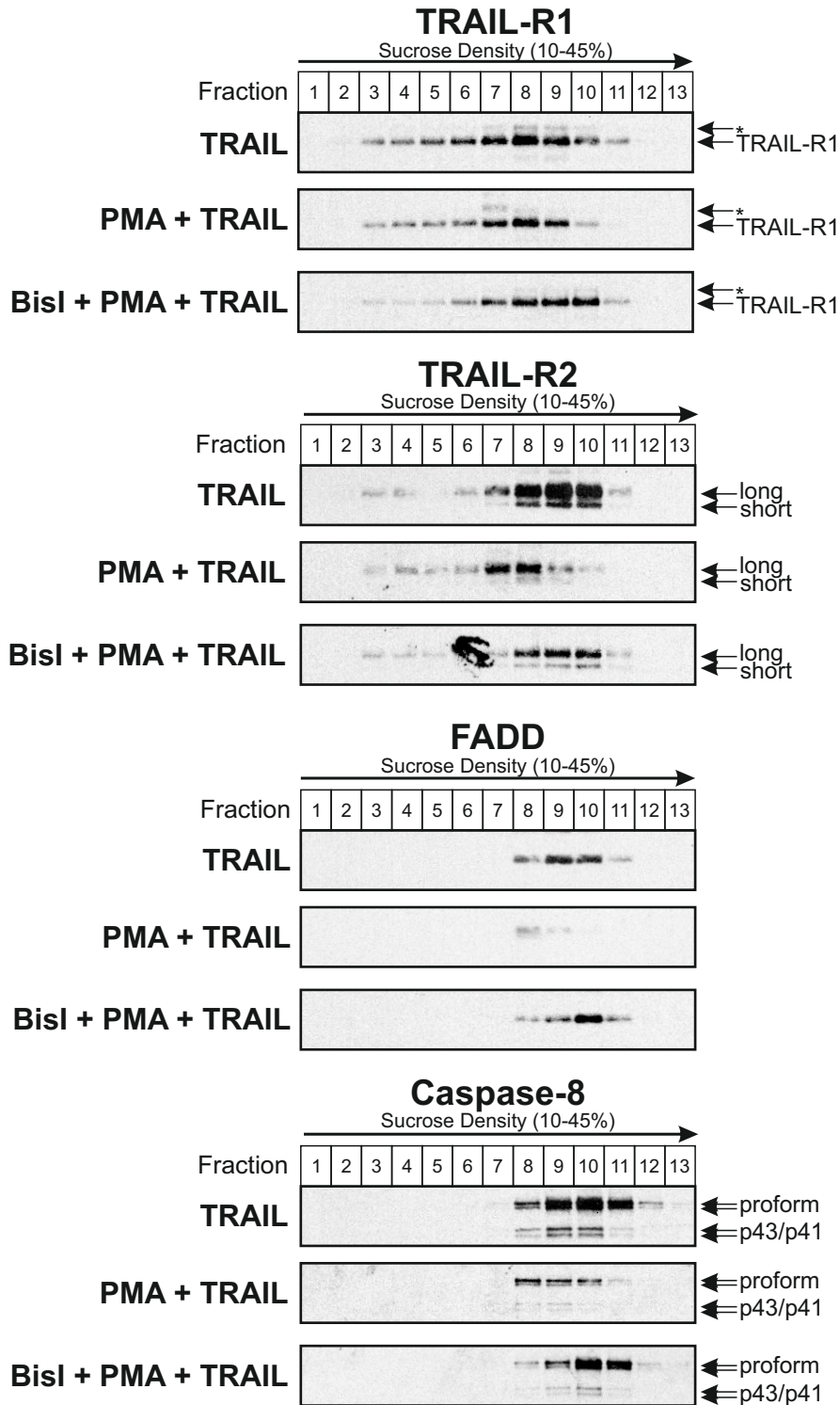


Figure 5.7: PKC Activation Inhibits the Aggregation of TRAIL-R2 to HMW-DISC and Impedes FADD Recruitment

HeLa cells ($6 \times T175$ flasks, $\sim 6 \times 10^7$) were pre-treated with either: 20 ng / ml PMA or 1 μ M BisI and 20 ng / ml PMA. Initially cells were treated with BisI for 30 min before addition of PMA for 30 min. After pre-treatment, cells were treated with 0.5 μ g/ml bTRAIL. Treated cells were then lysed and separated by centrifugation through 10-45% sucrose density gradients. TRAIL DISCs were then captured by incubation using streptavidin beads from the indicated fractions. Western blots were performed from the eluted fractions and were probed for TRAIL-R1, TRAIL-R2, FADD and Caspase-8.

with bTRAIL and were subsequently lysed, in phosphatase inhibitor-containing lysis buffer. TRAIL-DISCs were then isolated and subsequently immunoblotted for known DISC components. Figure 5.8A shows that the TRAIL receptors, FADD and caspase-8 were detected in each DISC sample. The level of FADD detected was reduced when the cells were pre-treated with PMA. In contrast, when cells were pre-treated with BisI before PMA, the amount of FADD recruited to the DISC was restored. This reduction in FADD recruitment mirrors that observed in the sucrose density fractionated DISCs (Figure 5.7) and our previously published results (Harper et al., 2003a). Importantly, the band corresponding to TRAIL-R1 does not appear to alter its position in either PMA or BisI pre-treated TRAIL DISC samples. An apparent higher molecular weight band (*) is observed in all three samples which could correspond to a glycosylated form of TRAIL-R1. This possible glycosylated TRAIL-R1 band (*) appears to diminish slightly in the PMA pre-treated sample and may be affected by PKC activation. PMA pre-treatment does however appear to have an effect on the position of TRAIL-R2 (Figure 5.8 A). The bands corresponding to the long and short isoforms of TRAIL-R2 migrate at an apparent higher molecular weight in the PMA pre-treated DISC (denoted by red arrows). This higher molecular weight shift of TRAIL-R2 is reversed when the cells are additionally pre-treated with BisI, indicating that the shift is being mediated by PKC.

This experiment was then repeated in Jurkat E6.1 cells (Figure 5.8B), where DISCs were isolated following treatment with biotinylated ILZ-TRAIL (bILZ-TRAIL) with or without pre-treatment with PMA and BisI as described above. Western blots of the isolated DISCs show that TRAIL-R2, FADD and caspase-8 were detected in each sample. No signal was detected for TRAIL-R1, confirming that Jurkat cells do not express TRAIL-R1 and signal exclusively through TRAIL-R2. The amount of FADD detected was reduced in the sample pre-treated with PMA, with the level being partially restored with additional BisI pre-treatment. In addition, the bands corresponding to TRAIL-R2 long and short isoforms could again be observed at a higher apparent molecular weight when Jurkat cells were pre-treated with PMA (red arrows). This effect was again reversed in the BisI pre-treated cells, demonstrating that PKC activation was responsible for the modification of TRAIL-R2. Therefore, in a second cell line in which

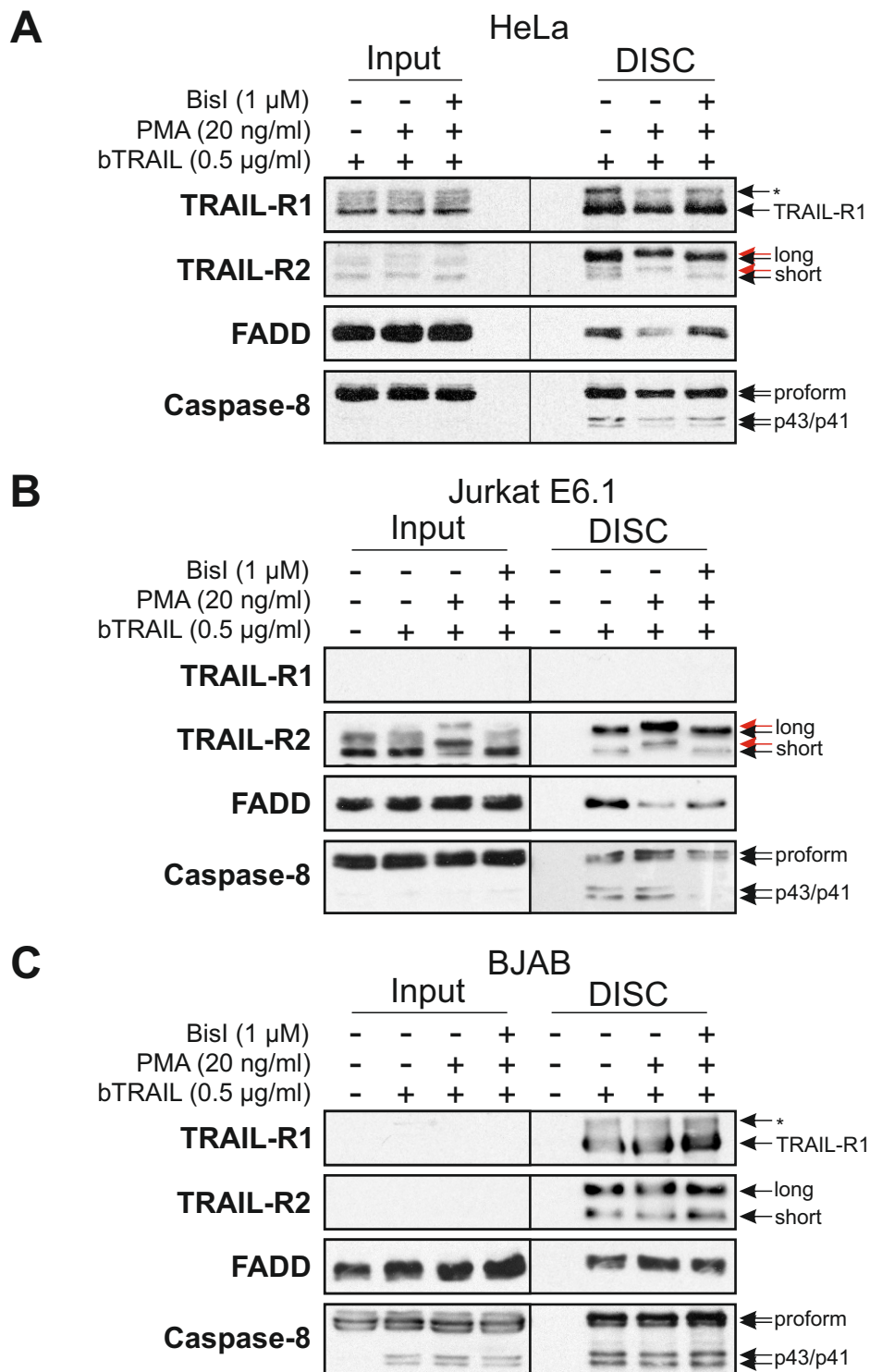


Figure 5.8: PKC Activation Modifies TRAIL-R2 and Inhibits FADD Recruitment to the DISC in HeLa and Jurkat E6.1 Cells but not in BJAB Cells

HeLa (A) (2 x T175 flasks, $\sim 2 \times 10^7$), Jurkat (B) or BJAB (C) (50×10^6) cells were pre-treated with either: 20 ng/ml PMA or 1 μ M Bisl and 20 ng/ml PMA. Initially cells were treated with Bisl for 30 min before addition of PMA for 30 min. After pre-treatment, cells were treated with 0.5 μ g/ml bTRAIL (A,C) or bILZ-TRAIL (B). Treated cells were lysed in DISC lysis buffer containing phosphatase inhibitors. DISCs were isolated by incubation with streptavidin beads and eluted into sample buffer. Western blots were performed from the eluted DISCs and probed for TRAIL-R1, TRAIL-R2, FADD and caspase-8.

PKC activation can inhibit TRAIL signalling (Figure 5.1), a reduction in FADD recruitment to the DISC correlates with a modification of TRAIL-R2, resulting in an increase in the apparent molecular weight of both the long and short isoforms. I then isolated DISCs from BJAB cells (Figure 5.8C), which do not show inhibition of TRAIL signalling by PKC activation (Figure 5.2), by treating with bTRAIL after pre-treatment with PMA or Bisl and PMA. Western blots of the isolated DISCs detected TRAIL-R1, TRAIL-R2, FADD and caspase-8. However, as opposed to that observed in the HeLa and Jurkat cells, PMA treatment had no effect on the amount of FADD recruited. In addition, there were no observable differences in the migration of the TRAIL-R2 long and short isoform bands when the cells were pre-treated with PMA. Therefore, reduced FADD binding and TRAIL-R2 modification correlate with inhibition of TRAIL signalling, and importantly were not observed in the cell line that was insensitive to PKC-mediated inhibition of TRAIL signalling.

5.2.8 PKC Activation Modifies both TRAIL-stimulated and Unstimulated TRAIL-R2

From the PMA pre-treated DISCs isolated from HeLa and Jurkat cells (Figures 5.8A and B), it is apparent that PKC activation is modifying TRAIL-R2 in the DISC. It is not however clear whether this modification is occurring solely in the DISC-associated TRAIL-R2 or whether PKC activation is modifying TRAIL-R2 globally. To determine the effect of PMA on unstimulated TRAIL-R2, the TRAIL DISC was isolated from HeLa cells, but in addition unstimulated (US) TRAIL receptors were isolated by the addition of bTRAIL post cell lysis. Western blots performed from the isolated samples for TRAIL-R1/R2 and FADD are shown in Figure 5.9. As expected, in the unstimulated (US) samples (Lanes 2-4) only TRAIL-R1/R2 were detected. FADD was specifically detected in the TRAIL DISC samples (Lanes 5-7), but as previously observed (Figure 5.8), the amount of FADD recruited was reduced in the PMA pre-treated DISC (Lane 6). Bisl partially restored the amount of FADD recruited (Lane 7), although not as much as previously observed in the SDG DISCs (Figure 5.7) or non-fractionated DISCs (Figure 5.8). The bands detected for TRAIL-R2 migrated at the position of an apparent higher molecular weight (red arrows) in the PMA pre-treated samples, both in the DISC (Lane 6) and when unstimulated (Lane 3). In addition, the TRAIL-R2 bands migrated at their

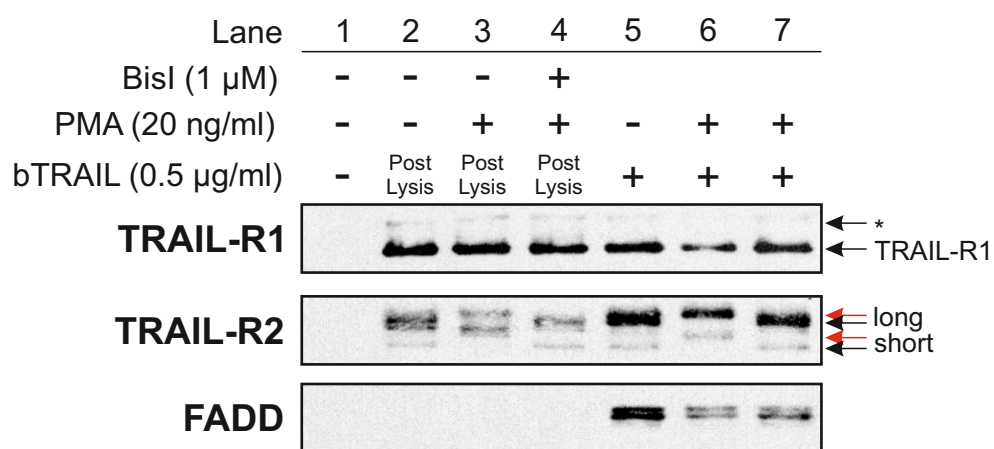


Figure 5.9: PKC Activation Modifies both TRAIL-Stimulated (DISC associated) and TRAIL-Unstimulated TRAIL-R2

HeLa cells (2 x T175 flasks, $\sim 2 \times 10^7$) were pre-treated with either: 20 ng/ml PMA or 1 μ M Bisl and 20 ng/ml PMA. Initially cells were treated with Bisl for 30 min before addition of PMA for 30 min. After pre-treatment, cells were treated with 0.5 μ g/ml bTRAIL. TRAIL DISCs were isolated (lanes 5-7). In addition, unstimulated (US) TRAIL receptors were isolated by adding bTRAIL only after the cells had been lysed (lanes 2-4). Western blots of the isolated DISCs (TT) and unstimulated receptor (US) samples were probed for the TRAIL receptors and FADD.

usual (lower molecular weight) positions when the cells were additionally pre-treated with BisI (Lanes 4 and 7). These data confirm that the PKC-mediated modification of TRAIL-R2 occurs on both TRAIL-stimulated (DISC-associated) and unstimulated TRAIL-R2.

5.2.9 PKC-mediated Phosphorylation of TRAIL-R2 results in Phosphorylation of a Serine/Threonine Residue

To characterise the PKC-induced modification of TRAIL-R2, two-dimensional gels were performed from DISCs isolated from HeLa cells which were treated with bTRAIL alone or pre-treated with PMA followed by bTRAIL (Figure 5.10). The samples were initially focussed over a pH 4-7 linear focussing strip for 35,000 Vh before being separated by SDS-PAGE and western blotted for TRAIL-R2. The western blots of the TRAIL alone treated sample (Figure 5.10: left panel) revealed distinct spots corresponding to the long and short isoforms of TRAIL-R2. The spot corresponding to the long isoform is located both higher and to the left of the short isoform spots. This is expected, as the long isoform has a higher predicted mass (48 kDa vs 45 kDa) as well as a predicted pI with a lower pH (pH 4.97 vs pH 4.99) (Bjellqvist et al., 1993). The long isoform spot also appears to be diffuse, indicating that it could contain multiple spots. This could imply that the long isoform is subjected to small post-translational modifications even in untreated cells. In addition, multiple spots are detected for the short isoform, which also could indicate other post-translational modifications. In the PMA treated sample (Figure 5.10: middle panel), spots corresponding to the long and short TRAIL-R2 isoforms were also detected. However, the long and short isoform spots appear to shift upwards (indicating a higher molecular weight) and to the left (indicating an increased negative charge). This shift is most apparent when the western blots for the untreated and PMA-treated samples are overlaid (Figure 5.10: right panel). This pattern of an upwards shift to the lower pH area of the gel would indicate that a phosphorylation event has occurred as the addition of a phosphate moiety would increase both the mass of a protein and add a negative charge. The addition of a single phosphate group is predicted to decrease the pI of the long and short isoforms to 4.93 and 4.94 (from 4.97 and 4.99) respectively (Bjellqvist et al., 1993). Additional phosphorylations would reduce the pI by similar increments. From the relatively small

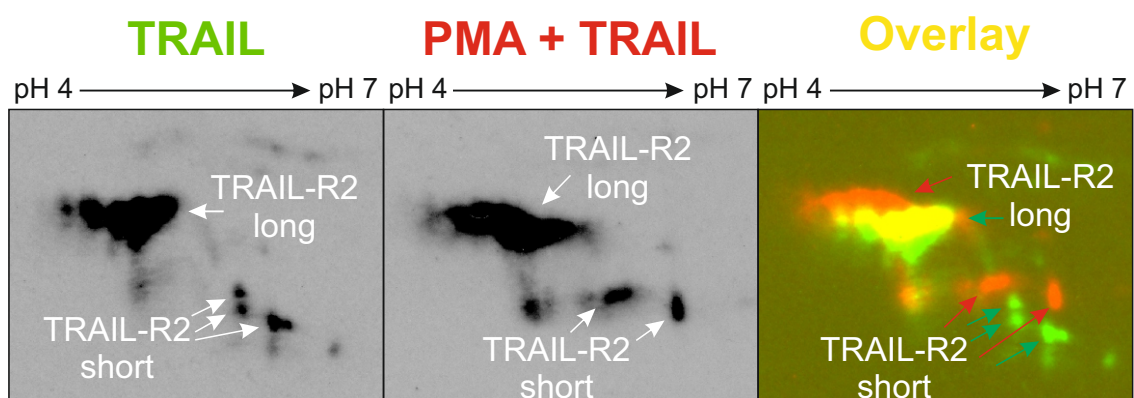


Figure 5.10: Two-dimensional Gels of TRAIL-R2 from PMA Treated HeLa Cells Indicate Phosphorylation Event

HeLa cells (2 x T175 flasks, 2×10^7) were not pre-treated (TRAIL, left panel) or pre-treated with 20 ng/ml PMA (PMA + TRAIL, middle panel) for 30 min followed by treatment with bTRAIL and the DISC isolated as described in Materials and Methods. DISC samples were subjected to two-dimensional electrophoresis (initially focussed for 35,000 v_h over linear pH 4-7 strips before separation by SDS-PAGE on 10% polyacrylamide gels), western blotted and probed for TRAIL-R2. Images shown are cropped versions of the full blots. Scanned TRAIL (left panel) and PMA + TRAIL (middle panel) western blot images were inverted and then merged using ImageJ. These images were then overlaid. The TRAIL only (left panel) and PMA + TRAIL (middle panel) western blots are coloured green and red respectively in the overlay (right panel). Overlapping regions between the two western blots are coloured yellow.

change in the horizontal position of the TRAIL-R2 spots, and the lack of multiple additional spots appearing in the PMA-treated sample, it is likely that PKC activation induces a single phosphorylation of TRAIL-R2.

To confirm that PKC activation mediated the phosphorylation of TRAIL-R2, DISCs isolated from HeLa cells treated with PMA followed by bTRAIL or bTRAIL alone were treated with lambda phosphatase (λ) (Figure 5.11 A). PMA treatment (Figure 5.11: Lanes 1 + 2 vs Lane 3) again caused an upward shift in the bands corresponding to the long and short TRAIL-R2 isoforms (denoted by red arrows). However, when the sample was treated with lambda phosphatase (Lane 4) the bands appeared at the normal, lower positions (black arrows). This confirmed that PKC modified TRAIL-R2 by phosphorylation. Lambda phosphatase has higher activity at removing serine/threonine phosphorylations, but does still show a lower level of activity towards tyrosine phosphorylations (Cohen and Cohen, 1989). Protein tyrosine phosphatase (PTP) however only removes phosphate groups from tyrosine residues (Zander et al., 1991). To determine whether the phosphorylation of TRAIL-R2 occurred on a serine/threonine residue or tyrosine residue, DISCs isolated from HeLa cells treated with PMA followed by bTRAIL or bTRAIL alone were treated with lambda phosphatase (λ) or protein tyrosine phosphatase (PTP) (Figure 5.11 B). PMA treatment (Figure 5.11 B: Lanes 1-3 vs Lane 4) again caused an upward shift in the bands corresponding to the long and short TRAIL-R2 isoforms (denoted by red arrows). The level of TRAIL-R2 observed in the bTRAIL alone treated sample (Lane 1) appears much lower than the other samples (Lanes 2-6). This can be explained by a poor transfer during western blotting (possibly due to an air bubble), as in the previous experiment (Figure 11 A), there was no difference in the amount of TRAIL-R2 detected. When the sample was treated with lambda phosphatase (Lane 5) the bands appeared at the normal, lower positions (black arrows). However, treatment with PTP (Lane 6) had no effect on the position of the TRAIL-R2 bands and they remained at the PMA-induced elevated positions (red arrows). This demonstrates that the PKC-induced phosphorylation of TRAIL-R2 occurs on a serine/threonine residue and not on a tyrosine residue.

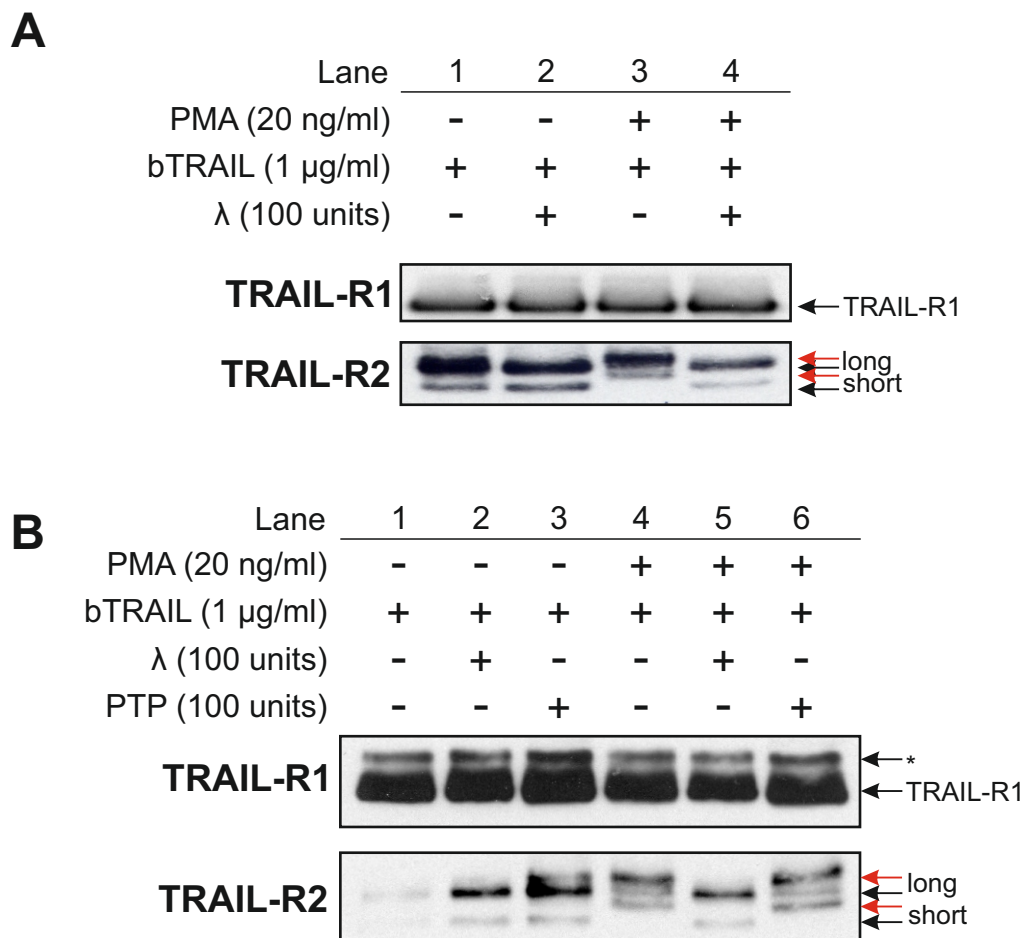


Figure 5.11: PKC-Induced Phosphorylation of TRAIL-R2 Occurs on Serine/Threonine Residue

(A) HeLa cells (2 x T175 flasks, $\sim 2 \times 10^7$) were treated with 0.5 µg/ml bTRAIL either alone or following pre-treatment with 20 ng/ml PMA for 30 min. TRAIL DISCs were isolated by incubation with streptavidin beads. Whilst still bound to the beads, each sample was then split into two samples, where one sample was then treated with lambda (λ) phosphatase (Lanes 2 and 4), whilst the other sample was re-suspended in the same buffer but without the addition of lambda phosphatase (Lanes 1 and 3) for 30 min at 37°C. After phosphatase treatment the samples were eluted into SDS-PAGE sample buffer and immunoblotted for TRAIL-R1 and TRAIL-R2.

(B) HeLa cells (2 x T175 flasks, $\sim 2 \times 10^7$) were treated with 0.5 µg/ml bTRAIL either alone or following pre-treatment with 20 ng/ml PMA for 30 min. Whilst still bound to the beads, each sample was split into three samples. One sample was then treated with lambda phosphatase (lanes 2 and 5), one with protein tyrosine phosphatase (PTP) (lanes 3 and 6), whilst the third sample was re-suspended and incubated in the same buffer but without the addition of the phosphatases (lanes 1 and 4) for 30 min at 37°C. After phosphatase treatment the samples were eluted into SDS-PAGE sample buffer and immunoblotted for TRAIL-R1 and TRAIL-R2.

5.2.10 *In Vitro* GST-TRAIL-R2-ICD Binding Assay Reveals Potential Sites of PKC-mediated Phosphorylation of TRAIL-R2

Having clearly demonstrated that PKC activation results in the loss of FADD binding to the TRAIL DISC and that this reduction correlates with both inhibition of TRAIL signalling and the phosphorylation of TRAIL-R2, it was important to identify the phosphorylation site. The results (Figure 5.11) showed that the PKC mediated phosphorylation of TRAIL-R2 occurs on both the long and short isoforms and would indicate that the site of phosphorylation would not be on the extracellular domain of TRAIL-R2, which is truncated in the short isoform. In addition, our previous study demonstrated that PMA treatment inhibited the recruitment of FADD to the intracellular domain (ICD) of the TRAIL receptors in an *in vitro* reconstituted DISC binding assay (Harper et al., 2003a). Considering that this effect could be achieved using only the ICD of TRAIL-R1/R2 increases the likelihood that the PKC-mediated phosphorylation occurred on a residue in the ICD of TRAIL-R2. All of the serine and threonine residues in the ICD of TRAIL-R2 are highlighted in Figure 5.12. By aligning the sequences of TRAIL-R1 and TRAIL-R2 it is therefore possible to identify serine and threonine residues which are present on TRAIL-R2 but not TRAIL-R1. These sites could potentially be sites for PKC-mediated phosphorylation of TRAIL-R2, as previous results have shown that TRAIL-R1 is not similarly phosphorylated. Assuming a similar mechanism occurs for CD95 (Figure 5.3), we can further narrow down the most likely phosphorylation sites if we consider that the serine/threonine residue would also be conserved in the CD95 ICD sequence. Using this argument, the residues S234, S261, S262, S308, T381, T384, T408 and S424 would be highly likely candidate phosphorylation sites as they are not conserved in TRAIL-R1. Importantly, of these residues, S261 and S424 are also conserved in CD95.

By mutating serine and threonine residues in the ICD of TRAIL-R2 and analysing their effect on the PMA-mediated inhibition of FADD recruitment by PMA treatment in an *in vitro* binding assay, it should be possible to identify the critical phosphorylation site.

Therefore, the intracellular domains (ICDs) of TRAIL-R1 and TRAIL-R2 were fused to a glutathione S-transferase (GST) tag and these GST-TRAIL-R1/2-ICD fusion proteins were expressed in *Escherichia coli* (Figure 5.13A) (Hughes et al., 2016). The

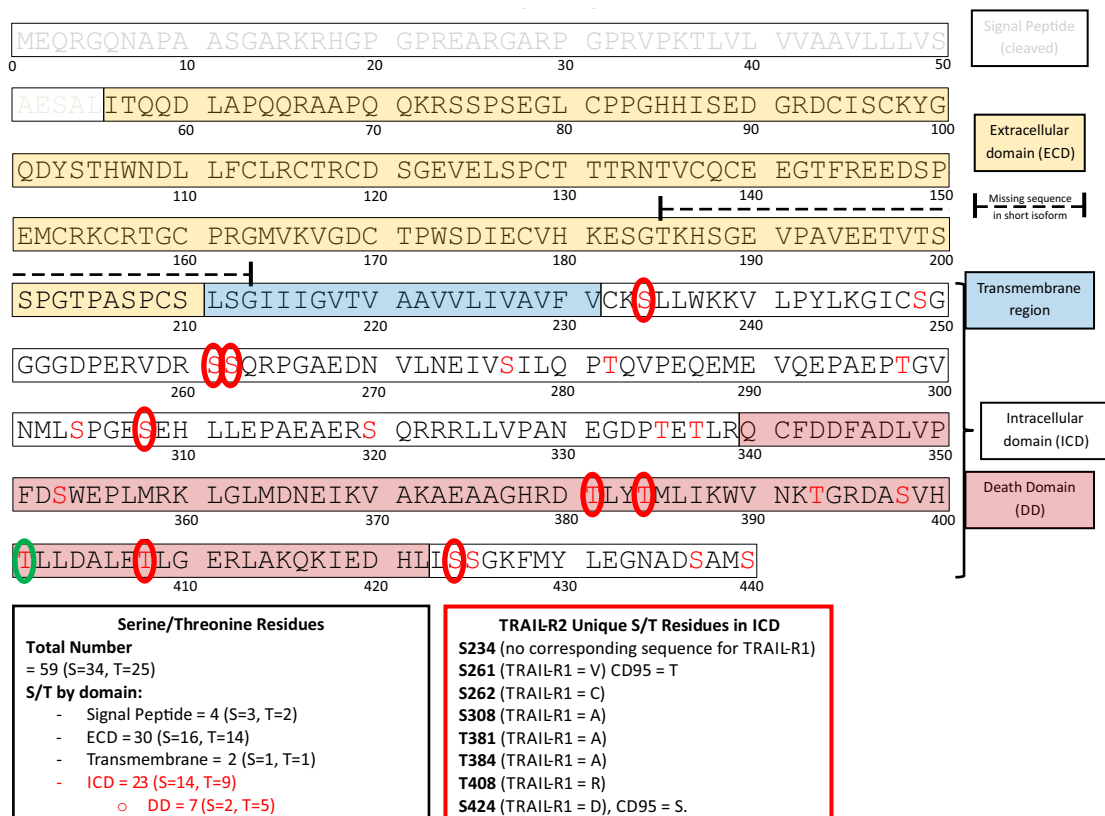


Figure 5.12: Potential Serine/Threonine Phosphorylation Sites in TRAIL-R2 Intracellular Domain

Graphical representation of the TRAIL-R2 amino acid sequence showing domains of the TRAIL-R2 protein. The signal peptide (white box, greyed out text) is truncated in the mature TRAIL-R2 protein. The extracellular domain (yellow box) and transmembrane region (blue box) contain the sequence which differs between the long and short TRAIL-R2 isoforms (indicated by dashed lines). The intracellular domain (white box, black text) contains within it the sequence for the death domain (pink filled box). Serine (S) and threonine (T) residues in the intracellular domain (ICD) of the TRAIL-R2 sequence are displayed by red text. Amino acid sequences of TRAIL-R2, TRAIL-R1 and CD95 were aligned using BLAST (Altschul *et al* 1990). Serine or threonine residues that are present in the TRAIL-R2 sequence but not conserved in the TRAIL-R1 sequence are displayed in the red box and highlighted by red circles. Serine or threonine residues which are present in TRAIL-R2, absent in TRAIL-R1 and also conserved in CD95 are also detailed in the red box.

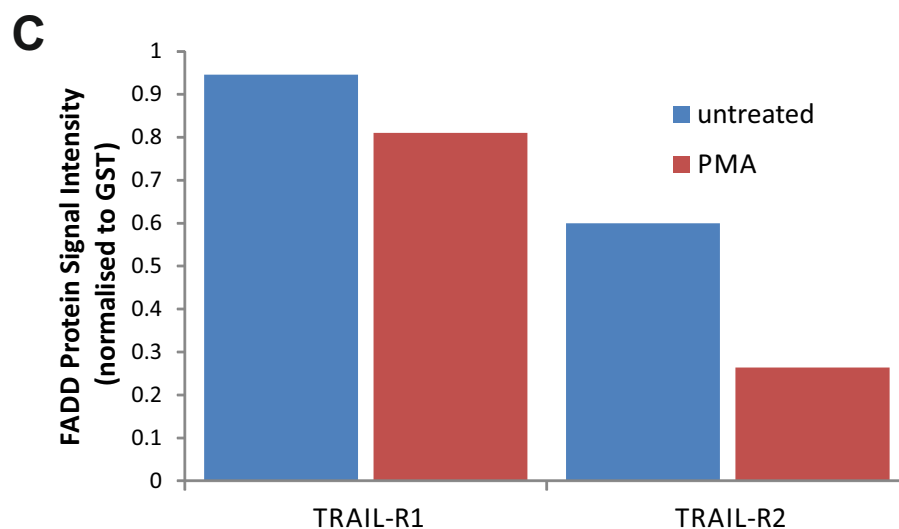
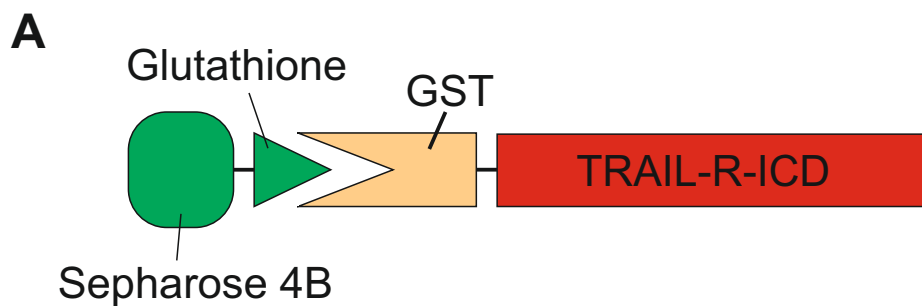


Figure 5.13: PMA Treatment Blocks FADD Recruitment to TRAIL-R2 Intracellular Domain

A) Diagram representing the structure of the TRAIL-Receptor intracellular domain (ICD)-GST fusion protein bound to glutathione-sepharose beads. **(B)** HeLa cells were treated either with or without PMA (20 ng/ml) for 30 min and lysates prepared. Cell lysates (5 mg) were then incubated with either GST-TRAIL-R1-ICD or GST-TRAIL-R2-ICD fusion proteins bound to glutathione-Sepharose beads (10 μ g) at 16°C for 16h. After washing with PBS, TRAIL-R1/R2 intracellular domain-interacting proteins were eluted in SDS sample buffer and analyzed for the presence of FADD and GST by western blotting **(B)**. The signal intensity of the detected bands were determined using a LI-COR, FADD values were normalised to the GST input values and plotted **(C)**.

fusion proteins were bound onto glutathione beads and incubated in lysates prepared from HeLa cells either untreated or treated with PMA. When incubated with lysates from untreated cells, both the TRAIL-R1 and TRAIL-R2 ICDs could recruit FADD, as visualised by western blot (Figure 5.13B, Lanes 1 and 3). The amount of FADD recruited was greater from the TRAIL-R2 ICD than with the TRAIL-R1 ICD. Pre-treatment of HeLa cells with PMA reduced the amount of FADD precipitated with both the TRAIL-R1 and TRAIL-R2 ICDs (Figure 5.13B, Lanes 2 and 4). When normalised to the amount of GST-ICD input (Figure 5.13C), it is apparent that although PMA treatment slightly reduced the amount of FADD recruited to the TRAIL-R1 ICD, the effect on FADD recruitment to the TRAIL-R2 ICD is far greater. As previous results had shown a clear role for TRAIL-R2, and that TRAIL-R1 was not phosphorylated by PKC, the impact of mutation of potential phosphorylation sites in TRAIL-R2 was further investigated.

Mutants were then constructed in which serine and threonine residues in the ICD of TRAIL-R2 (highlighted in Figure 5.12) were converted to alanine and the mutated GST-TRAIL-R1/R2-ICD expressed as before. These were either single mutations, or double mutations if two serine/threonine residues were within four amino acids. The GST-TRAIL-R2-ICD mutants were incubated with lysates prepared from Jurkat cells, either treated with PMA for 30 min or untreated. Figure 5.14 shows the amount of FADD detected from each TRAIL-R2 construct from either the untreated or PMA-treated cells. The western blots show that when incubated with wild-type GST-TRAIL-R2-ICD, PMA treatment reduced FADD binding. This reduction is comparable to the reduction previously observed using HeLa cell lysates (Figure 5.13C). Mutation of the residues: T381, S298-T401, S424-S425, T393 and S353 to alanine almost completely abolished FADD binding in both the untreated and PMA-treated samples. This reduction is most likely due to structural changes in the ICD which inhibit FADD binding, and are therefore likely unrelated to phosphorylation status. There was also a partial loss of FADD binding in the untreated samples when the residues: T298, S277, S320, S308, S249 and S304 were mutated to alanine. In these samples, FADD was still being recruited by the GST-TRAIL-R2-ICDs but at a lower level than observed for the wild-type. Mutation of the residues: T408, S261-S262, S437-S440 and T282 had very little effect on the ability of the GST-TRAIL-R2-ICD to recruit FADD in the untreated samples.

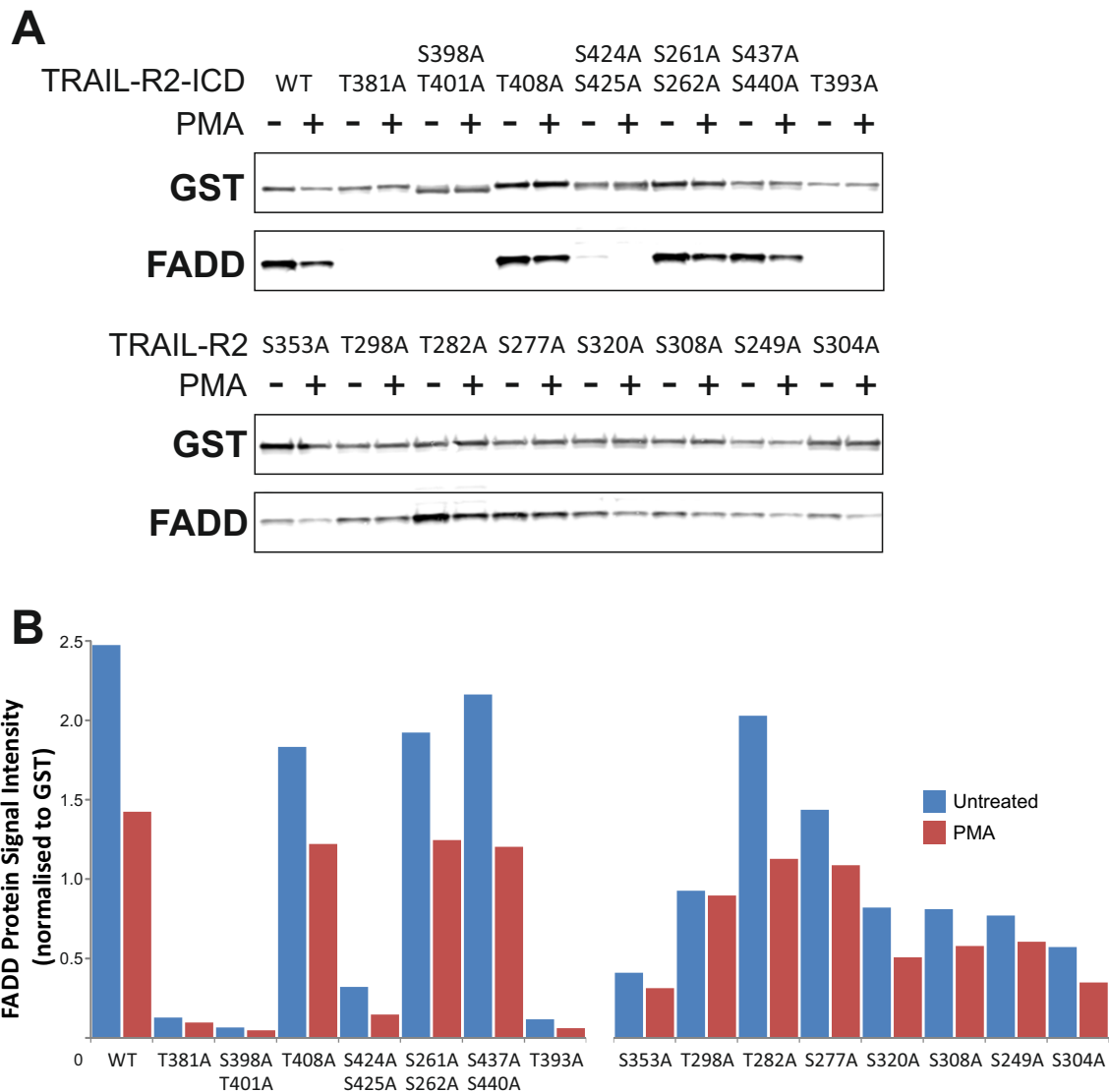


Figure 5.14: *In Vitro* Binding Assay Reveals Potential Sites of PKC-Mediated Phosphorylation of TRAIL-R2

Jurkat E6.1 cells were treated either with or without PMA (20 ng/ml) for 30 min and lysates prepared. Cell lysates (5 mg) were then incubated with GST-TRAIL-R2-ICD fusion proteins bound to glutathione-Sepharose beads (10 μ g) at 16°C for 16 h. The fusion proteins were either the wild-type (WT) TRAIL-R2-ICD, or constructs in which one or two serine and/or threonine residue(s) had been mutated to alanine. After washing with PBS, TRAIL-R2 intracellular domain-interacting proteins were eluted in SDS sample buffer and analyzed for the presence of FADD and GST by western blotting (A). The signal intensity of the detected bands were determined using a LI-COR, FADD values were normalised to the GST input values and plotted (B).

For those samples in which constitutive FADD binding has not been abolished by the mutations, the effect of PMA treatment can then be analysed. The majority of the samples show a reduction in the amount of FADD binding when the mutant GST-TRAIL-R2-ICD is incubated in the lysate prepared from PMA-treated cells. The PMA-induced inhibition of FADD binding is of a similar magnitude as observed in the wild type (WT) for the constructs in which residues: T408, S424-S425, S261-S262, S437-S440, T282, S320 and S304 were mutated to alanine. Interestingly, mutation of the residues S353, T298, S277, S308 and S249 to alanine reduced the inhibition of FADD binding caused by PMA treatment. Of these residues, it is only the mutation of residue T298 to alanine in which FADD binding is equal in both the untreated and PMA-treated samples. This highlights residues S277, S308, S249 and particularly T298 as being the most likely sites for a PKC-induced TRAIL-R2 phosphorylation which in turn inhibits the recruitment of FADD to TRAIL-R2.

5.3 Discussion

This chapter describes the investigation of the mechanism by which PKC activation inhibits death receptor-induced apoptosis through the analysis of TRAIL and CD95 signalling and TRAIL DISC formation in HeLa, Jurkat and BJAB cells. Taken together, this investigation has:

1. Demonstrated that PKC activation by PMA inhibits TRAIL-induced apoptosis in the HeLa and Jurkat, but not BJAB cell lines.
2. Confirmed that PKC activation by PMA can inhibit CD95-induced apoptosis in Jurkat cells.
3. Discovered that PMA can also block TRAIL-induced NF κ B signalling.
4. Demonstrated that knockdown of PKC β in HeLa cells, which only express PKC β , can prevent PKC-mediated inhibition of TRAIL-induced apoptosis.
5. Demonstrated that PMA treatment can inhibit FADD recruitment to the DISC by preventing TRAIL-R2 aggregation to HMW-DISC complexes.
6. Identified that PKC mediates the phosphorylation of TRAIL-R2 in cell lines which are sensitive to PKC-mediated inhibition of TRAIL signalling and identified possible sites of PKC-mediated phosphorylation.

I therefore propose the mechanism that PKC β phosphorylates the intracellular domain of TRAIL-R2 on a serine or threonine residue. This phosphorylation prevents the aggregation of TRAIL-R2 to form a high molecular weight (HMW) complex. By preventing its HMW aggregation, TRAIL-R2 is unable to recruit FADD into the DISC and thereby downstream TRAIL signalling to apoptosis or NF κ B activation is blocked.

5.3.1 Sensitivity of Cell Lines to PKC-mediated Inhibition of Death Receptor Signalling

This study confirmed that TRAIL-induced apoptosis can be inhibited by the activation of PKC in both the cervical carcinoma HeLa cell line and the leukemic T cell line, Jurkat E6.1. However, TRAIL-induced apoptosis in the Burkitt's lymphoma B cell line, BJAB was not inhibited by PKC. The reasons for the insensitivity of the BJAB cells to PKC are not completely clear. An earlier study attempted to explain the insensitivity of the lymphoblastoid B cell derived, SKW6.4 cell line, to PMA-mediated inhibition of anti-

CD95-induced apoptosis (Meng et al., 2002) by differences between Type I and Type II cells in regard to extrinsic apoptosis. They had observed PKC sensitivity in Jurkat cells, a type II cell line but not the type I SKW6.4 cells. In this study, PKC activation was also demonstrated to inhibit TRAIL signalling in Jurkat cells, but also in HeLa cells. HeLa cells have also been characterised as type II cells, as overexpression of BCL-2 can block extrinsic pathway-induced apoptosis (Mandal et al., 1996; Yasuhara et al., 1997). PKC activation did not inhibit TRAIL signalling in the type I, BJAB cell line (Kohlhaas et al., 2007), therefore implying that apoptotic cell type may impact upon PKC sensitivity. Type II cells form a less active DISC, thereby requiring amplification of initiator caspase-driven apoptotic signals by engagement of the intrinsic pathway (Kohlhaas et al., 2007; Ozören and El-Deiry, 2002). The more active type I cell DISC may therefore be able to overcome inhibition from PKC, whereas the type II cell DISC would be exquisitely sensitive. It is also however, noteworthy that both the BJAB and SKW6.4 cells are B cell derived cell lines, which may instead indicate a cell type specific effect.

Knockdown of PKC β in HeLa cells was shown to drastically reduce the ability of PMA to inhibit TRAIL-induced apoptosis (Figure 5.6). This was opposed to the effect of knocking down PKC α , which demonstrated no significant reduction in PMA inhibition. However, the role of the other conventional and novel PKC isoforms in inhibiting death receptor signalling cannot be completely ruled out and should be investigated. The knockdown of PKC β should also be repeated with a number of other targeting siRNA to rule out the possibility of off-target effects being responsible for the observed phenotype. Another approach would be to knockout PKC β using gene editing techniques such as CRISPR/cas9.

The observation that PKC β may be responsible for PKC-mediated inhibition of death receptor signalling correlates with other reports in the literature. Meng *et al.* (2010) demonstrated that the PKC β specific inhibitor, enzastaurin, could reverse the inhibition of both anti-CD95 and TRAIL-induced apoptosis by PMA in Jurkat cells. The role of PKC β was further clarified by similar results when PKC β expression was knocked down by shRNA. Interestingly, Inoue et al (2009) detected PKC β in TRAIL-DISCs isolated from CLL patient primary cells, although this observation could also

have been due to contamination with components of the B cell receptor (BCR) signalling machinery.

PKC isoforms have been shown to have remarkably different functions depending on the cell type and even stimulus involved (Steinberg, 2008). It could be that PKC β does not have the same inhibitory effect on death receptor signalling in B cells because instead in those cells it plays important functions in BCR signalling (Oellerich et al., 2011).

5.3.2 PKC-mediated Inhibition of Non-Apoptotic Death Receptor Signalling

In addition to the inhibition of TRAIL-induced apoptotic signalling, it was also demonstrated that PKC activation can block NF κ B signalling by TRAIL (Figure 5.4). This shows for the first time that PKC activation is able to block both the apoptotic and pro-survival TRAIL signalling arms, implying a complete shutdown of TRAIL signalling. This work should be expanded by investigating the effect of PKC activation on other TRAIL-induced pro-survival pathways such as JNK and p38 activation (Azijli et al., 2013). If PKC activation can indeed block both the apoptotic and pro-survival aspects of TRAIL signalling this could negatively impact on the use of a combined PKC inhibitor and TRAIL chemotherapeutic strategy. One of the negative outcomes of current TRAIL-based therapies is that many tumours are inherently resistant or quickly acquire resistance to TRAIL (reviewed in Abdulghani & El-Deiry 2010). In these cells, it has been shown that TRAIL treatment can actually increase tumour cell survival and proliferation by TRAIL-induced NF κ B activation (Ehrhardt et al., 2003). If PKC activation also blocks this pathway, then a combination of TRAIL and a PKC inhibitor could exacerbate the proliferative effect of TRAIL treatment in TRAIL resistant cell populations if the resistance to TRAIL-induced apoptosis is not PKC-mediated by an increase in NF κ B activation. In addition, it should be investigated whether PKC activation can block non-apoptotic signalling pathway activation by other death ligands, such as CD95L and TNF α , or whether this effect is specific to TRAIL signalling.

5.3.3 Effect of PKC Activation on DISC Formation

It has been suggested that in order to achieve a fully active signalling DISC the aggregation of TRAIL-R1/R2, FADD and caspase-8 to a complex with a much higher molecular weight than the predicted size of the trimerised receptors, FADD and caspase-8 chains alone is required (Dickens et al., 2012a). Therefore, the observation that PKC activation reduces the size of the TRAIL-R2 containing DISC (Figure 5.7) in HeLa cells provides a mechanism to explain how PKC can inhibit the recruitment of FADD to the complex. This also introduces the idea that PKC activation may not affect both TRAIL death receptors, TRAIL-R1 and TRAIL-R2 uniformly. Thus, in the same experiment, the size of the TRAIL-R1-containing complexes was reduced by a much smaller amount than observed for TRAIL-R2 (Figure 5.7). Although we cannot completely rule out the role of TRAIL-R1, a significant role for TRAIL-R2 over TRAIL-R1 correlates with the other data presented. The additional cell line that was shown to be sensitive to PKC-mediated inhibition of death receptor signalling was the Jurkat cell line (Figure 5.1). As Jurkat cells do not express TRAIL-R1, any inhibitory effect by PKC on the TRAIL receptors must be acting solely through TRAIL-R2. In addition, BJAB cells, which were insensitive to PKC-mediated inhibition of TRAIL signalling have been reported to signal pre-dominantly through TRAIL-R1 despite expression of functional TRAIL-R2 (Marion MacFarlane et al., 2005). It could therefore be that the reason for the BJAB insensitivity cell insensitivity to PMA is because PKC targets TRAIL-R2 and therefore has a much lower impact on TRAIL signalling in BJABs.

The idea that disruption of TRAIL-induced TRAIL-R2 aggregation could have a profound effect on the ability of TRAIL-R2 to induce apoptotic signalling fits with what is already known about TRAIL-R2 signalling. It has been reported in many cell lines that efficient TRAIL-R2 activation is only achieved when targeted with ligands that display higher order oligomerisation (Mühlenbeck et al., 2000). Ligands such as ILZ-TRAIL have proven more efficacious due to their ability to aggregate the TRAIL receptors (Kim et al., 2004). Therefore, PKC activation may directly inhibit TRAIL-induced apoptosis by blocking TRAIL-R2 aggregation. Conversely, the observed inhibition of TRAIL-R2 DISC aggregation by PKC could be due to a reduction in FADD binding. The recruitment of FADD could be required to stabilise the DISC, thus allowing greater aggregation to

occur. If FADD recruitment is reduced, then the highly aggregated DISC may become unstable and more likely to dissociate.

Meng et al (2010) reported a mechanism by which PKC activation blocked the anti-CD95 (CH11)-induced accumulation of CD95. They observed that after anti-CD95 treatment, the amount of CD95 detected on the cell surface increased. However, when the cells were pre-treated with PMA, anti-CD95 was unable to induce this increase. In light of the PMA effect observed here on TRAIL-R2 aggregation (Figure 5.7), it is possible that the effect observed by Meng et al (2010) could be the same PKC-induced inhibition of HMW death receptor complex formation. In a similar manner to that observed for the TRAIL receptors, ligand stimulation could cause the CD95 receptors to aggregate into large (HMW) complexes which would effectively trap them on the cell surface. As both TRAIL and CD95 signalling is blocked by PKC activation, it is likely that the underlying mechanisms of this effect would be similar between the two death receptors.

Further work should be carried out to confirm that the effect of PKC reducing the size of TRAIL-R2 containing HMW-DISCs is also observed in the Jurkat cell line. It would also be useful to examine the effects of PKC on HMW-DISC formation in BJAB cells to assess whether there is indeed any effect on TRAIL-R2 complex formation. In addition, SDG fractionation of the HMW-DISC could be repeated using the anti-CD95 antibody, CH11 to induce DISC formation in Jurkat cells. If PKC activation does indeed effect formation of the CD95-HMW complex then it would further indicate a universal mechanism for PKC-mediated inhibition of death receptor signalling.

5.3.4 PKC-mediated Phosphorylation of TRAIL-R2

This study demonstrated that PKC activation induced phosphorylation of TRAIL-R2, but not TRAIL-R1, in the PKC-sensitive HeLa and Jurkat cell lines but not in the PKC-insensitive BJAB cell line (Figure 5.8). This data again indicates that the mechanism by which PKC inhibits TRAIL signalling is through TRAIL-R2 and not TRAIL-R1. This correlates with a study in which PDAC cells, which largely signal through TRAIL-R1, could be sensitised to TRAIL-R2-induced death by treatment with a PKC inhibitor (Lemke et al., 2010). Therefore the apparent selectivity of certain cells to TRAIL-R1-

induced apoptosis could occur because TRAIL-R2 signalling is blocked by activated PKC.

The site of PKC-mediated phosphorylation of TRAIL-R2 was demonstrated to occur on a serine or threonine residue (Figure 5.11). This fits with a direct phosphorylation of TRAIL-R2 by PKC (as PKC is a serine/threonine kinase) however, we cannot discount that the phosphorylation may be indirect by another serine/threonine kinase activated by PKC. The exact site of phosphorylation has not been categorically defined, however mutation of the threonine 298 residue to alanine prevented further reduction of FADD recruitment by PMA in an *in vitro* TRAIL-R2-ICD binding assay (Figure 5.14). Mutation of the residues S353, T298, S277, S308 and S249 however also reduced the inhibitory effect of FADD, albeit by smaller amounts. These GST-TRAIL-R2-ICD mutant constructs should also be tested in lysates from HeLa cells treated with PMA to confirm the effects seen in Jurkat cells. The *in vitro* assay could not rule out the residues T381, S398, T401, S424, S425, and T393 as being the site of phosphorylation as mutation of these sites completely abolished FADD recruitment even in the absence of PMA. Some of these constructs contained mutations of two serine/threonine residues. It may therefore be possible to mitigate the structural effects of the mutation by re-making these constructs with only a single serine/threonine to alanine mutation. In addition to the mutation of serine/threonine residues to alanine to abolish potential phosphorylations, a mutation to aspartate/glutamate can act to mimic a phosphorylation. The use of such phosphomimetic mutations may add further insight to the phosphorylation site identity, however such mutations can have profound effects on protein structure so the resulting data would need to be interpreted with caution.

The potential phosphorylation sites identified here should also be tested in a cellular system. This could be achieved by transfecting the gene for the serine/threonine mutated TRAIL-R2 into a cell line which lacks TRAIL-R2 and observing the effects of PMA treatment on TRAIL-induced apoptosis. Another approach could be to edit the sequence of the TRAIL-R2 gene to replace the serine/threonine residue with alanine or a phosphomimetic using a CRISPR/cas9 gene editing-based approach.

When proteins are phosphorylated, there is usually a regulated equilibrium between the kinase phosphorylating the target protein and a phosphatase removing the phosphorylation. Härmälä-Braskén et al (2003) reported that inhibition of the PP2a family of phosphatases could inhibit apoptosis mediated by death ligands. In addition, components of the PP2a phosphatase complex were detected associated with the BJAB TRAIL-DISC (Chapter 4). Importantly, BJAB cells are sensitive to TRAIL-induced death and the action of the PP2a phosphatase could therefore function by removing inhibitory PKC-mediated phosphorylations.

Chapter 6: Final Overview

Chapter 6: Final Overview

The aim of this thesis was to identify and characterise novel mechanisms which regulate TRAIL signalling. This has been achieved through purification of the TRAIL DISC and unstimulated TRAIL-R1/R2 using both wild-type and TRAIL-R1/R2-specific TRAIL mutants. By improving an established platform, novel TRAIL DISC and unstimulated TRAIL-R1/R2-interacting proteins were quantifiably identified by label-free quantitative mass spectrometry (Figure 6.1). In addition, the mechanism by which activated PKC can inhibit TRAIL signalling was investigated (Figure 6.2). The major findings from this work are discussed below.

In Chapter 3, a platform to analyse the isolated TRAIL DISC by label-free quantitative mass spectrometry was improved upon to enable the detection of novel TRAIL DISC-interacting proteins. Using this platform enabled all known components of the TRAIL DISC to be identified. The platform was also utilised to enable the successful detection of unstimulated TRAIL-R1/R2. In addition to the known DISC components, the platform was also utilised to identify novel TRAIL DISC and TRAIL-R1/R2-interacting proteins. This led to the confirmation of an interaction, previously identified in our lab (Dickens et al, unpublished data), between transferrin receptor 1 (TfR1) and the TRAIL DISC. In addition, the catalytic subunit of the serine/threonine phosphatase, PP2A (PP2A-C) was also shown to interact with the TRAIL-DISC. Confirmation by western blot analysis revealed that TfR1 and PP2A-C not only interact with the TRAIL DISC, but can also be detected interacting with the unstimulated TRAIL receptors, TRAIL-R1/R2. Analysis of purified unstimulated TRAIL-R1/R2 also revealed a novel association with multiple members of the oxysterol binding protein related protein (ORP) family.

Chapter 4 built upon the improved platform developed in Chapter 3 to identify proteins which interact specifically with TRAIL-R1 or TRAIL-R2 in the DISC or with unstimulated TRAIL-R1/R2. This work revealed that ORP8 interacts with unstimulated TRAIL-R1 in BJAB cells, and with TRAIL-R1 and TRAIL-R2 in HeLa cells. In addition, PP2A-C, along with the regulatory subunit (B55 α) and scaffold subunit (A) of the PP2A holoenzyme, pre-associated with TRAIL-R1 and TRAIL-R2 in BJAB cells but were not detected in HeLa cells. The detection of the PP2A phosphatase holoenzyme indicates a

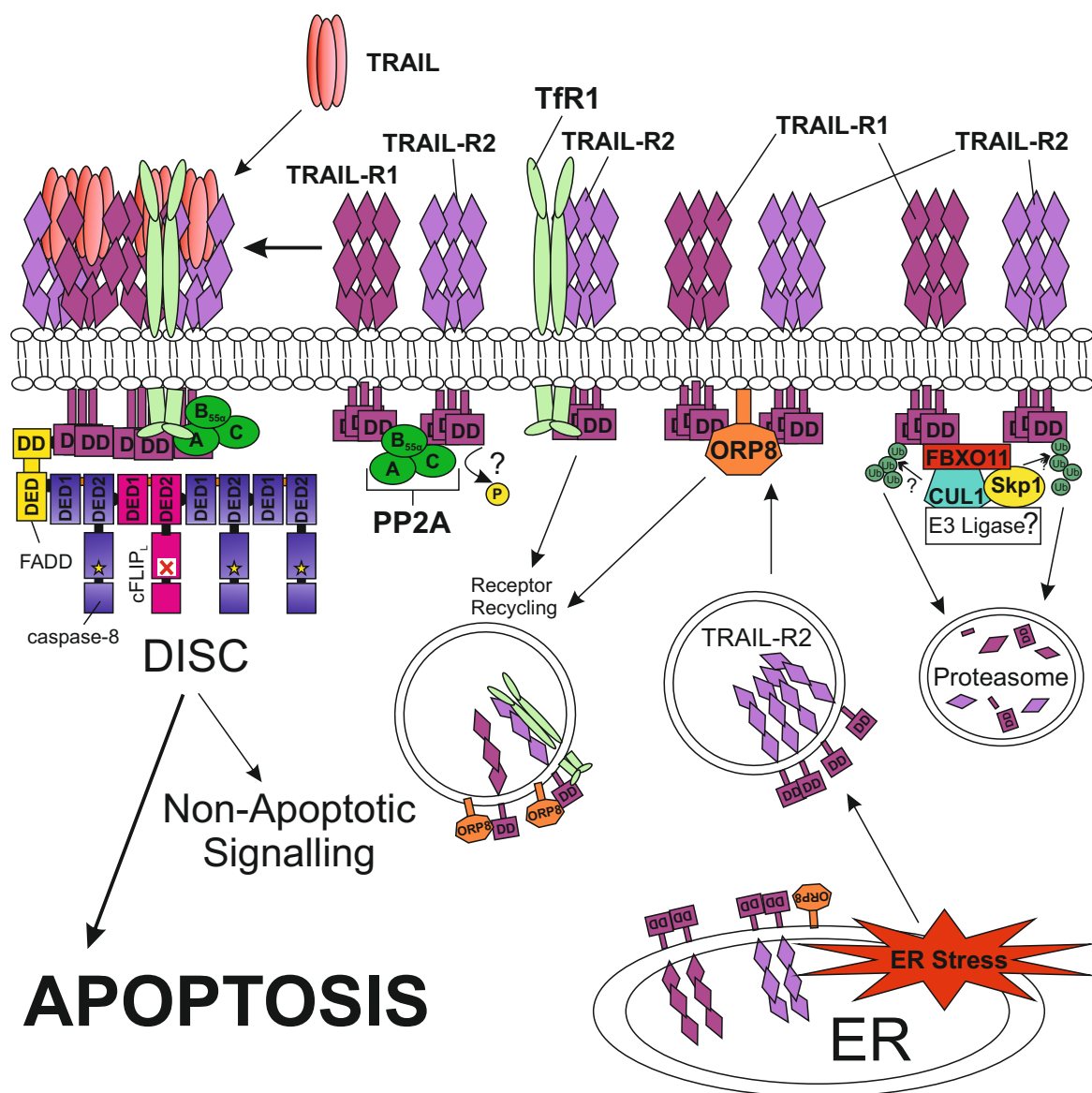


Figure 6.1: Schematic of Novel Potential Mechanisms of Regulation of TRAIL Signalling Identified in this Thesis

The serine/threonine phosphatase, PP2A, was identified interacting with both TRAIL-R1 and TRAIL-R2 in the TRAIL DISC and with unstimulated TRAIL-R1/R2. PP2A may be regulating TRAIL signalling by removing inhibitory phosphorylations on TRAIL-R1/TRAIL-R2. Transferrin receptor 1 (Tfr1) was confirmed to interact with the TRAIL DISC and unstimulated TRAIL-R2. Oxysterol-binding protein-related protein-8 (ORP8) was identified interacting with unstimulated TRAIL-R1 (BJAB & HeLa cells) and TRAIL-R2 (HeLa cells only). In HeLa cells, ORP8 was shown to effect TRAIL-R2 cell surface expression and may achieve this by regulating the endocytic recycling of TRAIL-R2 from the plasma membrane. Tfr1 has previously been shown in our lab to also effect TRAIL-R2 cell surface expression (Dickens et al, unpublished data) and may share a similar regulatory mechanism to ORP8. Alternatively, siRNA targeting of ORP8 may have caused ER stress and through activation of the ER stress response, inducing an upregulation of TRAIL-R2 cell surface expression. S-phase kinase associated protein-1 (Skp1), Cullin-1 (CUL1) and F-box only protein-11 (FBXO11) make up an SCF complex identified associated with unstimulated TRAIL-R1/R2. This SCF complex may regulate the ubiquitination and subsequent proteasomal degradation of TRAIL-R1/R2.

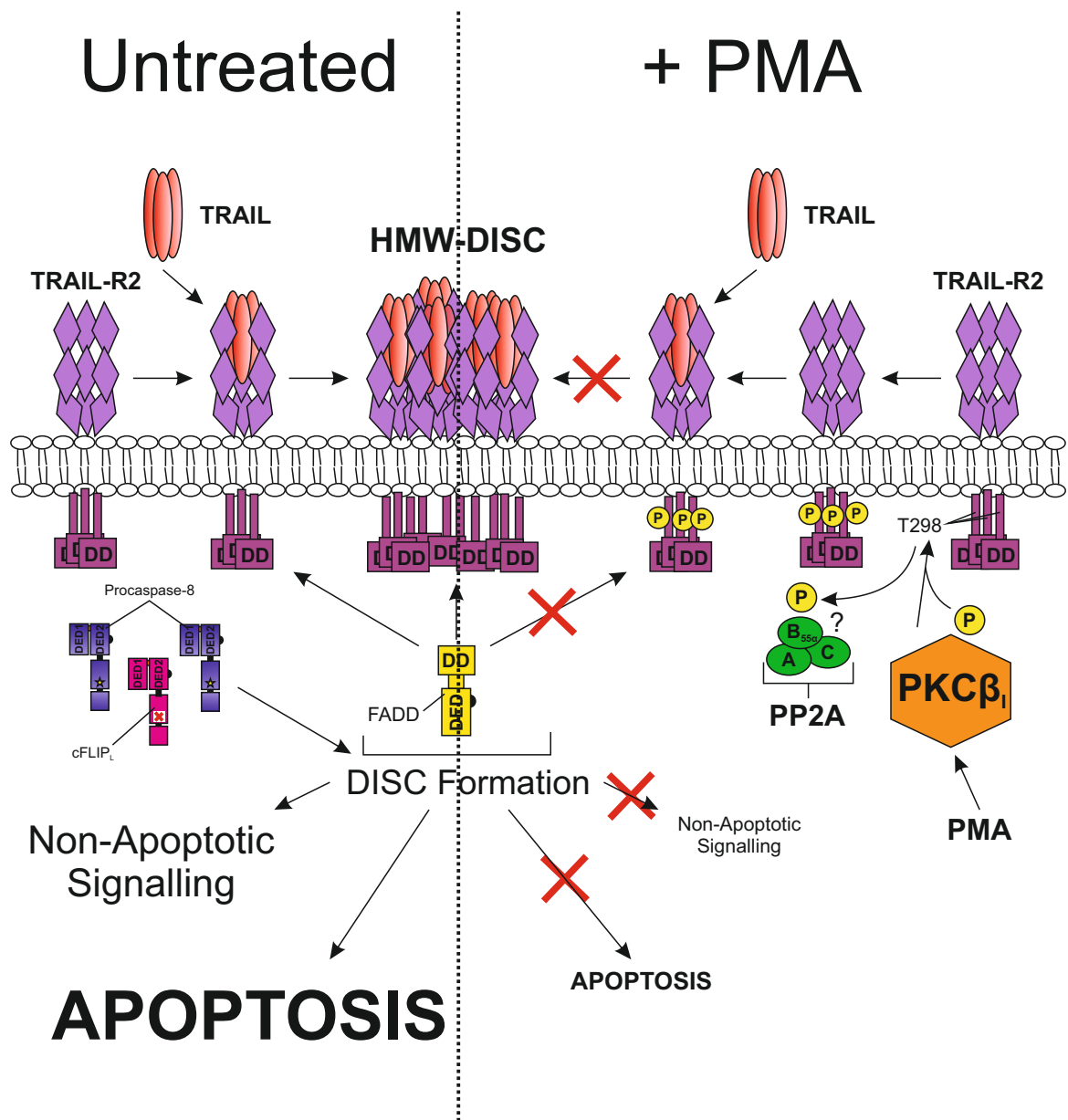


Figure 6.2: Schematic for the Proposed Mechanism Underlying PKC-mediated Inhibition of TRAIL Signalling

Activation of the Protein Kinase C β_1 isoform (PKC β_1) (e.g. PMA bytreatment, right side of figure) induces the phosphorylation of the intracellular domain of TRAIL-R2, most likely on residue threonine 298 (T298) (Chapter 5). The phosphorylation of TRAIL-R2 prevents the TRAIL-induced aggregation of TRAIL-R2 into high molecular weight (HMW)-DISC complexes. This inhibition of TRAIL-R2 aggregation prevents the recruitment of FADD and subsequent caspase-8 recruitment and activation. The loss of DISC formation, prevents the activation of both the apoptotic and non-apoptotic arms of TRAIL signalling. PP2A (Identified in Chapters 3 & 4) may regulate the de-phosphorylation of TRAIL-R2 and therefore oppose PKC-mediated inhibition of TRAIL signalling.

role for de-phosphorylation of TRAIL-R1/R2 in the regulation of TRAIL signalling. An S-phase kinase (Skp)-Cullin-F-box protein (SCF) complex composed of Skp1, CUL1 and F-box only protein 11 (FBXO11), also pre-associates with TRAIL-R1 and TRAIL-R2 in BJAB cells, but is not detected associated with TRAIL-R1/R2 in HeLa cells. SCF complexes regulate signalling pathways by ubiquitinating target proteins, resulting in their degradation by the proteasome (Xie et al., 2013). Proteasome inhibition has previously been shown to increase TRAIL-R1 and TRAIL-R2 protein levels (Johnson et al., 2003) and therefore Skp1, CUL1 and FBXO11 may regulate the targeting of TRAIL-R1/R2 for degradation.

The role of ORP8 in the regulation of TRAIL signalling was also investigated further. Targeted reduction of ORP8 expression using siRNA induces an increase in the levels of TRAIL-R2, but not TRAIL-R1, on the plasma membrane of HeLa cells. This increase in cell surface TRAIL-R2 sensitises HeLa cells to wild-type, TRAIL-R1-specific and TRAIL-R2 specific-TRAIL-induced apoptosis. ORP8 is known to interact with the endoplasmic reticulum (ER) and play important roles in maintaining cholesterol and lipid transport (Zhou et al., 2011). Loss of ORP8 may therefore induce ER stress, which has been reported to increase TRAIL-R2 expression (Lu et al., 2014a). A similar mechanism was reported for CD95, in which overexpression of ORP8 induces ER stress and sensitises cells to CD95L-induced apoptosis through an increase in CD95 cell surface expression (Zhong et al., 2015). Alternatively, the detection of an interaction between ORP8 and TRAIL-R1/R2 indicates a more specific regulatory mechanism. Due to the known role of ORP8 in lipid transport (Zhou et al., 2011), it may also have a role in the recycling of TRAIL-R2 from the plasma membrane. Reduction in ORP8 levels would therefore perturb this recycling and lead to increased cell surface levels of TRAIL-R2. A similar role for Tfr1 in TRAIL-R2 recycling has also been proposed, as in our lab siRNA targeting of Tfr1 causes TRAIL-R2 cell surface expression to increase (Dickens et al, unpublished data).

Of the novel proteins identified interacting with the TRAIL DISC or unstimulated TRAIL-R1/R2, only ORP8 is detected in both BJAB and HeLa cells. The PP2A, Skp1, CUL1 and FBXO11 interaction with TRAIL-R1/R2 was only detected in BJAB cells. These differences in TRAIL-R1/R2-interacting proteins indicate differential signalling between

the epithelial cell line, HeLa and haematopoietic line, BJAB. Similar differences have been described previously, as CUL3 has been shown to regulate TRAIL DISC formation in epithelial cell lines (Dickens et al., 2012a; Jin et al., 2009), but not in haematopoietic derived cell lines (Dickens et al., 2012a).

Chapter 5 describes the investigation of the mechanism by which activated PKC inhibits TRAIL signalling. I confirmed that PKC activation blocks TRAIL-induced apoptosis in HeLa and Jurkat cells (and anti-CD95-induced apoptosis in Jurkat cells) (Gómez-Angelats et al., 2000; Harper et al., 2003; Meng et al., 2010; Ruiz-Ruiz et al., 1999; Sarker et al., 2001), and showed for the first time that PKC activation inhibits TRAIL-induced NF κ B activation in HeLa cells. This demonstrates that activation of PKC can inhibit both the apoptotic and non-apoptotic arms of TRAIL signalling. The inhibitory effect of PKC can be blocked by siRNA targeting of the PKC β_1 isoform. PKC activation does not however inhibit TRAIL-induced apoptosis in the Burkitt's lymphoma, BJAB cell line, suggesting an alternative role for PKC β_1 in BJAB cells. This is consistent with the role of individual PKC isoforms varying between different cell types (Reviewed in Steinberg, 2008). The inhibition of apoptotic signalling correlates with a reduction in TRAIL-induced aggregation of TRAIL-R2 into high molecular weight (HMW) DISC complexes. This inhibition of TRAIL-R2 HMW-DISC aggregation prevents the recruitment of FADD, which in turn reduces caspase-8 recruitment and activation. The targeting of TRAIL-R2 by PKC was further evidenced by the detection of PKC-induced phosphorylation of the intracellular domain (ICD) of TRAIL-R2. In the PKC insensitive BJAB cells however, TRAIL-R2 phosphorylation is not observed. PKC activation can also block FADD recruitment to recombinant GST-TRAIL-R2-ICD *in vitro*, and mutation of TRAIL-R2 ICD serine/threonine residues revealed threonine 298 (T298) as the most likely PKC-mediated phosphorylation site. Although T298 is the strongest candidate from the data, there are a number of other possible sites which produced smaller effects (S277, S308, S249) or could not be analysed due to mutation-induced constitutive loss of FADD recruitment (S424, S425, S353, T381, T393 S398, T401). T298 is located in the TRAIL-R2 ICD between the transmembrane domain and the death domain. Phosphorylation of T298 may impede interactions between the intracellular domains of neighbouring TRAIL-R2 molecules and therefore prevent the

formation of TRAIL-induced HMW-DISC complexes. The detection of PP2A associated with TRAIL-R1/R2 in BJAB cells, but not HeLa cells (Chapter 3), may explain the insensitivity of BJAB cells to PKC-mediated inhibition of TRAIL signalling and lack of TRAIL-R2 phosphorylation. Moreover, the constitutive-association of PP2A with TRAIL-R2 may remove inhibitory, PKC-mediated phosphorylations on TRAIL-R2. The constitutive TRAIL-R2:PP2A interaction may also explain the exquisite sensitivity of BJAB cells to TRAIL-induced apoptosis. I therefore propose that the mechanism of PKC-mediated inhibition of TRAIL signalling occurs through the targeted phosphorylation of T298 in the ICD of TRAIL-R2. This phosphorylation prevents the aggregation of TRAIL-R2 into TRAIL HMW-DISC complexes, FADD recruitment and caspase-8 activation (Figure 6.2). The role of PKC activation on TRAIL DISC lipid raft association should be determined, as lipid rafts have been shown to impact upon TRAIL signalling in HeLa cells and could explain the effect of PKC activation on TRAIL DISC aggregation (Jin et al., 2009). As activation of PKC has also been shown to inhibit apoptosis-induced by anti-CD95 (Figure 5.3, Gómez-Angelats & Cidlowski, 2001; Meng et al., 2010; Ruiz-Ruiz et al., 1999) and TNF α (Harper et al., 2003), a similar regulatory mechanism may be involved. Therefore, it should be investigated if PKC activation can mediate the phosphorylation and subsequent inhibition of CD95 and TNFR1-induced signalling.

In conclusion, this thesis has identified and characterised novel mechanisms which regulate TRAIL signalling. PP2A and Skp1-Cul1-FBXO11 have the potential to regulate TRAIL signalling through the de-phosphorylation and ubiquitination of both TRAIL-R1 and TRAIL-R2. Conversely, ORP8 and PKC appear to specifically regulate TRAIL signalling by TRAIL-R2. By gaining a greater understanding of the mechanisms which regulate TRAIL signalling, new strategies may be developed to overcome the resistance to TRAIL-based therapeutics, which is currently hampering their use in the fight against cancer. In addition, understanding of the mechanisms which specifically regulate either TRAIL-R1 or TRAIL-R2 will enable therapeutics which target only one of the TRAIL death receptors to gain greater efficacy.

The data shown in this thesis has opened up new avenues for further study into the regulation of TRAIL signalling. Key experiments which should be completed in the near future to expand upon this research are summarised below.

1. The role of PP2A in regulating TRAIL signalling should be further investigated by using siRNA targeting or CRISPR/cas9 gene editing to knockdown/knockout the PP2A-B55 α subunit. Specific targeting of the B55 α subunit will reduce the number of PP2A regulated pathways effected and enable the specific role of PP2A in TRAIL signalling to be identified.
2. The role of the Skp1-CUL1-FBXO11 complex in regulating TRAIL-R1/R2 protein levels should be investigated by targeting of each of the SCF components with siRNA or cas9/CRISPR gene editing. In addition, isolation of unstimulated TRAIL-R1/R2 in the presence of de-ubiquitinase (DUB) inhibitors would reveal whether TRAIL-R1/R2 are being ubiquitinated.
3. The mechanism by which ORP8 regulates TRAIL-R2 surface expression should be investigated by co-targeting both ORP8 and CHOP with siRNA or CRISP/cas9. If the removal of CHOP expression abolishes the observed increase in TRAIL-R2 cell surface expression, then the upregulation of TRAIL-R2 is most likely being driven by the ER stress response.
4. It should be determined whether siRNA targeting of PKC β_1 can also relieve the inhibition of TRAIL-induced non-apoptotic signalling by PKC. This can be achieved by western blot analysis of TRAIL-induced phosphorylation of I κ B α in (PKC β_1 siRNA transfected) cells untreated or treated with PMA.
5. The role of the other potential PKC-mediated phosphorylation sites identified within the TRAIL-R2-ICD should be determined. Serine 424 was identified as a potential phosphorylation site due to its conservation in TRAIL-R2 and CD95 but not TRAIL-R1. The mutation of both S424 and S425 completely abolished FADD recruitment to the GST-TRAIL-R2-ICD. Mutating each of the residues individually should have a less dramatic effect on the TRAIL-R2 ICD structure and thereby enable the effect of PKC activation on FADD binding to be specifically evaluated. In addition, the effect of mutating T298 to alanine (and the other potential phosphorylation sites) on TRAIL signalling should be tested in a cellular system by transfecting a mutated TRAIL-R2 gene into a TRAIL-R2 null cell line or by using CRISPR/cas9 gene editing to induce the mutation.

Appendices

TRAIL-R1: 120/468 amino acids (26% coverage), 12 peptides, 14 spectra

MAPPARVHL	GAF LAVTPNP	GSAASGTEAA	AATPSKVWGS	SAGRIEPRGG	GRGALPTSMG	QHGPSARARA	GRAPGPRPAR
EASPRLRVHK	TFKFVVGVFL	LQVVPSSAAT	IKLHSDSIGT	QDWEH SPLGE	LCPPGSHRSE	HPGALNRCTE	GVGYTNASN
LFACLPCTAC	KSDDEERSFC	TTTRNTAQQG	KPGTFNRDNS	AEMGRKCSRQ	CPRGMVKVKD	STPWSDLQGV	HKESGNHNI
WVILVVTLLV	PLLLVAVLLV	CCIGSGGGG	DPKCMDRVCF	WRGLLRGPG	AEDNAHNEIL	SNADSLSTFV	SEQQMESQEP
ADLTGVTVQS	PGEAQCLLGP	AEAEGSQRRR	LLVPANGADP	TETLMLFFDK	FANIVPFDSW	DQLMRQLDLT	KNEIDVVRAG
TAGPGDALYA	MLMKVVNKTG	RNASIHTLLD	ALERMEERHA	KEKIQDLLVD	SGKFIYLEDG	TGSAVSL E	

TRAIL-R2: 226/440 amino acids (60% coverage), 20 peptides, 23 spectra

MEQRGQNAFA	ASGARKRHGP	GPREARGARP	GPRVPKTLVL	VVAAVLLLVLS	AESALITQDD	LAPQQRRAAPO	QKRSSPSEGL
CPPGHHSIED	GRDCISCKYQ	QDYSTHWNDL	LFGLRCTRCD	SGEVELSPCT	TTRNTVQDCE	EGTFREEDSP	EMCRKCRTOG
PRGMVKVGDG	TPWSDIEVH	KESGTHKSGE	APAVEETVTS	SPGTPASPCS	LSGIIIGVTV	AAVVLLVAVF	VCKSLWLKXV
LPYLKGIQSG	GGDPERVDR	SSORPGAEDN	VLNEIVSILQ	PTQVPEQEME	VQEPAEPTGV	NMLSPGSESH	LLEPAEAERS
QRRRLVLPAN	EGDPTETLRQ	CFDDFADLVP	FDSWEPLMRK	LGMLDNEIKV	AKAEAAGHRD	TLYTMLIKWV	NKTRGRDASVH
TLLDALETLG	ERLAKQKIED	HLLSSGKFMV	LEGNADSAM				

TRAIL-R4: 101/386 amino acids (26% coverage), 7 peptides, 7 spectra

MGLWQGSVPT	ASSARAGRYP	GARTASGTRP	WLLDPKILKF	VVFIVAIVLLP	VRVDSATIPR	QDEVPOQTVA	PQQRRSLKLE
ECCPAGSHRS	EYTGACNPCT	EGVDYTIASN	NLPSCLLCTV	CKSGQTNKSS	CTTTRDTVCQ	CEKGSFQDKN	SPEMCRTOCT
GPCRGMVKVKS	NCTPRSDIKC	KNESAASTGT	KTPAAEETVT	TILGMLASPY	HYLIIIVVLLV	IILAVVVVGF	SCRKKFISYL
KGIQSGGGGG	PERVHRVLEFR	RRGCPSPVPG	AEDNARHETL	SNRYLDTQV	SEGEIQGOEL	AELTGVTVES	PEEPORLLEQ
AEAEGRQR	LLVPVNDADS	ADISTLLDAS	ATLEECHAKE	TIQDQLVGS E	KLFYEEDEAG	SATSGL	

FADD: 101/208 amino acids (49% coverage), 7 peptides, 8 spectra

MDPFLVLLHS	VSSSLSSSEL	TELKFLCLGR	VGKRKLERVQ	SGLDLFSMLL	EONDLEPGHT	ELLRELLASL	RRHDLRLRVD
DPEAGAAAGA	APGEEDLQAA	FNVIQDNVQK	DWRRLARQLK	VSDTKIDSIE	DRYPRNLTER	VRESLRWKLN	TEKENATVAH
LVGALRSQGM	NLVADLVQEV	QQARDLQNR	GAMSPMSWNS	DASTSEAS			

Caspase-8: 272/479 amino acids (57% coverage), 23 peptides, 23 spectra

MDFSRNLYDI	GEQLDSEDLA	SLKFLSLDYI	PQRKQEPDKD	ALMLFQRLQE	KRMLEESNLS	FLKELLFRIN	RDLDLITYLN
TRKEEMEREL	QTPGRAQISA	YRVMLYQISE	EYRSSELRSF	KFLLLQEEISK	KLDDDMNLL	DIFIEMEKR	ILGEGKLDL
KRVCAQINKS	LLKIINDYEE	FSKERSSSLE	GSPDEFNNGE	ELCGVMTISD	SPREODESESO	TLDKVVYOMKS	KPRGYDLIIN
NHNFAKAREK	VPKLSHSIRDR	NGTHLDAGAL	TTTFEELHFE	KLPHDDCTVE	QIYEILKIYQ	LMDHSNMDCP	ICCLILSHGDK
GIIYGTDDGE	APIYELTSQF	TGLKCP SLAG	KPKVFFIQAG	QODNYQKQIP	VETDSEEQPY	LEMPLSSPQT	RYIPDEADFL
LMATVNNRV	SYRNPAGECTV	YIQSLQSLR	ERCPRQDDIL	TILTEVNYEV	SNKDDKKNMG	KQMPQPTFTL	RKKLVLFPSD

cFLIP: 135/480 amino acids (28% coverage), 13 peptides, 13 spectra

MSAEVIHOVE	EALDTEKEM	LLFLCRDYAI	DVPPNVRDL	LDLLRERGKL	SYGDLAELLY	RVRRFOLLKR	ILKMORKAVE
THLLRNPHLV	SDYRVLMAEI	GEDLDKSDVS	SLIFLMKDYM	GRGKISKEKS	FLLDLVLELEK	LNLVAPDOLD	LLEKCLKNIH
RIDLKTKIQK	YKQSVQAGT	SYRNVLQAAI	QKSLKDPSSN	FRLHNGRSKE	QRLKEQLGAD	QEPVKKSIQE	SEAFLPQSIIP
EEFYKMKSKP	LGICLIIDCI	GNETELLRDT	FTSLQYEVQK	FLHLSMHGIS	QILGQFACMP	EHRDYSDFV	VLVSRGGSQS
VYGVQDTHSG	LPHHIRRMF	MGDSCPVLG	KPRMFFIQNY	VYSEGQLED	SLLVVDGPAM	KNVEFKAKGR	GLCTVHREAD
FFWSLCTADM	SLLQEQSSP	SLYLQCLSQK	LRQERKRPLL	DLHIELNGYM	YDWNRSVSAK	EKYYVWLQHT	LRKKLILSYT

Caspase-10: 112/521 amino acids (21% coverage), 7 peptides, 7 spectra

MKSQQQHWYS	SSDNCKVSP	REKLLIIDS	LQVODVENLK	FLCIGLVPNK	KLEKSSASD	VFEHLLAEDL	LSEEDPFFLA
ELLVITRQKK	LLQHLNCKE	EVERLLPTRO	RVSIFRWLLY	ELSEGIDSEN	LKDMI FLKDD	SLPKTEMTSL	SFLAFLKQGG
KIDEDNLTCL	EDLCKTVVPK	LLRNIEKYKR	EKAIQIVTTP	VQKEAESYQG	EEELVSQTDV	KTFLEALPQE	SWQNKHAGSN
GNRATNGAPS	LVSRRMQGAS	ANTLNSETST	KRAAVYRMRN	NHRGLCVIVN	NHSFTSLKDR	OGTHKDAEIL	SHVFWLQFT
VHIHNNVTKV	EMEMVLQKQK	CNPAHADGDC	FVFCILTHGR	FGAVYSSDEA	LPIREIMSH	FTALQCPRLA	EKPKLFFIQ A
CQGEI IQPSV	SIEADALNPE	QAPTSLQDSI	PAEADFLGL	ATVPGYVSFR	HVEEGSWYIQ	SLCNHLKCLV	PRMLKFL EKT
MEIRGRKRTV	WGAKQISATS	LPTAISAQTP	RPPMRWSSV	S			

Appendix Figure 3.1: Amino Acid Coverage of Detected TRAIL DISC Components

Amino acid sequences for TRAIL-R1, TRAIL-R2, TRAIL-R4, FADD, caspase-8, cFLIP and caspase-10 are displayed. Peptides detected by mass spectrometry are highlighted in yellow, with modified residues being coloured green. The coverage of each shown is the greatest detected across all of the samples shown in Table 3.1. Also displayed are the total unique peptides and total unique spectra detected.

Accession Number	Protein	Sample (Protein (fmol))					
		Unstimulated			DISC		
		WT	R1	R2	WT	R1	R2
TR10A_HUMAN	TRAIL-R1	176.8	88.3	0.0	315.0	348.3	3.4
TR10B_HUMAN	TRAIL-R2	135.8	2.2	41.8	257.1	159.1	204.2
TR10D_HUMAN	TRAIL-R4	93.7	70.4	0.0	102.4	135.3	1.3
FADD_HUMAN	FADD	0.3	0.0	0.0	62.4	55.8	0.0
CASP8_HUMAN	Caspase-8	0.5	1.6	0.0	474.8	344.5	85.5
CFLAR_HUMAN	cFLIP	0.0	0.0	0.0	88.2	77.1	11.2
CASPA_HUMAN	Caspase-10	0.0	0.0	0.0	32.7	15.1	0.0
2AAA_HUMAN	Serine/threonine-protein phosphatase 2A 65 kDa regulatory subunit A	14.5	13.8	14.3	29.5	15.1	18.9
2ABA_HUMAN	Serine/threonine-protein phosphatase 2A 55 kDa regulatory subunit B alpha	8.6	6.6	0.0	7.4	6.2	10.4
ACYP2_HUMAN	Acylphosphatase-2	0.0	0.0	0.0	0.0	1.3	0.0
ADX_HUMAN	Adrenodoxin	0.0	0.0	0.0	7.1	0.0	0.0
ATP5I_HUMAN	ATP synthase subunit e	0.0	7.4	0.0	3.7	7.0	0.0
ATP5L_HUMAN	ATP synthase subunit g	0.0	8.0	0.0	4.3	9.7	0.0
ATX2L_HUMAN	Ataxin-2-like protein	16.2	6.3	77.3	9.3	16.5	37.8
BOLA2_HUMAN	BoLA-like protein 2	0.0	5.7	0.0	12.6	6.1	0.0
BTBD9_HUMAN	BTB/POZ domain-containing protein 9	8.6	0.0	0.0	0.0	0.0	0.0
CA131_HUMAN	Uncharacterized protein C1orf131	5.3	4.4	0.0	8.0	4.6	0.0
CAPZB_HUMAN	F-actin-capping protein subunit beta	14.5	9.8	0.0	20.7	22.9	0.0
CB047_HUMAN	Uncharacterized protein C2orf47	0.0	0.0	0.0	1.2	1.6	0.0
CH10_HUMAN	10 kDa chaperonin	0.0	2.8	0.0	5.0	4.0	0.0
CMC2_HUMAN	COX assembly mitochondrial protein 2 homolog	4.8	2.9	3.4	4.5	11.6	8.1
CTSL2_HUMAN	Cathepsin L2	8.9	3.5	0.0	109.3	1.6	0.0
CUL1_HUMAN	Cullin 1	18.6	3.4	132.1	6.9	12.8	76.1
CUL5_HUMAN	Cullin 5	6.3	1.8	1.5	4.7	1.5	2.6
CX7A2_HUMAN	Cytochrome c oxidase subunit 7A2	0.0	0.0	0.0	1.9	0.0	0.0
DCA10_HUMAN	DDB1- and CUL4-associated factor 10	14.0	14.8	17.9	0.0	1.9	3.9
DCTP1_HUMAN	CTP pyrophosphatase 1	0.0	4.1	0.0	0.0	1.1	0.0
DDX55_HUMAN	ATP-dependent RNA helicase DDX55	0.0	0.0	11.0	0.0	0.0	0.0
DNJB6_HUMAN	DnaJ homolog subfamily B member 6	0.0	2.8	0.0	0.0	10.2	0.0
DYL2_HUMAN	Dynein light chain 2	0.0	0.0	0.0	6.5	0.0	0.0
ENY2_HUMAN	Transcription and mRNA export factor ENY2	0.0	4.6	0.0	7.9	2.2	0.0

ERP44_HUMAN	Endoplasmic reticulum resident protein 44	6.3	9.7	0.0	0.0	10.7	0.0
F207A_HUMAN	Protein FAM207A	5.0	11.5	5.1	14.4	7.6	0.0
FBX11_HUMAN	F-box only protein 11	13.3	5.5	256.2	0.4	2.2	118.0
FBXW5_HUMAN	F-box/WD repeat-containing protein 5	93.9	85.9	30.0	32.2	73.7	63.7
GGA2_HUMAN	ADP-ribosylation factor-binding protein GGA2	2.9	5.9	0.0	0.0	6.8	0.0
GHC1_HUMAN	Mitochondrial glutamate carrier 1	0.0	0.0	0.0	2.8	9.0	1.8
GLYR1_HUMAN	Putative oxidoreductase GLYR1	4.9	4.4	33.1	8.2	0.0	0.0
GRSF1_HUMAN	G-rich sequence factor 1	1.7	4.0	24.3	3.5	0.0	3.6
K2C78_HUMAN	Keratin, type II cytoskeletal 78	0.0	1.0	0.9	0.0	2.4	1.6
LEG1_HUMAN	Galectin-1	0.0	0.0	0.0	6.9	0.0	0.0
LEG7_HUMAN	Galectin-7	0.0	8.5	0.0	0.0	0.0	0.0
LSM2_HUMAN	U6 snRNA-associated Sm-like protein LSM2	0.0	0.0	0.0	5.7	1.4	0.0
LSM6_HUMAN	U6 snRNA-associated Sm-like protein LSM6	0.0	9.1	0.0	10.5	4.0	0.0
LYPA1_HUMAN	Acyl-protein thioesterase 1	9.5	5.5	0.0	17.5	3.0	0.0
MEF2B_HUMAN	Myocyte-specific enhancer factor 2B	9.4	9.2	3.1	10.8	2.2	0.0
MIB2_HUMAN	E3 ubiquitin-protein ligase MIB2	4.6	9.8	0.0	0.0	0.0	0.0
MINA_HUMAN	lysine-specific demethylase and histidyl-hydroxylase MINA	0.5	1.4	16.8	2.4	0.0	0.0
MRE11_HUMAN	Double-strand break repair protein MRE11A	10.2	1.7	0.0	7.1	7.4	9.8
NBR1_HUMAN	Next to BRCA1 gene 1 protein	113.7	116.6	8.4	3.0	46.9	94.5
NC2B_HUMAN	Protein Dr1	7.6	2.8	0.0	11.2	2.4	0.0
NEUL4_HUMAN	Neuralized-like protein 4	69.0	22.0	17.1	0.3	56.0	6.7
NTPCR_HUMAN	Cancer-related nucleoside-triphosphatase	11.6	5.8	4.2	21.1	7.4	2.2
NUDC_HUMAN	Nuclear migration protein nudC	1.5	10.8	0.0	0.0	7.0	0.0
NUP50_HUMAN	Nuclear pore complex protein Nup50	9.4	6.5	0.4	18.1	6.5	0.0
NUP62_HUMAN	Nuclear pore complex protein p62	14.5	12.4	0.0	12.6	16.1	0.0
OSBL8_HUMAN	Oxysterol-binding protein-related protein 8	144.4	210.2	10.1	2.9	106.3	0.0
OSBL9_HUMAN	Oxysterol-binding protein-related protein 9	100.3	143.8	0.0	9.6	55.1	0.0
P20D2_HUMAN	Peptidase M20 domain-containing protein 2	54.9	57.8	31.5	10.6	50.6	25.2
PARP4_HUMAN	Poly [ADP-ribose] polymerase 4	52.2	41.1	7.6	8.8	21.3	61.4

PCM1_HUMAN	Pericentriolar material 1 protein	11.7	6.2	2.6	3.2	3.5	15.0
PHF14_HUMAN	PHD finger protein 14	10.4	6.8	0.0	4.9	4.0	3.3
PININ_HUMAN	Pinin	48.0	37.6	29.2	44.1	18.2	3.1
POGZ_HUMAN	Pogo transposable element with ZNF domain	9.8	11.0	1.0	5.7	6.0	1.5
PP2AA_HUMAN	Serine/threonine-protein phosphatase 2A catalytic subunit	5.7	2.9	12.0	9.8	6.2	0.0
PPIL1_HUMAN	Peptidyl-prolyl cis-trans isomerase-like 1	0.0	0.0	0.0	2.9	2.5	0.0
PRC2B_HUMAN	Proline-rich coiled-coil protein 2B	59.5	35.4	26.4	15.0	38.9	4.2
PSA_HUMAN	Puromycin-sensitive aminopeptidase	2.0	1.0	0.0	1.3	1.5	0.0
QCR2_HUMAN	Cytochrome b-c1 complex subunit 2	6.9	15.0	0.0	5.1	10.5	4.7
QPCTL_HUMAN	Glutaminyl-peptide cyclotransferase-like protein	0.0	1.1	0.0	2.8	3.4	0.0
RANG_HUMAN	Ran-specific GTPase-activating protein	0.0	3.3	0.0	8.4	5.1	0.0
RBM3_HUMAN	RNA-binding protein 3	4.2	3.8	0.0	20.3	1.7	0.0
RENT2_HUMAN	Regulator of nonsense transcripts 2	0.0	4.8	14.9	2.5	3.6	25.3
RIPK1_HUMAN	Receptor-interacting protein kinase 1	0.0	0.0	0.0	7.5	8.0	1.6
RL32_HUMAN	60S ribosomal protein L32	0.0	0.0	99.8	2.9	0.0	5.6
RL36L_HUMAN	60S ribosomal protein L36a-like	0.0	0.0	0.0	0.0	0.0	8.3
RM12_HUMAN	39S ribosomal protein L12	6.0	2.7	0.0	12.7	2.2	0.0
RMTL1_HUMAN	rRNA methyltransferase 3	2.9	1.0	24.5	0.0	0.0	1.5
RMXL1_HUMAN	RNA binding motif protein, X-linked-like-1	16.8	0.0	60.0	112.2	20.8	1.2
RNPS1_HUMAN	RNA-binding protein with serine-rich domain 1	22.3	20.8	17.9	49.8	11.4	0.0
RS28_HUMAN	40S ribosomal protein S28	0.0	31.8	0.0	38.6	13.3	0.0
S10A9_HUMAN	Calgranulin-B	0.0	1.1	0.0	0.0	7.5	0.0
SKP1_HUMAN	S-phase kinase-associated protein 1	41.2	22.9	15.6	21.3	27.2	31.9
SLIRP_HUMAN	stem-loop-interacting RNA-binding protein	0.0	0.0	0.0	16.7	0.0	0.0
SNP23_HUMAN	Synaptosomal-associated protein 23	0.0	0.0	0.0	0.0	1.5	4.0
SPB4_HUMAN	Serpin B4	0.6	9.6	0.0	0.0	0.0	0.0
SPF27_HUMAN	Pre-mRNA-splicing factor SPF27	2.8	3.1	0.0	15.2	0.0	0.0
SPT5H_HUMAN	Transcription elongation factor SPT5	45.2	18.7	66.7	3.3	4.0	4.3
SRFB1_HUMAN	Serum response factor-binding protein 1	7.0	7.8	0.0	18.7	0.0	0.0

SRPK1_HUMAN	SRSF protein kinase 1	6.8	3.7	95.2	8.8	2.1	13.4
SUCB1_HUMAN	Succinate--CoA ligase subunit beta	4.9	7.7	0.0	7.1	5.9	1.0
TFR1_HUMAN	Transferrin receptor protein 1	29.1	1.8	15.1	53.2	41.2	41.4
TI23B_HUMAN	Putative mitochondrial import inner membrane translocase subunit Tim23B	14.0	0.0	0.0	0.0	0.0	0.0
TOM20_HUMAN	Mitochondrial import receptor subunit TOM20	0.0	8.2	0.0	26.4	2.5	0.0
UBE3A_HUMAN	Ubiquitin-protein ligase E3A	17.2	3.7	0.1	0.2	6.3	33.6
USMG5_HUMAN	Up-regulated during skeletal muscle growth protein 5	0.0	3.6	0.0	3.9	3.9	0.0
VAPA_HUMAN	Vesicle-associated membrane protein A	1.3	8.2	0.0	0.0	5.0	0.0
VAPB_HUMAN	Vesicle-associated membrane protein B	3.0	18.5	0.0	0.0	9.0	0.0
XIAP_HUMAN	E3 ubiquitin-protein ligase XIAP	7.3	8.9	6.9	3.5	10.8	5.7
ZN638_HUMAN	Zinc finger protein 638	26.4	19.2	11.0	21.4	104.9	22.8
ZY11B_HUMAN	Protein zyg-11 homolog B	8.6	8.4	1.3	0.0	7.2	4.0

Appendix Table 4.1: All Proteins Identified by Label-free Quantitative Mass Spectrometry in Chapter 4

The amount of protein (fmol) for each protein detected in the DISC and unstimulated samples described in Chapter 4 are shown.

TRAIL-R1: 104/468 amino acids (22% coverage), 9 peptides, 15 spectra

MAPPARVHL	GAFLAVTPNP	GSAASGTEAA	AATPSKVWGS	SAGRIEPRGG	GRGALPTSMG	QHGPSARARA	GRAPGPRPAR
EASPRLRVK	TFKFVVVGVL	LOVVPSSAA	IKLHDQSIGT	QWEHSPLGE	LCPPGSHRSE	HFGACNRCTE	GVGYTNASHN
LFACLPTAC	KSDEEERSPC	TTTRNTACCC	KPGTFRNDNS	AEMCRKCSR	LPRGMVKVKD	CTPWSDIECV	HKESGNGHNI
WVILVVTLV	PLLVLAVLIV	CCCIGSGGG	DPKCMDRVCF	WRLGLLRGPG	AEDNAHNEIL	SNADSLSTFV	SEDOMESQEP
ADLTGVTVQS	PGEAQCLLGP	AEAEGSQRRR	LLVPANGADP	TETLMFFDK	FANIVPFDSW	DQLMRQLDLT	KNEIDVVRAG
TAGPGDALYA	MLMKWVNKTG	RNASIHTLLD	ALERMEERHA	KEKIQDLLVD	SGKFIYLEDG	TGSAVSL	

TRAIL-R2: 115/440 amino acids (26% coverage), 3 peptides, 3 spectra

MEQRGNAPA	ASGARKRHGP	GPREARGARP	GPRVPKTLVL	VVAAVLLLV	AESALITQDD	LAPQQRAAPO	QKRSSPSEGL
CPPGHHSID	GRCISCKYG	QDYSTHWNDL	LFCLRCTRCD	SGEVELSPCT	TTRNTVQCE	EGTFREEDSP	EMCRKCRGTGC
PRGMVKGDG	TPWSDIEVH	KESGTHKSGE	APAVEETVTS	SPGTPASPCS	LSGIIIGVTV	AAVVLI VAVF	VCKSLWLKVV
LPYLKGI	CGGDPERVDR	SSQRPGEADN	VLNEIVSILQ	PTQVPEQEME	VQPEAETGV	NMLSPGESEH	LLEPAEAERS
RRRLVLPAN	EGDPTETLRQ	CFDDFAADLV	FDSWEP LMRK	LGLMDNEIKV	AKAEAAGHRD	TLYTMLIKWV	NKTGRDASVH
TLLEDALETLG	ERLAKQKIED	HLLSSGKFMV	LEGNADSAM				

TRAIL-R4: 65/386 amino acids (17% coverage), 4 peptides, 5 spectra

MGLWGQSVPT	ASSARAGRYP	GARTASGTRP	WLLDPKILKF	VVFIVAVLLP	VRVDSATIPR	ODEVPOQTVA	PQQRRSLKKE
EECFAGSHRS	EYTGACNPCT	EGVDYTIASN	NLPSCLLCTQ	CKSGQTNKSS	CTTTRDTVCO	CEKGSFQDKN	SPEMCRTCRT
GCPRGMVKS	NCTPRSDIKC	KNESAASSTG	KTPAAEETVT	TILGMLASPY	HYLIIIVLVV	IILAVVVVGF	SCRKFFISYL
KGI	CSGGGGG	PERVHRVLF	RSQPSRVP	AEDNARNETL	SNRYLQPTQV	SEQEIIQQL	AELTSVTVES
AEAEGCQRRR	LLVPVNDADS	ADISTLLDAS	ATLEECHAKE	TIQDQLVGE	KLFYEDEAG	SATSCL	

FADD: 85/208 amino acids (41% coverage), 9 peptides, 9 spectra

MDPFLVLLHS	VSSLSLSSSEL	TELKFLCLGR	VGKRKLERVQ	SOLDLFSMLL	EONDLEPGHT	ELLRELLASL	RRHOLLRRVD
DFAACAAGA	APGEDLCAA	FNVICDNVKG	DVRRLRQDK	VSDTKIDSIE	DRYPRNLTER	VRESLRIWKN	TEKENATVAH
LVGALR	SCQM	NLVAIDLQEV	QQAARDLQNR	S	GAMSPMSWNS	DASTSEAS	

Caspase-8: 256/479 amino acids (53% coverage), 23 peptides, 26 spectra

MEGGRRARVY	IESKRNFLLQ	AFPTPPFAEH	VELGRLDGSE	TAMVPGKGA	DYILLPFFKM	DFSRNLYDIG	EQLDSEDLAS
LKFLSLDYIF	QRKQEPKDA	LWLFQRLQEK	RLEESNLSF	LKELLFRINR	LDLLITTYLNT	RKEMERELQ	TPORADISAV
RVMLYQISEE	VSRSELRSFK	FLLQEEISK	KLDDMMMLLD	FTEMEKRVII	LGECKLDILK	RVGAQINKSL	LKIIINDYEEF
SKERSSSLLEG	SPDEFNNGEE	LCGVMTISDS	PREQDSESQT	LDKVYQMKSK	PRGYCLINN	HNFAKAREKV	PKLHRSIRDNR
GTHLDAGALT	TTFEELHFEI	KPHDDCTVEQ	IYEILKLYQL	MDHSNMDCFI	CCILSHGDKG	I IYGTDQGEA	PIYELTSQFT
GLKCPSLAGK	PKVFFIQACQ	GDNYQKGI PV	ETDSEEQPYL	EMDLSSPQTR	YIPDEADFL	GMATVYNCVS	YRNPAGETWY
IQSLCQSLRE	RCPRGDDILT	ILTEVNYEVS	NKDDKKNMGK	GMPPQPTFLR	KLIVFPD		

cFLIP: 152/480 amino acids (32% coverage), 15 peptides, 15 spectra

MSAEVIHOVE	EALDTEKEM	LLFLCRDVAI	DVYPPNVRDL	LDILRERGKL	SVGDLAELLY	RVRRFDLLKR	ILKMDR KAVE
THLLRNPHLV	SDYRVLMAEI	GEDLDKSDVS	SLIFLMDQYM	GRGKISKEKS	FLDLVVELEK	LNLVAPDQD	LLEKCLKNIH
RIDLKTKIK	YRQSVQGAQT	SYRNVLQAAI	QKSLKDPNN	FLHNGRSKE	QRLKQLGAG	QEPVKSIOE	SEAFLOPSIR
EERLYMKSKP	LSIGLIIIDCI	QWETELLRDT	FTSLQYQNK	FLHLSMHGIS	QILGQFACMP	EHRDQDSFV	VLVSRGSSQS
VYGVDTQTHG	LPLHHIRRMF	MGDSCPYL	LAGPKMFFIQNY	VYSEGOLED	SLLVYDGPAM	KNVEFAQKR	GLCTVHREAD
FFWSLCTADM	SLEEGSHSSP	SLYLQCLSQK	LQERKRPLL	DLHIELNGYM	YDWNRSVSAK	EKYVYWLQHT	LRKKLILSYT

Caspase-10: 118/521 amino acids (23% coverage), 8 peptides, 8 spectra

MKSOGQHWYS	SSDNCKVSP	REKLLIIDS	LGVODVENLK	FLCIGLVPNK	KLEKSSASD	VFEHLLAEDL	LSEEDPFLA
ELLYIRQK	LLQLNCTKE	EVERLLPTRQ	RVSLFRNLV	ELSEGIDSEN	LKDMIFLLK	SLPKTMTSL	SFLAFLEKGG
KIDEDNLTC	EDLCKTVVPK	LLRNIEKYR	EKAIQIVTTP	VQKEAESYQG	EEELVSQTDV	KTFLEALPQE	SWQNKHAGSN
GNRATNGAPS	LVSRCMOGAS	ANTLNSETST	KRAAVYMMNR	NHRGLCVIVN	NHSFTSLKDR	GGTHKDAEIL	SHVFWLGF
VHIHNNVTKV	EMEMVLQKQK	CNPAHADGDC	FVFCILTHGR	FGAVYSSDEA	LIPIREIMSH	FTALQCPRLA	EKPKLFFIIQA
CQGEIIPQSV	SIEADALNPE	QAPTSLQDSI	PAEADFLGL	ATVPGYVSR	HVEEGSWYIQ	SLCNHLKLV	PRMLKFLK
MEIRGRKRTV	WGAKQISATS	LPTAISAQTP	RPPMRRWSSV	S			

Appendix Figure 4.1: Amino Acid Coverage of DISC Components Detected in Chapter 4

Amino acid sequences for TRAIL-R1 (WT DISC), TRAIL-R2 (WT DISC), TRAIL-R4 (WT DISC), FADD (WT DISC), caspase-8 (WT DISC), cFLIP (R1 DISC) and caspase-10 (WT DISC) are displayed. Peptides detected by mass spectrometry are highlighted in yellow, with modified residues being coloured green. The coverage of each shown is the greatest detected across all of the mass spectrometry analysed samples shown in Chapter 4. Also displayed are the total unique peptides and total unique spectra detected.

ORP8: 307/889 amino acids (35% coverage), 33 peptides, 36 spectra

MEGGLADGEP	DRISLLGDSK	DVLPSTVVA	NSDESQLLTP	QKMSQRQGGKE	AYPPTPKDLH	QPSLSPASHP	SQGFERQKED
ISQNKDESLE	SMKSKSESK	LYNGSEKDS	TSKLTKEES	LKVKKNVRE	EKKRATKELL	STITDPSVIV	MADWLKIRGT
LKSWKLLWCY	LKQVLLVLR	TKNGQWVGT	LLNACEIE	RPSSKDDGFCF	KLFHPLEQSI	WAVKGGPKGEA	VGSITQPLPS
SYLLIRATSE	SDGRCWMDAL	ELALKCSSLL	KRTMIREGKE	HDLSSVSDST	HYTFYGLLRA	NNLHSGDNFQ	LNDSEIEROH
KFLQDDMSDK	SDKENDEHD	ESDNEVMQSE	EESDITDTSER	QDSSYIEPEP	VEPLKETTYY	EQSHEELGEA	GEASOTETVS
EENKSLIWTLL	LKQVRPGMDL	SKVVLPTFIL	EPRSFLLDKL	DYYVHADFLS	EAALEENPYF	RLKKVYVWYL	SGFYKPKKGL
KKPYNPILGE	TFRCLWIHPR	TNSKTFYIAE	QVSHHPPISA	FYVSNRKGDF	CLSGSILAKS	KFYGNLSIAI	LEGEARLTFLL
NRGEDIYVMTM	PYAHCKGILY	GTMTLELGGT	VNITCOIKTGY	SATLEFKLKP	FLGSSDCVNO	ISGKLLKLGKE	VLATLEGHWD
SEVFTIDKKT	DNSEVFNPT	PDIKQWRLLR	HTVKFEEQD	FESEKLGWRV	TRAINAKDQT	EATQEKVYLE	EAQRQAARDR
KTKNEEWSCK	LFLDPLTGE	WHYKFASTRP	WDLNDMLOF	EKDGVIOTKV	KHRTPVVSP	KMKHKPTRQO	KKVAKGYSSP
EPDIQDSSGS	EAQSVKPSR	RKKGIELGDI	QSSIESIKQT	QEEIKRNIMA	LRNHLVSTP	ATDYFLQOKD	YFIIFLLILL
QVIINFMFK							

Skp1: 89/163 amino acids (55% coverage), 11 peptides, 11 spectra

MPSLKLQSSD	GEIFEVDFEI	AKQSVTIKT	MLEDLGMDEG	DDDPVPLPNV	NAAILKKVIO	WCTHHKDDPP	PPEDDENKEK
RDDIPVWDQ	EFLKVDQGL	FELILAAANYL	DIKGLLDVTC	KTVANMIKGG	TPEEIRKTFN	IKNDFTEEEE	AQVRKENQWC
EKE							

CUL1: 180/776 amino acids (23% coverage), 20 peptides, 21 spectra

MSSTRSQNPH	GLKQIGLDDI	WDDLRAAGIQ	VYTRQSMAS	RYMELYTHVY	NYCTSVHQSN	QARGAGVPPS	KSKKGGTPEG
AQFVGLLEYK	RLKEFLKNYL	TNLLKDGEDL	WDESVLKFFY	QWEDYRFSS	KVLNGICAYL	NRHWVRRRED	EGRKGYYEYI
SLALVTWRDC	LFRPLNKQVT	NAVLLKIEKE	RNGETINTRL	ISGVVQSYVE	LGLNEDDAFA	KGPTLTVYKE	SFESQFLADT
ERFYTRESTE	FLQONPVTEY	MKKAEARLLE	EQRPRVQVYL	ESTQDELARK	EQVLLIEKHL	EIHFTEFQNL	LDADKNEDLG
RMYNLVSRIO	DGLGELKLL	ETHIHNQGLA	AIEKCGEAL	NDPKMYVQTV	LDVHKKYNAL	VMSAFNNDAG	FVAALDKACG
RFINNNAVTK	MAQSSKSPFE	LLARYDSSL	KKSSKNPEEA	ELEDTLNQVM	VVFYKIEDKD	VFGKPYAKML	AKRLVHONS
SDDKEASML	KLQKAGGFY	TSKLQRMFD	IQVSKDLNEQ	EKKHLLHSEP	LDLDFSTQVL	SSGWPQQS	CTFALPSEL
RSYQRTAFY	ASRHSGRKLT	WLYQLSKGEL	VTCNFKNRYT	LGASTFGMAI	LLQYNTEDAY	TVQQLTDSIQ	IKMDILAQVL
QIILLKSKLLV	LEDENANVDE	VELKPDTLIK	LYLGKNNKL	RWINVPMKT	EOKQEQETH	KNIEEDRKL	IQAAIVRIMK
MRKVLKHQQL	LGEVLTQLSS	RFKPRVPVIK	KCIDILIEKE	YLERVDGKED	TYSYLA		

FBXO11: 244/927 amino acids (26% coverage), 21 peptides, 27 spectra

MNSVRAANRR	PRRVSRRPPV	QQQQQQPPQ	PPQPQQPPQ	PQQQPPPPQ	QQQQQQPPPP	PPPPPLPQE	RNNVGERDD
VPADVAEES	GPGAQNSPYQ	LRRLTLKPKR	TACPTKNSME	GASTSTENF	GHRRAKRARV	GKQDLSAAP	AEQYLQEKLP
DEVVLFKIFSY	LLEODLCRAA	CVCKRFSELA	NDPILGKRLY	MEVFETTRPM	MHPEPGKFYQ	INPEEYEHNP	PWKESFOOLY
KGAHVKPGFA	EHFYSNPARY	KGRENMLYYD	TJEDALGGVQ	EAHFDGLIFV	HSGIYDDEWI	YTESPMTD	AAPGRVADKV
IIEENTRDSSTF	VFMESSEDAY	VGYMTIRFNP	DDKSAQHNA	HHOLEITVNC	SPIIDHCIR	STRTVGSAVG	VSGQAAPTII
KHCNIISDCCN	VGLYITDHAQ	GIVYEDNEISN	NALAGIWKNN	HGNPIIRRNH	IHHGRDVGVF	TFDHGMGYFE	SCNIHRNRILA
GFEVKAYANP	TVVRCIHHG	QTGGIYVHEK	GRGGFIENKI	YANNFAGVWI	TSNSDPTIRG	NSIFNGNQQG	VYIFGGRGRL
IIEGNDIYQNA	LAGIQIRTNS	PIVLRHNKIH	DQGHGGIYVH	EKGQGVIEEN	EYVSNLTVL	WTEITGSPVL	RRNRHISGGK
VGVVYFDNNGH	GLVEDNDIYN	HMYSGVQIRT	GSNPRIIRNK	IWGGQNGGIL	VYNSGLGCE	DNEIFDNMA	GWVKTDSNP
TLRRNKIHG	DGGCIGFNG	GRGLLEENDI	FRNAQAQVLS	SNTSHPILRK	NRIFDGFAG	IEITNHATAT	LEGNQIFNRR
FGGLFLASGV	NVTMKNKIM	NQDAIENAV	SRGQCKYGLI	SYTSPMHDF	YRCHTCTTDD	RNAIYVNGIK	KCHGGHDFEF
IRHDRFFDGD	GAGTLSNPGT	LAGEPTHDT	TLYDSAPPIE	SNTLQHN			

PP2A-A: 110/589 amino acids (19% coverage), 9 peptides, 10 spectra

MAAADGDDSL	YPIAVLIDEL	RNEDVQLRLN	SIKKLLSTIAL	ALGVERTRSE	LLPFLTDTIY	DEDEVLLALA	EQLGFTTLLV
GGPEYVHCLL	PPLESLATVE	ETVVRDKAVE	SLRAISHEHS	PSDLEAHFVP	LVKRLAGGDW	FTSRTSACGL	FVVCYPRVSS
AVKAEALRQYF	RNLCSDDTPM	VRRAAASKLG	EFAKVLLEDN	VKSEIIPMFS	NLASDEQDSV	RLLAVEACNV	IAQLLPQEDL
EALVMPTLRQ	AAEDKSWRVH	YVADKFTLE	QKAVGPEITK	TDLVLPFQNL	KDCEAEVRA	AASHKVKFCF	ENLSDACREN
VIMSQILPCII	KELVSDANQH	VKSALASVIM	GLSPILKGDN	TIEHLLPLFL	AQLKDECEPV	RLNIISNLDC	VNEVIGIRQL
SQSLLPAIYE	LAEDAKWVRV	LAIIEYMPLL	AGQLGVEFFD	EKLNLSLMAW	LVDDHYAIRE	AATSNLKLKLV	EKFGEKAWHA
TIIIPKVLAMS	GDPNYLHRMT	TLFCINVLSE	VCGQDITTKH	MLPTVLRVAG	DPVANVRFNV	AKSLQKIGPI	LDNSTLQSEV
KPILEKLTQD	QDVVVKYFAQ	EALTVLSLA					

PP2A-B55α: 38/457 amino acids (8% coverage), 4 peptides, 4 spectra

MFPKFLSRSM	FHGAGGGNDI	QWCFSQVKGA	VDDVVAEADI	ISTVEFNHSG	ELLATGDKGG	RVVIFQQEQE	NKIQSHSRGE
YNVYSTFQSH	EPEFDYLLKSL	EIEEEKINKIR	WLPOKNAAQF	LLSTNDKTIK	LWKISERDKR	PEGYNLKEED	GRYRDPTTIV
TLRVPVFRPM	DLMVYASPRR	IFANAHTYHI	NCSINSDYIE	TYLSADDLRI	NLWHLIETDR	SFNIVDIKPA	NMEELTEVIT
AAEFHFNSSCN	TEFVYSSKGT	IRLCDMRASA	LCDRHNSKLF	EPEDEPSNRSF	FSEIISISID	VKFSHSGRYM	MTRDYLVSVKI
WDLNENRPPV	ETRYQVHEYLR	SKLCSLYEND	CIFDKFCECCW	NGSDSVVMTG	SYNFFRMFD	RNTKRDTITLE	ASRENNKPR
VLKPRKVCAS	GKRKKKEISV	DSLDRKKKIL	HTAWHPKENI	IAVATTNNLY	IFQDKVM		

PP2A-C: 27/309 amino acids (9% coverage), 3 peptides, 3 spectra

MDEKVFTELK	DQWIEQLNEC	KOLSESQVKS	LCEKAKEILT	KESNVQEVRC	PVTVCGDVHG	QFHDLMLFRR	IGGKSPDNTY
LFGMDYVDRG	YYSVETVTL	VALKVRYRER	HEITLRGNHS	RQITQVGYGF	DECLRKYGNA	NWVKYFTDLF	DYLLPLTALVD
GQIFGLHGGGL	SPSIDTLQHI	RALDRVLEVP	IEGPMCDLWS	SDPPDRGGWG	ISPRGAGYTF	QODISETFNH	ANGLTLVRSRA
HQLVMEGYNW	CHDRNVVTFI	SAPNYCYRCG	NQAAMELDD	TLKYSLQGD	PAPRRGEPHV	TRRTPDYFL	

RIPK1: 37/671 amino acids (6% coverage), 3 peptides, 3 spectra

MQPDMSLNI	KMKSSDFLES	AELDSGGFGK	VSLCFHRTQG	LMIMKTYVYK	PNCIEHNEAL	LEEAKMNNRL	RHSRVVKKLG
VIIIEEGKYSL	VEYMEKGNL	MHVYLKAEKST	PLSVQKRIIL	EIEIEGMCYLH	CKGVIHKDLK	PENILVDNDF	HIKIADLGLA
SFKMWSKLN	EEHNLREVD	GTAKKNGGTL	YVMAPEHLND	VNAKPTKESD	VYSFAVVLVA	VFANKEPEYN	AICEQOLIMC
IKSQRPPVD	DITEYCPREI	ISLMKLCWEA	NPEARPTFFG	IEEKFRPFYL	SQLEESVEED	VSLLKKEYSN	ENAVQTKMQS
LQLDCVAVPS	SRNSATEQP	GSLLHSSQGLG	MGPVEESWFA	PSLEHQPQEN	EPSLQSKLQD	EANYHLYGSR	MDRQTKRQRP
QNVAYNREEE	RRRVSHDPP	AQRRPYENFO	NTEGKGTAYS	SAASHGNNAV	QPSGLTSQPO	VLQYQNGLYS	SHGFGTRPLD
PGTAGRQVWY	RPIPSHMPSL	HNIPVPEFNY	LGNTPMFP	SLPPTDESIC	YTIYNSTGIQ	IQAYNVEIG	GTSSLLDST
NTHFKRPA	YQAFDNTT	SLTDKHLDP	RENLGKHWKN	CARKLGFTQS	QIDEIDHDYE	RDGLKEKVVYQ	MLQKWMYRE
IKGATVGLKA	QALHQCSRID	LLSSLIYVSQ	N				

Appendix Figure 4.2: Amino Acid Coverage of Novel TRAIL DISC and TRAIL-R1/R2 Interacting Proteins Detected in Chapter 4

Amino acid sequences for the novel TRAIL DISC/TRAIL-R1/R2 proteins which were confirmed by western blot are shown.: ORP8 (R1 US), Skp1 (WT US), CUL1 (R2 DISC), FBXO11 (R2 US), PP2A-A (WT US), PP2A-B55α (R1 DISC), PP2A-C (WT DISC) and RIPK1 (R1-DISC) are displayed. Peptides detected by mass spectrometry are highlighted in yellow, with modified residues being coloured green. The coverage of each shown is the greatest detected across all of the mass spectrometry analysed samples in Chapter 4. Also displayed are the total unique peptides and total unique spectra detected.

Bibliography

Bibliography

- Abbas, T., Mueller, A.C., Shibata, E., Keaton, M., Rossi, M., Dutta, A., 2013. CRL1-FBXO11 promotes Cdt2 ubiquitylation and degradation and regulates Pr-Set7/Set8-mediated cellular migration. *Mol. Cell* 49, 1147–58. doi:10.1016/j.molcel.2013.02.003
- Abdulghani, J., El-Deiry, W.S., 2010. TRAIL receptor signaling and therapeutics. *Expert Opin. Ther. Targets* 14, 1091–108. doi:10.1517/14728222.2010.519701
- Acehan, D., Jiang, X., Morgan, D.G., Heuser, J.E., Wang, X., Akey, C.W., 2002. Three-dimensional structure of the apoptosome: implications for assembly, procaspase-9 binding, and activation. *Mol. Cell* 9, 423–32.
- Adachi, M., Suematsu, S., Kondo, T., Ogasawara, J., Tanaka, T., Yoshida, N., Nagata, S., 1995. Targeted mutation in the Fas gene causes hyperplasia in peripheral lymphoid organs and liver. *Nat. Genet.* 11, 294–300. doi:10.1038/ng1195-294
- Aggarwal, B.B., Gupta, S.C., Kim, J.H., 2012. Historical perspectives on tumor necrosis factor and its superfamily: 25 years later, a golden journey. *Blood* 119, 651–65. doi:10.1182/blood-2011-04-325225
- Algeciras-Schimmich, A., Pietras, E.M., Barnhart, B.C., Legembre, P., Vijayan, S., Holbeck, S.L., Peter, M.E., 2003. Two CD95 tumor classes with different sensitivities to antitumor drugs. *Proc. Natl. Acad. Sci. U. S. A.* 100, 11445–50. doi:10.1073/pnas.2034995100
- Amarante-Mendes, G.P., Griffith, T.S., 2015. Therapeutic applications of TRAIL receptor agonists in cancer and beyond. *Pharmacol. Ther.* 155, 117–31. doi:10.1016/j.pharmthera.2015.09.001
- Ashkenazi, A., Pai, R.C., Fong, S., Leung, S., Lawrence, D.A., Marsters, S.A., Blackie, C., Chang, L., McMurtrey, A.E., Hebert, A., DeForge, L., Koumenis, I.L., Lewis, D., Harris, L., Bussiere, J., Koeppen, H., Shahrokh, Z., Schwall, R.H., 1999. Safety and antitumor activity of recombinant soluble Apo2 ligand. *J. Clin. Invest.* 104, 155–62. doi:10.1172/JCI6926

- Ashkenazi, A., Salvesen, G., 2014. Regulated cell death: signaling and mechanisms. *Annu. Rev. Cell Dev. Biol.* 30, 337–56. doi:10.1146/annurev-cellbio-100913-013226
- Azijli, K., Weyhenmeyer, B., Peters, G.J., de Jong, S., Kruyt, F. a E., 2013. Non-canonical kinase signaling by the death ligand TRAIL in cancer cells: discord in the death receptor family. *Cell Death Differ.* 20, 858–868. doi:10.1038/cdd.2013.28
- Bagnoli, M., Canevari, S., Mezzanzanica, D., 2010. Cellular FLICE-inhibitory protein (c-FLIP) signalling: a key regulator of receptor-mediated apoptosis in physiologic context and in cancer. *Int. J. Biochem. Cell Biol.* 42, 210–3. doi:10.1016/j.biocel.2009.11.015
- Banner, D.W., D’Arcy, A., Janes, W., Gentz, R., Schoenfeld, H.J., Broger, C., Loetscher, H., Lesslauer, W., 1993. Crystal structure of the soluble human 55 kd TNF receptor-human TNF beta complex: implications for TNF receptor activation. *Cell* 73, 431–45.
- Barnhart, B.C., Legembre, P., Pietras, E., Bubici, C., Franzoso, G., Peter, M.E., 2004. CD95 ligand induces motility and invasiveness of apoptosis-resistant tumor cells. *EMBO J.* 23, 3175–85. doi:10.1038/sj.emboj.7600325
- Basu, A., Sivaprasad, U., 2007. Protein kinase Cepsilon makes the life and death decision. *Cell. Signal.* 19, 1633–42. doi:10.1016/j.cellsig.2007.04.008
- Béaslas, O., Vihervaara, T., Li, J., Laurila, P.-P., Yan, D., Olkkonen, V.M., 2012. Silencing of OSBP-related protein 8 (ORP8) modifies the macrophage transcriptome, nucleoporin p62 distribution, and migration capacity. *Exp. Cell Res.* 318, 1933–45. doi:10.1016/j.yexcr.2012.05.026
- Békés, M., Salvesen, G.S., 2009. The CUL1 of caspase-8 ubiquitination. *Cell* 137, 604–6. doi:10.1016/j.cell.2009.04.052
- Bellail, A.C., Tse, M.C.L., Song, J.H., Phuphanich, S., Olson, J.J., Sun, S.Y., Hao, C., 2010. DR5-mediated DISC controls caspase-8 cleavage and initiation of apoptosis in human glioblastomas. *J. Cell. Mol. Med.* 14, 1303–17. doi:10.1111/j.1582-4934.2009.00777.x

- Berridge, M.J., 2009. Inositol trisphosphate and calcium signalling mechanisms. *Biochim. Biophys. Acta - Mol. Cell Res.* 1793, 933–940. doi:10.1016/j.bbamcr.2008.10.005
- Bidère, N., Su, H.C., Lenardo, M.J., 2006. Genetic disorders of programmed cell death in the immune system. *Annu. Rev. Immunol.* 24, 321–52. doi:10.1146/annurev.immunol.24.021605.090513
- Bjellqvist, B., Hughes, G.J., Pasquali, C., Paquet, N., Ravier, F., Sanchez, J.C., Frutiger, S., Hochstrasser, D., 1993. The focusing positions of polypeptides in immobilized pH gradients can be predicted from their amino acid sequences. *Electrophoresis* 14, 1023–31.
- Blanchard, H., Kodandapani, L., Mittl, P.R., Marco, S.D., Krebs, J.F., Wu, J.C., Tomaselli, K.J., Grütter, M.G., 1999. The three-dimensional structure of caspase-8: an initiator enzyme in apoptosis. *Structure* 7, 1125–33.
- Blankenship, J.W., Varfolomeev, E., Goncharov, T., Fedorova, A. V, Kirkpatrick, D.S., Izrael-Tomasevic, A., Phu, L., Arnott, D., Aghajan, M., Zobel, K., Bazan, J.F., Fairbrother, W.J., Deshayes, K., Vucic, D., 2009. Ubiquitin binding modulates IAP antagonist-stimulated proteasomal degradation of c-IAP1 and c-IAP2(1). *Biochem. J.* 417, 149–60. doi:10.1042/BJ20081885
- Boatright, K.M., Renatus, M., Scott, F.L., Sperandio, S., Shin, H., Pedersen, I.M., Ricci, J.E., Edris, W.A., Sutherlin, D.P., Green, D.R., Salvesen, G.S., 2003. A unified model for apical caspase activation. *Mol. Cell* 11, 529–41.
- Bodmer, J.-L., Schneider, P., Tschopp, J., 2002. The molecular architecture of the TNF superfamily. *Trends Biochem. Sci.* 27, 19–26.
- Boldin, M.P., Goncharov, T.M., Goltsev, Y. V, Wallach, D., 1996. Involvement of MACH, a novel MORT1/FADD-interacting protease, in Fas/APO-1- and TNF receptor-induced cell death. *Cell* 85, 803–15.
- Boldin, M.P., Varfolomeev, E.E., Pancer, Z., Mett, I.L., Camonis, J.H., Wallach, D., 1995. A novel protein that interacts with the death domain of Fas/APO1 contains a sequence motif related to the death domain. *J. Biol. Chem.* 270, 7795–8.

- Bononi, A., Agnoletto, C., De Marchi, E., Marchi, S., Patergnani, S., Bonora, M., Giorgi, C., Missiroli, S., Poletti, F., Rimessi, A., Pinton, P., 2011. Protein kinases and phosphatases in the control of cell fate. *Enzyme Res.* 2011, 329098. doi:10.4061/2011/329098
- Boyd, R.S., Jukes-Jones, R., Walewska, R., Brown, D., Dyer, M.J.S., Cain, K., 2009. Protein profiling of plasma membranes defines aberrant signaling pathways in mantle cell lymphoma. *Mol. Cell. Proteomics* 8, 1501–15. doi:10.1074/mcp.M800515-MCP200
- Bradford, M.M., 1976. A rapid and sensitive method for the quantitation of microgram quantities of protein utilizing the principle of protein-dye binding. *Anal. Biochem.* 72, 248–54.
- Bremer, E., 2013. Targeting of the tumor necrosis factor receptor superfamily for cancer immunotherapy. *ISRN Oncol.* 2013, 371854. doi:10.1155/2013/371854
- Burgett, A.W.G., Poulsen, T.B., Wangkanont, K., Anderson, D.R., Kikuchi, C., Shimada, K., Okubo, S., Fortner, K.C., Mimaki, Y., Kuroda, M., Murphy, J.P., Schwalb, D.J., Petrella, E.C., Cornella-Taracido, I., Schirle, M., Tallarico, J.A., Shair, M.D., 2011. Natural products reveal cancer cell dependence on oxysterol-binding proteins. *Nat. Chem. Biol.* 7, 639–47. doi:10.1038/nchembio.625
- Burns, T.F., Bernhard, E.J., El-Deiry, W.S., 2001. Tissue specific expression of p53 target genes suggests a key role for KILLER/DR5 in p53-dependent apoptosis in vivo. *Oncogene* 20, 4601–12. doi:10.1038/sj.onc.1204484
- Busuttil, V., Bottero, V., Frelin, C., Imbert, V., Ricci, J.-E., Auberger, P., Peyron, J.-F., 2002. Blocking NF-kappaB activation in Jurkat leukemic T cells converts the survival agent and tumor promoter PMA into an apoptotic effector. *Oncogene* 21, 3213–24. doi:10.1038/sj.onc.1205433
- Byun, H.S., Park, K.A., Won, M., Yang, K.-J., Shin, S., Piao, L., Kwak, J.Y., Lee, Z.-W., Park, J., Seok, J.H., Liu, Z.-G., Hur, G.M., 2006. Phorbol 12-myristate 13-acetate protects against tumor necrosis factor (TNF)-induced necrotic cell death by modulating the recruitment of TNF receptor 1-associated death domain and

- receptor-interacting protein into the TNF receptor 1 signaling complex: *Im. Mol. Pharmacol.* 70, 1099–108. doi:10.1124/mol.106.025452
- Cabal-Hierro, L., Lazo, P.S., 2012. Signal transduction by tumor necrosis factor receptors. *Cell. Signal.* 24, 1297–305. doi:10.1016/j.cellsig.2012.02.006
- Cain, K., Bratton, S.B., Cohen, G.M., 2002. The Apaf-1 apoptosome: a large caspase-activating complex. *Biochimie* 84, 203–14.
- Cain, K., Bratton, S.B., Langlais, C., Walker, G., Brown, D.G., Sun, X.M., Cohen, G.M., 2000. Apaf-1 oligomerizes into biologically active approximately 700-kDa and inactive approximately 1.4-MDa apoptosome complexes. *J. Biol. Chem.* 275, 6067–70.
- Cao, X., Pobezinskaya, Y.L., Morgan, M.J., Liu, Z., 2011. The role of TRADD in TRAIL-induced apoptosis and signaling. *FASEB J.* 25, 1353–8. doi:10.1096/fj.10-170480
- Carswell, E.A., Old, L.J., Kassel, R.L., Green, S., Fiore, N., Williamson, B., 1975. An endotoxin-induced serum factor that causes necrosis of tumors. *Proc. Natl. Acad. Sci. U. S. A.* 72, 3666–70.
- Chai, J., Wu, Q., Shiozaki, E., Srinivasula, S.M., Alnemri, E.S., Shi, Y., 2001. Crystal structure of a procaspase-7 zymogen: mechanisms of activation and substrate binding. *Cell* 107, 399–407.
- Chan, F.K., Chun, H.J., Zheng, L., Siegel, R.M., Bui, K.L., Lenardo, M.J., 2000. A domain in TNF receptors that mediates ligand-independent receptor assembly and signaling. *Science* 288, 2351–4.
- Chan, F.K.-M., 2007. Three is better than one: pre-ligand receptor assembly in the regulation of TNF receptor signaling. *Cytokine* 37, 101–7. doi:10.1016/j.cyto.2007.03.005
- Chang, D.W., Ditsworth, D., Liu, H., Srinivasula, S.M., Alnemri, E.S., Yang, X., 2003. Oligomerization is a general mechanism for the activation of apoptosis initiator and inflammatory procaspases. *J. Biol. Chem.* 278, 16466–9. doi:10.1074/jbc.C300089200

- Chang, L., Kamata, H., Solinas, G., Luo, J.-L., Maeda, S., Venuprasad, K., Liu, Y.-C., Karin, M., 2006. The E3 ubiquitin ligase itch couples JNK activation to TNF α -induced cell death by inducing c-FLIP(L) turnover. *Cell* 124, 601–13. doi:10.1016/j.cell.2006.01.021
- Chaudhary, P.M., Eby, M., Jasmin, A., Bookwalter, A., Murray, J., Hood, L., 1997. Death receptor 5, a new member of the TNFR family, and DR4 induce FADD-dependent apoptosis and activate the NF- κ B pathway. *Immunity* 7, 821–30.
- Chipuk, J.E., Moldoveanu, T., Llambi, F., Parsons, M.J., Green, D.R., 2010. The BCL-2 Family Reunion. *Mol. Cell* 37, 299–310. doi:10.1016/j.molcel.2010.01.025
- Choi, S.J., Lee, K.-H., Park, H.S., Kim, S.-K., Koh, C.-M., Park, J.Y., 2005. Differential expression, shedding, cytokine regulation and function of TNFR1 and TNFR2 in human fetal astrocytes. *Yonsei Med. J.* 46, 818–26. doi:10.3349/ymj.2005.46.6.818
- Cifone, M.G., De Maria, R., Roncaioli, P., Rippo, M.R., Azuma, M., Lanier, L.L., Santoni, A., Testi, R., 1994. Apoptotic signaling through CD95 (Fas/Apo-1) activates an acidic sphingomyelinase. *J. Exp. Med.* 180, 1547–52.
- Cohen, G.M., 1997. Caspases: the executioners of apoptosis. *Biochem. J.* 326 (Pt 1, 1–16.
- Cohen, P.T., Cohen, P., 1989. Discovery of a protein phosphatase activity encoded in the genome of bacteriophage lambda. Probable identity with open reading frame 221. *Biochem. J.* 260, 931–4.
- Conradt, B., Horvitz, H.R., 1998. The *C. elegans* protein EGL-1 is required for programmed cell death and interacts with the Bcl-2-like protein CED-9. *Cell* 93, 519–29.
- Cretney, E., Takeda, K., Yagita, H., Glaccum, M., Peschon, J.J., Smyth, M.J., 2002. Increased susceptibility to tumor initiation and metastasis in TNF-related apoptosis-inducing ligand-deficient mice. *J. Immunol.* 168, 1356–61.
- Daniel, D., Crawford, J., 2006. Myelotoxicity from chemotherapy. *Semin. Oncol.* 33,

74–85. doi:10.1053/j.seminoncol.2005.11.003

- Davids, M.S., Letai, A., 2012. Targeting the B-cell lymphoma/leukemia 2 family in cancer. *J. Clin. Oncol.* 30, 3127–35. doi:10.1200/JCO.2011.37.0981
- Degli-Esposti, M.A., Dougall, W.C., Smolak, P.J., Waugh, J.Y., Smith, C.A., Goodwin, R.G., 1997a. The novel receptor TRAIL-R4 induces NF-kappaB and protects against TRAIL-mediated apoptosis, yet retains an incomplete death domain. *Immunity* 7, 813–20.
- Degli-Esposti, M.A., Smolak, P.J., Walczak, H., Waugh, J., Huang, C.P., DuBose, R.F., Goodwin, R.G., Smith, C.A., 1997b. Cloning and characterization of TRAIL-R3, a novel member of the emerging TRAIL receptor family. *J. Exp. Med.* 186, 1165–70.
- Delhase, M., Hayakawa, M., Chen, Y., Karin, M., 1999. Positive and negative regulation of IkappaB kinase activity through IKKbeta subunit phosphorylation. *Science* 284, 309–13.
- Denecker, G., Hoste, E., Gilbert, B., Hochepped, T., Ovaere, P., Lippens, S., Van den Broecke, C., Van Damme, P., D’Herde, K., Hachem, J.-P., Borgonie, G., Presland, R.B., Schoonjans, L., Libert, C., Vandekerckhove, J., Gevaert, K., Vandenabeele, P., Declercq, W., 2007. Caspase-14 protects against epidermal UVB photodamage and water loss. *Nat. Cell Biol.* 9, 666–74. doi:10.1038/ncb1597
- Desbarats, J., Birge, R.B., Mimouni-Rongy, M., Weinstein, D.E., Palerme, J.-S., Newell, M.K., 2003. Fas engagement induces neurite growth through ERK activation and p35 upregulation. *Nat. Cell Biol.* 5, 118–25. doi:10.1038/ncb916
- Desbarats, J., Newell, M.K., 2000. Fas engagement accelerates liver regeneration after partial hepatectomy. *Nat. Med.* 6, 920–3. doi:10.1038/78688
- Dickens, L.S., 2009. PROTEOMIC AND MOLECULAR CHARACTERISATION OF TRAIL-INDUCED SIGNALLING COMPLEXES. University of Leicester.
- Dickens, L.S., Boyd, R.S., Jukes-Jones, R., Hughes, M. a, Robinson, G.L., Fairall, L., Schwabe, J.W.R., Cain, K., Macfarlane, M., 2012a. A death effector domain chain DISC model reveals a crucial role for caspase-8 chain assembly in mediating

- apoptotic cell death. *Mol. Cell* 47, 291–305. doi:10.1016/j.molcel.2012.05.004
- Dickens, L.S., Powley, I.R., Hughes, M. a, MacFarlane, M., 2012b. The “complexities” of life and death: death receptor signalling platforms. *Exp. Cell Res.* 318, 1269–77. doi:10.1016/j.yexcr.2012.04.005
- Domina, A.M., Vrana, J.A., Gregory, M.A., Hann, S.R., Craig, R.W., 2004. MCL1 is phosphorylated in the PEST region and stabilized upon ERK activation in viable cells, and at additional sites with cytotoxic okadaic acid or taxol. *Oncogene* 23, 5301–15. doi:10.1038/sj.onc.1207692
- Duan, S., Cermak, L., Pagan, J.K., Rossi, M., Martinengo, C., di Celle, P.F., Chapuy, B., Shipp, M., Chiarle, R., Pagano, M., 2012. FBXO11 targets BCL6 for degradation and is inactivated in diffuse large B-cell lymphomas. *Nature* 481, 90–3. doi:10.1038/nature10688
- Duiker, E.W., Mom, C.H., de Jong, S., Willemse, P.H.B., Gietema, J.A., van der Zee, A.G.J., de Vries, E.G.E., 2006. The clinical trail of TRAIL. *Eur. J. Cancer* 42, 2233–40. doi:10.1016/j.ejca.2006.03.018
- Duriez, P.J., Shah, G.M., 1997. Cleavage of poly(ADP-ribose) polymerase: a sensitive parameter to study cell death. *Biochem. Cell Biol.* 75, 337–49.
- Earnshaw, W.C., Martins, L.M., Kaufmann, S.H., 1999. Mammalian caspases: structure, activation, substrates, and functions during apoptosis. *Annu. Rev. Biochem.* 68, 383–424. doi:10.1146/annurev.biochem.68.1.383
- Eberstadt, M., Huang, B., Chen, Z., Meadows, R.P., Ng, S.C., Zheng, L., Lenardo, M.J., Fesik, S.W., 1998. NMR structure and mutagenesis of the FADD (Mort1) death-effector domain. *Nature* 392, 941–5. doi:10.1038/31972
- Eck, M.J., Sprang, S.R., 1989. The structure of tumor necrosis factor-alpha at 2.6 Å resolution. Implications for receptor binding. *J. Biol. Chem.* 264, 17595–605.
- Ehrhardt, H., Fulda, S., Schmid, I., Hiscott, J., Debatin, K.-M., Jeremias, I., 2003. TRAIL induced survival and proliferation in cancer cells resistant towards TRAIL-induced apoptosis mediated by NF-κB. *Oncogene* 22, 3842–3852.

doi:10.1038/sj.onc.1206520

Eichhorn, P.J.A., Creighton, M.P., Bernards, R., 2009. Protein phosphatase 2A regulatory subunits and cancer. *Biochim. Biophys. Acta - Rev. Cancer* 1795, 1–15. doi:10.1016/j.bbcan.2008.05.005

Eichhorn, P.J.A., Creighton, M.P., Wilhelmsen, K., van Dam, H., Bernards, R., 2007. A RNA Interference Screen Identifies the Protein Phosphatase 2A Subunit PR55 γ as a Stress-Sensitive Inhibitor of c-SRC. *PLoS Genet.* 3, e218. doi:10.1371/journal.pgen.0030218

Eichhorn, P.J. a, Creighton, M.P., Bernards, R., 2009. Protein phosphatase 2A regulatory subunits and cancer. *Biochim. Biophys. Acta* 1795, 1–15. doi:10.1016/j.bbcan.2008.05.005

Ellis, H.M., Horvitz, H.R., 1986. Genetic control of programmed cell death in the nematode *C. elegans*. *Cell* 44, 817–29.

Emery, J.G., McDonnell, P., Burke, M.B., Deen, K.C., Lyn, S., Silverman, C., Dul, E., Appelbaum, E.R., Eichman, C., DiPrinzio, R., Dodds, R.A., James, I.E., Rosenberg, M., Lee, J.C., Young, P.R., 1998. Osteoprotegerin is a receptor for the cytotoxic ligand TRAIL. *J. Biol. Chem.* 273, 14363–7.

Enari, M., Sakahira, H., Yokoyama, H., Okawa, K., Iwamatsu, A., Nagata, S., 1998. A caspase-activated DNase that degrades DNA during apoptosis, and its inhibitor ICAD. *Nature* 391, 43–50. doi:10.1038/34112

Esposito, D., Sankar, A., Morgner, N., Robinson, C. V, Rittinger, K., Driscoll, P.C., 2010. Solution NMR investigation of the CD95/FADD homotypic death domain complex suggests lack of engagement of the CD95 C terminus. *Structure* 18, 1378–90. doi:10.1016/j.str.2010.08.006

Fabre, B., Lambour, T., Bouyssié, D., Menneteau, T., Monsarrat, B., Burlet-Schiltz, O., Bousquet-Dubouch, M.-P., 2014. Comparison of label-free quantification methods for the determination of protein complexes subunits stoichiometry. *EuPA Open Proteomics* 4, 82–86. doi:10.1016/j.euprot.2014.06.001

- Fadok, V.A., Bratton, D.L., Rose, D.M., Pearson, A., Ezekewitz, R.A., Henson, P.M., 2000. A receptor for phosphatidylserine-specific clearance of apoptotic cells. *Nature* 405, 85–90. doi:10.1038/35011084
- Ferlay, J., Soerjomataram, I., Dikshit, R., Eser, S., Mathers, C., Rebelo, M., Parkin, D.M., Forman, D., Bray, F., 2015. Cancer incidence and mortality worldwide: sources, methods and major patterns in GLOBOCAN 2012. *Int. J. cancer* 136, E359-86. doi:10.1002/ijc.29210
- Finnberg, N., Klein-Szanto, A.J.P., El-Deiry, W.S., 2008. TRAIL-R deficiency in mice promotes susceptibility to chronic inflammation and tumorigenesis. *J. Clin. Invest.* 118, 111–23. doi:10.1172/JCI29900
- Flusberg, D.A., Roux, J., Spencer, S.L., Sorger, P.K., 2013. Cells surviving fractional killing by TRAIL exhibit transient but sustainable resistance and inflammatory phenotypes. *Mol. Biol. Cell* 24, 2186–200. doi:10.1091/mbc.E12-10-0737
- Fuentes-Prior, P., Salvesen, G.S., 2004. The protein structures that shape caspase activity, specificity, activation and inhibition. *Biochem. J.* 384, 201–32. doi:10.1042/BJ20041142
- Gasparian, M.E., Chernyak, B. V., Dolgikh, D.A., Yagolovich, A. V., Popova, E.N., Sycheva, A.M., Moshkovskii, S.A., Kirpichnikov, M.P., 2009. Generation of new TRAIL mutants DR5-A and DR5-B with improved selectivity to death receptor 5. *Apoptosis* 14, 778–787. doi:10.1007/s10495-009-0349-3
- Gómez-Angelats, M., Bortner, C.D., Cidlowski, J.A., 2000. Protein kinase C (PKC) inhibits fas receptor-induced apoptosis through modulation of the loss of K⁺ and cell shrinkage. A role for PKC upstream of caspases. *J. Biol. Chem.* 275, 19609–19. doi:10.1074/jbc.M909563199
- Gómez-Angelats, M., Cidlowski, J.A., 2001. Protein kinase C regulates FADD recruitment and death-inducing signaling complex formation in Fas/CD95-induced apoptosis. *J. Biol. Chem.* 276, 44944–52. doi:10.1074/jbc.M104919200
- Gonzalvez, F., Lawrence, D., Yang, B., Yee, S., Pitti, R., Marsters, S., Pham, V.C., Stephan, J.-P., Lill, J., Ashkenazi, A., 2012. TRAF2 Sets a threshold for extrinsic

- apoptosis by tagging caspase-8 with a ubiquitin shutoff timer. *Mol. Cell* 48, 888–99. doi:10.1016/j.molcel.2012.09.031
- Grosse-Wilde, A., Kemp, C.J., 2008. Metastasis suppressor function of tumor necrosis factor-related apoptosis-inducing ligand-R in mice: implications for TRAIL-based therapy in humans? *Cancer Res.* 68, 6035–7. doi:10.1158/0008-5472.CAN-08-0078
- Guicciardi, M.E., Gores, G.J., 2009a. Life and death by death receptors. *FASEB J.* 23, 1625–37. doi:10.1096/fj.08-111005
- Guicciardi, M.E., Gores, G.J., 2009b. Life and death by death receptors. *FASEB J.* 23, 1625–37. doi:10.1096/fj.08-111005
- Gyrd-Hansen, M., Darding, M., Miasari, M., Santoro, M.M., Zender, L., Xue, W., Tenev, T., da Fonseca, P.C.A., Zvelebil, M., Bujnicki, J.M., Lowe, S., Silke, J., Meier, P., 2008. IAPs contain an evolutionarily conserved ubiquitin-binding domain that regulates NF-kappaB as well as cell survival and oncogenesis. *Nat. Cell Biol.* 10, 1309–17. doi:10.1038/ncb1789
- Hadji, A., Ceppi, P., Murmann, A.E., Brockway, S., Pattanayak, A., Bhinder, B., Hau, A., De Chant, S., Parimi, V., Kolesza, P., Richards, J., Chandel, N., Djaballah, H., Peter, M.E., 2014. Death induced by CD95 or CD95 ligand elimination. *Cell Rep.* 7, 208–22. doi:10.1016/j.celrep.2014.02.035
- Han, J.H., Moon, A.R., Chang, J.H., Bae, J., Choi, J.M., Lee, S.H., Kim, T.-H., 2016. Potentiation of TRAIL killing activity by multimerization through isoleucine zipper hexamerization motif. *BMB Rep.* 49, 282–7.
- Hanahan, D., Weinberg, R.A., 2011. Hallmarks of cancer: the next generation. *Cell* 144, 646–74. doi:10.1016/j.cell.2011.02.013
- Hanahan, D., Weinberg, R.A., 2000. The hallmarks of cancer. *Cell* 100, 57–70.
- Härmälä-Braskén, A.-S., Mikhailov, A., Söderström, T.S., Meinander, A., Holmström, T.H., Damuni, Z., Eriksson, J.E., 2003. Type-2A protein phosphatase activity is required to maintain death receptor responsiveness. *Oncogene* 22, 7677–86.

doi:10.1038/sj.onc.1207077

- Harper, N., Farrow, S.N., Kaptein, A., Cohen, G.M., MacFarlane, M., 2001. Modulation of tumor necrosis factor apoptosis-inducing ligand- induced NF-kappa B activation by inhibition of apical caspases. *J. Biol. Chem.* 276, 34743–52. doi:10.1074/jbc.M105693200
- Harper, N., Hughes, M. a, Farrow, S.N., Cohen, G.M., MacFarlane, M., 2003a. Protein kinase C modulates tumor necrosis factor-related apoptosis-inducing ligand- induced apoptosis by targeting the apical events of death receptor signaling. *J. Biol. Chem.* 278, 44338–47. doi:10.1074/jbc.M307376200
- Harper, N., Hughes, M., MacFarlane, M., Cohen, G.M., 2003b. Fas-associated death domain protein and caspase-8 are not recruited to the tumor necrosis factor receptor 1 signaling complex during tumor necrosis factor-induced apoptosis. *J. Biol. Chem.* 278, 25534–41. doi:10.1074/jbc.M303399200
- Harper, N., MacFarlane, M., 2008. Recombinant TRAIL and TRAIL receptor analysis. *Methods Enzymol.* 446, 293–313. doi:10.1016/S0076-6879(08)01618-2
- Haynes, N.M., Hawkins, E.D., Li, M., McLaughlin, N.M., Hämmerling, G.J., Schwendener, R., Winoto, A., Wensky, A., Yagita, H., Takeda, K., Kershaw, M.H., Darcy, P.K., Smyth, M.J., 2010. CD11c+ dendritic cells and B cells contribute to the tumoricidal activity of anti-DR5 antibody therapy in established tumors. *J. Immunol.* 185, 532–41. doi:10.4049/jimmunol.0903624
- He, L., Jang, J.H., Choi, H.G., Lee, S.M., Nan, M.H., Jeong, S.J., Dong, Z., Kwon, Y.T., Lee, K.S., Lee, K.W., Chung, J.K., Ahn, J.S., Kim, B.Y., 2013. Oligomycin A enhances apoptotic effect of TRAIL through CHOP-mediated death receptor 5 expression. *Mol. Carcinog.* 52, 85–93. doi:10.1002/mc.21831
- Hengartner, M.O., Ellis, R.E., Horvitz, H.R., 1992. *Caenorhabditis elegans* gene *ced-9* protects cells from programmed cell death. *Nature* 356, 494–9. doi:10.1038/356494a0
- Higuchi, H., Yoon, J.-H., Grambihler, A., Werneburg, N., Bronk, S.F., Gores, G.J., 2003. Bile acids stimulate cFLIP phosphorylation enhancing TRAIL-mediated apoptosis.

- J. Biol. Chem. 278, 454–61. doi:10.1074/jbc.M209387200
- Hill, J.M., Morisawa, G., Kim, T., Huang, T., Wei, Y., Wei, Y., Werner, M.H., 2004. Identification of an expanded binding surface on the FADD death domain responsible for interaction with CD95/Fas. J. Biol. Chem. 279, 1474–81. doi:10.1074/jbc.M304996200
- Hirata, H., Takahashi, A., Kobayashi, S., Yonehara, S., Sawai, H., Okazaki, T., Yamamoto, K., Sasada, M., 1998. Caspases are activated in a branched protease cascade and control distinct downstream processes in Fas-induced apoptosis. J. Exp. Med. 187, 587–600.
- Holmström, T.H., Schmitz, I., Söderström, T.S., Poukkula, M., Johnson, V.L., Chow, S.C., Krammer, P.H., Eriksson, J.E., 2000. MAPK/ERK signaling in activated T cells inhibits CD95/Fas-mediated apoptosis downstream of DISC assembly. EMBO J. 19, 5418–28. doi:10.1093/emboj/19.20.5418
- Horak, P., Pils, D., Haller, G., Pribill, I., Roessler, M., Tomek, S., Horvat, R., Zeillinger, R., Zielinski, C., Krainer, M., 2005. Contribution of epigenetic silencing of tumor necrosis factor-related apoptosis inducing ligand receptor 1 (DR4) to TRAIL resistance and ovarian cancer. Mol. Cancer Res. 3, 335–43. doi:10.1158/1541-7786.MCR-04-0136
- Hsu, H., Huang, J., Shu, H.B., Baichwal, V., Goeddel, D. V., 1996a. TNF-dependent recruitment of the protein kinase RIP to the TNF receptor-1 signaling complex. Immunity 4, 387–96.
- Hsu, H., Shu, H.B., Pan, M.G., Goeddel, D. V., 1996b. TRADD-TRAF2 and TRADD-FADD interactions define two distinct TNF receptor 1 signal transduction pathways. Cell 84, 299–308.
- Hsu, H., Xiong, J., Goeddel, D. V., 1995. The TNF receptor 1-associated protein TRADD signals cell death and NF-kappa B activation. Cell 81, 495–504.
- Hughes, M.A., Langlais, C., Cain, K., MacFarlane, M., 2013. Isolation, characterisation and reconstitution of cell death signalling complexes. Methods 61, 98–104. doi:10.1016/j.ymeth.2013.02.006

- Hughes, M.A., Powley, I.R., Jukes-Jones, R., Horn, S., Feoktistova, M., Fairall, L., Schwabe, J.W.R., Leverkus, M., Cain, K., MacFarlane, M., 2016. Co-operative and Hierarchical Binding of c-FLIP and Caspase-8: A Unified Model Defines How c-FLIP Isoforms Differentially Control Cell Fate. *Mol. Cell* 61, 834–849. doi:10.1016/j.molcel.2016.02.023
- Hughes, M. a, Harper, N., Butterworth, M., Cain, K., Cohen, G.M., MacFarlane, M., 2009. Reconstitution of the death-inducing signaling complex reveals a substrate switch that determines CD95-mediated death or survival. *Mol. Cell* 35, 265–79. doi:10.1016/j.molcel.2009.06.012
- Igney, F.H., Behrens, C.K., Krammer, P.H., 2000. Tumor counterattack--concept and reality. *Eur. J. Immunol.* 30, 725–31. doi:10.1002/1521-4141(200003)30:3<725::AID-IMMU725>3.0.CO;2-D
- Inoue, S., Harper, N., Walewska, R., Dyer, M.J.S., Cohen, G.M., 2009. Enhanced Fas-associated death domain recruitment by histone deacetylase inhibitors is critical for the sensitization of chronic lymphocytic leukemia cells to TRAIL-induced apoptosis. *Mol. Cancer Ther.* 8, 3088–97. doi:10.1158/1535-7163.MCT-09-0451
- Israël, A., 2010. The IKK complex, a central regulator of NF-kappaB activation. *Cold Spring Harb. Perspect. Biol.* 2, a000158. doi:10.1101/cshperspect.a000158
- Ito, T., Deng, X., Carr, B., May, W.S., 1997. Bcl-2 phosphorylation required for anti-apoptosis function. *J. Biol. Chem.* 272, 11671–3.
- Itoh, N., Nagata, S., 1993. A novel protein domain required for apoptosis. Mutational analysis of human Fas antigen. *J. Biol. Chem.* 268, 10932–7.
- Jin, Z., El-Deiry, W.S., 2006. Distinct signaling pathways in TRAIL- versus tumor necrosis factor-induced apoptosis. *Mol. Cell. Biol.* 26, 8136–48. doi:10.1128/MCB.00257-06
- Jin, Z., Li, Y., Pitti, R., Lawrence, D., Pham, V.C., Lill, J.R., Ashkenazi, A., 2009. Cullin3-based polyubiquitination and p62-dependent aggregation of caspase-8 mediate extrinsic apoptosis signaling. *Cell* 137, 721–35. doi:10.1016/j.cell.2009.03.015

- Jo, M., Kim, T.H., Seol, D.W., Esplen, J.E., Dorko, K., Billiar, T.R., Strom, S.C., 2000. Apoptosis induced in normal human hepatocytes by tumor necrosis factor-related apoptosis-inducing ligand. *Nat. Med.* 6, 564–7. doi:10.1038/75045
- Johnson, T.R., Stone, K., Nikrad, M., Yeh, T., Zong, W.-X., Thompson, C.B., Nesterov, A., Kraft, A.S., 2003. The proteasome inhibitor PS-341 overcomes TRAIL resistance in Bax and caspase 9-negative or Bcl-xL overexpressing cells. *Oncogene* 22, 4953–63. doi:10.1038/sj.onc.1206656
- Kägi, D., Vignaux, F., Ledermann, B., Bürki, K., Depraetere, V., Nagata, S., Hengartner, H., Golstein, P., 1994. Fas and perforin pathways as major mechanisms of T cell-mediated cytotoxicity. *Science* 265, 528–30.
- Kaneki, M., Kharbanda, S., Pandey, P., Yoshida, K., Takekawa, M., Liou, J.R., Stone, R., Kufe, D., 1999. Functional role for protein kinase C β as a regulator of stress-activated protein kinase activation and monocytic differentiation of myeloid leukemia cells. *Mol. Cell. Biol.* 19, 461–70.
- Kang, T.-B., Oh, G.-S., Scandella, E., Bolinger, B., Ludewig, B., Kovalenko, A., Wallach, D., 2008. Mutation of a self-processing site in caspase-8 compromises its apoptotic but not its nonapoptotic functions in bacterial artificial chromosome-transgenic mice. *J. Immunol.* 181, 2522–32.
- Karray, S., Kress, C., Cuvellier, S., Hue-Beauvais, C., Damotte, D., Babinet, C., Lévi-Strauss, M., 2004. Complete loss of Fas ligand gene causes massive lymphoproliferation and early death, indicating a residual activity of gld allele. *J. Immunol.* 172, 2118–25.
- Kayagaki, N., Yamaguchi, N., Nakayama, M., Eto, H., Okumura, K., Yagita, H., 1999. Type I interferons (IFNs) regulate tumor necrosis factor-related apoptosis-inducing ligand (TRAIL) expression on human T cells: A novel mechanism for the antitumor effects of type I IFNs. *J. Exp. Med.* 189, 1451–60.
- Keller, N., Mares, J., Zerbe, O., Grütter, M.G., 2009. Structural and biochemical studies on procaspase-8: new insights on initiator caspase activation. *Structure* 17, 438–48. doi:10.1016/j.str.2008.12.019

- Kerr, J.F., Wyllie, A.H., Currie, A.R., 1972. Apoptosis: a basic biological phenomenon with wide-ranging implications in tissue kinetics. *Br. J. Cancer* 26, 239–57.
- Kersse, K., Vanden Berghe, T., Lamkanfi, M., Vandenabeele, P., 2007. A phylogenetic and functional overview of inflammatory caspases and caspase-1-related CARD-only proteins. *Biochem. Soc. Trans.* 35, 1508–11. doi:10.1042/BST0351508
- Kim, J.-Y., Lee, J.-Y., Kim, D.-G., Koo, G.-B., Yu, J.-W., Kim, Y.-S., 2011. TRADD is critical for resistance to TRAIL-induced cell death through NF- κ B activation, *FEBS Letters*. doi:10.1016/j.febslet.2011.05.034
- Kim, M.-H., Billiar, T.R., Seol, D.-W., 2004. The secretable form of trimeric TRAIL, a potent inducer of apoptosis. *Biochem. Biophys. Res. Commun.* 321, 930–5. doi:10.1016/j.bbrc.2004.07.046
- Kischkel, F.C., Hellbardt, S., Behrmann, I., Germer, M., Pawlita, M., Krammer, P.H., Peter, M.E., 1995. Cytotoxicity-dependent APO-1 (Fas/CD95)-associated proteins form a death-inducing signaling complex (DISC) with the receptor. *EMBO J.* 14, 5579–88.
- Kischkel, F.C., Lawrence, D.A., Chuntharapai, A., Schow, P., Kim, K.J., Ashkenazi, A., 2000. Apo2L/TRAIL-Dependent Recruitment of Endogenous FADD and Caspase-8 to Death Receptors 4 and 5. *Immunity* 12, 611–620. doi:10.1016/S1074-7613(00)80212-5
- Kohlhaas, S.L., Craxton, A., Sun, X.-M., Pinkoski, M.J., Cohen, G.M., 2007. Receptor-mediated endocytosis is not required for tumor necrosis factor-related apoptosis-inducing ligand (TRAIL)-induced apoptosis. *J. Biol. Chem.* 282, 12831–41. doi:10.1074/jbc.M700438200
- Koivunen, J., Aaltonen, V., Peltonen, J., Zugaza, J.L., Sinnett-Smith, J., Lint, J. Van, Rozengurt, E., Paolucci, L., Rozengurt, 2006. Protein kinase C (PKC) family in cancer progression. *Cancer Lett.* 235, 1–10. doi:10.1016/j.canlet.2005.03.033
- Kojima, H., Shinohara, N., Hanaoka, S., Someya-Shirota, Y., Takagaki, Y., Ohno, H., Saito, T., Katayama, T., Yagita, H., Okumura, K., 1994. Two distinct pathways of specific killing revealed by perforin mutant cytotoxic T lymphocytes. *Immunity* 1,

357–64.

- Krammer, P.H., 2000. CD95's deadly mission in the immune system. *Nature* 407, 789–95. doi:10.1038/35037728
- Labbé, K., Saleh, M., 2008. Cell death in the host response to infection. *Cell Death Differ.* 15, 1339–49. doi:10.1038/cdd.2008.91
- Lavrik, I., Krueger, A., Schmitz, I., Baumann, S., Weyd, H., Krammer, P.H., Kirchhoff, S., 2003. The active caspase-8 heterotetramer is formed at the CD95 DISC. *Cell Death Differ.* 10, 144–145. doi:10.1038/sj.cdd.4401156
- Lee, H.-W., Lee, S.-H., Lee, H.-W., Ryu, Y.-W., Kwon, M.-H., Kim, Y.-S., 2005. Homomeric and heteromeric interactions of the extracellular domains of death receptors and death decoy receptors. *Biochem. Biophys. Res. Commun.* 330, 1205–12. doi:10.1016/j.bbrc.2005.03.101
- Lee, K.-H., Feig, C., Tchikov, V., Schickel, R., Hallas, C., Schütze, S., Peter, M.E., Chan, A.C., 2006. The role of receptor internalization in CD95 signaling. *EMBO J.* 25, 1009–23. doi:10.1038/sj.emboj.7601016
- Lee, S.Y., Reichlin, A., Santana, A., Sokol, K.A., Nussenzweig, M.C., Choi, Y., 1997. TRAF2 Is Essential for JNK but Not NF- κ B Activation and Regulates Lymphocyte Proliferation and Survival. *Immunity* 7, 703–713.
- Lee, T.H., Shank, J., Cusson, N., Kelliher, M.A., 2004. The kinase activity of Rip1 is not required for tumor necrosis factor-alpha-induced I κ B kinase or p38 MAP kinase activation or for the ubiquitination of Rip1 by Traf2. *J. Biol. Chem.* 279, 33185–91. doi:10.1074/jbc.M404206200
- Legembre, P., Barnhart, B.C., Zheng, L., Vijayan, S., Straus, S.E., Puck, J., Dale, J.K., Lenardo, M., Peter, M.E., 2004a. Induction of apoptosis and activation of NF- κ B by CD95 require different signalling thresholds. *EMBO Rep.* 5, 1084–9. doi:10.1038/sj.embor.7400280
- Legembre, P., Schickel, R., Barnhart, B.C., Peter, M.E., 2004b. Identification of SNF1/AMP kinase-related kinase as an NF- κ B-regulated anti-apoptotic kinase

- involved in CD95-induced motility and invasiveness. *J. Biol. Chem.* 279, 46742–7. doi:10.1074/jbc.M404334200
- Lemke, J., Noack, A., Adam, D., Tchikov, V., Bertsch, U., Röder, C., Schütze, S., Wajant, H., Kalthoff, H., Trauzold, A., 2010. TRAIL signaling is mediated by DR4 in pancreatic tumor cells despite the expression of functional DR5. *J. Mol. Med. (Berl)*. 88, 729–40. doi:10.1007/s00109-010-0619-0
- Li, H., Zhu, H., Xu, C.J., Yuan, J., 1998. Cleavage of BID by caspase 8 mediates the mitochondrial damage in the Fas pathway of apoptosis. *Cell* 94, 491–501.
- Li, P., Nijhawan, D., Budihardjo, I., Srinivasula, S.M., Ahmad, M., Alnemri, E.S., Wang, X., 1997. Cytochrome c and dATP-dependent formation of Apaf-1/caspase-9 complex initiates an apoptotic protease cascade. *Cell* 91, 479–89.
- Li, W., Zhang, X., Olumi, A.F., 2007. MG-132 sensitizes TRAIL-resistant prostate cancer cells by activating c-Fos/c-Jun heterodimers and repressing c-FLIP(L). *Cancer Res.* 67, 2247–55. doi:10.1158/0008-5472.CAN-06-3793
- Li, Y., Wang, H., Wang, Z., Makhija, S., Buchsbaum, D., LoBuglio, A., Kimberly, R., Zhou, T., 2006. Inducible resistance of tumor cells to tumor necrosis factor-related apoptosis-inducing ligand receptor 2-mediated apoptosis by generation of a blockade at the death domain function. *Cancer Res.* 66, 8520–8. doi:10.1158/0008-5472.CAN-05-4364
- Lin, Y., Devin, A., Cook, A., Keane, M.M., Kelliher, M., Lipkowitz, S., Liu, Z.G., 2000. The death domain kinase RIP is essential for TRAIL (Apo2L)-induced activation of I κ B kinase and c-Jun N-terminal kinase. *Mol. Cell. Biol.* 20, 6638–45.
- Liu, X., Guo, S., Liu, X., Su, L., 2015. Chaetocin induces endoplasmic reticulum stress response and leads to death receptor 5-dependent apoptosis in human non-small cell lung cancer cells. *Apoptosis* 20, 1499–507. doi:10.1007/s10495-015-1167-4
- Lowin, B., Hahne, M., Mattmann, C., Tschopp, J., 1994. Cytolytic T-cell cytotoxicity is mediated through perforin and Fas lytic pathways. *Nature* 370, 650–2. doi:10.1038/370650a0

- Lu, M., Lawrence, D.A., Marsters, S., Acosta-Alvear, D., Kimmig, P., Mendez, A.S., Paton, A.W., Paton, J.C., Walter, P., Ashkenazi, A., 2014a. Opposing unfolded-protein-response signals converge on death receptor 5 to control apoptosis. *Science* 345, 98–101. doi:10.1126/science.1254312
- Lu, M., Marsters, S., Ye, X., Luis, E., Gonzalez, L., Ashkenazi, A., 2014b. E-cadherin couples death receptors to the cytoskeleton to regulate apoptosis. *Mol. Cell* 54, 987–98. doi:10.1016/j.molcel.2014.04.029
- Lutz, R.J., 2000. Role of the BH3 (Bcl-2 homology 3) domain in the regulation of apoptosis and Bcl-2-related proteins. *Biochem. Soc. Trans.* 28, 51–6.
- Lydeard, J.R., Schulman, B.A., Harper, J.W., 2013. Building and remodelling Cullin-RING E3 ubiquitin ligases. *EMBO Rep.* 14, 1050–1061. doi:10.1038/embor.2013.173
- MacFarlane, M., Ahmad, M., Srinivasula, S.M., Fernandes-Alnemri, T., Cohen, G.M., Alnemri, E.S., 1997. Identification and molecular cloning of two novel receptors for the cytotoxic ligand TRAIL. *J. Biol. Chem.* 272, 25417–20.
- MacFarlane, M., Harper, N., Snowden, R.T., Dyer, M.J.S., Barnett, G.A., Pringle, J.H., Cohen, G.M., 2002. Mechanisms of resistance to TRAIL-induced apoptosis in primary B cell chronic lymphocytic leukaemia. *Oncogene* 21, 6809–18. doi:10.1038/sj.onc.1205853
- MacFarlane, M., Inoue, S., Kohlhaas, S.L., Majid, a, Harper, N., Kennedy, D.B.J., Dyer, M.J.S., Cohen, G.M., 2005. Chronic lymphocytic leukemic cells exhibit apoptotic signaling via TRAIL-R1. *Cell Death Differ.* 12, 773–82. doi:10.1038/sj.cdd.4401649
- MacFarlane, M., Kohlhaas, S.L., Sutcliffe, M.J., Dyer, M.J.S., Cohen, G.M., 2005. TRAIL receptor-selective mutants signal to apoptosis via TRAIL-R1 in primary lymphoid malignancies. *Cancer Res.* 65, 11265–70. doi:10.1158/0008-5472.CAN-05-2801
- MacFarlane, M., Merrison, W., Dinsdale, D., Cohen, G.M., 2000. Active caspases and cleaved cytokeratins are sequestered into cytoplasmic inclusions in TRAIL-induced apoptosis. *J. Cell Biol.* 148, 1239–54.
- Mahalingam, D., Szegezdi, E., Keane, M., de Jong, S., Samali, A., 2009. TRAIL receptor

- signalling and modulation: Are we on the right TRAIL? *Cancer Treat. Rev.* 35, 280–8. doi:10.1016/j.ctrv.2008.11.006
- Mahmood, Z., Shukla, Y., 2010. Death receptors: targets for cancer therapy. *Exp. Cell Res.* 316, 887–99. doi:10.1016/j.yexcr.2009.12.011
- Mandal, M., Maggirwar, S.B., Sharma, N., Kaufmann, S.H., Sun, S.-C., Kumar, R., 1996. Bcl-2 Prevents CD95 (Fas/APO-1)-induced Degradation of Lamin B and Poly(ADP-ribose) Polymerase and Restores the NF- κ B Signaling Pathway. *J. Biol. Chem.* 271, 30354–30359. doi:10.1074/jbc.271.48.30354
- Marconi, M., Ascione, B., Ciarlo, L., Vona, R., Garofalo, T., Sorice, M., Gianni, A.M., Locatelli, S.L., Carlo-Stella, C., Malorni, W., Matarrese, P., 2013. Constitutive localization of DR4 in lipid rafts is mandatory for TRAIL-induced apoptosis in B-cell hematologic malignancies. *Cell Death Dis.* 4, e863. doi:10.1038/cddis.2013.389
- Marsters, S.A., Sheridan, J.P., Pitti, R.M., Huang, A., Skubatch, M., Baldwin, D., Yuan, J., Gurney, A., Goddard, A.D., Godowski, P., Ashkenazi, A., 1997. A novel receptor for Apo2L/TRAIL contains a truncated death domain. *Curr. Biol.* 7, 1003–6.
- Martin, D.A., Siegel, R.M., Zheng, L., Lenardo, M.J., 1998. Membrane oligomerization and cleavage activates the caspase-8 (FLICE/MACH α 1) death signal. *J. Biol. Chem.* 273, 4345–9.
- Medema, J.P., Scaffidi, C., Kischkel, F.C., Shevchenko, A., Mann, M., Krammer, P.H., Peter, M.E., 1997. FLICE is activated by association with the CD95 death-inducing signaling complex (DISC). *EMBO J.* 16, 2794–804. doi:10.1093/emboj/16.10.2794
- Meng, X.W., Heldebrant, M.P., Flatten, K.S., Loegering, D.A., Dai, H., Schneider, P.A., Gomez, T.S., Peterson, K.L., Trushin, S.A., Hess, A.D., Smith, B.D., Karp, J.E., Billadeau, D.D., Kaufmann, S.H., 2010. Protein kinase C β modulates ligand-induced cell surface death receptor accumulation: a mechanistic basis for enzastaurin-death ligand synergy. *J. Biol. Chem.* 285, 888–902. doi:10.1074/jbc.M109.057638
- Meng, X.W., Heldebrant, M.P., Kaufmann, S.H., 2002. Phorbol 12-myristate 13-acetate inhibits death receptor-mediated apoptosis in Jurkat cells by disrupting

- recruitment of Fas-associated polypeptide with death domain. *J. Biol. Chem.* 277, 3776–83. doi:10.1074/jbc.M107218200
- Mérino, D., Lalaoui, N., Morizot, A., Schneider, P., Solary, E., Micheau, O., 2006. Differential inhibition of TRAIL-mediated DR5-DISC formation by decoy receptors 1 and 2. *Mol. Cell. Biol.* 26, 7046–55. doi:10.1128/MCB.00520-06
- Miaczynska, M., Pelkmans, L., Zerial, M., 2004. Not just a sink: endosomes in control of signal transduction. *Curr. Opin. Cell Biol.* 16, 400–6. doi:10.1016/j.ceb.2004.06.005
- Micheau, O., Shirley, S., Dufour, F., 2013. Death receptors as targets in cancer. *Br. J. Pharmacol.* 169, 1723–44. doi:10.1111/bph.12238
- Micheau, O., Tschopp, J., 2003. Induction of TNF receptor I-mediated apoptosis via two sequential signaling complexes. *Cell* 114, 181–90.
- Mitsiades, N., Poulaki, V., Mitsiades, C., Tsokos, M., 2001. Ewing's sarcoma family tumors are sensitive to tumor necrosis factor-related apoptosis-inducing ligand and express death receptor 4 and death receptor 5. *Cancer Res.* 61, 2704–12.
- Motz, G.T., Santoro, S.P., Wang, L.-P., Garrabrant, T., Lastra, R.R., Hagemann, I.S., Lal, P., Feldman, M.D., Benencia, F., Coukos, G., 2014. Tumor endothelium FasL establishes a selective immune barrier promoting tolerance in tumors. *Nat. Med.* 20, 607–15. doi:10.1038/nm.3541
- Mühlenbeck, F., Schneider, P., Bodmer, J.L., Schwenzler, R., Hauser, A., Schubert, G., Scheurich, P., Moosmayer, D., Tschopp, J., Wajant, H., 2000. The tumor necrosis factor-related apoptosis-inducing ligand receptors TRAIL-R1 and TRAIL-R2 have distinct cross-linking requirements for initiation of apoptosis and are non-redundant in JNK activation. *J. Biol. Chem.* 275, 32208–13. doi:10.1074/jbc.M000482200
- Muzio, M., Chinnaiyan, A.M., Kischkel, F.C., O'Rourke, K., Shevchenko, A., Ni, J., Scaffidi, C., Bretz, J.D., Zhang, M., Gentz, R., Mann, M., Krammer, P.H., Peter, M.E., Dixit, V.M., 1996. FLICE, a novel FADD-homologous ICE/CED-3-like protease, is recruited to the CD95 (Fas/APO-1) death--inducing signaling complex. *Cell* 85,

817–27.

Nagata, S., 1997. Apoptosis by death factor. *Cell* 88, 355–65.

Nagata, S., Enari, M., Sakahira, H., Yokoyama, H., Okawa, K., Iwamatsu, A., 1998. A caspase-activated DNase that degrades DNA during apoptosis, and its inhibitor ICAD. *Nature* 391, 43–50. doi:10.1038/34112

Nagata, S., Suzuki, J., Segawa, K., Fujii, T., 2016. Exposure of phosphatidylserine on the cell surface. *Cell Death Differ.* 23, 952–61. doi:10.1038/cdd.2016.7

Naismith, J.H., Devine, T.Q., Kohno, T., Sprang, S.R., 1996. Structures of the extracellular domain of the type I tumor necrosis factor receptor. *Structure* 4, 1251–62.

Naismith, J.H., Sprang, S.R., 1998. Modularity in the TNF-receptor family. *Trends Biochem. Sci.* 23, 74–9.

Natoni, A., MacFarlane, M., Inoue, S., Walewska, R., Majid, A., Knee, D., Stover, D.R., Dyer, M.J.S., Cohen, G.M., 2007. TRAIL signals to apoptosis in chronic lymphocytic leukaemia cells primarily through TRAIL-R1 whereas cross-linked agonistic TRAIL-R2 antibodies facilitate signalling via TRAIL-R2. *Br. J. Haematol.* 139, 568–77. doi:10.1111/j.1365-2141.2007.06852.x

Ngo, M., Ridgway, N.D., 2009. Oxysterol binding protein-related Protein 9 (ORP9) is a cholesterol transfer protein that regulates Golgi structure and function. *Mol. Biol. Cell* 20, 1388–99. doi:10.1091/mbc.E08-09-0905

Nikolov, M., Schmidt, C., Urlaub, H., 2012. Quantitative mass spectrometry-based proteomics: an overview. *Methods Mol. Biol.* 893, 85–100. doi:10.1007/978-1-61779-885-6_7

O’Connell, J., O’Sullivan, G.C., Collins, J.K., Shanahan, F., 1996. The Fas counterattack: Fas-mediated T cell killing by colon cancer cells expressing Fas ligand. *J. Exp. Med.* 184, 1075–82.

Oellerich, T., Bremes, V., Neumann, K., Bohnenberger, H., Dittmann, K., Hsiao, H.-H., Engelke, M., Schnyder, T., Batista, F.D., Urlaub, H., Wienands, J., 2011. The B-cell

- antigen receptor signals through a preformed transducer module of SLP65 and CIN85. *EMBO J.* 30, 3620–34. doi:10.1038/emboj.2011.251
- Ogasawara, J., Watanabe-Fukunaga, R., Adachi, M., Matsuzawa, A., Kasugai, T., Kitamura, Y., Itoh, N., Suda, T., Nagata, S., 1993. Lethal effect of the anti-Fas antibody in mice. *Nature* 364, 806–9. doi:10.1038/364806a0
- Ohtsuka, T., Buchsbaum, D., Oliver, P., Makhija, S., Kimberly, R., Zhou, T., 2003. Synergistic induction of tumor cell apoptosis by death receptor antibody and chemotherapy agent through JNK/p38 and mitochondrial death pathway. *Oncogene* 22, 2034–44. doi:10.1038/sj.onc.1206290
- Oliver, P.G., LoBuglio, A.F., Zhou, T., Forero, A., Kim, H., Zinn, K.R., Zhai, G., Li, Y., Lee, C.H., Buchsbaum, D.J., 2012. Effect of anti-DR5 and chemotherapy on basal-like breast cancer. *Breast Cancer Res. Treat.* 133, 417–26. doi:10.1007/s10549-011-1755-0
- Olkonen, V.M., Li, S., 2013. Oxysterol-binding proteins: Sterol and phosphoinositide sensors coordinating transport, signaling and metabolism. *Prog. Lipid Res.* doi:10.1016/j.plipres.2013.06.004
- Ouyang, W., Yang, C., Zhang, S., Liu, Y., Yang, B., Zhang, J., Zhou, F., Zhou, Y., Xie, C., 2013. Absence of death receptor translocation into lipid rafts in acquired TRAIL-resistant NSCLC cells. *Int. J. Oncol.* 42, 699–711. doi:10.3892/ijo.2012.1748
- Ozören, N., El-Deiry, W.S., 2002. Defining characteristics of Types I and II apoptotic cells in response to TRAIL. *Neoplasia* 4, 551–7. doi:10.1038/sj.neo.7900270
- Ozören, N., Fisher, M.J., Kim, K., Liu, C.X., Genin, A., Shifman, Y., Dicker, D.T., Spinner, N.B., Lisitsyn, N.A., El-Deiry, W.S., 2000. Homozygous deletion of the death receptor DR4 gene in a nasopharyngeal cancer cell line is associated with TRAIL resistance. *Int. J. Oncol.* 16, 917–25.
- Ozsoy, H.Z., Sivasubramanian, N., Wieder, E.D., Pedersen, S., Mann, D.L., 2008. Oxidative stress promotes ligand-independent and enhanced ligand-dependent tumor necrosis factor receptor signaling. *J. Biol. Chem.* 283, 23419–28. doi:10.1074/jbc.M802967200

- Pan, G., Ni, J., Wei, Y.F., Yu, G., Gentz, R., Dixit, V.M., 1997a. An antagonist decoy receptor and a death domain-containing receptor for TRAIL. *Science* 277, 815–8.
- Pan, G., O'Rourke, K., Chinnaiyan, A.M., Gentz, R., Ebner, R., Ni, J., Dixit, V.M., 1997b. The receptor for the cytotoxic ligand TRAIL. *Science* 276, 111–3.
- Pennarun, B., Meijer, A., de Vries, E.G.E., Kleibeuker, J.H., Kruyt, F., de Jong, S., 2010. Playing the DISC: turning on TRAIL death receptor-mediated apoptosis in cancer. *Biochim. Biophys. Acta* 1805, 123–40. doi:10.1016/j.bbcan.2009.11.004
- Peter, M.E., Hadji, A., Murmann, A.E., Brockway, S., Putzbach, W., Pattanayak, A., Ceppi, P., 2015. The role of CD95 and CD95 ligand in cancer. *Cell Death Differ.* 22, 885–6. doi:10.1038/cdd.2015.25
- Petroski, M.D., Deshaies, R.J., 2005. Function and regulation of cullin-RING ubiquitin ligases. *Nat. Rev. Mol. Cell Biol.* 6, 9–20. doi:10.1038/nrm1547
- Pitti, R.M., Marsters, S.A., Ruppert, S., Donahue, C.J., Moore, A., Ashkenazi, A., 1996. Induction of apoptosis by Apo-2 ligand, a new member of the tumor necrosis factor cytokine family. *J. Biol. Chem.* 271, 12687–90.
- Pop, C., Fitzgerald, P., Green, D.R., Salvesen, G.S., 2007. Role of proteolysis in caspase-8 activation and stabilization. *Biochemistry* 46, 4398–407. doi:10.1021/bi602623b
- Pop, C., Salvesen, G.S., 2009. Human caspases: activation, specificity, and regulation. *J. Biol. Chem.* 284, 21777–81. doi:10.1074/jbc.R800084200
- Pop, C., Timmer, J., Sperandio, S., Salvesen, G.S., 2006. The apoptosome activates caspase-9 by dimerization. *Mol. Cell* 22, 269–75. doi:10.1016/j.molcel.2006.03.009
- Rasper, D.M., Vaillancourt, J.P., Hadano, S., Houtzager, V.M., Seiden, I., Keen, S.L., Tawa, P., Xanthoudakis, S., Nasir, J., Martindale, D., Koop, B.F., Peterson, E.P., Thornberry, N. a, Huang, J., MacPherson, D.P., Black, S.C., Hornung, F., Lenardo, M.J., Hayden, M.R., Roy, S., Nicholson, D.W., 1998. Cell death attenuation by “Usurpin”, a mammalian DED-caspase homologue that precludes caspase-8 recruitment and activation by the CD-95 (Fas, APO-1) receptor complex. *Cell*

- Death Differ. 5, 271–88. doi:10.1038/sj.cdd.4400370
- Ravi, R., Bedi, G.C., Engstrom, L.W., Zeng, Q., Mookerjee, B., Gélinas, C., Fuchs, E.J., Bedi, A., 2001. Regulation of death receptor expression and TRAIL/Apo2L-induced apoptosis by NF-kappaB. *Nat. Cell Biol.* 3, 409–16. doi:10.1038/35070096
- Raychaudhuri, S., Prinz, W. a, 2010. The diverse functions of oxysterol-binding proteins. *Annu. Rev. Cell Dev. Biol.* 26, 157–77. doi:10.1146/annurev.cellbio.042308.113334
- Reed, J.C., Zha, H., Aime-Sempe, C., Takayama, S., Wang, H.-G., 1996. Structure—Function Analysis of Bcl-2 Family Proteins. Springer US, pp. 99–112. doi:10.1007/978-1-4899-0274-0_10
- Ren, Y.-G., Wagner, K.W., Knee, D.A., Aza-Blanc, P., Nasoff, M., Deveraux, Q.L., 2004. Differential regulation of the TRAIL death receptors DR4 and DR5 by the signal recognition particle. *Mol. Biol. Cell* 15, 5064–74. doi:10.1091/mbc.E04-03-0184
- Riedl, S.J., Fuentes-Prior, P., Renatus, M., Kairies, N., Krapp, S., Huber, R., Salvesen, G.S., Bode, W., 2001. Structural basis for the activation of human procaspase-7. *Proc. Natl. Acad. Sci. U. S. A.* 98, 14790–5. doi:10.1073/pnas.221580098
- Riedl, S.J., Shi, Y., 2004. Molecular mechanisms of caspase regulation during apoptosis. *Nat. Rev. Mol. Cell Biol.* 5, 897–907. doi:10.1038/nrm1496
- Rieger, J., Naumann, U., Glaser, T., Ashkenazi, A., Weller, M., 1998. APO2 ligand: a novel lethal weapon against malignant glioma? *FEBS Lett.* 427, 124–8.
- Rock, K.L., Kono, H., 2008. The inflammatory response to cell death. *Annu. Rev. Pathol.* 3, 99–126. doi:10.1146/annurev.pathmechdis.3.121806.151456
- Rodriguez, J., Lazebnik, Y., 1999. Caspase-9 and APAF-1 form an active holoenzyme. *Genes Dev.* 13, 3179–84.
- Rossin, A., Derouet, M., Abdel-Sater, F., Hueber, A.-O., 2009. Palmitoylation of the TRAIL receptor DR4 confers an efficient TRAIL-induced cell death signalling. *Biochem. J.* 419, 185–92, 2 p following 192. doi:10.1042/BJ20081212
- Rouvier, E., Luciani, M.F., Golstein, P., 1993. Fas involvement in Ca(2+)-independent T

- cell-mediated cytotoxicity. *J. Exp. Med.* 177, 195–200.
- Ruiz-Ruiz, C., Robledo, G., Font, J., Izquierdo, M., López-Rivas, A., 1999. Protein kinase C inhibits CD95 (Fas/APO-1)-mediated apoptosis by at least two different mechanisms in Jurkat T cells. *J. Immunol.* 163, 4737–46.
- Safa, A.R., Day, T.W., Wu, C.-H., 2008. Cellular FLICE-like inhibitory protein (C-FLIP): a novel target for cancer therapy. *Curr. Cancer Drug Targets* 8, 37–46.
- Sandu, C., Gavathiotis, E., Huang, T., Wegorzewska, I., Werner, M.H., 2005. A mechanism for death receptor discrimination by death adaptors. *J. Biol. Chem.* 280, 31974–80. doi:10.1074/jbc.M506938200
- Sarker, M., Ruiz-Ruiz, C., López-Rivas, A., 2001. Activation of protein kinase C inhibits TRAIL-induced caspases activation, mitochondrial events and apoptosis in a human leukemic T cell line. *Cell Death Differ.* 8, 172–81. doi:10.1038/sj.cdd.4400791
- Scaffidi, C., Fulda, S., Srinivasan, A., Friesen, C., Li, F., Tomaselli, K.J., Debatin, K.M., Krammer, P.H., Peter, M.E., 1998. Two CD95 (APO-1/Fas) signaling pathways. *EMBO J.* 17, 1675–87. doi:10.1093/emboj/17.6.1675
- Scaffidi, C., Schmitz, I., Zha, J., Korsmeyer, S.J., Krammer, P.H., Peter, M.E., 1999. Differential modulation of apoptosis sensitivity in CD95 type I and type II cells. *J. Biol. Chem.* 274, 22532–8.
- Schaefer, U., Voloshanenko, O., Willen, D., Walczak, H., 2007. TRAIL: a multifunctional cytokine. *Front. Biosci.* 12, 3813–24.
- Schleich, K., Warnken, U., Fricker, N., Oztürk, S., Richter, P., Kammerer, K., Schnölzer, M., Krammer, P.H., Lavrik, I.N., 2012. Stoichiometry of the CD95 death-inducing signaling complex: experimental and modeling evidence for a death effector domain chain model. *Mol. Cell* 47, 306–19. doi:10.1016/j.molcel.2012.05.006
- Schlessinger, J., 1988. Signal transduction by allosteric receptor oligomerization. *Trends Biochem. Sci.* 13, 443–7. doi:10.1016/0968-0004(88)90219-8
- Schneider, P., Thome, M., Burns, K., Bodmer, J.L., Hofmann, K., Kataoka, T., Holler, N.,

- Tschopp, J., 1997. TRAIL receptors 1 (DR4) and 2 (DR5) signal FADD-dependent apoptosis and activate NF-kappaB. *Immunity* 7, 831–6.
- Schneider, P., Thome, M., Burns, K., Bodmer, J.-L., Hofmann, K., Kataoka, T., Holler, N., Tschopp, J., 1997. TRAIL Receptors 1 (DR4) and 2 (DR5) Signal FADD-Dependent Apoptosis and Activate NF-κB. *Immunity* 7, 831–836. doi:10.1016/S1074-7613(00)80401-X
- Schneider-Brachert, W., Tchikov, V., Neumeyer, J., Jakob, M., Winoto-Morbach, S., Held-Feindt, J., Heinrich, M., Merkel, O., Ehrenschwender, M., Adam, D., Mentlein, R., Kabelitz, D., Schütze, S., 2004. Compartmentalization of TNF receptor 1 signaling: internalized TNF receptorsomes as death signaling vesicles. *Immunity* 21, 415–28. doi:10.1016/j.immuni.2004.08.017
- Scott, F.L., Stec, B., Pop, C., Dobaczewska, M.K., Lee, J.J., Monosov, E., Robinson, H., Salvesen, G.S., Schwarzenbacher, R., Riedl, S.J., 2009. The Fas-FADD death domain complex structure unravels signalling by receptor clustering. *Nature* 457, 1019–22. doi:10.1038/nature07606
- Secchiero, P., Gonelli, A., Carnevale, E., Milani, D., Pandolfi, A., Zella, D., Zauli, G., 2003. TRAIL promotes the survival and proliferation of primary human vascular endothelial cells by activating the Akt and ERK pathways. *Circulation* 107, 2250–6. doi:10.1161/01.CIR.0000062702.60708.C4
- Senftleben, U., Cao, Y., Xiao, G., Greten, F.R., Krähn, G., Bonizzi, G., Chen, Y., Hu, Y., Fong, A., Sun, S.C., Karin, M., 2001. Activation by IKKalpha of a second, evolutionary conserved, NF-kappa B signaling pathway. *Science* 293, 1495–9. doi:10.1126/science.1062677
- Senju, S., Negishi, I., Motoyama, N., Wang, F., Nakayama, K., Nakayama, K., Lucas, P.J., Hatakeyama, S., Zhang, Q., Yonehara, S., Loh, D.Y., 1996. Functional significance of the Fas molecule in naive lymphocytes. *Int. Immunol.* 8, 423–31.
- Sessler, T., Healy, S., Samali, A., Szegezdi, E., 2013. Structural determinants of DISC function: new insights into death receptor-mediated apoptosis signalling. *Pharmacol. Ther.* 140, 186–99. doi:10.1016/j.pharmthera.2013.06.009

- Shamas-Din, A., Kale, J., Leber, B., Andrews, D.W., 2013. Mechanisms of action of Bcl-2 family proteins. *Cold Spring Harb. Perspect. Biol.* 5, a008714. doi:10.1101/cshperspect.a008714
- Sheikh, M.S., Huang, Y., Fernandez-Salas, E.A., El-Deiry, W.S., Friess, H., Amundson, S., Yin, J., Meltzer, S.J., Holbrook, N.J., Fornace, A.J., 1999. The antiapoptotic decoy receptor TRID/TRAIL-R3 is a p53-regulated DNA damage-inducible gene that is overexpressed in primary tumors of the gastrointestinal tract. *Oncogene* 18, 4153–9. doi:10.1038/sj.onc.1202763
- Sheridan, J.P., Marsters, S.A., Pitti, R.M., Gurney, A., Skubatch, M., Baldwin, D., Ramakrishnan, L., Gray, C.L., Baker, K., Wood, W.I., Goddard, A.D., Godowski, P., Ashkenazi, A., 1997. Control of TRAIL-induced apoptosis by a family of signaling and decoy receptors. *Science* 277, 818–21.
- Shi, Y., 2004. Caspase activation: revisiting the induced proximity model. *Cell* 117, 855–8. doi:10.1016/j.cell.2004.06.007
- Shin, M.S., Kim, H.S., Lee, S.H., Park, W.S., Kim, S.Y., Park, J.Y., Lee, J.H., Lee, S.K., Lee, S.N., Jung, S.S., Han, J.Y., Kim, H., Lee, J.Y., Yoo, N.J., 2001. Mutations of tumor necrosis factor-related apoptosis-inducing ligand receptor 1 (TRAIL-R1) and receptor 2 (TRAIL-R2) genes in metastatic breast cancers. *Cancer Res.* 61, 4942–6.
- Shiozaki, E.N., Shi, Y., 2004. Caspases, IAPs and Smac/DIABLO: mechanisms from structural biology. *Trends Biochem. Sci.* 29, 486–94. doi:10.1016/j.tibs.2004.07.003
- Siegel, R.M., Frederiksen, J.K., Zacharias, D.A., Chan, F.K., Johnson, M., Lynch, D., Tsien, R.Y., Lenardo, M.J., 2000. Fas preassociation required for apoptosis signaling and dominant inhibition by pathogenic mutations. *Science* 288, 2354–7.
- Siegel, R.M., Martin, D.A., Zheng, L., Ng, S.Y., Bertin, J., Cohen, J., Lenardo, M.J., 1998. Death-effector filaments: novel cytoplasmic structures that recruit caspases and trigger apoptosis. *J. Cell Biol.* 141, 1243–53.
- Silva, J.C., Gorenstein, M. V, Li, G.-Z., Vissers, J.P.C., Geromanos, S.J., 2006. Absolute quantification of proteins by LCMSE: a virtue of parallel MS acquisition. *Mol. Cell.*

Proteomics 5, 144–56. doi:10.1074/mcp.M500230-MCP200

- Simons, K., Toomre, D., 2000. Lipid rafts and signal transduction. *Nat. Rev. Mol. Cell Biol.* 1, 31–9. doi:10.1038/35036052
- Símová, S., Klíma, M., Cermak, L., Sourková, V., Andera, L., 2008. Arf and Rho GAP adapter protein ARAP1 participates in the mobilization of TRAIL-R1/DR4 to the plasma membrane. *Apoptosis* 13, 423–36. doi:10.1007/s10495-007-0171-8
- Skaar, J.R., Pagan, J.K., Pagano, M., 2013. Mechanisms and function of substrate recruitment by F-box proteins. *Nat. Rev. Mol. Cell Biol.* 14, 369–81. doi:10.1038/nrm3582
- Slee, E.A., Harte, M.T., Kluck, R.M., Wolf, B.B., Casiano, C.A., Newmeyer, D.D., Wang, H.G., Reed, J.C., Nicholson, D.W., Alnemri, E.S., Green, D.R., Martin, S.J., 1999. Ordering the cytochrome c-initiated caspase cascade: hierarchical activation of caspases-2, -3, -6, -7, -8, and -10 in a caspase-9-dependent manner. *J. Cell Biol.* 144, 281–92.
- Slupe, A.M., Merrill, R.A., Strack, S., Slupe, A.M., Merrill, R.A., Strack, S., 2011. Determinants for Substrate Specificity of Protein Phosphatase 2A. *Enzyme Res.* 2011, 398751. doi:10.4061/2011/398751
- Song, J.H., Tse, M.C.L., Bellail, A., Phuphanich, S., Khuri, F., Kneteman, N.M., Hao, C., 2007. Lipid rafts and nonrafts mediate tumor necrosis factor related apoptosis-inducing ligand induced apoptotic and nonapoptotic signals in non small cell lung carcinoma cells. *Cancer Res.* 67, 6946–55. doi:10.1158/0008-5472.CAN-06-3896
- Spector, M.S., Desnoyers, S., Hoepfner, D.J., Hengartner, M.O., 1997. Interaction between the *C. elegans* cell-death regulators CED-9 and CED-4. *Nature* 385, 653–6. doi:10.1038/385653a0
- Sprick, M.R., Weigand, M.A., Rieser, E., Rauch, C.T., Juo, P., Blenis, J., Krammer, P.H., Walczak, H., Ashkenazi, A., Dixit, V., Ashkenazi, A. 2000. FADD/MORT1 and Caspase-8 Are Recruited to TRAIL Receptors 1 and 2 and Are Essential for Apoptosis Mediated by TRAIL Receptor 2. *Immunity* 12, 599–609. doi:10.1016/S1074-7613(00)80211-3

- Srinivasula, S.M., Hegde, R., Saleh, A., Datta, P., Shiozaki, E., Chai, J., Lee, R.A., Robbins, P.D., Fernandes-Alnemri, T., Shi, Y., Alnemri, E.S., 2001. A conserved XIAP-interaction motif in caspase-9 and Smac/DIABLO regulates caspase activity and apoptosis. *Nature* 410, 112–6. doi:10.1038/35065125
- Stegehuis, J.H., de Wilt, L.H.A.M., de Vries, E.G.E., Groen, H.J., de Jong, S., Kruijt, F.A.E., 2010. TRAIL receptor targeting therapies for non-small cell lung cancer: current status and perspectives. *Drug Resist. Updat.* 13, 2–15. doi:10.1016/j.drug.2009.11.001
- Steinberg, S.F., 2008. Structural basis of protein kinase C isoform function. *Physiol. Rev.* 88, 1341–78. doi:10.1152/physrev.00034.2007
- Stennicke, H.R., Deveraux, Q.L., Humke, E.W., Reed, J.C., Dixit, V.M., Salvesen, G.S., 1999. Caspase-9 can be activated without proteolytic processing. *J. Biol. Chem.* 274, 8359–62.
- Stennicke, H.R., Ryan, C.A., Salvesen, G.S., 2002. Reprieval from execution: the molecular basis of caspase inhibition. *Trends Biochem. Sci.* 27, 94–101.
- Sun, M., Song, L., Li, Y., Zhou, T., Jope, R.S., 2008. Identification of an antiapoptotic protein complex at death receptors. *Cell Death Differ.* 15, 1887–900. doi:10.1038/cdd.2008.124
- Suzuki, J., Denning, D.P., Imanishi, E., Horvitz, H.R., Nagata, S., 2013. Xk-related protein 8 and CED-8 promote phosphatidylserine exposure in apoptotic cells. *Science* 341, 403–6. doi:10.1126/science.1236758
- Szegezdi, E., Reis, C.R., Van Der Sloot, A.M., Natoni, A., O ’reilly, A., Reeve, J., Cool, R.H., O ’dwyer, M., Knapper, S., Serrano, L., Quax, W.J., Samali, A., 2011. Targeting AML through DR4 with a novel variant of rhTRAIL. *J. Cell. Mol. Med* 15, 2216–2231. doi:10.1111/j.1582-4934.2010.01211.x
- Tait, S.W.G., Green, D.R., 2013. Mitochondrial regulation of cell death. *Cold Spring Harb. Perspect. Biol.* 5. doi:10.1101/cshperspect.a008706
- Tait, S.W.G., Green, D.R., 2010. Mitochondria and cell death: outer membrane

- permeabilization and beyond. *Nat. Rev. Mol. Cell Biol.* 11, 621–32.
doi:10.1038/nrm2952
- Takahashi, T., Tanaka, M., Brannan, C.I., Jenkins, N.A., Copeland, N.G., Suda, T., Nagata, S., 1994. Generalized lymphoproliferative disease in mice, caused by a point mutation in the Fas ligand. *Cell* 76, 969–76.
- Tanaka, H., Hoshikawa, Y., Oh-hara, T., Koike, S., Naito, M., Noda, T., Arai, H., Tsuruo, T., Fujita, N., 2009. PRMT5, a novel TRAIL receptor-binding protein, inhibits TRAIL-induced apoptosis via nuclear factor-kappaB activation. *Mol. Cancer Res.* 7, 557–69. doi:10.1158/1541-7786.MCR-08-0197
- Tawa, P., Hell, K., Giroux, A., Grimm, E., Han, Y., Nicholson, D.W., Xanthoudakis, S., 2004. Catalytic activity of caspase-3 is required for its degradation: stabilization of the active complex by synthetic inhibitors. *Cell Death Differ.* 11, 439–47. doi:10.1038/sj.cdd.4401360
- Tecchio, C., Huber, V., Scapini, P., Calzetti, F., Margotto, D., Todeschini, G., Pilla, L., Martinelli, G., Pizzolo, G., Rivoltini, L., Cassatella, M.A., 2004. IFNalpha-stimulated neutrophils and monocytes release a soluble form of TNF-related apoptosis-inducing ligand (TRAIL/Apo-2 ligand) displaying apoptotic activity on leukemic cells. *Blood* 103, 3837–44. doi:10.1182/blood-2003-08-2806
- Thomas, L.R., Johnson, R.L., Reed, J.C., Thorburn, A., 2004. The C-terminal tails of tumor necrosis factor-related apoptosis-inducing ligand (TRAIL) and Fas receptors have opposing functions in Fas-associated death domain (FADD) recruitment and can regulate agonist-specific mechanisms of receptor activation. *J. Biol. Chem.* 279, 52479–86. doi:10.1074/jbc.M409578200
- Thomas, L.R., Stillman, D.J., Thorburn, A., 2002. Regulation of Fas-associated death domain interactions by the death effector domain identified by a modified reverse two-hybrid screen. *J. Biol. Chem.* 277, 34343–8. doi:10.1074/jbc.M204169200
- Thorburn, A., Behbakht, K., Ford, H., 2008. TRAIL receptor-targeted therapeutics: resistance mechanisms and strategies to avoid them. *Drug Resist. Updat.* 11, 17–

24. doi:10.1016/j.drug.2008.02.001

- Thornberry, N.A., Lazebnik, Y., 1998. Caspases: enemies within. *Science* 281, 1312–6.
- Trauzold, A., Wermann, H., Arlt, A., Schütze, S., Schäfer, H., Oestern, S., Röder, C., Ungefroren, H., Lampe, E., Heinrich, M., Walczak, H., Kalthoff, H., 2001. CD95 and TRAIL receptor-mediated activation of protein kinase C and NF-kappaB contributes to apoptosis resistance in ductal pancreatic adenocarcinoma cells. *Oncogene* 20, 4258–69. doi:10.1038/sj.onc.1204559
- Tschopp, J., Bodmer, J.-L., Holler, N., Reynard, S., Vinciguerra, P., Schneider, P., Juo, P., Blenis, J., 2000. TRAIL receptor-2 signals apoptosis through FADD and caspase-8. *Nat. Cell Biol.* 2, 241–243. doi:10.1038/35008667
- Tur, V., van der Sloot, A.M., Reis, C.R., Szegezdi, E., Cool, R.H., Samali, A., Serrano, L., Quax, W.J., 2008. DR4-selective tumor necrosis factor-related apoptosis-inducing ligand (TRAIL) variants obtained by structure-based design. *J. Biol. Chem.* 283, 20560–8. doi:10.1074/jbc.M800457200
- Turriziani, B., Garcia-Munoz, A., Pilkington, R., Raso, C., Kolch, W., von Kriegsheim, A., 2014. On-beads digestion in conjunction with data-dependent mass spectrometry: a shortcut to quantitative and dynamic interaction proteomics. *Biology (Basel)*. 3, 320–32. doi:10.3390/biology3020320
- Vääräniemi, J., Palovuori, R., Lehto, V.P., Eskelinen, S., 1999. Translocation of MARCKS and reorganization of the cytoskeleton by PMA correlates with the ion selectivity, the confluence, and transformation state of kidney epithelial cell lines. *J. Cell. Physiol.* 181, 83–95. doi:10.1002/(SICI)1097-4652(199910)181:1<83::AID-JCP9>3.0.CO;2-G
- Valley, C.C., Lewis, A.K., Mudaliar, D.J., Perlmutter, J.D., Braun, A.R., Karim, C.B., Thomas, D.D., Brody, J.R., Sachs, J.N., 2012. Tumor necrosis factor-related apoptosis-inducing ligand (TRAIL) induces death receptor 5 networks that are highly organized. *J. Biol. Chem.* 287, 21265–78. doi:10.1074/jbc.M111.306480
- van de Kooij, B., Verbrugge, I., de Vries, E., Gijsen, M., Montserrat, V., Maas, C., Neefjes, J., Borst, J., 2013. Ubiquitination by the membrane-associated RING-CH-

- 8 (MARCH-8) ligase controls steady-state cell surface expression of tumor necrosis factor-related apoptosis inducing ligand (TRAIL) receptor 1. *J. Biol. Chem.* 288, 6617–28. doi:10.1074/jbc.M112.448209
- van Dijk, M., Halpin-McCormick, A., Sessler, T., Samali, A., Szegezdi, E., 2013. Resistance to TRAIL in non-transformed cells is due to multiple redundant pathways. *Cell Death Dis.* 4, e702. doi:10.1038/cddis.2013.214
- van Roosmalen, I.A.M., Quax, W.J., Kruyt, F.A.E., 2014. Two death-inducing human TRAIL receptors to target in cancer: Similar or distinct regulation and function? *Biochem. Pharmacol.* 91, 447–456. doi:10.1016/j.bcp.2014.08.010
- VanHook, A.M., 2014. Avoiding Inflammation During Apoptosis. *Sci. Signal.* 7, ec89-ec89. doi:10.1126/scisignal.2005314
- Varfolomeev, E., Goncharov, T., Fedorova, A. V, Dynek, J.N., Zobel, K., Deshayes, K., Fairbrother, W.J., Vucic, D., 2008. c-IAP1 and c-IAP2 are critical mediators of tumor necrosis factor alpha (TNFalpha)-induced NF-kappaB activation. *J. Biol. Chem.* 283, 24295–9. doi:10.1074/jbc.C800128200
- Varfolomeev, E., Maecker, H., Sharp, D., Lawrence, D., Renz, M., Vucic, D., Ashkenazi, A., 2005. Molecular determinants of kinase pathway activation by Apo2 ligand/tumor necrosis factor-related apoptosis-inducing ligand. *J. Biol. Chem.* 280, 40599–608. doi:10.1074/jbc.M509560200
- von Karstedt, S., Conti, A., Nobis, M., Montinaro, A., Hartwig, T., Lemke, J., Legler, K., Annawanter, F., Campbell, A.D., Taraborrelli, L., Grosse-Wilde, A., Coy, J.F., El-Bahrawy, M.A., Bergmann, F., Koschny, R., Werner, J., Ganten, T.M., Schweiger, T., Hoetzenecker, K., Kenessey, I., Hegedüs, B., Bergmann, M., Hauser, C., Egberts, J.-H., Becker, T., Röcken, C., Kalthoff, H., Trauzold, A., Anderson, K.I., Sansom, O.J., Walczak, H., 2015. Cancer cell-autonomous TRAIL-R signaling promotes KRAS-driven cancer progression, invasion, and metastasis. *Cancer Cell* 27, 561–73. doi:10.1016/j.ccell.2015.02.014
- Wagner, K.W., Punnoose, E. a, Januario, T., Lawrence, D. a, Pitti, R.M., Lancaster, K., Lee, D., von Goetz, M., Yee, S.F., Totpal, K., Huw, L., Katta, V., Cavet, G.,

- Hymowitz, S.G., Amler, L., Ashkenazi, A., 2007. Death-receptor O-glycosylation controls tumor-cell sensitivity to the proapoptotic ligand Apo2L/TRAIL. *Nat. Med.* 13, 1070–7. doi:10.1038/nm1627
- Wajant, H., Pfizenmaier, K., Scheurich, P., 2003. Tumor necrosis factor signaling. *Cell Death Differ.* 10, 45–65. doi:10.1038/sj.cdd.4401189
- Walczak, H., Miller, R.E., Ariail, K., Gliniak, B., Griffith, T.S., Kubin, M., Chin, W., Jones, J., Woodward, A., Le, T., Smith, C., Smolak, P., Goodwin, R.G., Rauch, C.T., Schuh, J.C., Lynch, D.H., 1999. Tumoricidal activity of tumor necrosis factor-related apoptosis-inducing ligand in vivo. *Nat. Med.* 5, 157–63. doi:10.1038/5517
- Walker, N.P., Talanian, R. V, Brady, K.D., Dang, L.C., Bump, N.J., Ferez, C.R., Franklin, S., Ghayur, T., Hackett, M.C., Hammill, L.D., 1994. Crystal structure of the cysteine protease interleukin-1 beta-converting enzyme: a (p20/p10)₂ homodimer. *Cell* 78, 343–52.
- Wang, C.Y., Mayo, M.W., Korneluk, R.G., Goeddel, D. V, Baldwin, A.S., 1998. NF-kappaB antiapoptosis: induction of TRAF1 and TRAF2 and c-IAP1 and c-IAP2 to suppress caspase-8 activation. *Science* 281, 1680–3.
- Wang, L., Du, F., Wang, X., 2008. TNF-alpha induces two distinct caspase-8 activation pathways. *Cell* 133, 693–703. doi:10.1016/j.cell.2008.03.036
- Wang, L., Yang, J.K., Kabaleeswaran, V., Rice, A.J., Cruz, A.C., Park, A.Y., Yin, Q., Damko, E., Jang, S.B., Raunser, S., Robinson, C. V, Siegel, R.M., Walz, T., Wu, H., 2010. The Fas-FADD death domain complex structure reveals the basis of DISC assembly and disease mutations. *Nat. Struct. Mol. Biol.* 17, 1324–9. doi:10.1038/nsmb.1920
- Wang, P.-Y., Weng, J., Anderson, R.G.W., 2005. OSBP is a cholesterol-regulated scaffolding protein in control of ERK 1/2 activation. *Science* 307, 1472–6. doi:10.1126/science.1107710
- Wassenaar, T.A., Quax, W.J., Mark, A.E., 2008. The conformation of the extracellular binding domain of Death Receptor 5 in the presence and absence of the activating ligand TRAIL: a molecular dynamics study. *Proteins* 70, 333–43.

doi:10.1002/prot.21541

- Watanabe-Fukunaga, R., Brannan, C.I., Copeland, N.G., Jenkins, N.A., Nagata, S., 1992. Lymphoproliferation disorder in mice explained by defects in Fas antigen that mediates apoptosis. *Nature* 356, 314–7. doi:10.1038/356314a0
- Westphal, D., Dewson, G., Czabotar, P.E., Kluck, R.M., 2011. Molecular biology of Bax and Bak activation and action. *Biochim. Biophys. Acta - Mol. Cell Res.* 1813, 521–531. doi:10.1016/j.bbamcr.2010.12.019
- Whibley, C., Pharoah, P.D.P., Hollstein, M., 2009. p53 polymorphisms: cancer implications. *Nat. Rev. Cancer* 9, 95–107. doi:10.1038/nrc2584
- WHO, 2014. World Cancer Report 2014. Int. Agency Res. Cancer, WHO.
- Wiley, S.R., Schooley, K., Smolak, P.J., Din, W.S., Huang, C.P., Nicholl, J.K., Sutherland, G.R., Smith, T.D., Rauch, C., Smith, C.A., 1995. Identification and characterization of a new member of the TNF family that induces apoptosis. *Immunity* 3, 673–82.
- Wilson, K.P., Black, J.A., Thomson, J.A., Kim, E.E., Griffith, J.P., Navia, M.A., Murcko, M.A., Chambers, S.P., Aldape, R.A., Raybuck, S.A., 1994. Structure and mechanism of interleukin-1 beta converting enzyme. *Nature* 370, 270–5. doi:10.1038/370270a0
- Wu, G.S., Burns, T.F., McDonald, E.R., Jiang, W., Meng, R., Krantz, I.D., Kao, G., Gan, D.D., Zhou, J.Y., Muschel, R., Hamilton, S.R., Spinner, N.B., Markowitz, S., Wu, G., el-Deiry, W.S., 1997. KILLER/DR5 is a DNA damage-inducible p53-regulated death receptor gene. *Nat. Genet.* 17, 141–3. doi:10.1038/ng1097-141
- Wu, G.S., Burns, T.F., Zhan, Y., Alnemri, E.S., El-Deiry, W.S., 1999. Molecular cloning and functional analysis of the mouse homologue of the KILLER/DR5 tumor necrosis factor-related apoptosis-inducing ligand (TRAIL) death receptor. *Cancer Res.* 59, 2770–5.
- Wu, G.S., Kim, K., el-Deiry, W.S., 2000. KILLER/DR5, a novel DNA-damage inducible death receptor gene, links the p53-tumor suppressor to caspase activation and apoptotic death. *Adv. Exp. Med. Biol.* 465, 143–51. doi:10.1007/0-306-46817-

- Wu-Zhang, A.X., Newton, A.C., 2013. Protein kinase C pharmacology: refining the toolbox. *Biochem. J.* 452, 195–209. doi:10.1042/BJ20130220
- Wyles, J.P., Ridgway, N.D., 2004. VAMP-associated protein-A regulates partitioning of oxysterol-binding protein-related protein-9 between the endoplasmic reticulum and Golgi apparatus. *Exp. Cell Res.* 297, 533–47. doi:10.1016/j.yexcr.2004.03.052
- Xiao, T., Towb, P., Wasserman, S.A., Sprang, S.R., 1999. Three-dimensional structure of a complex between the death domains of Pelle and Tube. *Cell* 99, 545–55.
- Xie, C.-M., Wei, W., Sun, Y., 2013. Role of SKP1-CUL1-F-box-protein (SCF) E3 ubiquitin ligases in skin cancer. *J. Genet. Genomics* 40, 97–106. doi:10.1016/j.jgg.2013.02.001
- Xu, J., Xu, Z., Zhou, J.-Y., Zhuang, Z., Wang, E., Boerner, J., Wu, G.S., 2013. Regulation of the Src-PP2A interaction in tumor necrosis factor (TNF)-related apoptosis-inducing ligand (TRAIL)-induced apoptosis. *J. Biol. Chem.* 288, 33263–71. doi:10.1074/jbc.M113.508093
- Xu, J., Zhou, J.-Y., Xu, Z., Kho, D.-H., Zhuang, Z., Raz, A., Wu, G.S., 2014. The role of Cullin3-mediated ubiquitination of the catalytic subunit of PP2A in TRAIL signaling. *Cell Cycle* 13, 3750–8. doi:10.4161/15384101.2014.965068
- Xue, D., Shaham, S., Horvitz, H.R., 1996. The *Caenorhabditis elegans* cell-death protein CED-3 is a cysteine protease with substrate specificities similar to those of the human CPP32 protease. *Genes Dev.* 10, 1073–83.
- Yagita, H., Takeda, K., Hayakawa, Y., Smyth, M.J., Okumura, K., 2004. TRAIL and its receptors as targets for cancer therapy. *Cancer Sci.* 95, 777–83.
- Yamaguchi, H., Wang, H.-G., 2004. CHOP is involved in endoplasmic reticulum stress-induced apoptosis by enhancing DR5 expression in human carcinoma cells. *J. Biol. Chem.* 279, 45495–502. doi:10.1074/jbc.M406933200
- Yang, C.H., Pfeffer, S.R., Sims, M., Yue, J., Wang, Y., Linga, V.G., Paulus, E., Davidoff, A.M., Pfeffer, L.M., 2015. The oncogenic microRNA-21 inhibits the tumor

- suppressive activity of FBXO11 to promote tumorigenesis. *J. Biol. Chem.*
doi:10.1074/jbc.M114.632125
- Yang, H., Chen, X., Wang, X., Li, Y., Chen, S., Qian, X., Wang, R., Chen, L., Han, W.,
Ruan, A., Du, Q., Olumi, A.F., Zhang, X., 2014. Inhibition of PP2A activity confers a
TRAIL-sensitive phenotype during malignant transformation. *Mol. Cancer Res.* 12,
217–27. doi:10.1158/1541-7786.MCR-13-0441
- Yang, J.K., Wang, L., Zheng, L., Wan, F., Ahmed, M., Lenardo, M.J., Wu, H., 2005.
Crystal structure of MC159 reveals molecular mechanism of DISC assembly and
FLIP inhibition. *Mol. Cell* 20, 939–49. doi:10.1016/j.molcel.2005.10.023
- Yang, X., Chang, H.Y., Baltimore, D., 1998. Essential role of CED-4 oligomerization in
CED-3 activation and apoptosis. *Science* 281, 1355–7.
- Yasuhara, N., Sahara, S., Kamada, S., Eguchi, Y., Tsujimoto, Y., 1997. Evidence against a
functional site for Bcl-2 downstream of caspase cascade in preventing apoptosis.
Oncogene 15, 1921–1928. doi:10.1038/sj.onc.1201370
- Yeager, C.E., Olsen, E.A., 2011. Treatment of chemotherapy-induced alopecia.
Dermatol. Ther. 24, 432–42. doi:10.1111/j.1529-8019.2011.01430.x
- Zander, N.F., Lorenzen, J.A., Cool, D.E., Tonks, N.K., Daum, G., Krebs, E.G., Fischer, E.H.,
1991. Purification and characterization of a human recombinant T-cell protein-
tyrosine-phosphatase from a baculovirus expression system. *Biochemistry* 30,
6964–70.
- Zerafa, N., Westwood, J.A., Cretney, E., Mitchell, S., Waring, P., Iezzi, M., Smyth, M.J.,
2005. Cutting edge: TRAIL deficiency accelerates hematological malignancies. *J.*
Immunol. 175, 5586–90.
- Zhang, L., Fang, B., 2005. Mechanisms of resistance to TRAIL-induced apoptosis in
cancer. *Cancer Gene Ther.* 12, 228–37. doi:10.1038/sj.cgt.7700792
- Zhang, X.D., Franco, A., Myers, K., Gray, C., Nguyen, T., Hersey, P., 1999. Relation of
TNF-related apoptosis-inducing ligand (TRAIL) receptor and FLICE-inhibitory
protein expression to TRAIL-induced apoptosis of melanoma. *Cancer Res.* 59,

2747–53.

- Zheng, H., Shen, M., Zha, Y.-L., Li, W., Wei, Y., Blanco, M.A., Ren, G., Zhou, T., Storz, P., Wang, H.-Y., Kang, Y., 2014. PKD1 phosphorylation-dependent degradation of SNAIL by SCF-FBXO11 regulates epithelial-mesenchymal transition and metastasis. *Cancer Cell* 26, 358–73. doi:10.1016/j.ccr.2014.07.022
- Zhong, W., Qin, S., Zhu, B., Pu, M., Liu, F., Wang, L., Ye, G., Yi, Q., Yan, D., 2015. Oxysterol-Binding Protein (OSBP)-Related Protein 8 (ORP8) Increases Sensitivity of Hepatocellular Carcinoma Cells to Fas-Mediated Apoptosis. *J. Biol. Chem.* doi:10.1074/jbc.M114.610188
- Zhou, T., Li, S., Zhong, W., Vihervaara, T., Béaslas, O., Perttilä, J., Luo, W., Jiang, Y., Lehto, M., Olkkonen, V.M., Yan, D., 2011. OSBP-related protein 8 (ORP8) regulates plasma and liver tissue lipid levels and interacts with the nucleoporin Nup62. *PLoS One* 6, e21078. doi:10.1371/journal.pone.0021078
- Zhu, H., Zhang, L., Huang, X., Davis, J.J., Jacob, D.A., Teraishi, F., Chiao, P., Fang, B., 2004. Overcoming acquired resistance to TRAIL by chemotherapeutic agents and calpain inhibitor I through distinct mechanisms. *Mol. Ther.* 9, 666–73. doi:10.1016/j.ymthe.2004.02.007
- Zou, H., 1999. An APAF-1 Cytochrome c Multimeric Complex Is a Functional Apoptosome That Activates Procaspase-9. *J. Biol. Chem.* 274, 11549–11556. doi:10.1074/jbc.274.17.11549